Journal Pre-proofs

NMR investigations of glycan conformation, dynamics, and interactions

Jesús Angulo, Ana Ardá, Sara Bertuzzi, Angeles Canales, June Ereño-Orbea, Ana Gimeno, Marcos Gomez-Redondo, Juan C. Muñoz-García, Paola Oquist, Serena Monaco, Ana Poveda, Luca Unione, Jesús Jiménez-Barbero

PII: S0079-6565(24)00024-4
DOI: https://doi.org/10.1016/j.pnmrs.2024.10.002
Reference: JPNMRS 1555

To appear in: *Progress in Nuclear Magnetic Resonance Spectroscopy*

Received Date: 27 June 2024
Accepted Date: 7 October 2024

Please cite this article as: J. Angulo, A. Ardá, S. Bertuzzi, A. Canales, J. Ereño-Orbea, A. Gimeno, M. Gomez-Redondo, J.C. Muñoz-García, P. Oquist, S. Monaco, A. Poveda, L. Unione, J. Jiménez-Barbero, NMR investigations of glycan conformation, dynamics, and interactions, *Progress in Nuclear Magnetic Resonance Spectroscopy* (2024), doi: https://doi.org/10.1016/j.pnmrs.2024.10.002

NMR investigations of glycan conformation, dynamics, and interactions

Jesús Angulo,[a] Ana Ardá,[b,c] Sara Bertuzzi,[b] Angeles Canales,[d] June Ereño-Orbea,[b,c] Ana Gimeno,[b,c] Marcos Gomez-Redondo,[b] Juan C. Muñoz-García,[a] Paola Oquist,[d] Serena Monaco,[e] Ana Poveda,[b] Luca Unione,[b,b] Jesús Jiménez-Barbero*[b,c,f,g]

[a] Institute for Chemical Research (IIQ), CSIC-University of Seville, 49 Américo Vespucio, 41092 Seville, Spain.

[b] Center for Cooperative Research in Biosciences (CIC bioGUNE), Basque Research and Technology Alliance (BRTA), 48160 Derio, Bizkaia, Spain.

[c] Ikerbasque, Basque Foundation for Science, Plaza Euskadi 5, 48009 Bilbao, Spain.

[d] Departamento de Química Orgánica, Facultad Ciencias Químicas, Universidad Complutense de Madrid, Avd. Complutense s/n, C.P. 28040 Madrid, Spain

[e] School of Pharmacy, University of East Anglia, Norwich Research Park, NR47TJ Norwich, UK.

[f] Department of Organic & Inorganic Chemistry, Faculty of Science and Technology, University of the Basque Country, EHU-UPV, 48940 Leioa, Bizkaia, Spain.

[g] Centro de Investigacion Biomedica En Red de Enfermedades Respiratorias, 28029 Madrid, Spain.

Table of Contents

ABSTRACT

Glycans are ubiquitous in nature, decorating our cells and serving as the initial points of contact with any visiting entities. These glycan interactions are fundamental to host-pathogen recognition and are related to various diseases, including inflammation and cancer. Therefore, understanding the conformations and dynamics of glycans, as well as the key features that regulate their interactions with proteins, is crucial for designing new therapeutics. Due to the intrinsic flexibility of glycans, NMR is an essential tool for unravelling these properties. In this review, we describe the key NMR parameters that can be extracted from the different experiments, and which allow us to deduce the necessary geometry and molecular motion information, with a special emphasis on assessing the internal motions of the glycosidic linkages. We specifically address the NMR peculiarities of various natural glycans, from histo-blood group antigens to glycosaminoglycans, and also consider the special characteristics of their synthetic analogues (glycomimetics). Finally, we discuss the application of NMR protocols to study glycan-related molecular recognition events, both from the carbohydrate and receptor perspectives, including the use of stable isotopes and paramagnetic NMR methods to overcome the inherent degeneracy of glycan chemical shifts.

Keywords: Glycans, molecular recognition, glycoproteins, lectins, conformation

1. Introduction

Glycans are everywhere. From the simplest monosaccharides to the most convoluted glycostructures, they are one of the most sophisticated assemblies found on earth. Considering the number of residues they are comprised of, carbohydrates can be found as monosaccharides, oligosaccharides, and polysaccharides, as well as coupled with other biological entities to make glycolipids and glycoproteins, glycoconjugates in general. [1] The plethora of biological processes they are involved in makes understanding their role in molecular recognition events a crucial point to completely comprehend the full scope of the response to these events. [2-6]

Since sugar-mediated binding events are essential for cell-cell, cell-matrix, and cell-pathogen communication and meticulously modulate the physiology of the cell in health and disease, this research field is constantly expanding. [3] In the light of this, understanding the basis of

the structural diversity of carbohydrates, linkages to other biomolecules, and cellular distribution is of paramount importance.

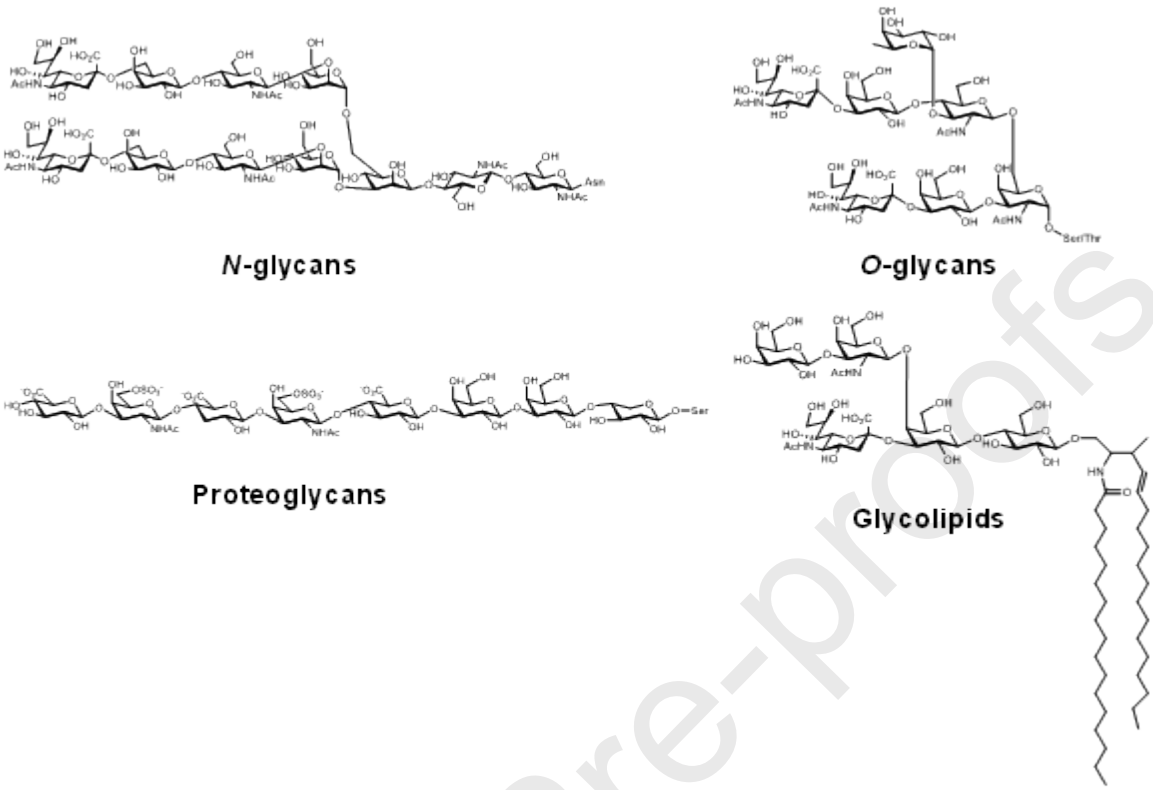

Scheme 1. The glycan world. Glycans may show different types of chemical structure in Nature.

The most common text abbreviation scheme for monosaccharides uses three letters, while for their visual representation, the pictorial notation universally recognized is the so-called Symbol Nomenclature for Glycans (SNFG), [7] which assigns a precise shape and a colour to each component (Scheme 2).

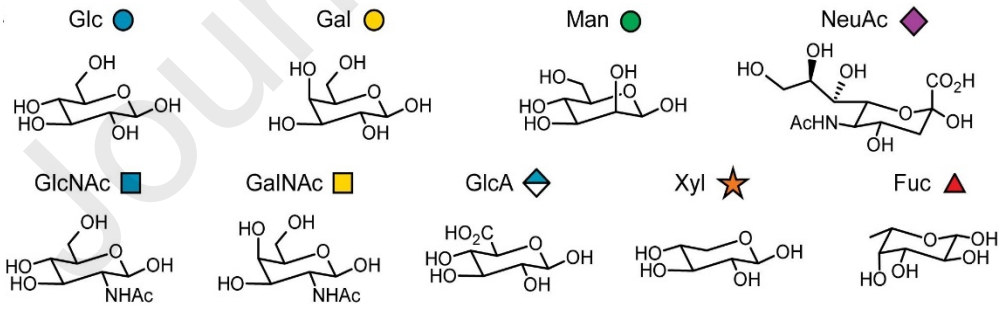

Scheme 2. Structure of the nine main recurrent monosaccharides in the mammalian *glycome* with their three-letter abbreviations and SNFG symbols.

Thus, the observed variety in nature does not strictly depend on the available number of sugar building blocks, but it is rooted, instead, in the chemical complexity of the monosaccharides and in the different natures of the linkages that join them together.

1.1. Techniques to unravel glycan conformation and monitor sugar-lectin interactions

The comprehensive study of the fine details that govern the binding events occurring between glycans and lectins is a major focus of this review. A collection of complementary techniques is described that over the years has allowed characterization of these systems at different levels of resolution. [8]

X-ray crystallography has been for decades the biophysical technique most often employed to elucidate the structure of lectin-sugar complexes at atomic resolution [9, 10]. Regarding glycans alone, their intrinsic flexibility can generate crystal heterogeneity, thus limiting the quality (resolution) of the crystal. The larger the glycan, the harder it is to obtain structures with good resolution. Nevertheless, this technique has some general limitations, since initial trials to find the correct crystallization conditions can require enormous effort in terms of time, and, notably, not all proteins can be crystalized. In addition, it has been demonstrated that deposited structures of sugar-lectin complexes may need further validation and refinement because of erroneous conformations or wrong linkages of the carbohydrate counterpart. [11, 12]

Recent advances in cryo-electron microscopy (cryo-EM) also provide the possibility to study protein-glycan recognition at atomic level, [13] overcoming the problem of the generation of crystals. Samples can be prepared at low concentrations before vitrification. A great advantage of cryo-EM with respect to X-ray crystallography is that conformational flexibility is not an obstacle and, in principle, full glycoproteins can be analysed, thus determining the 3D arrangement of their atoms at good resolution. However, one limitation of the technique is size; in fact, complexes smaller than ≈ 40 kDa are hardly detected. This is not a problem for highly glycosylated entities (such as viruses, glycoproteins or glycolipids), or for the study of multimeric assemblies or lattices (lectins generating trimers, dimers, tetramers in solution), but prevents the detailed analysis of small lectin-carbohydrate complexes. [14, 15]

Surface plasmon resonance (SPR) [16] and biolayer interferometry (BLI) [17] are biophysical techniques that measure association and dissociation kinetic constants. In both cases, the ligand or the receptor have to be immobilized on a sensor chip, but no additional tags are required for the detection. These techniques can be used to study lectin-sugar complexes, providing thermodynamic and kinetic parameters of the interaction. However, optimization of the protocol can be challenging. Moreover, the fact that one of the components is immobilized on a surface can affect its proper presentation to binding partners, depending on the particular system.

High-throughput microarrays also involve immobilization on solid surfaces. [18] These methods are a fundamental tool used in glycoscience to rapidly detect binding hits and guide the rational design of lectin binders. Both glycan and lectin arrays have been developed in a way that hundreds of glycans or lectins can be tested simultaneously in a single experiment. [19] Focusing on the glycoarray technique, glycans are usually covalently linked to a solid surface [20] where the binding events are detected through fluorescence measurements. Lectins can be directly labelled with a fluorescent tag, or alternatively detection can be achieved by exploiting a fluorescent-tagged anti-lectin antibody. However, there are some limitations of the technique. At first, large amounts of glycans are densely packed in the spots, a condition that may not occur in Nature. Furthermore, the type and length of the linker used, as well as the chemical characteristics of the surface, can also affect binding, mainly influencing orientation, packing, and presentation of the glycan. [21]

Isothermal titration calorimetry (ITC) offers the unique possibility to obtain the thermodynamic parameters that regulate a binding event. [22] No labelling is required, for either the ligand or the lectin, and growing advances in detection methods are allowing experiments to be performed with rather low quantities of sample. [23] Moreover, the data are collected in

solution without any need to immobilize one component of the complex. The heat released upon interaction of the partners is plotted against ligand concentration. Then, the binding constant (K_D), the reaction stoichiometry (n) and the enthalpy (ΔH) of the recognition process can be accurately calculated. In addition, the entropy (ΔS) can be estimated indirectly. Interactions with affinity constants in the nM-μM range can generally be studied with ITC, and most sugar-lectin associations falls in this range. [24] Protein concentration can be increased in the case of systems with low affinity, to optimize the experiment. However, affinity in the mM range is usually incompatible with the determination of reliable constants. [25]

2. NMR to the rescue

Due to the vast number of monosaccharide building blocks in nature and the conformational plasticity of their dihedral angles in solution, NMR spectroscopy has become universally accepted as the best approach to accessing the conformational details of glycans, usually in combination with computational procedures.

The versatility of NMR provides several descriptive parameters (chemical shifts, couplings, NOEs, relaxation rates …) that can be exploited in many ways depending on the nuclei studied, and the configuration of the pulse sequences and experiments (Table 1). In turn, such versatility has given rise to hundreds of experiments designed for different purposes: characterization of unknown molecules (organic synthesis, natural products…), [26] structure elucidation, [27, 28] ligand screening in drug discovery, [29] estimation of affinities, [30, 31] conformational information, [32, 33] reaction kinetics, [34] and molecular recognition. [35, 36]

Table 1. NMR strategies applied in the study of glycans and their interactions.

	NMR observables	NMR Experiments	Specific applications
Structural characterization (Assignment)	Chemical shifts	1D ^{1}H 2D ^{1}H-^{13}C-HSQC	Identification of anomeric protons and non-hydroxylated groups (aglicone, acetyl groups…). [320,321] Identification of anomalous chemical shifts arising from specific environment perturbations or conformational behaviors. [107]
	Scalar couplings	1D ^{1}H	Short-range correlations. Stereochemistry of sugars.
		2D ^{1}H-^{13}C-HSQC	Identification of C-H pairs. Identification of methylene groups (usually H_6) with ^{13}C-edited pulse sequences.
		2D ^{1}H-^{1}H COSY	Homonuclear short-range correlations ($^{3}J_{HH}$).
		2D ^{1}H-^{1}H TOCSY	Homonuclear long-range correlations (each sugar ring as an independent spin system).
		3D ^{1}H-^{13}C-HSQC-TOCSY	Homonuclear-heteronuclear correlation to avoid massive signal overlap in complex glycans. Requires ^{13}C-labeling.
		2D ^{1}H-^{13}C-HMBC	Heteronuclear long-range correlation. Identification of glycosidic linkages.

	Nuclear Overhauser and Rotating-frame Overhauser Effects	2D ^{1}H-^{1}H NOESY	Homonuclear through-space correlations. [113, 114]
		2D ^{1}H-^{1}H ROESY	Homonuclear through-space correlations for glycans with close-to-zero NOEs.
		3D ^{1}H-^{13}C-HSQC-NOESY	Homonuclear-heteronuclear correlation to avoid massive signal overlap in complex glycans. Requires ^{13}C labeling.
	Diffusion	2D DOSY	Deconvolution of 1D spectra by molecular size (size, [240-242] purity [249]).
	Pseudocontact shifts (PCSs)	1D ^{1}H 2D ^{1}H-^{13}C-HSQC	Breaking of chemical shift degeneracy in complex pseudosymmetric glycans. [270],[276]
Conformational studies	Scalar couplings	1D ^{1}H	Ring conformations (puckering). Torsional angles.
		1D ^{13}C	Ring conformations (puckering). Torsional angles. Glycosidic torsionals. ^{13}C labeling strongly advisable. [396]
	Nuclear Overhauser and Rotating-frame Overhauser Effects	2D ^{1}H-^{1}H NOESY/ROESY	Intra-residue: Ring conformations (puckering). Inter-residue: Glycosidic torsions. [105, 115-118]
	Pseudocontact shifts (PCSs)	1D ^{1}H 2D ^{1}H-^{13}C-HSQC	Conformational space of complex structures deduced from anisotropic perturbations. [270, 276, 277]
	Paramagnetic Relaxation Enhancements (PREs)	1D ^{1}H 2D ^{1}H-^{13}C-HSQC	Conformation of complex oligosaccharides [214] and presentation glycosphingolipids in micelles [289] as deduced from effects on relaxation rates
	Residual Dipolar Coupling	1D ^{1}H 2D ^{1}H-^{13}C-HSQC	Conformation of oligosaccharides using paramagnetic tags [274] or alignment media. [222, 271, 302-311] ^{13}C labeling strongly advisable. [312-314]
	Relaxation	^{13}C-{^{1}H}-CPMG	Structure, dynamics and local motions. [353-355]
Glycan-receptor interactions	*Ligand-based NMR Experiments*		
	Saturation Transfer Difference	^{1}H STD-NMR	Identification of binders. Ligand epitope mapping. [454]
		DEEP-STD	Information about type of amino acid residues in the binding site. [459]

		2D ^{1}H-STD-TOCSY 2D ^{1}H-^{13}C STD-HSQC	Ligand epitope mapping applied to complex glycans displaying acute signal crowding [531]. Heteronuclear versions usually require ^{13}C labelling. [533, 398, 399, 538]
		^{19}F STD/ ^{1}H STD-TOCSYreF	Ligand epitope mapping by direct ^{19}F observation or relaying on ^{1}H-^{19}F coupling constants. [543, 544]
	Nuclear Overhauser and Rotating-frame Overhauser Effects	2D Transferred-NOESY	Binding of small glycans to large receptors. Intermolecular ligand-receptor NOEs. [574, 577, 581, 582, 584-586]
		2D Transferred-ROESY	Chemical exchange between free and bound ligands. [120]
		2D ^{1}H-^{13}C-HSQC-NOESY	Intermolecular glycan-receptor NOEs separated in the ^{13}C dimension. [46, 391]
	Pseudocontact shifts (PCSs)	2D-^{13}C-HSQC	Detailed analysis of the epitope mapping in complex glycans. [276, 287]
	Residual Dipolar Couplings (RDCs)	2D ^{1}H-^{13}C-HSQC	Ligand bound-state conformation. [243]
	Diffusion	2D-DOSY	Changes in relative molecular sizes by complex formation.
	Relaxation	^{19}F-{^{1}H}-CPMG	Identification of binders. Screening of ^{19}F-labeled compound libraries. Affinity determination by competition experiments. [224-235]
	Receptor-based NMR Experiments		
	Chemical shifts	2D ^{1}H-^{1}H TOCSY/NOESY	Protein binding site mapping. [608-610]
		2D ^{1}H-^{13}C-HSQC	Probing specific interactions.[616-623]
		2D-^{15}N-HSQC	Epitope mapping from the receptor point of view. Requires ^{15}N-labeling. Binding constants and binding dynamics (titration). [624-629]
		1D ^{19}F	Binding detection by protein observed ^{19}F. [665]

	Relaxation	^{19}F-{^{1}H}-CPMG	Affinity determination by changes in peak intensity. [664]
	Paramagnetic Relaxation Enhancement (PRE)	2D ^{1}H-^{15}N-HSQC	Epitope mapping from the receptor point of view. [273, 291-294]
	Residual Dipolar Couplings (RDCs)	2D-^{15}N-TROSY	Distance-derived constraints provide information on the conformation of the protein in the bound state. [311]
	Diffusion	2D-DOSY	Changes in oligomeric state of the protein upon ligand binding.

2.1. Assignments

Obviously, in the carbohydrate field, the first step in any NMR-based structural, conformational or molecular recognition study is the assignment of the NMR-active nuclei of the glycan. [37] This task comprises different steps, including the identification of the monosaccharide constituents, their absolute configurations, the possible existence of substitutions at the hydroxyl moieties (sulphate, phosphate, acetate, …, etc), the anomeric configuration of every monosaccharide, and the types of glycosidic linkage between neighbours, as well as the existence of branching points. [38] This analysis requires considerable effort, which in many cases has to be complemented by the use of other structural techniques. [39] In sugars, protons (^{1}H) are the most commonly used nuclei for structural determination by NMR. The vast majority of carbohydrate protons provide ^{1}H NMR signals that lie in a narrow spectral region, between δ 3.2 and 4.2 ppm, due to their similar chemical environment, as they are all bound to carbon atoms bearing hydroxyl groups (C_2, C_3, C_4, and C_6 in hexapyranosides). Obviously, *O*-substitution provides chemical shift changes that can be exploited to assess the location of the substituent. Hydroxyl groups also contain key information on hydrogen bonding interactions, and their assignments have been widely targeted. Technically, these OH moieties are rather difficult to detect, given the existence of fast exchange with bulk water, as carbohydrate analysis by NMR is usually carried out in D_2O. DMSO can be employed as solvent to facilitate assignment, and even monitor the presence of intra or intermolecular hydrogen bonds, but a DMSO solution is obviously far from physiological conditions. Nevertheless, different technical approximations have been carried out to be able to observe sugar OH signals, [40-43] mainly using rather low temperatures, mixtures [44] with deuterated acetone, methanol, or DMSO, and high concentrations (even in the M range). The application to glycans of the Looped projected spectroscopy (L-PROSY) method, in the form of a homonuclear NOESY experiment, has allowed the detection of cross peaks between the hydroxyl and the nonlabile protons of significant intensity for a sialic acid tetrasaccharide. Since glycan hydroxyl groups exchange with bulk water at a fast rate (between tens and thousands of times per second at room temperature), there are technical challenges that should be carefully considered for the success of the experiment. [45] In particular, frequency-selective π/2 pulses were employed bracketing the evolution time, targeting only the exchangeable hydroxyl protons in a looping scheme that should be optimised by considering that sugar hydroxyl exchange with water at a rate of $10-10^3$ s^{-1} at room temperature. In most cases it is essential to use multidimensional NMR to solve the overlapping problem by expanding the NMR correlations to additional dimensions. For instance, it is possible to detect the hydroxyl groups by using ^{13}C-correlations in HSQC-TOCSY type experiments, even using ^{13}C at natural isotopic abundance. [45] This approach has also been extended to ^{13}C-labelled Man-containing glycans in the presence of a receptor (cyanovirin-N, see also in Section 6.2).

Standard isotope-edited NOESY and TOCSY experiments allowed their assignment and the deduction of their orientation in the bound stale, along with the determination of their hydrogen-bonding patterns, through the analysis of the observed inter- and intra-molecular NOEs. [46]

A)

B)

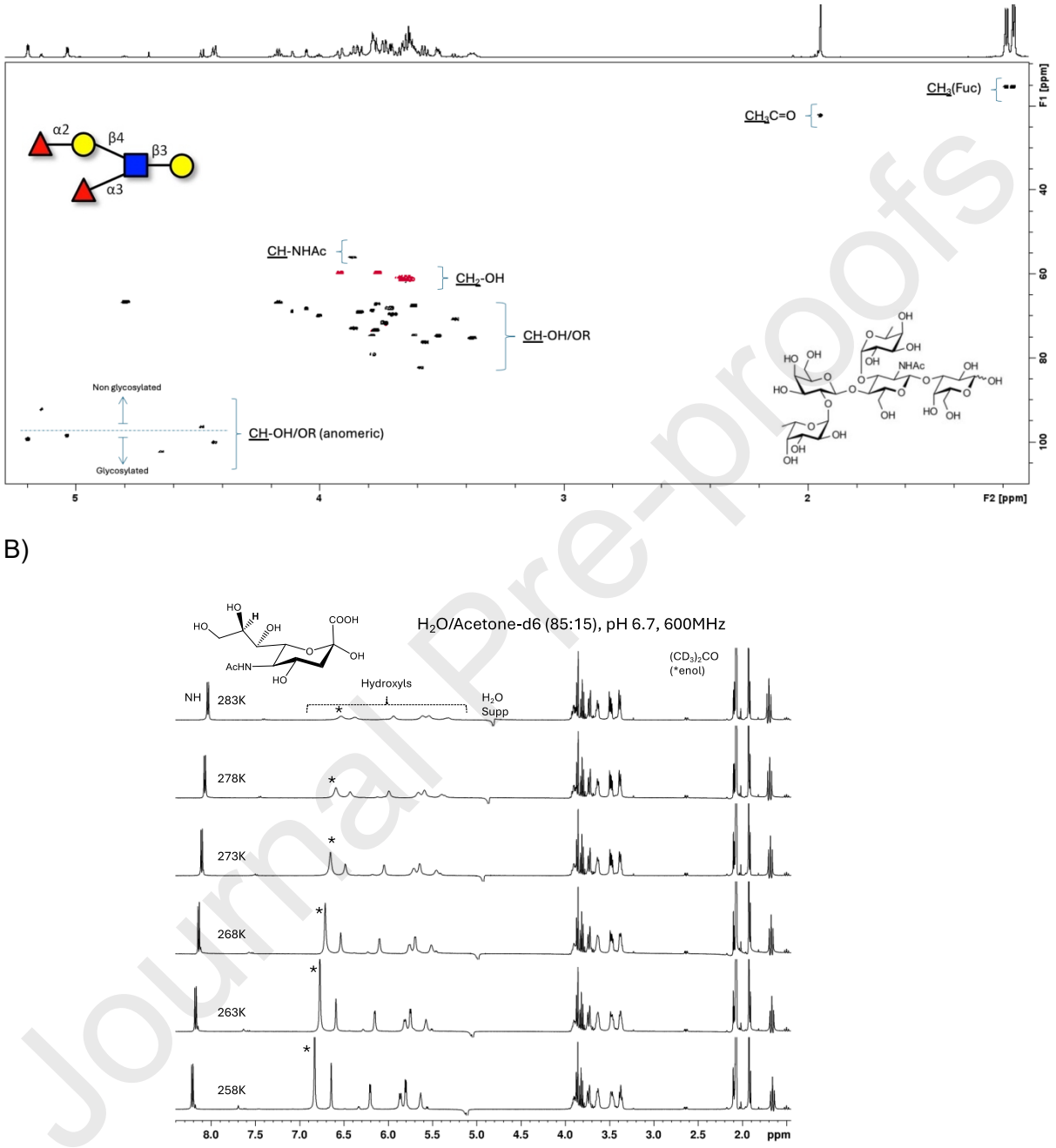

Figure 1. Top. A typical ^{1}H-^{13}C HSQC spectrum for a glycan, in this case, the Lewis Y pentasaccharide: Fucα1-2Galβ1-4(Fucα1-3)GlcNAcβ1-3Gal. The different regions are highlighted. Bottom. B. The ^{1}H NMR spectra of sialic acid in H_2O recorded at different temperatures. Under the appropriate experimental conditions, the hydroxyl groups may also be detected.

Therefore, the NMR assignment of glycans is usually based on the combination of different standard homonuclear (COSY, TOCSY; NOESY, ROESY) and heteronuclear (HMQC/HSQC, HMBC, HSQC-TOCSY) experiments (Figure 2). These methods and their selective versions have been extensively described and reviewed. [47, 48] At any point in the assignment process, the structural features of different sugar residues can be evaluated. For instance, the structure of the monosaccharide units is usually determined from vicinal $^{3}J_{H,H}$ coupling constants, [49] which contain torsion angle information according to Karplus-like relationships, combined with intra-residue NOE effects (the comparison between TOCSY and NOESY experiments allows the protons within a given monosaccharide ring to be distinguished from those belonging to the neighbouring residues). The use of diverse Karplus-like relationships to assess the configuration of sugars based on vicinal proton-proton coupling constants (and other heteronuclear alternatives, see below) has been widely applied. [49]

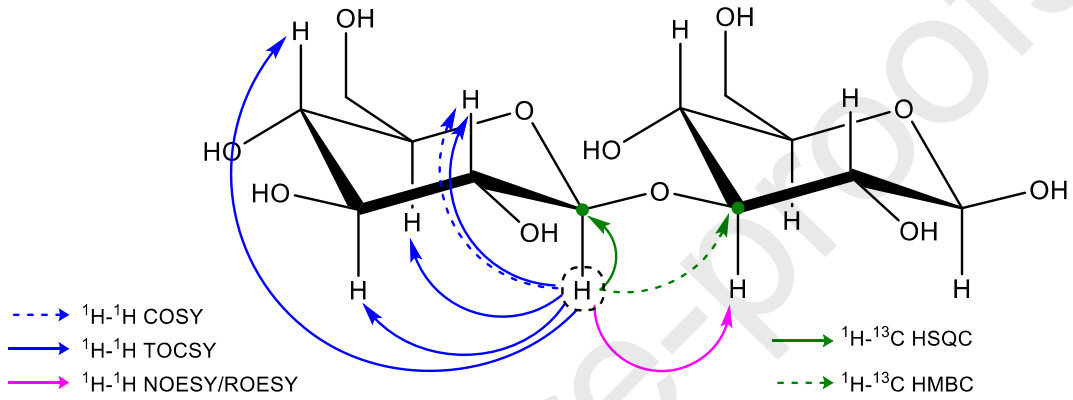

Figure 2. The standard ^{1}H, ^{13}C NMR experiments for assigning the NMR resonance signals of a glycan. From the anomeric proton H_1, COSY and TOCSY experiments reveal the spin system for a given monosaccharide ring. ^{1}H-^{13}C HSQC allows assignment of the corresponding ^{13}C nuclei. Transfer of information to a neighbouring ring may be obtained through NOE (through space) or through ^{1}H-^{13}C HMBC (using long-range interglycosidic $^{3}J_{CH}$ couplings). Intraresidue NOE interactions allow assessment of the relative orientations of protons within a ring, and, therefore, the spatial orientations of hydroxyl substituents.

From a global perspective, the J/NOE combination provides direct information on the chemical nature of the monosaccharide ring, which together with ^{1}H and ^{13}C chemical shifts (obtained through standard ^{1}H-^{13}C HMQC or HSQC correlation experiments) usually identifies the particular monosaccharide moiety, its anomeric configuration, and the existence of any chemical substitutions at the OH groups (or NH for amino sugars). [50] Obviously, the use of ^{1}H-^{31}P and/or ^{1}H-^{15}N correlation experiments unequivocally identifies the existence of phosphorus or amino substitutions and their positions. The positions of the glycosidic linkages are derived from NOESY and/or ^{1}H-^{13}C HMBC correlation experiments. Usually, glycan protons only show NOEs within a residue, or to protons in immediately contiguous residues. Therefore, analysis of the NOESY data should provide a first indication of the sequence, which can then be complemented by ^{1}H-^{13}C HMBC. This can provide an unambiguous result, but can be difficult to acquire, due to insufficient material and to the intrinsic low sensitivity of this experiment for large molecules, caused in turn by relaxation effects during the long *J*-coupling evolution period (tens of ms). Nevertheless, these experiments, sometimes combined with HSQC-TOCSY experiments, are of paramount importance for deducing the structures of polysaccharides.

Interestingly, there are general features in the NMR spectra of oligo and polysaccharides that have been exploited to develop computational tools to provide ^{13}C chemical shift predictions

for a given glycan. These predictions can be compared to the experimentally observed data, providing an excellent tool for identifying the primary sequence of a given saccharide, [51, 52] including the identities of the component monosaccharides, their furanose or pyranose nature, the α/β-anomeric configurations, the attachment positions of the glycosidic linkages between the units, the existence of branching, and eventually, the sequence. Thus, NMR is the key methodology to assess the existence of novel monosaccharide entities found in newly discovered polysaccharides and glycolipids from different animals and plants, including their chemical modifications, which may include rather rare substituents. [53] It is also noteworthy that many labs have developed and applied different computational tools to quantitatively estimate the expected NMR parameters that a given glycan should show, based on the very large amount of experimental data that has been accumulated during the last decades. [54]

As typical example, Silipo et al. [55] have carried out the structural analysis of the core oligosaccharide of the lipopolysaccharide present on the outer layer of the membrane of *Acetobacter pasteurianus* CIP103108, one of the most widely used bacteria for acetic acid and vinegar production, using NMR spectroscopy supported by MS methods. The study of the NMR vicinal coupling constants $^{3}J_{H,H}$ and intra-residue NOE effects allowed for the identification of each sugar residue as well as their relative configuration. A combination of ^{1}H-^{13}C HSQC, ^{1}H-^{31}P HSQC HMBC, ROESY, TOCSY supported by MS compositional analysis provided the data to suggest a highly branched and negatively charged structure, with a Kdo residue (3-deoxy-d-*manno*-oct-2-ulosonic acid) at its core, two phosphate groups next to each other, followed by a Glc-(1-4)-α-GlcA, a Rha-Glc disaccharide at O_5 and a rather unusual Ko (d-*manno*-oct-2-ulosonic acid) residue at O_8 [55].

2.2. Towards the conformation. The key parameters

Once the NMR assignment is completed, we are in a position to start the NMR-based study of the conformational behavior of the target glycan [56], which is the first step in the process of understanding structure-function relationships [57]. The conformational behaviour of oligo- and polysaccharides is defined by their torsion angles (Figure 3) around the glycosidic linkages, dubbed Φ and Ψ respectively, and the pendant C_5-C_6 hydroxymethyl group (ω torsion*)* [58]. The latter torsion can populate three staggered conformations (Figure 3): *gauche-gauche* (*gg*), *gauche-trans* (*gt*) and *trans-gauche* (*tg*), whose populations depend on the orientation of the hydroxyl group at C_4 (either axial or equatorial) [59].

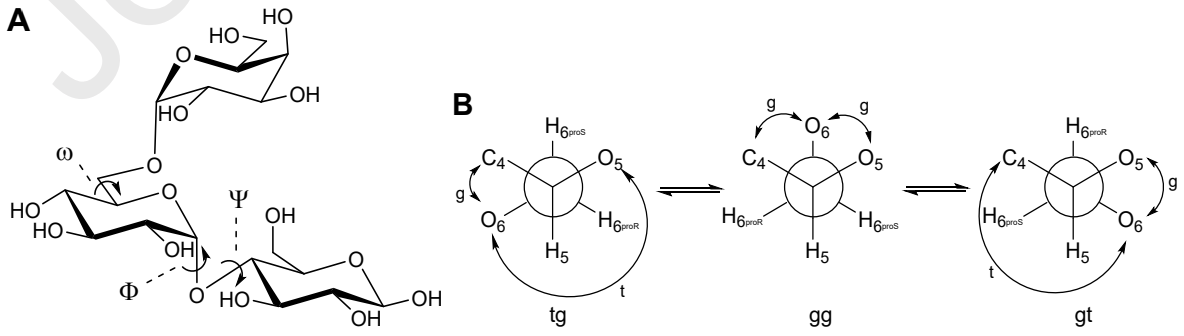

Figure 3. A) The torsion angles that define the conformation around the glycosidic linkages. Φ defines the torsion around C_1-O_1, while Ψ refers to C_X-O_1, where C_X is the attached carbon. In case of linkages involving the hydroxymethyl C_6 atom, an additional torsion angle (ω) is required to define the conformation around C_5-C_6. B) Newman projections of the three staggered geometries that the substituents can adopt around the C_5-C_6 linkage (*trans-gauche* or *tg*, *gauche-gauche* or *gg*, *gauche-trans* or *gt*). The first term refers to the relative orientation between O_5 and O_6 (gauche or trans) and the second to that between C_4 and O_6.

The conformational preferences around Φ are controlled by the so-called *exo*-anomeric effect, [60] (Figure 4), typical of molecules that show two oxygens (or highly electronegative atoms) attached to one carbon atom. For such species, there is an orbital-mediated stabilization of certain conformations, which show the proper arrangement between a particular lone pair at the glycosidic oxygen and the σ* orbital of the C_1-O_5 bond within the ring. Only two of the three staggered possible conformations at Φ are favoured by this steroelectronic effect (Figure 4), and one of the two (anti- Φ) is usually destabilized by steric forces. As a consequence, the most populated conformation is the *exo*-syn-Φ. Finally, the conformation around Ψ is under steric control. [61] Indeed, there are more possibilities of conformational averaging around Ψ than around Φ.

Thus it is accepted, and it has been demonstrated, that all Φ torsion angles in natural glycans display values in the exo-anomeric region, especially with the syn-Φ orientation and a very minor, or even negligible, participation of the anti-Φ alternative. Obviously, for those glycomimetics that do not show the exo-anomeric effect, this is not the case. [62] Indeed, the presence of non-exoanomeric conformations has been experimentally demonstrated for *C*-glycosyl compounds which feature an interglycosidic carbon atom instead of the natural oxygen (see also section 3.2 on glycomimetics).

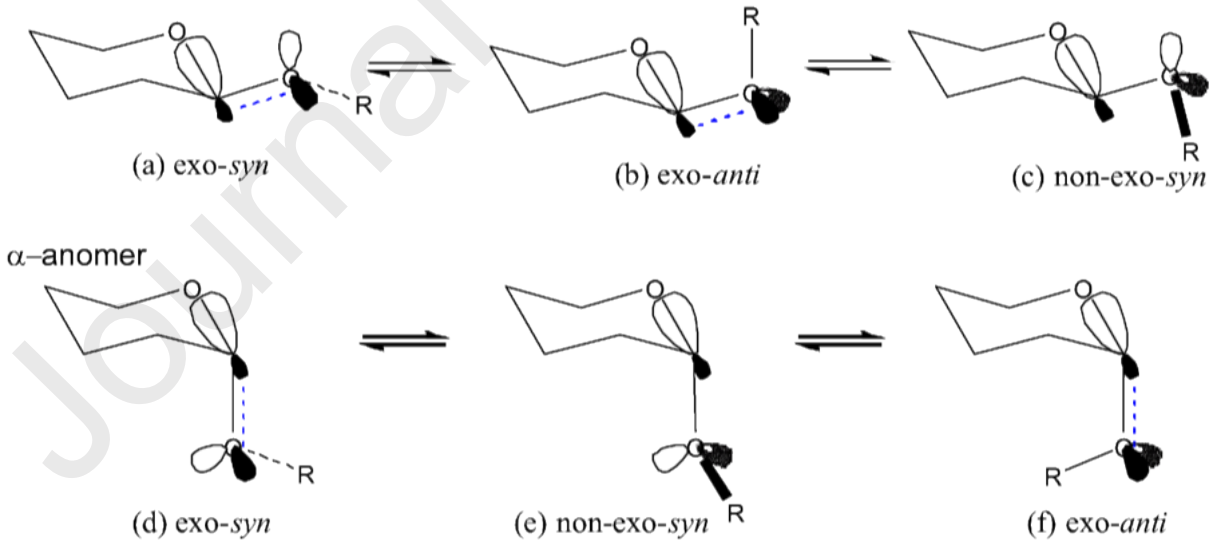

Figure 4. The exo-anomeric effect and torsion Φ values. The two exo-conformations (a and d, syn-exo; b and f, anti-exo) are stabilized by the overlap between the σ* orbital of the C1-O5 bond and one lone pair at the interglycosidic oxygen. The non-exo conformer does not show that stabilization and is never detected in natural glycosides. The presence of anti-conformers in torsion Φ (H_1-C_1-O_1-R), with values close to 180º, depends on the orientation of the substituents at the ring. The syn-exo conformers, with Φ (O_5-C_1-O_1-R) values ca. +60/-60º, are stabilized by the exo-anomeric effect and do not display steric conflicts.

2.2.1. *Vicinal coupling constants (carbon-proton and more) and torsion angles*

The conformation around the glycosidic linkages is usually deduced through extensive analysis of NOE data (see also Section 2.2.2). [63] However, it is obvious that interglycosidic vicinal carbon-proton coupling constants also contain conformational information (Figure 5), since they also show a dihedral-like Karplus-type relationship. [64, 65] Different equations have been proposed over the years to attempt to define a quantitative relationship between the actual $^{3}J_{CH}$ coupling values and the corresponding torsion angles. [65-67]

Obviously, like proton-proton couplings, [68] these $^{3}J_{CH}$ couplings depend not only on the torsion angle, but also on the electronegativity and relative orientation of the substituents along the coupling pathway. [65-67] This means that the substituents attached at C_1 (regarding Φ) and at C_4 (regarding Ψ) are also important and may strongly modify the coupling constant for a given value of torsion angle. Unfortunately, given the intrinsic chemical nature of sugars, to obtain conformationally rigid models for interglycosidic H-C-O-C torsions displaying a variety of dihedral angle values has remained elusive. Nevertheless, various empirical equations have been proposed to interpret the experimental $^{3}J_{COCH}$ values, with the best results obtained when using different equations to evaluate $^{3}J_{C1\text{-}O\text{-}C\text{-}HX}$ (for Φ) and $^{3}J_{CX\text{-}O\text{-}C\text{-}H1}$ (for Ψ). [65-67] Moreover, different equations have been proposed based on diverse theoretical methods, including DFT calculations, which have also been extended to employ other vicinal coupling constants that contain geometric information on the conformational ensemble around the glycosidic torsion angles, as $^{3}J_{C2\text{-}C1\text{-}O\text{-}CX}$ and $^{3}J_{C1\text{-}O\text{-}Cx\text{-}Cx\pm1}$. [69] It has been reported that DFT-calculated long-range ($^{2}J_{CH}$, $^{3}J_{CH}$, $^{4}J_{CH}$, $^{2}J_{CC}$, $^{3}J_{CC}$) coupling constants in sugars can be estimated with a high degree of accuracy, better than 5%. [70]

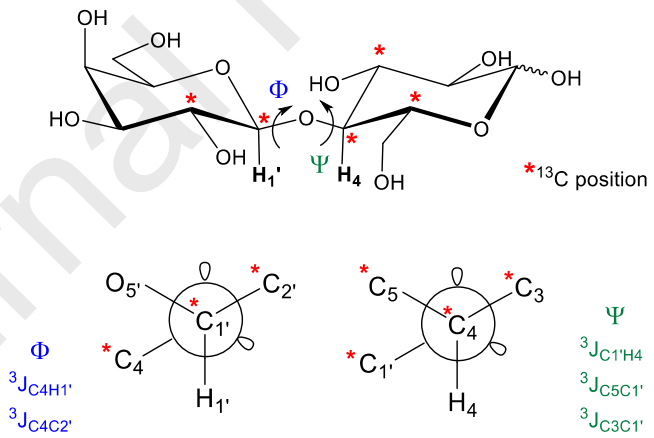

Figure 5. ^{13}C-based coupling constants that contain conformational information about glycosidic torsions. $^{3}J_{C4H1'}$ and $^{3}J_{C4C2'}$ encode information on Φ, whereas $^{3}J_{H4C1'}$, $^{3}J_{C5C1'}$, and $^{3}J_{C3C1'}$ contain information on Ψ.

It is well known that the relationships between the $^{3}J_{CH}$, and $^{3}J_{CC}$ coupling values and the torsion angles for these pathways are more complicated than those for $^{3}J_{HH}$, since there are many more substituents on the coupling routes, whose orientations will influence differently the actual ^{3}J value, even for the same torsion angle. [71] Moreover, since at least one of the coupled nuclei is ^{13}C, the maximum expected values (in Hz) for $^{3}J_{CC}$ are smaller (maximum ca. 5 Hz) than those for $^{3}J_{CH}$ (maximum *ca*. 8 Hz), and much smaller than those for $^{3}J_{HH}$.

Moreover, since the variation of the values among the possible interglycosidic conformers is not expected to be very high, good accuracy in the measurement is therefore essential. Experimentally, the quantitative measurement of these couplings can be challenging, especially when natural compounds, with natural ^{13}C abundance, are employed. Nevertheless, the use of very high or ultra-high field spectrometers, combined with cryogenic probes, may enable the experimental determination of such coupling constants with high accuracy, provided that the target molecule is available in sufficient quantity. Either selective excitation or regular sequences can be employed to measure these relatively small coupling constant values. Alternatively, the use of ^{13}C-labelled molecules, when available, greatly facilitates access to these NMR parameters. Different labelling schemes have been employed, including single labelling approaches, double ^{13}C labels, and up to complete uniform labelling. Interestingly, one-bond and geminal coupling constants, such as $^1J_{CH}$, $^1J_{CC}$, $^2J_{CH}$, and $^2J_{CC}$, also depend on the fine chemical structure around the coupled nuclei, along with the orientation around the torsion angles involving them. However, the parametrization of a reliable equation for these couplings is practically impossible. For instance, in a typical pyranose ring, $^1J_{C1,C2}$ depends on the chemical nature and orientation of the attached substituents but also on the orientations of the substituents attached at C_1–O_1 and C_2–O_2. Moreover, for $^1J_{CX,HX}$, the coupling values are also influenced by the vicinal torsion angles around the C_{x+1}-O_{x+1} and C_{x-1}-O_{x-1} linkages, except obviously for $^1J_{C1,H1}$, for which only the C_2–O_2 bond should be considered.

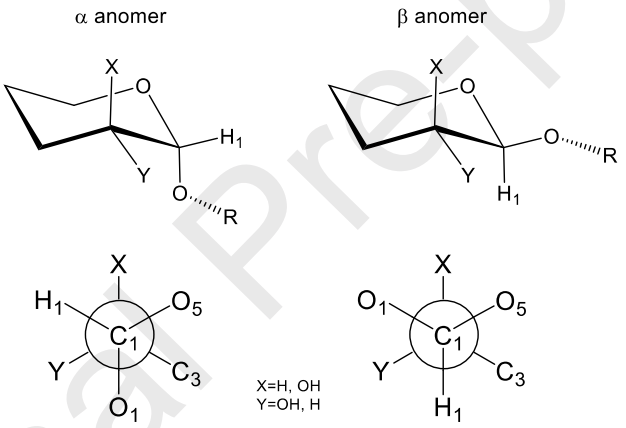

Figure 6. Representation of the the orientations of the substituents that modulate the $^1J_{C1,H1}$ value, for α (left) and β-anomers (right). The relative disposition of X and Y (OH or H) with respect to H_1 also affects the magnitude of $^1J_{C1,H1}$.

The estimation of diverse coupling constants involving ^{13}C nuclei ($^1J_{CH}$, $^1J_{CC}$, $^2J_{CH}$, $^2J_{CC}$, $^3J_{CC}$) has been used as experimental tool to investigate the distribution of glycan conformers in solution, by employing computing programs developed *ad hoc* for this task (*MA'AT* analysis). [67, 70-71] $^1J_{CH}$ coupling constants have also been extensively employed to unravel the the anomeric configuration. [65-67] The $^1J_{CH}$ value has an inverse relationship with the carbon–proton bond length at the anomeric center, which in turn depends on its s-character. The anomeric effect results in axially oriented C_1–H_1 bonds being longer than their equatorial analogues. Therefore, the β-sugar series display smaller $^1J_{C1,H1}$ couplings (*ca.* 160 Hz, axial C_1–H_1) than their α-counterparts configuration (*ca* 170 Hz, equatorial C_1–H_1). This experimental evidence is instrumental in distinguishing α- from β-anomers in those cases in which O_2 is axial and $^3J_{H1,H2}$ is small for both α- and β-anomers.

2.2.1.1. The hydroxymethyl group.

The study of the conformation around the more flexible exocyclic hydroxymethyl (CH_2OH) group of monosaccharides and (1-6)-linked oligo- and poly-saccharides is based on the estimation of the relative populations of the three model staggered rotamers defining the so-called ω torsion angle around the C_5-C_6 linkage: *gauche-gauche* (*gg*), *gauche-trans* (*gt)*, and *trans-gauche* (*tg)*. [59, 72] Here the first term refers to the O_5-C_5-C_6-O_6 torsion and the second to the C_4-C_5-C_6-O_6 torsion (Figure 3B). The experimental values of the measured vicinal $^3J_{H5,H6proR}$ and $^3J_{H5,H6proS}$ coupling constants are compared to those expected for the canonical rotamers, estimated through empirical equations or quantum mechanical calculations. [73] Since two experimental couplings are measured and the sum of the three populations should amount to 100%, the system can be solved in a straightforward manner. The key point is to be able to measure the coupling values in a satisfactory way and to be able to unambiguously determine the H_{6proR} and H_{6proS} stereo-assignment. In principle, this can be achieved through the analysis of the pattern of the intraresidue NOE measurements between H4 and the two H6 nuclei, depending on the orientation of H_4 (axial for Glc-type molecules and equatorial for Gal-type sugars). This type of analysis has been carried out extensively in many different glycans, allowing the conclusion that D-Glc and D-Man derivatives, regardless of the substitution at O_6, present near equal *gg* and *gt* populations and a near complete absence of the *tg* conformation both in solution [74] and in the solid state. [75] This propensity for the ω-torsion angle to adopt *gg/gt* conformations in D-Glc/Man has been attributed to the *gauche* effect [76] and to unfavourable 1,3-diaxial O_4/O_6 interactions operating in the *tg* rotamer. D-Gal moieties, in contrast, show a markedly different conformational distribution around the C_5–C_6 bond, where *gg* contributions are almost negligible, probably due to unfavourable 1,3-diaxial O4/O6 interactions (see Scheme 1 for the difference between D-Glc/Man and D-Gal). Based on quantum mechanical (QM) methods and molecular dynamics simulations (MD) in explicit water, Woods and coworkers reported that water plays a key role in determining the conformation around ω, [77] by disrupting the intramolecular HB (hydrogen bonding) networks within Gal monosaccharides that stabilize the *gg* conformers. Measurement of a combination of the standard $^3J_{H5,H6}$ with other $^nJ_{C,H}$ and $^nJ_{CC}$ couplings has been proposed to provide a fully integrated perspective on the conformation around hydroxymethyl groups. [69]

2.2.2. NOEs

The analysis of the conformation around glycosidic linkages typically relies on the analysis of inter-residue NOEs that connect protons around the glycosidic linkages, measured through nuclear Overhauser effect (NOE)-type experiments, NOESY and ROESY. [78] The NOE between two nuclei depends on the inverse of the sixth power of the distance between them ($\propto r^{-6}$), and therefore the inter-residue NOEs report on the Φ and Ψ torsions. [79] In addition to its $1/r^6$ dependence, the NOE is also influenced by the spectrometer frequency and displays a complex timescale dependence, in which the overall molecular tumbling may interact with kinetics of the conformational exchange involved in internal motions. In any case, the NOE-based approach works well when there are enough NOEs that are sensitive to molecular shape. Nevertheless, taking into account the mobility of most glycosidic linkages, most glycan conformational studies combine NOE data with computational chemistry calculations (molecular mechanics and/or molecular dynamics). Often, however, challenges stem from the insufficient number of NOEs across the glycosidic linkages, since usually only one or two NOEs are observable per linkage. [80]

A typical NOE-based analysis starts by identifying all intra- and inter-residue NOEs for the target glycan. [81] Intra- and inter-residue NOEs can be distinguished by comparing scalar coupling connectivities from COSY- and TOCSY-based experiments with through-space connectivities from NOE/ROE experiments. Intra-residue NOEs are then used to assess the actual chemical structure of every monosaccharide moiety (in combination with vicinal $^{3}J_{H,H}$ values, if available) and thus discard (or verify) the existence of conformational mobility at the individual ring level (see below in the glycosaminoglycan section). The intensities of the intra-residue NOEs may be used as internal standards to estimate (unknown) inter-residue proton-proton distances that are related to the torsion angle values. Different approaches can be applied for this task, from the isolated spin pair approximation to the full matrix relaxation approach, or some tactics in between, estimating internal motion or effective correlation times for specific proton pairs. [82] For instance, the combination of ROESY and NOESY at one or more magnetic fields [83] and the off-resonance ROESY experiment [84, 85] have been employed, since they allow the extraction of effective correlation times for different regions of a molecule and, thus, determination of different internal motion timescales and, eventually, inter-proton distances.

These NOE-based distances are then compared to those expected for different 3D molecular models of the glycan under investigation. For this task, different approaches have been employed over the years, from the Hard Sphere Exo-Anomeric (HSEA) method [86] to molecular mechanics and dynamics calculations, using the latest force field developments in the computational arena, or using quantum mechanics. [87] All these methods aim at obtaining reliable 3D structures that correspond to possible energy minima of the molecule to back up the experimental results (essentially ^{3}J and NOEs, and unsual chemical shifts). Obviously, NOEs do not directly (or inversely) depend on the inter-proton distance, but on its inverse sixth power. [78] Thus, the interpretation of the observed NOEs relies heavily on contributions from those conformers that show short distances between the corresponding proton pairs. Thus, although these conformers may have low populations, provided that the inter-proton distance is short enough, the corresponding NOE will still be observed. This fact was translated to the concept of an “exclusive NOE”, which defines a short inter-proton distance that only occurs in one of the possible conformers of the target glycan. If this NOE is observed, the corresponding conformer must be participating at least to some degree in the conformational equilibrium, with a population that can later be assessed by proper quantitative analysis. The exclusive NOE approach is a safe method to check the presence of different glycan conformers in equilibrium and has been extensively used (Figure 7).

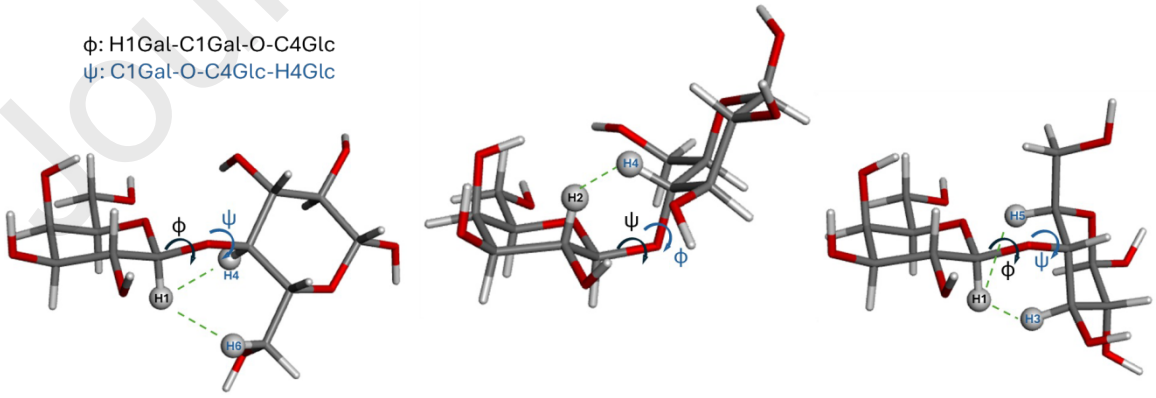

syn-exo-ϕ/syn-ψ
ϕ: 60; ψ: 0

anti-exo-ϕ/syn-ψ
ϕ: 180; ψ: 0

syn-exo-ϕ/anti-ψ
ϕ:60; ψ: 180

Figure 7. The concept of exclusive NOEs. For this lactose-type disaccharide, in the syn-exo-Φ/syn-Ψ conformation, there is a close distance for the H_1 Gal/H_4 Glc and H_1 Gal/H_6 Glc proton pairs. The presence of these NOEs in the NOESY spectrum indicates that this conformer is present in the conformational equilibrium, since these two proton pairs are far apart in the alternative syn-exo-Φ/anti-Ψ and anti-exo-Φ/syn-Ψ geometries, which are also local minima according to computational methods. In the same way, the presence of the H_2 Gal/H_4 Glc NOE demonstrates that the anti-exo-Φ/syn-Ψ should be considered as one of the contributing conformers. Finally, provided that cross peaks for the H_1 Gal/H_3 Glc and H_1 Gal/H_5 Glc proton pairs are detected in the NOESY experiment, there is a contribution from the syn-exo-Φ/anti-Ψ conformer.

3. NMR and the conformations of glycans

3.1 The natural glycans

Early NMR-based conformational studies were focused on the histo-blood group oligosaccharide and Lewis antigens and their constituent disaccharides. [86] The initial analysis of the NOE data, at that time at relatively low magnetic fields, along with the presence of particular chemical shift features, allowed the deduction that these molecules showed a fairly well-defined 3D shape. [87, 88] This proposal has been retained over the years [89] and it is generally accepted that these molecules can be defined by a major conformation around their glycosidic linkages, [90-92] although with the participation of low population conformers, depending on the particular antigen. [93] Interestingly, these minor geometries may also be recognized by certain receptors [94, 95] in a conformational selection process, with the corresponding entropy penalty associated to the interaction event. [96] Although the binding of minor conformers has only rarely been observed in the interactions of natural glycans with receptors, especially lectins, [97] this phenomenon has been widely detected by NMR for glycomimetics, [98] and also in the first step of the catalysis mediated by carbohydrate-active enzymes, especially glycosyl hydrolases. [99] Moreover, in the histo blood group oligosaccharide and Lewis antigen families, [100-103] the glycosidic linkages display different degrees of mobility depending on the particular chemical architecture of the saccharide. [104] Using a careful temperature-dependent NOE analysis, positive and negative NOEs [105] were observed for specific proton pairs located at different regions of one Lewis-like antigen, showing the existence of different effective correlation times for proton pairs within the same molecule and therefore, of different internal motions at distinct timescales. A similar phenomenon has also been observed for a macrolide antibiotic. [106]

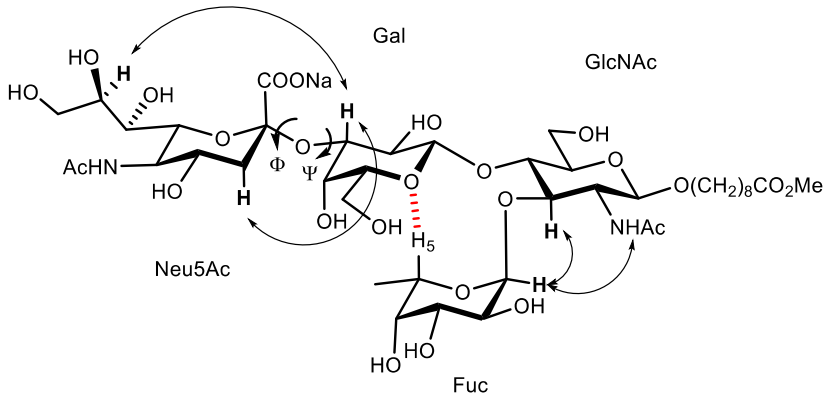

Figure 8. The key NOEs that define the conformation around the Neu5Ac-Gal and Fuc-GlcNAc glycosidic linkages of the sialyl LeX antigen. The extreme downfield shift of Fuc H5 indicates its close proximity to Gal O5, demonstrating the existence of a particular (turn-like conformation) for the glycosidic torsions of Gal-GlcNAc-Fuc trisaccharide moiety.

As a leading example, the LeX (Lewis X) antigen (Gal[Fucα(1→3)]β(1→4)GlcNAc) displays a particular structural feature. The first NMR-based structural and conformational analyses, described many years ago, showed that Fuc H_5 displays a particular highly deshielded chemical shift (δ 4.84 ppm), approximately 0.5 ppm at lower field than that for the corresponding disaccharides. Interestingly, this "anomalous" chemical shift is ubiquitous in a series of oligosaccharides, [107] which not only belong to the Lewis series of antigens and mammalian saccharides, including the biomedically relevant sialyl LeX antigen (Figure 8), but also exist in bacteria, amphibians, and marine invertebrates. The key consensus structural sequence can be identified as **X**-β1,4-[Fucα1,3]-**Y** and **X**-β1,3-[Fucα1,4]-**Y**, defined as a secondary structural element in glycans and dubbed by Schubert and coworkers as [3,4]F-branch (Figure 8). **Y**, in principle, should be Glc, GlcNAc or GlcA, while **X** could be Gal, GalNAc, Glc, or GlcNAc. [108] This unusual chemical shift for H5 Fuc was identified early to be due to the close proximity of Gal O_5 in the Lewis antigens, and later extended to all glycans displaying this structural motif. [109] The investigations by Schubert and coworkers led to the conclusion that there is a non-conventional C-H···O hydrogen bond [110] between Fuc H_5 and Gal O5 that provides additional stabilization to the lowest energy conformer, which also shows the particular combination of Φ (always at the favorable exo-anomeric region) and Ψ torsion angles to become a highly favored geometry. In fact, the use of $^{1}H,^{13}C$-HSQC heteronuclear experiments optimized for small couplings showed the key cross peak between Gal H1 and Fuc C5 in fucose in a sialyl-Lewis^x glycan, thus demonstrating the presence of electron density along the three-bond Gal H_1-Gal C_1-Gal O_5···H_5 Fuc pathway. [111, 112] This type of non-conventional C-H···O hydrogen bond has also been evidenced in linear Galα(1→4)Gal oligosaccharides. [113] Here, the interaction takes place between Gal $H_{5'}$ and Gal O_3 at the preceding residue. The existence of this structural motif in glycans has been further exploited by Delbianco and cowokers to design the first glycan hairpin. [114] A [3,4]F-like branch, but substituting Fuc at **Y** by Rha, with an equatorial OH_4 group, and changing the typical Gal unit in the Lewis antigens to Glc (also with equatorial OH_4), provides a turn unit that can be extended in parallel at both O_4 atoms of the two moieties that generate the C-H···O interaction. Importantly, a series of Glcβ(1→4)Glc moieties were attached at both entities. These cellulose-like chains are known to display a straight structure and show a tendency to provide inter-strand interactions. The success of the design to provide the target glycan hairpin topology was demonstrated by inter-strand NOEs (measured using labelled ^{13}C-Glc monosaccharides placed at specific positions), in addition to the typical NOEs and chemical shift deshielding observed at the turn motif. The driving forces that provide the impetus for generating this type of glycan hairpin have also been scrutinized using a similar NMR approach (NOE, δ analysis). [115]

The conformations of the histo blood group antigens have also been extensively studied. [116-118] The A and B tetrasaccharide antigens are also branched entities, with a different location of the αFuc unit, now attached to Gal O2 instead of GlcNAc O3 in the Lewis antigens (Scheme 3). The conformational behavior of the component disaccharides and trisaccharides has also been widely discussed and elucidated on the basis of the typical NOE/computational approach. Thus, NMR-based analysis of the conformational preferences of the branched tetrasaccharides, compared to those carried out for the Galβ(1→3)Glc/GlcNAc, Galβ(1→4)Glc/GlcNAc, Fucα(1→3)Gal, GalNAc/Galα(1→3)Gal disaccharides and the Fucα(1→2)Galβ(1→4)GlcNAc/Glc (H-type II/VI), Fucα(1→2)Galα (1→3)GlcNAc/Glc (H-type I/IV), GalNAc/Galα(1→3)Galβ(1→3)GlcNAc/Glc, and GalNAc/Galα(1→3)Galβ(1→4)GlcNAc/Glc trisaccharides, allowed the conclusion that the branched oligomers display a well-defined major conformation in solution. [119-122] The

presence of the branched Fuc in the tetrasaccharide antigens moiety leads to interactions at the vicinal αGal/GalNAc and αGlc/GlcNAc residues that preclude the existence of significant motion around the vicinal glycosidic linkages.

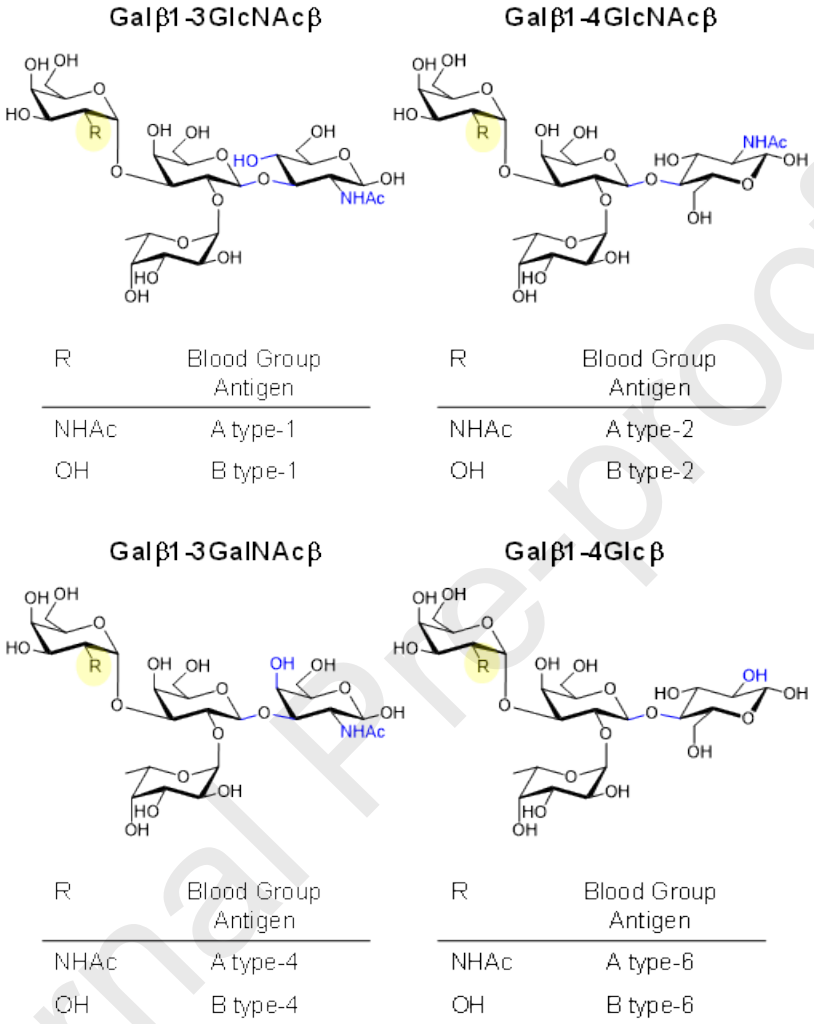

Scheme 3. The histo-blood group antigens and their different linkage types. The structural differences are highlighted.

Systematic NMR-based analysis of many different glycosidic linkages [123-126] has allowed the conclusion that, for disaccharides, the factors that determine their conformation comprise mainly the configuration at $C_{1'}$ (α or β) and the attached carbon C_X at the $C_{1'}$-O-C_x glycosidic linkage, as well as the chemical architectures at the surroundings of the participating $C_{1'}$ and C_X atoms; in other words, the configuration and substitution at $C_{2'}$ (either axial or equatorial, either O-substituted or N-substituted), the existence or not of additional substituents at $C_{1'}$ (eg. $C_{1'}$ is quaternary in sialic acid derivatives and in sucrose), and the configuration and substitution at C_{X+1} and C_{X-1}. For instance, the conformation around Φ/Ψ for Galβ(1→4)Glc, Glcβ(1→4)Glc, and Glcβ(1→4)Man should be very similar, while some differences should be expected respect to those for GalNAcβ(1→4)Glc, GlcNAcβ(1→4)Glc, and GlcNAcβ(1→4)Man due to the larger volume of the NAc versus the OH group at $C_{2'}$. The trends among these

conformational behaviors have been extensively investigated through NOE analysis assisted by computations and long-range heteronuclear couplings.

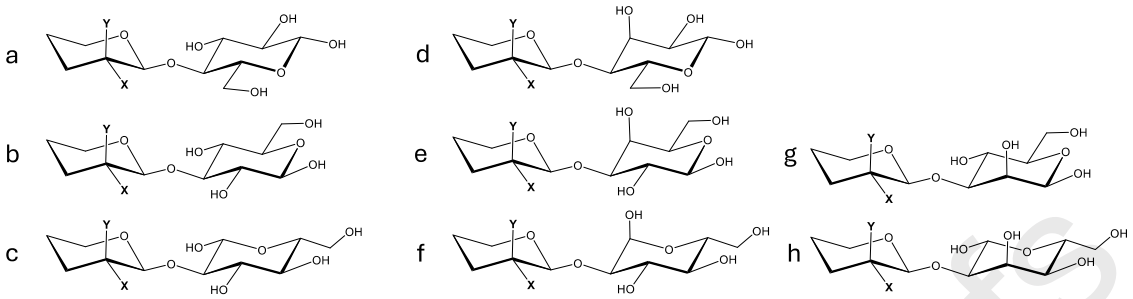

Figure 9. For natural *O*-glycosides, the conformation around Φ is regulated by the exo-anomeric effect, independently of the nature of X and Y. The major conformation around the Ψ torsion angle depends on the orientation and chemical nature of the substituents flanking the glycosylated position of the aglycone. For instance, glycosides a, b, and c, with β1-4, β1-3, and β1-2 linkages to β-Glc moieties will display a similar orientation around Ψ, since in each of these cases both substituents flanking the glycosylation position are equatorial. Some slight influence of the hydroxymethyl group (in a) versus the hydroxyl (in b and c) should be expected. An analogous situation may be expected for d (β1-4 to β-Allose), e (β1-3 to β-Gal), and f (β1-2 to α-Glc) and similarly for g (β1-3 to β-Man) and h (β1-2 to β-Allose).

As mentioned in section 2.1, the orientation of the hydroxyl groups in a glycan help determine the conformation of the saccharide and its molecular recognition properties, since they are involved in key intra- and inter-molecular hydrogen bonds. [127] Therefore, detection of these exchangeable moieties and evaluation of their interaction properties has been the target of investigations over many years, as described in section 2.2. [40-46]

3.1.1. Glycosaminoglycans

From a chemical perspective, GAGs are extensive unbranched polysaccharide chains characterized by repeating disaccharide units. Fundamentally, these units consist of a D-hexosamine residue (namely, D-glucosamine (D-GlcN) or D-galactosamine (D-GalN)) paired with a uronic acid component (D-glucuronic acid (D-GlcA) or L-iduronic acid (L-IdoA)). This structural formation underpins the nomenclature of glycosaminoglycans. The classification of GAGs into different families is based on the nature of these repeating units (Scheme 4), delineating distinct classes such as hyaluronan (HA), keratan sulfate (KS), chondroitin sulfate (CS), heparan sulfate (HS), heparin (HEP), and dermatan sulfate (DS).

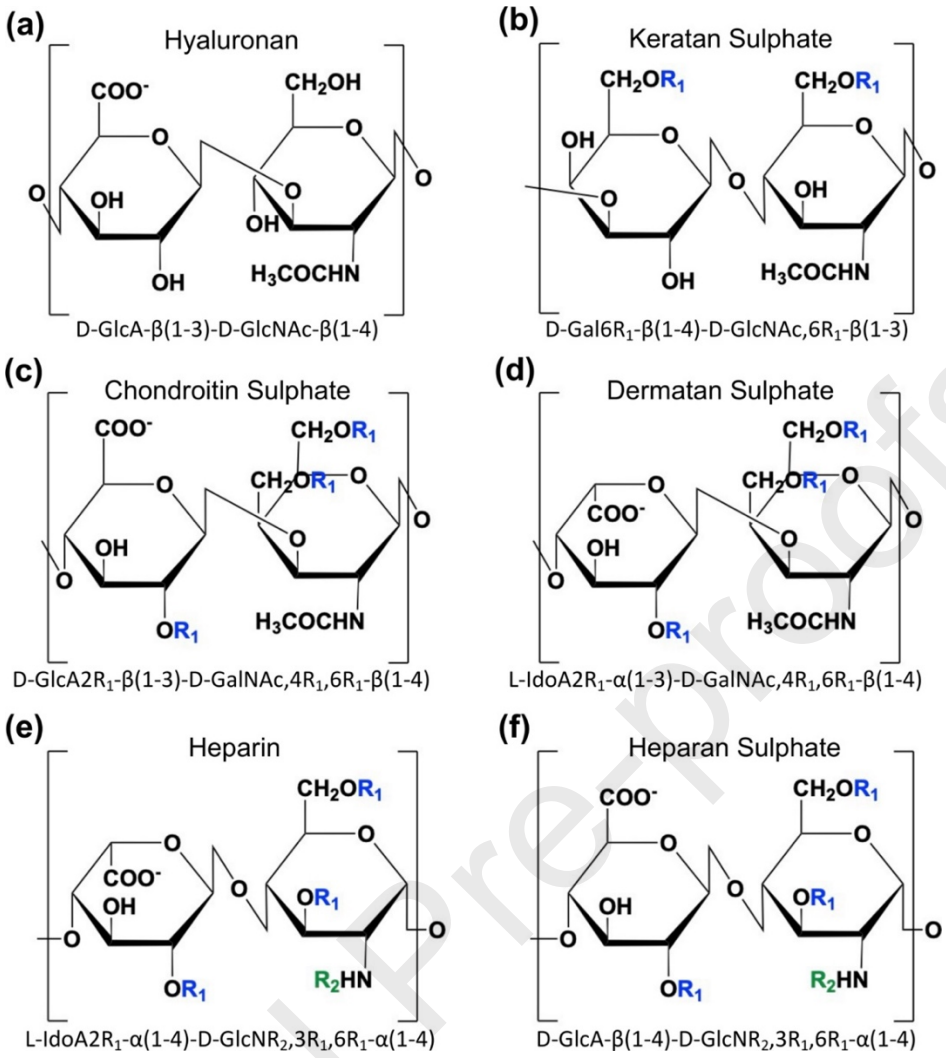

Scheme 4. Haworth representations of the chemical structures of the canonical disaccharide repeating units of hyaluronan –HA– (a); keratan sulfate –KS– (b); chondroitin sulfate –CS– (c); dermatan sulfate –DS– (d); heparin –Hep– (e); and heparan sulfate –HS– (f). R_1 = H/SO_3, R_2 = $COCH_3$/SO_3^-.

The intricate nature of GAGs arises from their multifaceted structural attributes. These include a significant degree of polymerization and size polydispersity, alongside sequence microheterogeneity, pronounced negative charge density, and the presence of potentially isomeric building blocks. Also, the inherent microheterogeneity of GAGs precludes their representation by a singular, definitive sequence. The biosynthetic pathways of GAGs have been deciphered to a large extent. [128] Their tremendous biosynthetic versatility leads to a multitude of possible substitution patterns, making GAGs potent information-containing biomolecules.

Over the past few decades, research has increasingly focused on molecular recognition processes involving glycosaminoglycans (GAGs), and their interactions with signalling proteins. [129-132] These interactions, owing to their biological significance and prevalence, have been the subject of extensive study. Here, we will pay special attention to heparin (HEP), [133] since it is the GAG most studied by NMR. The use of heparin

contaminated with chondroitin sulfate generates a rapid- and acute-onset anaphylactic reaction. NMR is therefore essential to properly characterize the different GAGs. [134, 135]

The use of NMR spectroscopy to study the structure and interactions of glycosaminoglycans (GAGs) and heparin has a rich history, spanning several decades. Indeed, there are numerous NMR studies that have addressed the structure, conformation, and interactions of all the members of the GAG family: [136] hyaluronan, [137- 139] keratan sulfate, [140] chondroitin sulfate, [141-143] and dermatan sulfate. [144] We consider GAGs, and especially heparan sulfate and heparin [145, 146], as a particularly significant category of glycans, given their wide biological importance and their intrinsic structural, conformational and dynamic features. In the 1970s and 1980s, pioneering work by researchers including Linhardt, Perlin, Lindahl, and Casu laid the foundations for the application of NMR to the analysis of GAGs and their interactions with proteins. [147-152].These early studies focused on using 1D ^{1}H NMR to elucidate the structural features of these complex polysaccharides. A key milestone was the characterization of the antithrombin-binding pentasaccharide sequence in heparin using NMR in the 1980s. [147-152] This demonstrated the potential of NMR to provide detailed structural information about biologically important GAG motifs.

As NMR technology advanced in the 1990s and 2000s, researchers were able to apply more sophisticated 2D and 3D NMR experiments to the study of GAGs and heparin. Thus, in the 1990s 2D NMR techniques like COSY, TOCSY, and NOESY/ROESY were used to characterise the structural variations of different heparin fractions .[153] It was not until a couple of decades later that 2D NMR was also applied to the analysis of GAG impurities, to study the contamination of heparin. [154]

The development of isotope-labelling strategies, such as the use of ^{13}C and ^{15}N-labeled GAGs, further expanded the capabilities of NMR for structural elucidation and the study of GAG-protein interactions. For instance, in the early 2000s, 2D TOCSY and ^{1}H,^{15}N-HSQC, and 3D ^{1}H,^{15}N-TOCSY-HSQC and ^{1}H,^{15}N-NOESY-HSQC NMR experiments allowed resolution of the structure of hyaluronan oligomers and assessment of their dynamics. [155] Quantitative 1D ^{1}H and ^{13}C and 2D ^{1}H-^{13}C HSQC NMR experiments were also applied to characterize and quantify sugar residues and substituent groups in heparins. [156, 157] Further, diffusion NMR experiments like DOSY were employed to analyse heparin solutions and identify low molecular weight impurities in them. [154, 158]

Overall, NMR has broadly been used to investigate the conformational behaviour of heparin and other glycosaminoglycans (GAGs), using approaches ranging from chemical shift analysis to full characterization through conformational studies, as well as their interactions with their biological receptors. [159-165] GAGs are intrinsically involved in many events of biological and biomedical interest, with heparin representing the paradigm given its worldwide application as an antithrombotic and anticoagulant factor.

3.1.1.1. Heparin: The L-IdoA ring.

Heparin is constituted by disaccharide repeating units comprising 1,4-linked hexopyranosyluronic acid and 2-amino-2-deoxyglucopyranose (glucosamine) residues. [149, 166] The uronic acid components predominantly include L-idopyranosyluronic acid (L-iduronic acid, L-IdoA) and to a lesser extent D-glucopyranosyluronic acid (D-glucuronic acid, D-GlcA). Notably, heparin is distinguished by its remarkably high negative charge density, attributed to the abundance of sulfate (OSO_3^-) and carboxylate (COO^-) groups. This structural feature is exemplified in the typical heparin disaccharide, containing an average of 2.7 sulfate groups. A frequently occurring structure within heparin is the trisulfated disaccharide L-IdoA2S-α(1-4)-D-GlcNS,6S. However, the molecule exhibits microheterogeneity due to variations in substitution patterns, such as the presence of acetyl or sulfate groups on the glucosamine residue and the potential for 3-*O* and 6-*O* position substitutions. Additionally, the uronic acid

residue can also possess a 2-*O*-sulfate group (Scheme 5). Heparin's molecular weight (MW) typically ranges from 5-40 kDa, with an average around 15 kDa, and, as mentioned above, it carries a substantial negative charge (roughly -75). The physicochemical properties of heparin are intrinsically related to the structure, sequence, conformation, flexibility, molecular weight, and charge density of the GAG. [167, 168] The inherent structural variability of heparin, characterized by high heterogeneity and polydispersity, presents significant challenges in its characterization. Further, it has been shown by NMR that heparin conformation is sensitive to temperature within the 280-305 K temperature range. However, the well-known hydrogen bond between the *N*-sulfamido group of the glucosamine residue and the 3-OH group of L-IdoA, as well as calcium binding via the iduronate residues, are not significantly affected by temperature. The unusual conformational flexibility of the iduronate ring most likely has a role in this behaviour. [168]

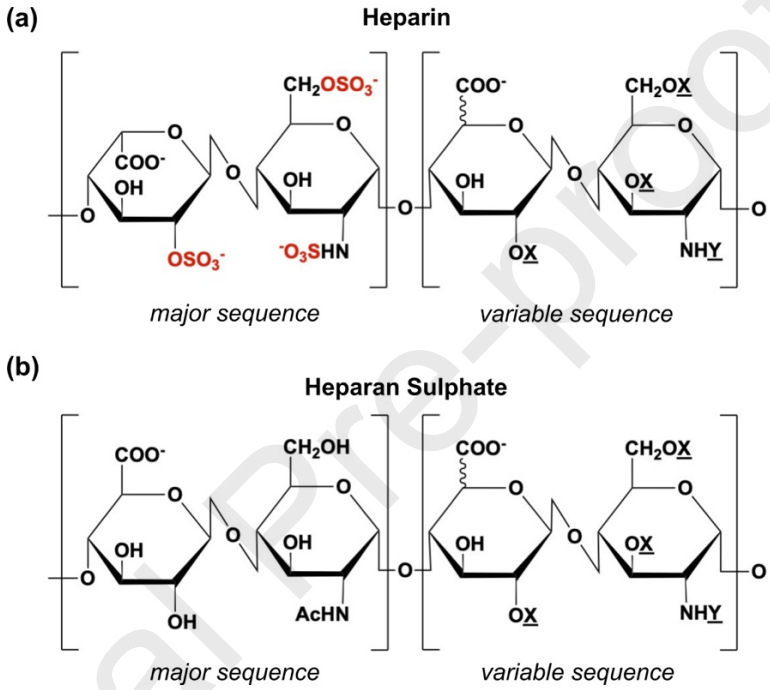

Scheme 5. Haworth representations of the major and minor disaccharide repeating units in heparin (a) and heparan sulfate (b). (X=H/SO_3^-, Y=Ac/SO_3^-/H).

In this context, NMR is essential for checking the compositions and conformations of such biomolecules. Zhang *et al.* described a relatively simple NMR-based approach to structural analysis of heparins. [169]They summarized the chemical shifts and $^3J_{H-H}$ couplings for all the anomeric protons of a synthetic library of 66 heparins, using chemical shift patterns to infer the presence or the absence of sulfate groups in certain positions of the flanking sugars and the presence of certain disaccharide fragments. [169] Heparan sulfate is similar to heparin, but is composed of a repeating linear copolymer of a uronic acid 1-4 linked to a glucosamine residue. [170] While D-glucuronic acid is more prevalent in heparan sulfate, substantial amounts of L-iduronic acid can be present. Heparan sulfate typically possesses about one sulfate group per disaccharide, although this can vary. [170, 171] These chains bind various proteins and are crucial in numerous physiological processes, including blood coagulation, cell adhesion, lipid metabolism, and growth factor regulation [172]. Although heparin and heparan sulfate share structural similarities, they can be distinguished by their differential sensitivity to GAG-degrading microbial enzymes, the heparin lyases. [173]

The conformation of heparin and its components has been extensively investigated since its discovery, employing NMR assisted by various other techniques. Owing to its nature and topology, *i.e.* a rigid helix with a complete turn every four residues, discontinuous interactions with the same side of a protein surface are expected, grouping each three contiguous sulfate groups on alternate sides (Fig. 10). Additionally, the number and distribution of sulfate groups play a key role in the specificity of its interactions. Another key structural aspect of the heparin or HS structure is that while it is fairly rigid from the backbone perspective (global conformation), at the same time it is rather flexible at the local level, *i.e.* when the conformational equilibrium of the iduronate ring is considered.

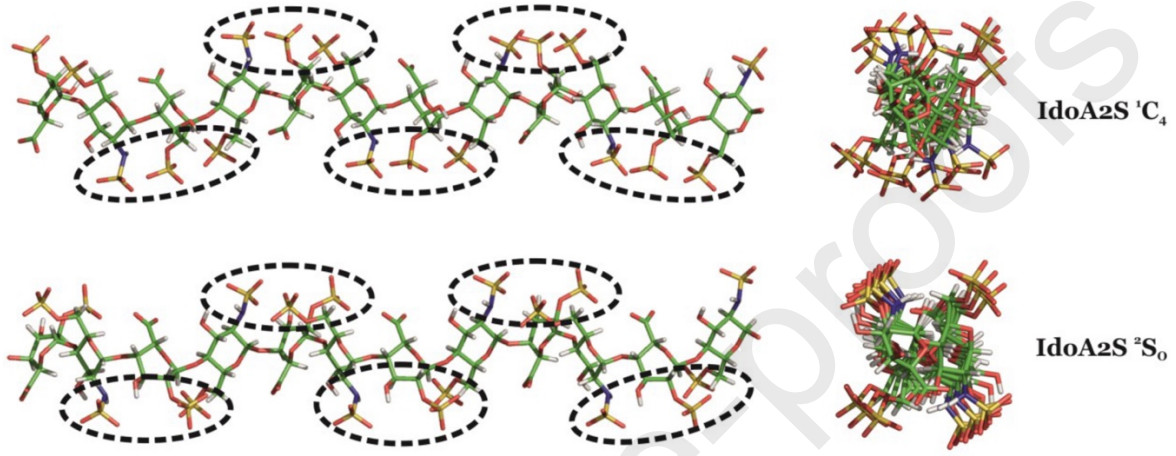

Fig 10. The major conformation of heparin determined by NMR and molecular modelling from a dodecasaccharide representative of the regular region of heparin. The iduronate residues are shown in $^1C_4$ (top) or the ^2S_O (bottom) ring conformations. Groups of three contiguous sulfate substituents on the same side of the molecule are highlighted with dashed circles.

For years, the conformation and dynamics of heparin have been analysed, paying attention to the behaviour around the glycosidic linkages and to the geometry of the individual monosaccharides that comprise the oligosaccharide chain, especially to the rather flexible iduronic acid moiety (L-IdoA). L-iduronic acid, biosynthesized through a single epimerization at the C_5 position of D-glucuronic acid, confers unique properties on iduronate-containing biomolecules. In the manner of most of L-hexopyranoses, it could be expected that a L-IdoA residue would adopt a $^1C_4$ chair conformation as its sole most stable conformer. However, in reality the iduronate ring may adopt several conformations of comparable energy, which explains the particularly good ability of iduronate-containing GAGs to control the activity of proteins such as chemokines, growth factors and blood coagulation enzymes.

It was deduced earlier that the IdoA ring could adopt a variety of conformations (the two chairs $^4C_1$ and $^1C_4$ as well as the $^2S_0$ skew boat), depending on its sulfation pattern and that at the vicinal sugar moieties. [151, 174] From a technical NMR perspective, since the changes in the ring conformation alter both the dihedral angles between vicinal hydrogen atoms and the distances between them, one can employ NMR spectroscopy to track such ring puckers by monitoring the spin-spin vicinal coupling constants ($^3J_{HH}$) and the proton-proton NOEs. Thus, over past decades, extensive solution NMR experiments as well as theoretical calculations have been performed to better understand the conformational flexibility of the iduronate ring. As a result, the picture describing the L-IdoA ring puckering, initially thought to be depicted by the equilibrium between the $^1C_4$ and $^4C_1$ chair conformers, was further extended when evidence appeared showing that the $^2S_0$ skew-boat pucker plays a critical role in the

control of blood coagulation. [151, 174-177] This $^{2}S_{O}$ conformer (or pucker) can be easily identified by NMR because it produces an intra-ring exclusive NOE cross-peak corresponding to the close contact between H_2 and H_5 protons, which are not at an NOE distance in either the $^{1}C_4$ or the $^{4}C_1$ chairs. [178] Moreover, the experimental determination of $^{3}J_{HH}$ couplings of an iduronic monosaccharide, or as the non-reducing terminal in oligosaccharides, indicate the presence of a mixture of both the $^{4}C_1$ and $^{1}C_4$ chairs with an additional contribution from the $^{2}S_{O}$ skew-boat. Specifically, an internal L-IdoA2S ring in heparin-like molecules shows a conformational equilibrium between the $^{1}C_4$ chair and the $^{2}S_{O}$ skew-boat puckers (Fig. 11), with a negligible or non-existent population of the $^{4}C_1$ chair. [178-180] Interestingly, this conformational equilibrium also occurs in fluorinated carba-analogues of the L-idose ring. [181] In the natural heparin polymer, it has previously been shown that the $^{1}C_4$ and $^{2}S_{O}$ conformers may interconvert with little change to the geometry of the glycosidic linkages to adjacent residues in the polysaccharide chain (C_4-O_4 and C_1-O_1 bonds present similar orientations in both forms); [182] this anticipated the idea, later demonstrated, that the global conformation of the oligo- or polysaccharide is independent of the iduronate conformational plasticity. [183] When discussing iduronate flexibility, the existence of fast pseudorotational interconversion along the boats and skew-boats conformational space must also be considered. [182-186]

The skew-boat $^{2}S_{O}$ occupancy in the L-IdoA and L-IdoA2S conformational equilibria has biological significance. Thus, inhibition of the coagulation cascade is thought to be initiated by antithrombin binding heparin with the iduronate residue in the $^{2}S_{O}$ conformation. Indeed, synthetic heparins presenting $^{2}S_{O}$-biased iduronate analogues are highly potent. [187] A complete exploration of the low-energy conformations for the iduronate ring (L-IdoA and L-IdoA2S) by MD simulations showed that iduronate residues undergo a microsecond puckering equilibrium ($^{1}C_4$-$^{4}C_1$ conformations exchange of the iduronate ring on the microsecond time scale), the composition of which depends on their substitution pattern (L-IdoA 2-*O*-sulfation stabilizes the $^{1}C_4$ conformer) and epimerization (C_5 epimerization leads to the $^{4}C_1$ chair). Furthermore, these MD calculations explained how enzymatic chemical modifications (epimerization and sulphation) can fine-tune the free energy landscape of the iduronate ring and may mediate protein selectivity.

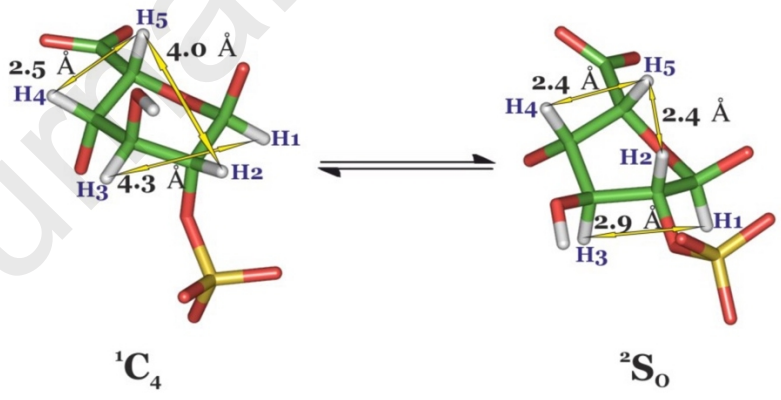

Figure 11. 3D model of the typical $^{1}C_4$-$^{2}S_{O}$ conformational equilibrium displayed by the iduronate ring in heparin chains. Note the variation of the H_2-H_5 and H_1-H_3 distances, outside the NOE range in the $^{1}C_4$ chair conformer and within the NOE range in the $^{2}S_{O}$ skew-boat pucker (exclusive NOEs).

For years, it has been widely accepted that the driving force that determines the conformational equilibrium of the iduronate residue in heparin oligosaccharides is the

electrostatic repulsion between anionic charges on neighbouring residues. Particularly for the regular region of heparin (iduronate in the L-IdoA2S form), due to the presence of three contiguous sulfate groups, NSO_3-(GlcN)-$2OSO_3$-(IdoA)-$6OSO_3$-(GlcN), on the same side of the helix, it is tempting to speculate that the electrostatic "stress" existing on that part of the molecule might be the origin of the singular conformational plasticity of the iduronate ring. While the flexibility of the backbones of polysaccharides is usually associated only with rotation of the monosaccharide residues around the glycosidic bonds, the extra flexibility induced by the presence of an equilibrium between two or more conformations of monosaccharide residues is a peculiar characteristic of iduronate-containing glycosaminoglycans, which could contribute to their binding properties and biological "versatility". These features contrast with the poor binding and biological properties of other glycosaminoglycans having approximately the same degree of sulfation and molecular weight, but the more rigid glucuronic acid as the major uronic acid.

Different factors that can be studied by NMR act as modulators of the conformational equilibrium of the iduronate ring. [178-186] Thus, the type of counterion present may shift the equilibrium towards one of the puckers, by interactions with specific sites of the polysaccharide. This is the case for Ca^{2+} ions, which drive the equilibrium towards the $^1C_4$ chair in heparin-like oligosaccharides. Furthermore, this equilibrium is highly sensitive to intramolecular factors such as 2-*O*-sulfation of the iduronate residue and the sulfation pattern of the adjacent GlcN rings. Thus, for internal L-IdoA or L-IdoA2S residues in heparin and heparan sulfate sequences, though only the $^1C_4$ and ^2S_O puckers participate in the conformational equilibrium, this is displaced towards the ^2S_O conformation when L-IdoA2S is 4-*O*-substituted with a 3-*O*-sulfated GlcNS residue (54-69% according to $^3J_{HH}$ at room temperature). On the other hand, for IdoA2S the conformational equilibrium is shifted towards the $^1C_4$ chair pucker, as long as it is at the non-reducing terminus. In the case of a terminal non-sulfated L-IdoA residue, the $^4C_1$ form also contributes significantly to the equilibrium. In addition, the presence of 6-*O*-sulphated glucosamine at the reducing end and next to a L-IdoA2S residue increases the population of the ^2S_O conformer of the latter, and makes its conformational equilibrium insensitive to temperature. In contrast, 6-OH glucosamine at the reducing end leads to an increased population of L-IdoA2S ^2S_O conformer at higher temperatures.

The global conformation of heparin is determined by the geometry (Φ and Ψ) of its glycosidic linkages; rigid and flexible behaviours have been observed for the GlcN-IdoA and IdoA-GlcN linkages, respectively. Obviously, the conformational space sampled by Φ is restricted by the exo-anomeric effect, and so it commonly presents a narrow distribution of values around the *syn* geometry. On the other hand, Ψ is not limited by the anomeric effect, although it displays a major geometry (*syn*) within GlcN-IdoA linkages and provides a significant flexibility to IdoA-GlcN linkages. This additional flexibility of the Ψ torsion is characterized by the appearance of *anti*-Ψ conformations (±180º) together with the more common *syn*-Ψ disposition. From the NMR viewpoint, while the *syn*-Ψ geometry can be identified by the presence of the $H_{1'}$-H_4 and $H_{1'}$-H_6 NOE cross-peaks, the *anti*-Ψ conformation produces $H_{1'}$-H_3, $H_{1'}$-H_5 and $H_{5'}$-H_6 exclusive NOEs. This allows experimental identification of the existence of conformational flexibility around the IdoA-GlcN linkages in solution. The NOE information can be complemented by $^3J_{CH}$ analysis to define the extent of flexibility.

Regarding molecular recognition by protein receptors, heparin has been shown to bind to several proteins, such as antithrombin III (AT-III), [187-189] fibroblast growth factors (FGF1 and FGF2), [190-192] the C-type lectin langerin, [193] chemokines, [194, 195] and apical surface proteins. [196] Thus, it was reported years ago that the effective interaction with the antithrombin III protein (AT-III) involved the skew boat ^2S_O geometry of the IdoA2S ring of heparin instead of the more common $^1C_4$ chain conformation of the unbound state. This structure-binding relationship was further taken as indicative of a structure-function effect

(antithrombotic activity), although this point is arguable. In any case, the existence of conformational flexibility in heparin molecules is thoroughly documented [197-200] and, therefore, their interactions with receptors brings entropic consequences. Conformational selection processes have been described in different systems, such as heparin binding to AT-III and FGF2, which selects the $^{2}S_{O}$ conformation of the 2-*O*-sulfated iduronate residue. [201] Further, experimental evidence has indicated the existence of flexibility of heparin in the bound state. [202] Unravelling the conformational behaviour and interactions of heparin molecules remains a major topic of research.

3.2. Glycomimetics

The development of glycan analogues is a therapeutic strategy to investigate in varied pathological contexts. However, it is well known that natural glycans are rarely employed as pharmacological drivers. They display rather low metabolic stability and high hydrophilicity, and unfortunately these features correlate with low drug bioavailability. Sugar mimetics (glycomimetics) have therefore been proposed. We will not describe here dramatic modifications of the sugar chemical structure, just those that concern the replacement of the exocyclic oxygen of the natural sugar to provide *C*-glycosyl, *N*-glycosyl, and *S*-glycosyl analogues, depending on the atom that replaces the oxygen (Scheme 6). The topology of the glycosidic linkage remains the same, just changing the interglycosidic linkage. However, detailed NMR spectroscopic analysis of these molecules has demonstrated that these analogues display diverse conformational behaviour. [203]

3.2.1. C-glycosyl compounds

Obviously, the lack of the glycosidic oxygen means that the exo-anomeric effect no longer acts, and therefore the conformations around Φ/Ψ are now solely ruled by van der Waals and dipolar interactions. From the NMR perspective, for C-glycosyl compounds the presence of the interglycosidic carbon atom, with two additional substituents (usually at least one of which is a hydrogen atom), provides additional *J*-coupling and NOE information that can be used to assess conformational behaviour. Indeed, for C-glycosidic linkages defined as $C_{1'}$-$C_{interglycosidic}$-C_X, there will be vicinal coupling constants between $H_{1'}$ and the protons at C_{inter}, as well as between those protons and H_X, provided that C_{inter} is not a quaternary center. [204] For a CH_2-interglycosidic arrangement, the two protons at the glycosidic carbon are diastereotopic and provide a very useful set of coupling constants and NOE information. [205, 206]

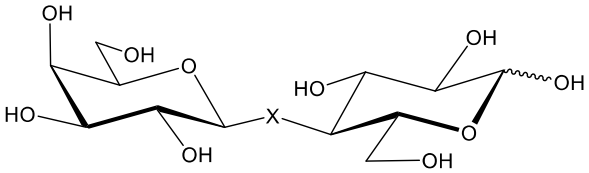

X=CH_2, NH, S, Se

Scheme 6. Glycomimetics: *C*- (X=CH_2), *N*- (X=NH), *S*- (X=S), and *Se*- (X=Se) glycosyl compounds. Their conformational behavior has been exhaustively studied by NMR methods. For X=CH_2, the two diastereotopic protons at the methylene group provide a very useful set of coupling constants and NOEs.

Exhaustive NMR investigations of different families of *C*-glycosyl compounds, comparable to those carried out for the corresponding natural *O*-glycosyl compounds, have allowed estimation of the populations (negligible for the natural molecules) of non-exo anomeric conformers for a diverse set of glycomimetics, and, therefore, experimental estimation of the magnitude of the steroelectronic component (at least 2 kcal/mol) of the *exo*-anomeric stabilization. In a subsequent study, NMR analysis of the conformations of pairs of *C*-glycosyl compounds with either axial or equatorial orientation of O2' allowed quantification of the steric destabilization (*ca.* 1.5 kcal/mol) provided by the interaction of the aglycone in a non-*exo*-anomeric orientation and the equatorial O2'.

Interestingly, *C*-glycosyl compounds have also been used as probes to monitor glycan-receptor molecular recognition events, [203, 207] providing important clues for understanding the specific interactions that rule these essential processes. In particular, transferred-NOESY NMR experiments (see below) have been widely employed to deduce the bound conformations of these mimetics, to compare them to those of the natural analogues and to evaluate the relative roles of conformational entropy and binding enthalpy in some of these events. Since *C*-glycosyl compounds are more flexible than their natural counterparts, differences in the bound geometries of *O*- and *C*-glycosyl molecules have been reported for some cases. Nevertheless, in most cases, the existence of identical bound conformations for both species has been demonstrated. Additional studies have been carried out for *S*- and *N*-glycosyl compounds, now solely based on NOE analysis, given the lack of non-exchangeable protons at the interglycosidic position.

3.2.2. Selenium-, thio-, and imino-glycosides

The conformations of other glycomimetics have also been studied. In particular, the conformations of thio-analogues of oligosaccharides, generated by substituting the interglycosidic oxygen by sulfur, have been characterized in considerable depth. Obviously, the C-S-C bond angle and the C-S distances are rather different from the corresponding C-O-C angle and C-O distances in the naturally occurring compounds, so it is expected that the conformational behavior will be different, considering also that the strength of the exo-anomeric effect will differ for the O-C-O and O-C-S arrangements at the glycosidic centre. The use of NMR measurements, especially inter-residue NOEs and vicinal heteronuclear $^{3}J_{CH}$ couplings, demonstrated that there are conformational differences between the two families, [208] both in the free state and when bound to protein receptors. The thio-glycoside analogues are more flexible [209] and sample a larger conformational space, as exemplified by galabiose and its S-linked-4 thiodisaccharide analogue, [210] and in maltose heteroanalogues. [211] Nevertheless, they can still be used as probes for glycosidases [212], since they are slowly hydrolyzed by these enzymes. Moreover, dithioglycoside analogues have also been studied. In this case, NMR experiments have indicated that the conformational flexibility around the C-S and S-S bonds is even larger for these analogues. [213]

The seleno analogues (C-Se-C at the pseudoglycosidic linkage) are also interesting from an NMR perspective, since ^{77}Se is an NMR-active nucleus that can be used to transfer information through the corresponding ^{1}H-^{77}Se and ^{13}C-^{77}Se coupling constants. [214] In fact, Se-glycosides have been proposed as possible spy molecules for NMR screening, using selective ^{1}H, ^{77}Se heteronuclear Hartmann-Hahn transfer [215] and ^{77}Se-edited CPMG-HSQMBC NMR experiments [216] for efficient use in competition NMR experiments.

The conformations of different imino-glycosyl analogues [217, 218], which have an NH moiety at the pseudoglycosidic linkage, have been also investigated. As with the thio-glycoside analogues described above, the lack of the exo-anomeric effect makes these molecules more flexible, especially around Φ, as demonstrated by NOE-based methodologies. They have been employed as oligosaccharide surrogates as molecular probes and in medical chemistry

campaigns [219]. Other glycomimetics will be described below in the molecular recognition section 6.1.

3.2.3. The power of ^{19}F-NMR: Fluorine-containing sugars

Fluorine-containing sugars (Scheme 7) are a special case within glycomimetics, since they have been widely employed in the glycosciences for years. In particular, the systematic replacement of every hydroxyl group of a given sugar by a fluorine atom has been used as a molecular probe for deducing the strength and relevance of hydrogen bonds in glycan-lectin complexes. A review of fluorinated carbohydrates has been recently presented, also describing the typical ^{19}F-NMR-based experimental approaches, [220] therefore here we will just highlight the most relevant details of fluorinated glycans and the applications of ^{19}F NMR to their study. It is very clear that ^{19}F detection-based NMR experiments constitute a great method to monitor fluorosugar conformation and fluoroglycan-receptor interactions, either directly or through competition approaches. In early studies, N-CF_3-acetyl GlcNAc analogues (Scheme 7a) were employed as probes for assessing their binding properties to different lectins, through the detection of ^{19}F chemical shift perturbations and/or transverse relaxation-mediated line broadening effects when the complexes were formed. [221-223]

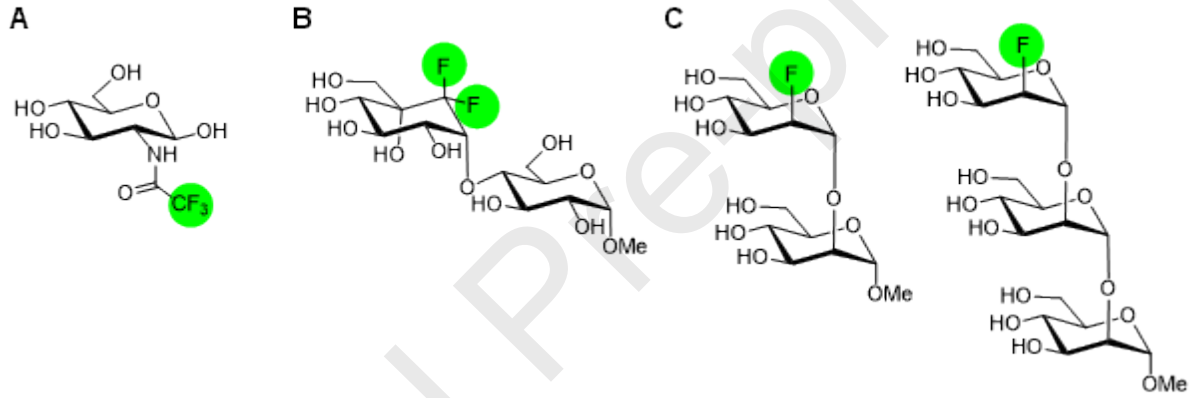

Scheme 7. A and B: Some fluorinated sugar analogues that have been synthesised and exhaustively studied by NMR. [221-224] C: Fluorinated Man-containing glycans studied by Gronenborn and coworkers [235].

Closely related with the work on glycomimetics described above, Sollogoub and coworkers [224] employed CF_2 substitution of the endocyclic O_5 atom of a disaccharide (Scheme 7b) to further assess the importance of the stereoelectronic component (orbital mediated interactions) of the exo-anomeric effect. On this basis, the conformational properties of maltose (Glcα(1→4)Glc), a regular disaccharide, its carba analogue (with a methylene group replacing the endocyclic oxygen involved in the exo-anomeric effect), and its CF_2-carba mimetic (with a CF_2 group at that position) were investigated. The conformational preferences found by NMR were fairly clear: the torsion angle value around Φ of maltose is governed by the exo-anomeric effect, and a single Φ conformer dominates the conformational equilibrium. This preference is lost for the CH_2 carba analogue, since a significant population of *non-exo*-anomeric conformers was detected through analysis of the exclusive NOEs. However, ^{1}H-^{1}H and ^{1}H-^{19}F NOEs demonstrated that the exo-anomeric predominance was restored for the CF_2 carba analogue. Theoretical calculations supported the initial hypothesis that the presence of the CF_2 moiety would induce polarization of the C_1-CF_2 bond, enough to favor the hyperconjugation of the lone pair at the exocyclic oxygen with the $\sigma^*_{C1\text{-}CF2}$ bond, thus restoring the exo-anomeric effect and the preferential exo conformation.

3.2.3.1. ^{19}F NMR and fluorine-containing sugars in the bound state

The key techniques for unravelling the interactions of glycans with their receptors by ligand-based NMR (STD-NMR, Tr-NOESY and their variants) will be described in the section below, highlighting the importance of ^{19}F NMR for monitoring glycan-receptor binding. It is evident that besides facilitating the interpretation of NMR spectra, the presence of ^{19}F nuclei may reveal information on molecular interactions. Different investigations have accentuated the benefits of fluorosugar ligands for assessing recognition events. Many protocols have been employed to study the interactions of fluorine-containing glycans, but here we will highlight ^{19}F relaxation-based and ^{19}F STD NMR methodologies (see below). Relaxation-mediated broadening effects using ^{19}F nuclei have allowed fine details of lectin-glycan interactions to be assessed with exquisite selectivity. [225] For instance, the introduction of a ^{19}F tag in the NAc moieties of GlcNAcβ(1→4)GlcNAc (N,N'-diacetyl chitobiose) allowed identification of the non-reducing moiety as the key epitope for establishing interactions with wheat germ agglutinin lectin. Furthermore, the use of diverse different mono-, di-, or tri-fluorination patterns (CH_2F, -CHF_2, -CF_3) showed that the analogue containing the difluorinated tag has a higher affinity towards this lectin than the other analogues, including the natural disaccharide. [225] It was hypothesised that this affinity increase is due to the large polarization of the C-H bond at the -CHF_2 tag, which allows it to establish a stabilizing CH-π stacking interaction with a tyrosine residue located at the lectin binding site.

This -CHF_2 substitution pattern at acetamide moieties has been recently extended to monitor Siglec- (sialic acid-binding immunoglobulin-type lectin-) sialic acid interactions through competitive experiments based on the FAXS (Fluorine chemical shift Anisotropy and eXchange for Screening) methodology developed by Dalvit and coworkers. [226] This approach relies on the intrinsic chemical shift anisotropy of ^{19}F nuclei. A ^{19}F-labeled entity is employed that is designed as a medium-weak binder for the target receptor, and is dubbed the spy molecule. [227, 228] For monitoring Siglec binding, a spy molecule has been proposed that consists of a sialic acid derivative decorated with the -NH(CO)CHF_2 moiety at C_5 (instead of NHAc). [229] In the presence of a certain amount of the Siglec receptor, the initial ^{19}F spectrum of the spy molecule shows a relatively broad ^{19}F signal that encodes the chemical exchange between the free and bound ligand, through its effect on the transverse relaxation R_2. The initial intensity of this signal can be adjusted by altering the ligand/receptor molar ratio, the total echo time in the CPMG-like pulse sequence, or the inter pulse delay in the CPMG train. Clearly, any molecule that also binds competitively to Siglecs, and is added to the NMR tube containing the Siglec and the spy molecule, should trigger the displacement of the spy molecule, with a concomitant sharpening of its ^{19}F NMR signal. Moreover, provided that the binding affinity of the spy molecule to the target receptor is known, this methodology can be used to estimate quantitatively the association constants of the competitors, even if they are high affinity ligands.

The FAXS ^{19}F NMR approach has also been used for screening and quantifying the binding affinity of a library of trifluoroacetamide analogues of ManNAc versus langerin, a C-type lectin receptor. [230] The experimental data was combined with the results of a computational screening protocol to predict a variety of initial hits, which were synthesised and tested. Resulting from this, a glycomimetic with a significant higher affinity than the natural ManNAc was identified. It is evident that this methodology affords a fast estimation of interaction features, with minimum use of material.

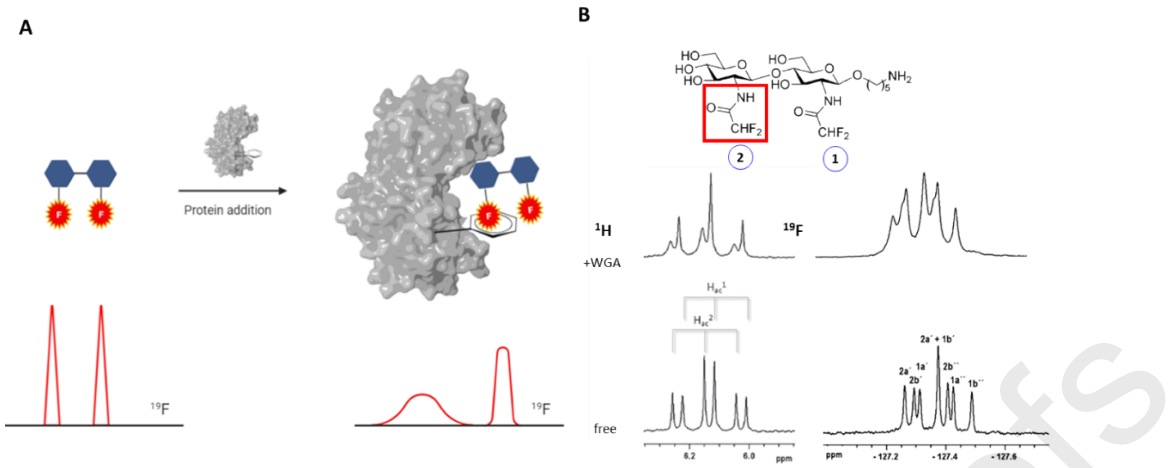

Figure 12. A. Schematic representation of the line broadening of the ^{19}F signal upon binding. Differential line broadening of the fluorine peak can be observed caused by the different interactions established upon binding. B. Distinct line broadening observed during the binding of ^{19}F N,N'-diacetyl chitobiose to WGA. Adapted from reference [225].

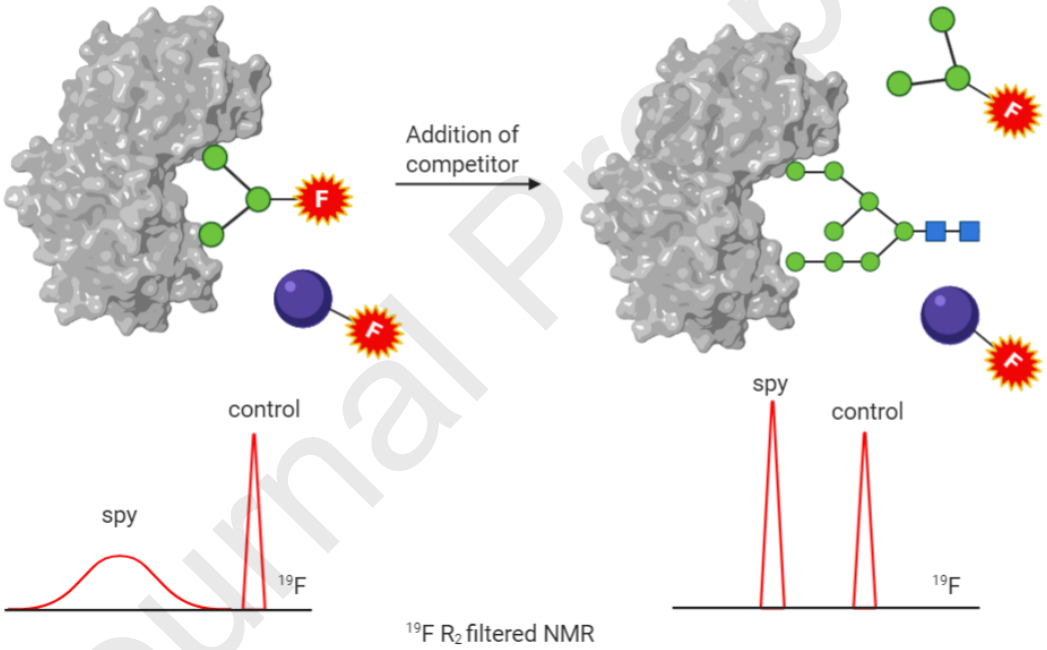

Figure 13. Schematic diagram of the FAXS experiment. (Left) Initially, signals of the spy molecule appear very broad while the signals of the control (non-binder) are very sharp. (Right) After the addition of a competitive ligand, the spy molecule is displaced, leading to a recovery of the spy signal peak.

Transverse relaxation rates are key parameters for detecting binding. In this context, ^{19}F NMR R_2-filtered experiments provide a fantastic tool for scrutinizing glycan-lectin-protein interactions. The methodology is fairly simple: R_2 values for the ^{19}F-containing glycans are estimated for the free ligand (R_2, free) and in the presence of the lectin (R_2, bound). The decay of the ^{19}F NMR intensities allows binding to be assessed. [231] Rather weak interactions can also be unravelled. Interestingly, the binding promiscuity of lectins of diverse origin could be disentangled in a one-shot and fast NMR experiment, since even for a large molecular library,

the typical problems of ^{1}H signal overlap that occur with sugar mixtures are absent in the case of ^{19}F NMR spectra. [232] In addition, analysis of the data obtained for a library of monosaccharides in which each hydroxyl group is replaced by a fluorine atom allowed the sugar selectivity of the particular lectin and the key hydroxyl groups involved in the interaction to be simultaneously defined. Thus, screening and chemical mapping were both achieved with a single NMR experiment. [232]

The same concept has been also employed to screen a ^{19}F-labelled library of Lewis type 2 glycans against different mammalian and bacterial lectins, [233] and to assess the binding of different glycomimetics to the bacterial lectin BambL. [234]

Other ^{19}F-NMR experiments have been employed to monitor glycan recognition. A seminal study described the interaction of ^{19}F-containing analogues of Manα(1→2)Man and Manα(1→2)Manα(1→2)-Man with Cyanovirin-N, an anti-HIV lectin [235]. The ^{19}F NMR signals of the 2F-Man unit at the non-reducing end (Scheme 5c) were used to deduce not only the binding pose of the glycan but also to measure the kinetics and thermodynamics of the interaction. 2D ^{19}F-^{19}F exchange experiments were also used to detect an alternative binding mode for the trisaccharide, which had not been found by typical ^{1}H-based NMR methods [46]. All of the ^{19}F-NMR-based conclusions were corroborated by ^{1}H-^{15}N HSQC chemical shift perturbation analysis on the lectin and ITC measurements on the system.

4. More experimental NMR tools

4.1. DOSY

Given the complexity and intrinsic heterogeneity of glycans, especially those isolated from natural sources, determining the degree of purity and size may become a true challenge. In many cases, Diffusion Ordered NMR SpectroscopY (DOSY-NMR) [236] may be used to deduce the purity of the glycan preparation under scrutiny, given its ability to combine *in-situ* translational diffusion resolution and spectroscopy, without the requirement of previous treatment of the formulation. The use of an appropriate pulse sequence with magnetic field gradient pulses (defined by gradient length, power, and shape) at specific times allows detection of the presence of individual species, even in a complex mixture, according to their size, which is inversely related to its translational diffusion coefficient. The observed NMR signal intensities are used to determine the diffusion coefficient, which encodes the molecular size of the molecule. On this basis, DOSY-NMR methods have been extensively employed to analyze glycan mixtures, and to assess molecular interactions, given the tremendous change in the translational diffusion coefficient that takes place when a free saccharide is bound by a given protein receptor. DOSY can also be employed to monitor possible changes in the oligomeric state of a system when interaction takes places, depending on the monitored NMR-active nuclei, either from the ligand or from the receptor. Interesting applications of DOSY can be found for assessing the exchange rate of the hydroxyl groups of glycans with water and hence detecting those that are involved in intramolecular hydrogen bonds. [237] It has been used for assessing the degree of multivalency of glycodendrimers [238] and as quality control for the purity of polysaccharides, [239-242], especially for glycosaminoglycans (see section 3.1.1), given their high interest to the pharma, cosmetic, and food industries. [243-248] The degree of contamination of heparin saccharides by oversulfated chondroitin sulfate has been a matter of special interest. [249]

DOSY NMR has also been employed as alternative or complement to size exclusion chromatography for the analysis of oligosaccharides, with specific applications to chitooligosaccharides [250] and their complexes with chitin-binding proteins. [251] It has been exhaustively used for the detection of glycan complexes, [252] including those with boronic acids [253] and metals [254], and to detect carbohydrate-carbohydrate interactions between

specific charged oligosaccharides and glycan-containing nanoparticles. [255] Interestingly, it has also been used as a direct tool to demonstrate the natural tendency of certain monosaccharides to interact with aromatic moieties, [256] present just as isolated species, without the need to adopt the 3D structure that exists in the lectin binding sites. The experiment can also be applied to discriminate between the anomeric forms of simple sugars and diverse phenyl D-glucosides. [257] The concatenation of the DOSY scheme with the transfer of information to other heteronuclei, for instance by using ^{19}F or ^{13}C modules, expands its range of application to other dimensions, thus allowing complex systems and mixtures to be studied. [258, 259]

4.2. Paramagnetic NMR

Paramagnetic NMR has found application across a diverse range of biological systems. This methodology was initially developed for metalloproteins, taking advantage of the metal binding site to replace a naturally bound metal by a paramagnetic ion. [260] Further developments introduced the use of lanthanide binding tags (LBT) or proteins fused with lanthanide binding peptides to extend the methodology to systems lacking natural metal binding sites. [261-263] The use of paramagnetic NMR is especially convenient for gaining insights into flexible molecules, where the maximum occurrence of each possible conformation can be inferred. [264] Therefore, various paramagnetic NMR approaches have been extensively applied to unravel the conformation and interactions of different biomolecules, including glycans. [265-267] In such cases, different chelating units have been designed, [268] mainly based on ethylenediamine [269] and phenylene diamine tetraacetic acid [270], which are attached to the glycan by chemical synthesis. Paramagnetic NMR has proven to be especially useful in the glycan field, since these biomolecules are characterized by severe signal overlap and sparse inter-glycosidic NOEs that hamper the 3D structural elucidation of the molecule. Using paramagnetic NMR approaches, key parameters with conformational information are generated, including pseudo-contact shifts (PCSs), [266, 267] residual dipolar couplings (RDCs) [271, 272] and paramagnetic relaxation enhancements (PREs), [273] offering one-of-a-kind insights into the structure, conformation, and dynamics of glycans.

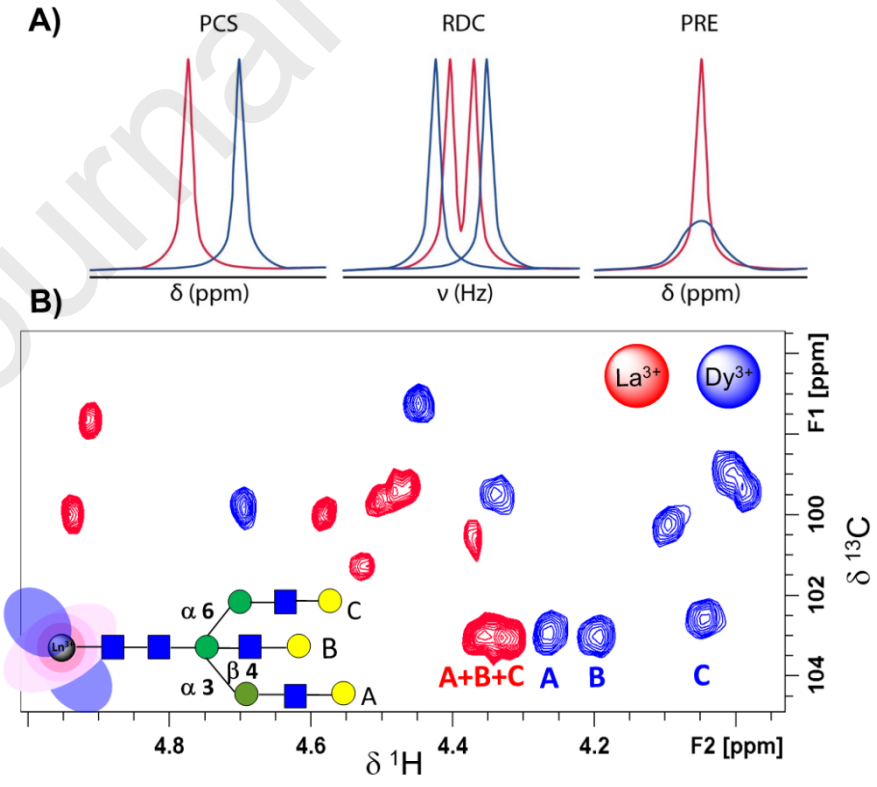

Figure 14. A) Schematic representation of the effects induced by paramagnetic metals, pseudo contact shifts, residual dipolar couplings and paramagnetic relaxation enhancements. B) Superimposition of the ^{1}H-^{13}C HSQC NMR spectrum of a biantennary bisected N-glycan acquired in diamagnetic conditions (La^{3+}, red colour) and paramagnetic conditions (Dy^{3+}, blue colour). The signals of the H_1 Gal protons that are overlapped in the presence of lanthanum split into three different signals; glycan units located at the two arms cannot be distinguished and as a result only one set of signals was detected for each monosaccharide (sialic acid, Gal and GlcNAc). In contrast, in paramagnetic conditions (Dy^{3+}) two sets of signals were detected and all the glycan signals were individually assigned. Adapted from reference [275].

4.2.1. Pseudo-contact shifts (PCSs)

The most widely used parameter in glycan structural studies is the pseudo contact shift. [263] PCSs arise from dipolar interactions between the unpaired electron of the paramagnetic ion and the nuclei in its vicinity, leading to changes in their chemical shifts in the NMR spectrum (Figure 14). The key feature of this effect is that it diminishes more slowly with distance (r^{-3} dependence) than the NOE (r^{-6} dependence), and therefore provides relatively long-range structural information. The PCS also depends on the shape of the paramagnetic susceptibility tensor ($\Delta\chi$), as can be seen from the following equation:

$$\Delta\delta^{PCS} = \frac{1}{12\pi r^3}\left[\Delta\chi_{ax}\,(3\cos^2\theta\ -1) + \ \frac{3}{2}\,\Delta\chi_{rh}\ \sin^2\theta\ \cos 2\varphi\ \right] \text{[1]}$$

where r is the distance from the nuclear spin to the metal ion; $\Delta\delta^{PCS}$ indicates the difference between the chemical shifts in the diamagnetic and paramagnetic samples; and θ and φ are the polar coordinates that describe the position of the nuclear spin with respect to the axes of the $\Delta\chi$ tensor ($\Delta\chi_{ax}$, $\Delta\chi_{rh}$).

The paramagnetic susceptibility tensor depends on the paramagnetic metal employed (Eu^{3+}, Ce^{3+}, Er^{3+}, Yb^{3+}, Tb^{3+}, Dy^{3+} or Tm^{3+}), so that different sets of data can be acquired by using different paramagnetic ions, thus obtaining complementary structural information. [274]

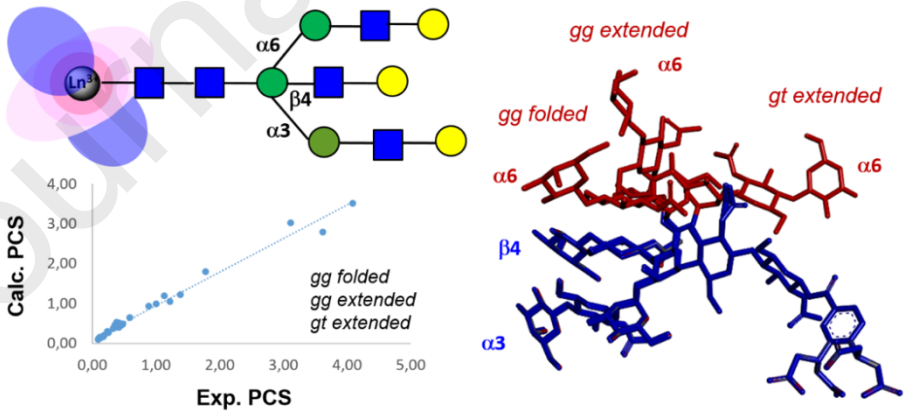

Figure 15. Conformational analysis of a biantennary bisected N-glycan by using PCSs. An ensemble of conformations were obtained and the theoretical PCSs were calculated for each geometry by using a specific software, Mnova StereoFitter. In this bisected N-glycan, a conformational equilibrium of three conformations with different orientations of the alpha 1-6 branch were required for obtaining a good fit between the experimental and calculated PCS data: extended *gauche-gauche* (*gg*), folded *gauche-gauche* (*gg*) and extended *gauche-trans* (gt). Adapted from reference [275].

In this context, PCSs have been successfully used to perform conformational analysis of complex-type (biantennary, [270] triantennary, [275] tetraantennary [276]) and high-mannose glycans. [265, 269, 277-281] Figure 15 shows the chemical shift changes observed in the glycan signals of a bisected complex type N-glycan upon dysprosium complexation. Interestingly, the increase in signal dispersion allows the individual assignment of the protons located in the different arms. [275] The combination of NMR data with molecular modelling allows characterization of the structural mobility of these flexible systems. In this context, it is important to highlight that pseudo-contact shifts are very sensitive to conformational changes, and therefore are especially useful in glycan structural studies. The analysis combined NMR and molecular modelling, and the protocol involved obtaining an ensemble of conformations by molecular dynamic simulations, calculation of theoretical PCSs for each geometry, and comparison with the experimental data by using specialized software such as the Mnova Stereo Fitter module. [282] Both individual conformers and combinations of conformers with different populations are evaluated to obtain the best overall correlation between experimental and calculated data; an example of a fitting is shown in Figure 15. In this case, three different families of conformers are required to fit the experimental data. [275] Following this protocol, the conformational space explored by different type of glycans has been characterized in detail. [268-273, 275-281]

In addition, PCSs have been applied to characterize molecular recognition processes. Glycan-lectin interactions are usually weak and, therefore, the chemical shift perturbations detected in lectin ^{1}H-^{15}N HSQC titrations are limited. In this context, the use of glycans conjugated with paramagnetic probes is a very useful tool. It allows a better characterization of the interaction surface, since the paramagnetic effect increases the changes in the protein signals upon glycan addition. This method has been applied to characterize the recognition of lactose by galectin-3, [283] complementing alternative previous approaches that applied PRE effects, [284] as well as to the interactions between heparan sulfate and Robo1-Ig1-2. [285] These methodologies nicely complement the typical receptor-based NMR approaches that will be described below and the PRE analysis that will be described in the next section.

The combination of paramagnetic NMR with ligand-based NMR methodologies (STD-NMR, see below) can also provide detailed information on binding features for complex glycans, which are rather difficult, or even impossible, to unravel using standard approaches. In particular, the use of paramagnetic lanthanide ions removes the overlap of the NMR signals of the repeating units located at different arms, which normally precludes the assignment of peaks to individual residues within a given arm (Figure 16). Following this protocol, the interaction features of each residue of an N-glycan tetraantennary oligosaccharide with *Datura stramonium* seed Lectin (DSL) and *Ricinus communis* agglutinin (RCA 120) were unequivocally characterized by monitoring the changes in linewidth of the different ^{1}H-^{13}C cross peaks for every residue. [286] This proof-of-concept study was successfully extended to investigate the interaction of rather complex and extended biantennary sialylated N-glycans involved in influenza virus attachment to epithelial cells. This methodology has provided a new

experimental insight for the understanding of the molecular basis of the interaction of these N-glycans with viral proteins. Recent H3N2 virus variants have evolved specificity to recognize long chain sialylated glycans, as also demonstrated by the combination of X-Ray and NMR methodologies. [287]

Figure 16. Biantennary sialylated N-glycan derivative bearing a lanthanide binding tag designed for performing recognition studies with influenza virus hemagglutinins. STD-NMR spectra were obtained for the biantennary glycan in the presence of two different hemagglutinin variants (Vic/11 and HK/68). The observed different STD patterns allowed detection of differences in the specific binding epitope for both variants. Only Vic/11 recognizes monosaccharides GlcNAc6 and 6'. Adapted from reference [287].

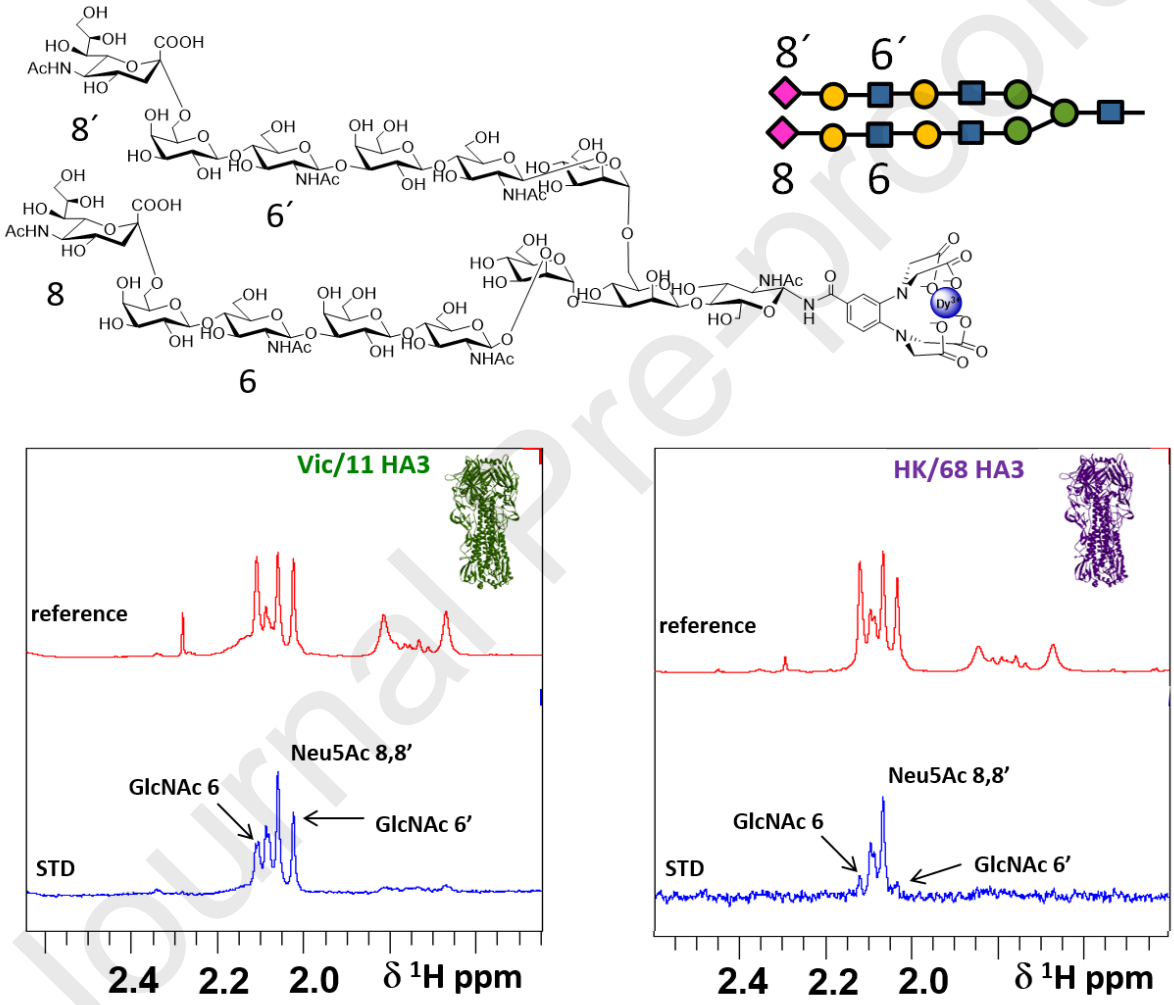

Obviously, the characterization of the molecular recognition features of such long chains is rather challenging, since repetitions of the N-acetyllactosamine (LacNAc) scaffold that are present cannot be distinguished in standard NMR experiments. Thus, the target glycans were conjugated to a lanthanide binding tag, and once the signals could be distinguished due to the different PCSs experienced by the different ^{1}H and ^{13}C NMR active nuclei at the diverse residues, STD-NMR experiments (see below) were carried out in the presence of hemagglutinins from different influenza variants. This study established that both arms are accessible for lectin recognition and, a different binding epitope was detected for H3 Victoria/11 vs Hong Kong/68 H3 variants, highlighting the importance of evolution for glycan

recognition. [286-288] Recent studies also show the potential of glycan conjugates bearing lanthanide binding tags to facilitate interpretation of competition experiments between similar glycans with different chain lengths that would normally display overlapping signals. [288]

4.2.2. Paramagnetic Relaxation Enhancement (PRE)

Paramagnetic metals also generate a local magnetic field that interacts with nearby nuclear spins, leading to faster relaxation rates, causing the signals from the nuclei that are spatially closest to the paramagnetic center to show line broadening (Fig. 14A). This effect is distance-dependent, PRE being proportional to r^{-6}.

The PRE rate, R_2^{PRE}, induced by a paramagnetic metal arises from the dipole-dipole interaction between a nucleus and an unpaired electron with an isotropic g-tensor at high magnetic field is described by the following equation:

$$R_2^{PRE} = \frac{1}{15}\left(\frac{\mu_0}{4\pi}\right)^2 \frac{\gamma_H^2 g^2 \mu_B^2 S(S+1)}{r^6}\left\{4\tau_c + \frac{3\tau_c}{1+(\omega_H\tau_c)^2}\right\} \quad (2)$$

where μ_0 indicates the permeability of vacuum; γ_H is the gyromagnetic ratio of the proton; *g* is the electron *g*-factor; *S* represents the spin quantum number; *r* is the distance between the paramagnetic center and the observed nucleus; and τ_c is the effective correlation time that is related to the electron spin-lattice relaxation time (τ_e) and the rotational correlation time (τ_m), with $\tau_c = (1/\tau_e + 1/\tau_m)^{-1}$. [273, 274]

The PRE can be measured by using paramagnetic lanthanides or spin labels (such as TEMPO or nitroxide structures). Following this approach, the conformation of a high-mannose undecasaccharide N-glycan was unravelled by using a spin label. The study was focused on the transverse relaxation rates (R_2) of anomeric protons, before and after radical quenching with ascorbic acid of the covalently-attached nitroxide group. The results showed that the glycan adopts a major folded-back conformation, in which two (1→6) branches of the glycan point towards the reducing terminus of the whole molecule. In detail, the Man moiety residues in the D2 and D3 branches display faster relaxation rates changes than those in the D1 branch. [289]

This concept has also been employed to describe the presentation of glycosphingolipids, particularly GM1, when anchored at phospholipid bicelles, which mimic the natural membrane. Interestingly, the use of membrane-anchored and soluble paramagnetic probes showed that the membrane-bound glycolipid displays a well-defined orientation, with fairly plastic dynamic behavior. [273] This presents the external epitope to interact with its receptors, as later corroborated by interrogating its interaction with galectins using standard receptor-based NMR methods. [290]

This methodology has also been widely used to explore the location of lectin binding sites, taking advantage of the changes in relaxation of the protein nuclei that are close to the paramagnetic center attached to the ligand. During the interaction, nuclei in the binding site residues will experience a dramatic increase in their relaxation rates, thereby highlighting the binding site. PREs are often quantified by observing the reduction in cross-peak intensities in 2D ^{1}H-^{15}N HSQC experiments. This decrease is caused by the faster transverse relaxation of the spin during the INEPT transfer and refocusing stages of the experiment. As mentioned above, [273] this methodology allowed determination of the structure of the complex formed by galectin-3 with lactose, thus complementing the PCS methodology [283] and standard approaches. [120] Recent studies have applied PRE effects to characterize the interaction of glycans with noroviruses. Norovirus is a highly contagious RNA virus that is known for carbohydrate-mediated host cell attachment. It is believed that norovirus attachment occurs via interaction with Histo Blood Group Antigens (HBGAs) on the host cell surface. The sugar

α-L-fucose is the minimal binding motif for genotype II (GII) noroviruses, with so-called P-dimer proteins being the minimal functional entity for HBGA recognition in this type of virus. In this context, an α-L-fucose (L-Fuc) derivative carrying a lanthanide binding tag was synthesized, and served as a non-covalent paramagnetic probe to assist the assignment of (^{2})H,(^{15}N)-labeled protruding domains (P-dimers) of norovirus using PCSs and PREs. This approach paved the way for novel NMR experiments giving access to information on the binding site not easily available from other experimental techniques. [291]

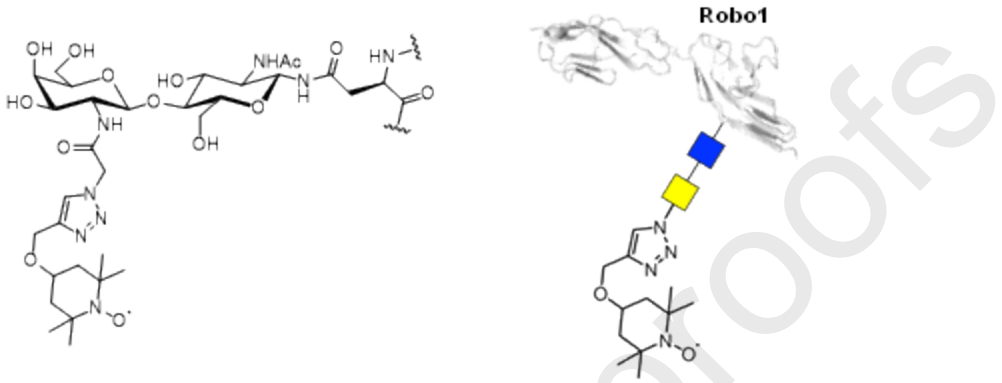

Scheme 8. The PRE approach: the paramagnetic tag (in this case, a nitroxide spin label) can be attached either to the glycan or to the protein receptor. Adapted from reference [293].

Nitroxide spin labelling has also been used for detailed interaction studies of CCL5 (RANTES) with cell surface glycosaminoglycans (GAGs). [292]. In particular, the structure and dynamics of CCL5-GAG interactions were probed using chondroitin sulfate ligands decorated with lanthanide binding tags. Two hexasaccharide fragments were employed that differed in the sulfation position at the non-reducing end GalNAc (see section 3.1.1). The binding orientations of the two ligands were different, with CCL5 showing more specificity for the sulfation pattern exhibited by one particular ligand, as deduced from the measured PRE perturbations. This methodology has also been employed to characterize the binding of heparan sulfate oligosaccharides decorated with a paramagnetic tag to Robo1, [293] corroborating the previous conclusions deduced from PCSs [284] and describing the dynamics and recognition features of the event (Scheme 6). It has also been applied to enzymes, allowing detection of the binding of diverse glycan substrates to N-acetylglucosaminyltransferase V. [294].

4.2.3. Residual Dipolar Couplings (RDCs)

In solution, the isotropic tumbling of molecules averages out the contributions from different internuclear orientations with respect to the magnetic field, and in these conditions the dipolar coupling cannot be detected. In contrast, in solid state NMR, dipolar couplings are operative, often generating extremely complex (or broad) signal patterns that can be simplified through fast rotation of the sample containing the molecule at the magic angle. In partially-aligned samples, residual dipolar couplings (RDCs) can be seen in solution, whose magnitudes depend on the degree of alignment obtained and on other intrinsic and geometric factors (see equations below). The advantage is that sharp NMR lines are preserved without the need for fast sample spinning, while information about the orientations of the different ^{1}H-^{1}H or ^{1}H-^{13}C vectors in the glycan can be obtained. Suitable partial alignment can be induced by using external alignment media, [295, 296] or by self-alignment with paramagnetic tags attached to the molecule; [274] the latter is a useful method that serves as a viable alternative to using alignment media in situations where the molecule of interest would interact with the media. Indeed, it has been reported that, depending on the chemical nature of the molecules providing the alignment, direct interactions between solute and alignment media may distort the results,

especially for flexible saccharides, whose conformation may be influenced by the environment. This has been described for different glycans. [297, 298]

The magnetic susceptibility tensor χ^{mol} of a molecule describes the proportionality between the applied magnetic field and the magnetic moment induced in a molecule. It is represented by a tensor, denoted by the symbol χ^{mol}. In the presence of a paramagnetic metal, the unpaired electron provides a paramagnetic contribution (χ) to this tensor (Eq. 3), which is anisotropic due to the orbital contribution to the electron magnetic moment.

$$\chi^{mol} = \chi + \chi^{dia} \qquad (3)$$

As a consequence, the energy of the system differs depending on the molecular orientation with respect to the external magnetic field. The lower energy states are more strongly populated, thereby inducing a partial alignment of the molecules.

The RDC of two partially aligned spins (for instance a ^{1}H-^{13}C pair) resulting from a paramagnetic alignment is defined by Equation 4 and Figure 4.

$$\text{RDC}\ (Hz) = \frac{1}{4\pi}\frac{B_0^2}{15kT}\frac{\gamma_C\gamma_H\hbar}{2\pi r_{CH}^3}\Delta\chi_{ax}^{mol}(3\cos^2\theta - 1) + \frac{3}{2}\Delta\chi_{rh}^{mol}\sin^2\theta\cos 2\Phi \qquad (4)$$

where B_0 is the external magnetic field, k is Boltzmann's constant, T is the temperature in kelvin, γ_C and γ_H are the gyromagnetic ratios of the C and H nuclei, ħ is Planck's constant, and r_{CH} is the distance between C and H. θ and Φ determine the polar coordinates of the C-H bond vector in the principal axis frame of the magnetic susceptibility tensor.

The angle θ is defined as the angle between the vector CH and the z-axis of the tensor $\Delta\chi^{mol.}$ In contrast, Φ is the angle describing the position of the projection of vector CH on the *xy*-plane of the tensor $\Delta\chi^{mol}$, relative to the x-axis.

$\Delta\chi_{ax}^{mol}$ and $\Delta\chi_{rh}^{mol}$ are the axial and rhombic components of the magnetic susceptibility tensor, defined as :

$$\Delta\chi_{ax}^{mol} = \chi_{zz}^{mol} - \frac{\chi_{xx}^{mol}+\chi_{yy}^{mol}}{2} = \frac{3}{2}(\chi_{zz}^{mol} - \bar{\chi}^{mol}) \qquad (5)$$

$$\Delta\chi_{rh}^{mol} = \chi_{xx}^{mol} - \chi_{yy}^{mol} \qquad (6)$$

Technically, RDCs (Hz) are calculated as the difference in coupling values observed between diamagnetic and paramagnetic conditions (Fig. 14 A) for a given pair of spins. ^{1}H-^{1}H or ^{1}H-^{13}C couplings can be measured by comparing a spectrum acquired in an isotropic medium (where any splitting observed is simply J) and one acquired from an oriented sample (where the observed splitting is RDC + J). In paramagnetic experiments, the isotropic medium uses a diamagnetic tag, usually the La^{3+} or Lu^{3+} complex, and the oriented sample uses the Dy^{3+}, Tb^{3+} or Tm^{3+} complex. Different approaches are used to measure these couplings, a simple one is the direct measurement of signal splitting in IPAP experiments [299] or using constant-time methods. [300] For small couplings, is very convenient to acquire quantitative experiments for coupling measurements, such as CT-COSY. [301]

There are few examples of RDC measurements in glycans by using paramagnetic alignment, [274] but the measurement of RDCs in a lactose conjugated with a lanthanide binding tag at 900 MHz has been described. Even at this high magnetic field a rather low orienting ability was seen for the paramagnetic tag. Alternatively, the conformations of different families of

glycans have been described by using RDC data obtained using external alignment media, [271] including those for hyaluronic acids, [302] dermatan sulfate, [144] the human milk oligosaccharides, [303-306] the Lewis and histo blood antigens, [89, 307], and a variety of flexible glycans of diverse size and nature. [308-311] The use of ^{13}C-labeled sugars allowed many more RDCs to be obtained, which were helpful for precise analysis. [312-314]

For glycan-protein complexes, the measurement of RDCs allowed unravelling of the conformation of the ^{13}C-labelled Galα1−4Galβ1−4Glc trisaccharide ligand when bound to the B-subunit homopentamer of the toxin derived from *Escherichia coli* O157, [315] and the core Man3 trisaccharide bound to the mannose-binding protein trimer. [316] Nevertheless, the RDCs observed under these conditions represent an average over bound and unbound states, and contributions from the free state can well outweigh contributions from the bound state; the result is that structural information about the bound conformation may be lost. To overcome this problem, new approaches have been devised to enhance the alignment, and hence increase the RDCs in the bound state. An elegant approach has been described that consists of modifying the protein to improve its alignment in a liquid crystal medium. [317] The method is based on the addition of a propyl chain to the C-terminus of a protein (galectin-3), which allows its insertion within the liquid crystal alignment medium utilized for the RDC measurements. This protocol leads to much larger RDCs for the bound state and therefore allows a better definition of the orientation of the ligand relative to the protein in situations where ligands are exchanging rapidly on and off of a protein. Under these conditions, one-bond ^{13}C-^{1}H and intra-ring ^{1}H-^{1}H RDCs were measured to evaluate the alignment of the ligand (lactose). In lactose, fourteen one-bond ^{13}C-^{1}H couplings were expected, seven from the glucose ring and seven from the galactose ring. Under these conditions, the ^{13}C-^{1}H splittings were easily measured using ^{13}C-^{1}H coupled HSQC experiments. These quantities provided excellent agreement with the back-calculated values of bound-state RDCs, and suggested that the conformation used to represent bound lactose correctly models the observed small amplitude of motion within the binding site. Such a procedure gives a fairly precise structural analysis of a ligand-protein interaction, particularly emphasizing the bound-state information. Moreover, the dynamics and allosteric mechanism of the two-domain glucose-galactose binding protein has been unravelled by exhaustive analysis of the PCS and RDC data. An engineered lectin displaying a lanthanide binding tag, which self-aligns in the magnetic field, [318] was employed to characterize the ensemble of conformations adopted by the protein.

5. From isolated glycans to intact glycoproteins

The analysis of glycoproteins has been a challenge for NMR scientists for decades. Generally speaking, the glycan chains in glycoproteins may be classified according to the type of linkage that attaches them to the protein chain. *N*-glycans are attached to the side chain amide group of asparagine (Asn), whereas *O*-glycans are linked to the side chain hydroxyl groups of serine (Ser) or threonine (Thr), or, less often, of hydroxylysine (Hyl). There are also rare *S*- and *C*-glycosyl linkages, to Cys and Trp. [319] Initial NMR studies focused on the determination of the primary structure of the *N*- and *O*-glycan chains, detached from the glycoprotein, and of the NMR analysis of their small oligosaccharide fragments, also isolated from natural sources or synthesized in the laboratory. Vliegenthart and coworkers [320, 321] developed the concept of "structural reporter groups" for the initial structural assignment and interpretation of ^{1}H-NMR spectrum of a glycan chain. In short, they proposed that the first step of the NMR analysis of a complex glycan would aim at assigning the NMR signals that display specific chemical shifts at clearly distinguishable positions in the spectrum. If possible, their coupling constants and their line widths should also be estimated. With this essential information, a first assignment of the primary structure of the glycan should be accomplished. The key structural reporter groups were defined as: a) the anomeric H_1 protons; b) protons shifted out of the bulk region due to glycosylation shifts or due to the influence of substituents, such as sulfate, phosphate, alkyl and acyl groups; c) deoxy sugar protons; and d) protons of alkyl and acyl substituents like methyl, acetyl, glycolyl, etc. With this information in hand, the primary

structures of a tremendous number of glycans of different types were identified by NMR (Figure 17), from the common pentasaccharide core of N-glycans, containing a 1-4 linked βMan residue, which acts as branching point, passing to the high-Man-9 structure that contains three antennae; to complex N-glycans that gather N-acetyllactosamine units in two, three, or four antennae, decorated or not with sialic acid moieties; and to hybrid type structures, which contain features of both the high-Man and N-acetyllactosamine-type structures; or further extensions at specific branching points with either GlcNAc or xylose (Xyl) residues.

This formidable task provided the basis for further developments in the field when 2D and 3D NMR methods became accessible. [322] With these methods, many research groups made key advances in the study of the conformation of these chemically diverse and complex glycans in the late 1980's and the 1990's. [39] As mentioned above, when discussing the general NMR-based approach to deducing the conformations of small oligosaccharides, combinations of NOE, vicinal homo- and hetero-nuclear coupling constants, assisted by molecular mechanics and dynamics calculations were employed to provide a view of the ensemble of shapes that could represent the conformational behavior of a given *N*-glycan. [323]

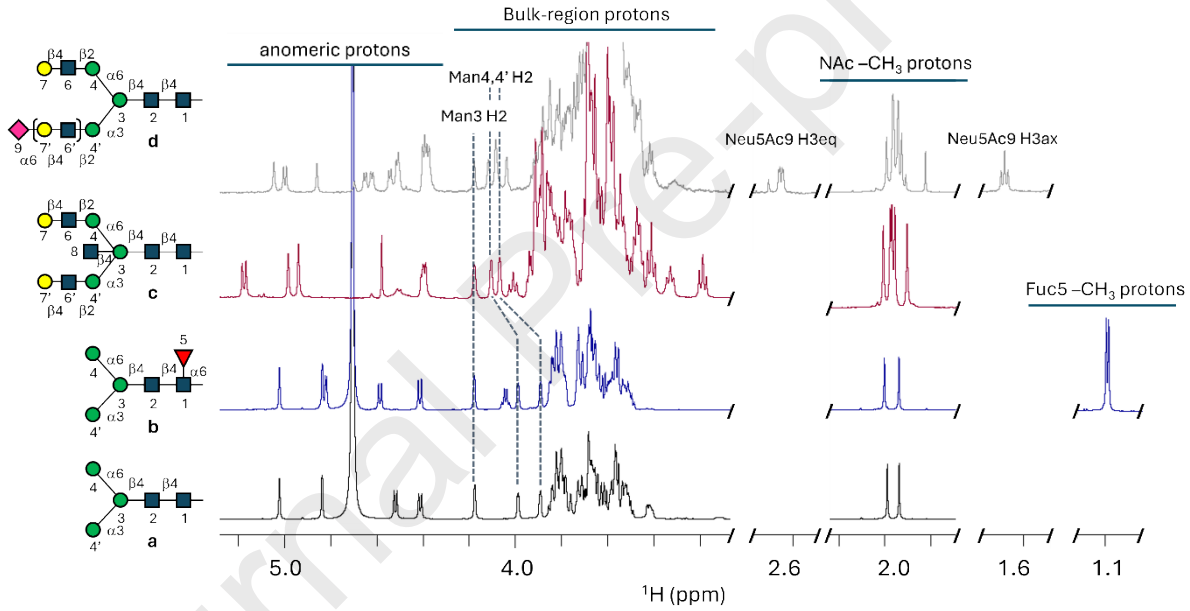

Figure 17: Expanded structural-reporter-group regions of the ^{1}H-NMR spectra of different N-glycan structures (**a**-**d**). From **a** to **b**, the methyl protons at ca. 1.1 ppm report on the presence of the 6-deoxy hexose, the fucose(5), α1-6 linked to the GlcNAc(1). In **a**, **b** and **c,** the glycosylation of mannose is indicated by the shift from the bulk-region of the H_2 protons of residues 4 and 4'. In **c** and **d**, the sialylation of the galactose, residue 7', is indicated by the presence of the H_{3eq} and H_{3ax} of the Neu5Ac, residue 9. The relative intensity scale of the expanded N-acetyl and methyl protons region differs from that of the other parts of the spectrum, for clarity.

In this way, the *N*-glycans of the high-Man, [324] complex-type, [325] and hybrid-type families were studied, as well as their smaller fragments (Man oligosaccharides, LacNAc oligosaccharides). [326] As landmarks, the behavior of the 1-6Man glycosidic linkages was also scrutinized, depending on their positions in the antennae (either Manα1-6Manβ, Manα1-6Manα, or GlcNAcβ1-6Manα), [327, 328] and studies on the effect of branching were carried

out. [329] The 1-6 linkages display an additional torsional degree of freedom, so the geometries around them are now defined by Φ, Ψ, and ω (see section 2.2 above). Since ω usually shows two distinct conformational regions (*gg* and *gt* for Glc/Man; *gt* and *tg* for Gal), a large degree of conformational mobility is expected. Interestingly, the intrinsically flexible 1-6 linkages did not all behave in the same way, so the accessible conformational space was more limited than expected in several cases, especially for those linkages closer to the Manβ branching point of *N*-glycans. [328] Studies of linear tri-, tetra-, or penta-saccharides demonstrated that, generally speaking, the conformational distribution for each glycosidic linkage was fairly independent of the others, [330] although some interactions could be expected when the additional glycosylation site was contiguous to the glycosidic linkage studied (as in the Lewis X trisaccharide in section 3.1 above). This fact poses an intrinsic problem for assessing the global conformational behavior of these *N*-glycans. Most NMR parameters that carry conformational information (vicinal *J*, NOE, sometimes T_1 relaxation) only provide short-range geometrical information, either through-space or through-bond. Therefore, the determination of the 3D structure of a 17-mer glycan (Scheme 9) relies on building up the proper geometry for each of the 16 glycosidic linkages of the molecule, whose conformational properties are generally not correlated. [87]

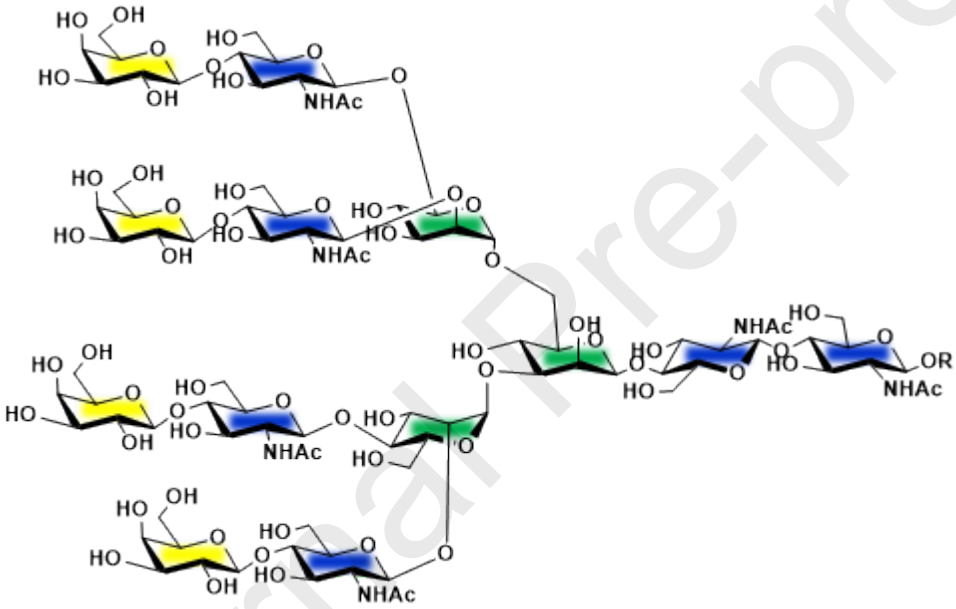

Scheme 9. An NMR challenge: a canonical tetraantennae *N*-glycan.

Thus, when each of the glycosidic linkages that compose a particular glycan are assumed to be flexible, the conformational space that the glycan is proposed to sample often seems to be very large. [39] Alternatively, simplified models based on one single conformer for each glycosidic linkage (one or two for ω angles), with only small librations around the global minimum are also frequently proposed. [331] These considerations motivated the use of other NMR parameters to deduce the conformation from a global perspective, especially pseudo-contact shifts (PCS), [201, 202] measured using paramagnetic NMR methods, and residual dipolar couplings (RDC), [196] obtained under partially aligned conditions. PCS methods allow deducing long-range distances, while RDC contain angular information, as described in sections 4.2.1 and 4.2.3. Moreover, the description of the conformation of a glycan should focus not only on the structural aspects, but also on the extent of motion and the time scales for these motions. Thus, different protocols have been employed to assess these key parameters, which are also described in the corresponding sections of this article.

The conclusions of the NMR-based conformational analysis of these molecules were also used as a benchmark to validate the utility of the different computational methods that were growing, from diverse force fields for molecular mechanics and dynamics calculations [332] to semi-empirical calculations, [333] which later passed into *ab-initio* methods. [334] Specific protocols to deal with sugars were also used to be able to reflect the structural consequences of anomeric effects and to deal with the high polarity of glycans, including the use of various explicit solvent models. Different applications of these approaches, including rigid and adiabatic relaxed energy maps, [335] Monte Carlo simulations, [81] simulated annealing MD, [91] NMR-based time-averaged restrained MD, [336] along with the careful comparison of results of these approaches with the experimental NMR data, their successes, and their failures, have been also extensively described for glycans of diverse chemical architecture and complexity. [39, 48, 57, 337] The tremendous advances in computational power and in the precision of computational approaches over many years has progressively allowed a better representation of the conformation and dynamics of glycans, including the possibility of accessing information about processes on the microsecond time scale, five or six orders of magnitude longer than when the first MD simulations for glycans were carried out more than 30 years ago. [87, 103, 338, 339]

5.1. Internal motions

The extent of molecular motions around the glycosidic linkages of glycans was an open question for years. [340, 341] Moreover, from the analysis of different publications it was evident that the concept of flexibility was rather subjective, ranging from the recognition of certain torsional oscillations around the glycosidic bonds within a particular Φ/Ψ region, to the appreciation of the simultaneous presence of two or more significantly different geometries (that is, the simultaneous presence of syn- and anti- conformers for Φ and/or Ψ (Figure 7), or *gg, gt*, or *gt* rotamers around ω for glycans with 1-6 glycosidic linkages). All these changes involve a major change in the orientations of the monosaccharide rings. The existence of flexibility is of prime importance in molecular recognition events, since the entropy term is generally unfavourable for most glycan interaction processes. [120] Obviously, when dealing with flexible molecules, given that the observed NMR data arise from the contributions of all the conformations that exist in solution, the use of an NOE-based approach, in conjunction with restrained molecular mechanics or molecular dynamics, to generate “the NMR structure” could lead to a virtual conformation, as first described by Jardetzky, [342] and then by Carver for glycans, [343] since this virtual ”averaged” geometry could explain all the NOEs even though the glycan may never adopt this exact conformation.

It has been well established for years that different features related to internal motions in biomolecules, and especially glycans, can be unravelled by using various NMR methods. [344] For instance, the amplitudes of the motions, the time scales, and the existence of different mobilities in different regions of a glycan can be disentangled by using homo- and/or hetero-nuclear relaxation measurements. [345] Different motional models can be employed to correlate the experimental NMR results with the molecular motions. The Lipari-Szabo approach has been extensively used. [346] This was initially proposed for proteins, based on the heteronuclear relaxation parameters obtained for amide N-H signals. This approach can be extended to glycans, considering that the order parameter S^2 encodes the amplitude of motion that is faster than overall tumbling for a given X-Y vector that connects any pair of spin 1/2 nuclei. [82, 347] For glycans, X is usually ^{13}C or ^{1}H and Y is ^{1}H For fully restricted motions (i.e. when only global tumbling of the whole molecule is present), $S^2=1$, while for completely unrestricted internal motions $S^2=0$. The approach also takes into account the global motion correlation time (τ_c), and the effective correlation time (τ_e), which depend on the timescales of the global and internal motions for the corresponding X-Y vector. The use of ^{13}C-^{1}H heteronuclear T_1, T_2 and NOE values to derive a description of molecular motion according to the Lipari-Szabo model was adopted by different research groups, [348-350] demonstrating, in general, the extent of external motions around the different glycosidic linkages of oligo- and

polysaccharides. This approach provided fair estimations of the internal motional time scales around the glycosidic linkages, within the range of tens of picoseconds, [104, 351] at least one order of magnitude faster than those estimated for the overall molecular tumbling, which obviously depends on the size and shape of the glycan. [352]

^{1}H NMR-based relaxation methods, employing selective and/or non selective T_1 and/or NOE measurements though NOESY and/or ROESY experiments (including off-resonance ROESY), have also been widely applied to deduce the extent of motion around glycan linkages. [84, 104] Given the relationships between the longitudinal relaxation rate ($1/T_1$) and cross relaxation rates, along longitudinal (σ_{NOE}), transverse (σ_{ROE}), or tilted axeis ($\sigma_{tiltedROE}$), with the spectral density function, the measurement of these parameters at different magnetic fields (at least two), or the determination of at least two of these parameters, allows determination of the effective motional correlation times in a straightforward manner. [83-85] Indeed, the ROESY experiment, initially called CAMELSPIN (*Cross-Relaxation Appropriate for Minimolecules Emulated by Locked SPIN*) by Bothner-By, [353] exploited the dependence of σ_{ROE} on the spectral density function to abolish the almost-zero NOE found for a tetrasaccharide molecule at 620 MHz in a regular NOESY experiment.

$$\sigma_{NOESY} = (k^2/10)[6J(2\omega)-J(0)] \quad (7)$$

$$\sigma_{ROESY} = (k^2/10)[2J(0)+3J(\omega)] \quad (8)$$

$$k=(\mu_0/8\pi^2)h\gamma^2r^{-3}. \quad (9)$$

On this basis, using either heteronuclear or homonuclear relaxation methods, or even both simultaneously, the existence of internal motions at different time scales in the same glycan was probed in a variety of systems, from simple disaccharide entities to large polysaccharide structures. [354, 355] Therefore, the presence of specific local dynamics for diverse glycosidic linkages was demonstrated, also within a given global energy region well-defined by a particular Φ/Ψ value. [82] For instance, for Lewis X tetrasaccharide analogues (see section 3.1), global motion correlation times slightly lower than 1 ns were estimated, with internal motion correlation times between 30 and 90 ps, depending on the particular monosaccharide residue. [83] For large polysaccharides, it had earlier been demonstrated that relaxation parameters are basically independent of chain length, given the dominant contribution of so-called segmental motions to the spectral density function, [356, as is typical of polymers. Indeed, many large polysaccharides, even those with molecular weights of tens of kDa, show sharp NMR signals, and their conformational behaviour can be studied, in a reductionistic manner, in a similar way to that of the constituent oligosaccharide repeating unit. [357]

5.2. Labelling with NMR-active stable isotopes and more

The NMR study of the conformation and dynamics of isolated glycan moieties, even relatively large complex systems, reached a status of maturity during the early years of this century. Nevertheless, some challenges remained, especially regarding characterisation of the conformational behavior and molecular recognition features of oligo- and poly-saccharides containing repeated single mono- or di-saccharide entities. In such cases, given (again) the averaged nature of NMR spectra, the NMR signals recorded correspond to those expected for just a mono- or di-saccharide. Despite this, access to detailed conformational information has been achieved in recent years thanks to the ability to place ^{13}C labels selectively in *ad hoc* chosen sites in the target molecules, thus characterising the conformational features of particular glycosidic linkages, or the existence of interactions at particular sites of a glycan.

The use of ^{13}C-labelled glycans for NMR studies started in the last years of the last century, allowing detailed structural, conformational, and interaction studies to be carried out. [358] Starting from *in vivo* technologies to create enriched yeast and bacterial cell wall materials for NMR studies, chemical and chemoenzymatic synthesis protocols have been used to prepare a variety of scientifically valuable saccharide samples that contain one or several residues labeled with ^{13}C or with other stable NMR-active isotopes (^{15}N). [359-363].^{13}C labeling makes possible precise determinations of heteronuclear $^{3}J_{C,X}$ couplings, dynamic aspects through ^{13}C-based relaxation experiments, and intra- and inter-molecular NOEs through ^{13}C-filtered or ^{13}C-edited experiments. [364] In addition, it offers extraordinary rewards for glycan NMR-based investigations, [365] given the tremendous spectral dispersion of ^{13}C and the possibility of employing 2D and 3D NMR heteronuclear experiments combining ^{13}C and ^{1}H data (or even ^{15}N, if also available) [366, 367] to alleviate signal overlap. [368] Accordingly, novel protocols have been established that allow the overexpression of target glycans in systems that have been genetically engineered. In particular, the synthesis of high-Man-8 and -9 glycans with uniform ^{13}C-labelling has been achieved in an engineered yeast, with ^{13}C-Glc as the carbon source. [368] Alternatively, the high-Man9 glycan has also been synthesised using an adenovirus expression system, allowing the NMR study of its interaction with two lectins, microvirin, and DC-SIGN. [369]

As an alternative, *in vitro* chemoenzymatic labeling approaches have also been successfully developed. In this case, however, the corresponding sugar nucleotide donor has to be available in its ^{13}C-labeled form. Chemical synthesis protocols [370] have also been of great importance in preparing ^{13}C-labelled glycans with either selective [371] or uniform labelling. In this way, a number of mono-, [372-376] di-, [377, 378] oligo-, [379, 380] and poly-saccharides have been made available for the scientific community to study their conformation, dynamics and interactions, including heparin, [299, 381] other glycosaminoglycans, [382-384] polysialic acids, [385] and different polysaccharides. [386, 387]

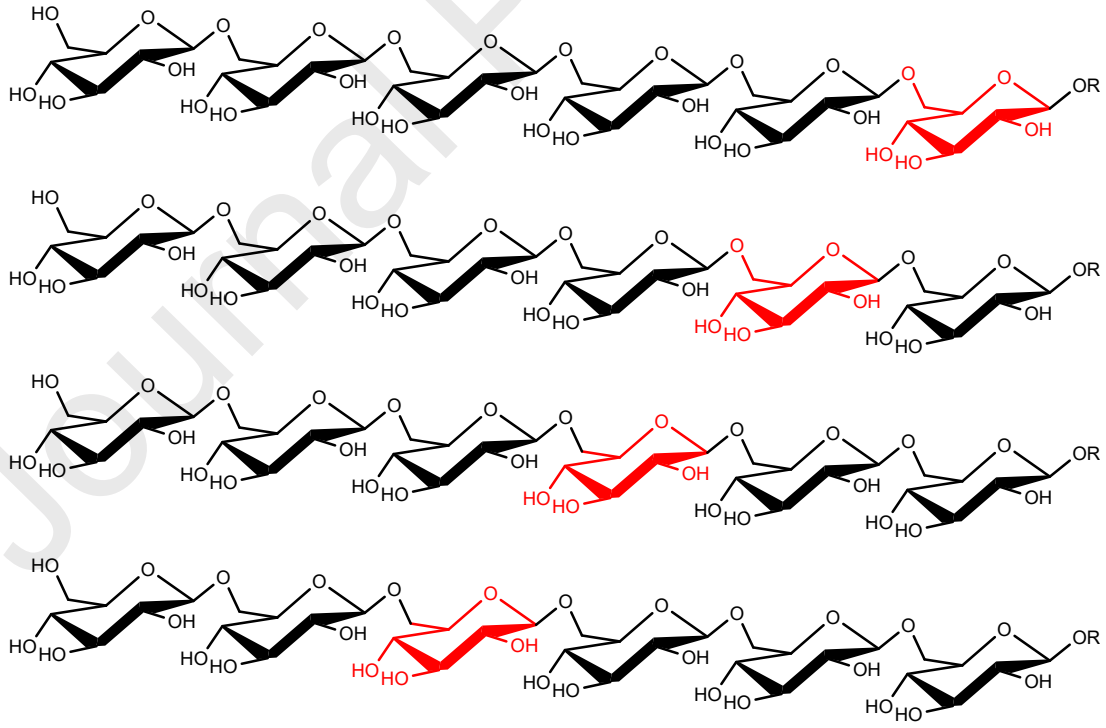

Figure 18. The NMR parameters required to assess diverse conformational features of a hexasaccharide formed by identical β1-6Glc units could be measured in the NMR spectra recorded for the target molecule, which contained a particular ^{13}C-labelled Glc moiety at a specific position (in red) of the chain. The same experiments were repeated for molecules that

only differ in the position of the ^{13}C-labelled Glc residue within the chain. In this way, specific NOEs and J_{CH} couplings could be measured at each specific site [396].

For uniformly labeled molecules, the existence of ^{13}C-^{13}C coupling constants allows TOCSY-type transfers to be used. [53] However, they evolve [362] in the indirect dimension in HSQC-type experiments, complicating the assignment of the NMR signals. The application of constant-time periods (CT) or virtual decoupling protocols to simplify the spectra have been extensively discussed. [53, 362]

The existence of labeled glycans allows detection of key intra- and inter-molecular interactions, and thus also the conformational features of a glycan in its complex with a receptor. [318, 388, 389, 390] In fact, the use of ^{13}C/^{15}N doubly-labeled lectins bound to ^{13}C-labeled glycans allowed determination of the fine details of the interaction between cyanovirin-N (CV-N) and the Manα(1−2)Manα(1−2)ManαOMe (Man3) trisaccharide core of N-glycan at high resolution. [391] As follow up, the orientation of the hydroxyl groups of the trisaccharide in the lectin binding site was elucidated, along with the hydrogen bond network in the complex. [46, 392]

More recently, with advances in the chemical synthesis of glycans, it is now possible to have access to milligram amounts of pure and well-defined oligosaccharides. In particular, the automated glycan assembly (AGA) method [393-395] has made it possible to obtain synthetic oligosaccharides bearing sugar residues specifically labelled with stable NMR active nuclei (^{13}C, ^{19}F), [396, 397] thus overcoming the chemical shift degeneracy of homo-oligosaccharides. As a key example, the conformation of a hexasaccharide consisting of 6 identical Glc units linked through β1-6 linkages was determined (Figure 18). First, different hexasaccharides (differing only in the positioning of isotopic labels) were synthesised with just one or two ^{13}C-labelled Glc units at specific positions of the oligosaccharide chain, thus making accessible specific structural and conformational information at each position and glycosidic linkage. In this way, the presence of certain populations of a helix-like geometry was deduced. [396] This was later further characterized through residual dipolar coupling (RDC) analysis in different orienting media. [222] This specific-labelling-based approach has also been employed to identify the binding epitopes of homo-oligomer poly LacNAc moieties when interacting with their receptors, [398] by using STD-HSQC experiments (see below in section 6.1.1.2). This concept was further applied to the study of interactions between complex sialylated N-glycans, containing several LacNAc, and diverse variants of influenza hemagglutinin. [399]

The next challenge was therefore accessing detailed information on the conformations, dynamics, and interaction features of intact glycoproteins. As initial steps in the use of ^{13}C-glycans, *in-vitro* labeling methodologies have been employed to prepare N-glycans that display specifically ^{13}C-labeled Neu5Ac, [400, 401] Gal, [402] GlcNAc, [403] Glc, [214] and Man [404] residues at individually defined positions.

5.3. N- and O-glycans in glycoproteins

In glycoproteins, the glycans are present in a specific manner, being attached to a given Asn (*N*-glycan) or Ser/Thr (*O*-glycan) residue within the polypeptide chain (Scheme 1). The glycan entities in glycoproteins are intrinsically heterogeneous, a fact that is linked to their biosynthesis. [405] The glycans provide glycoproteins with an additional layer of chemical and biochemical complexity, since the presence of the glycans affects their stability, processing, and biological function. The first example of a 3D NMR structure of an intact glycoprotein was

reported in 1995 by Wagner and coworkers, [406] focused on CD2, a T-cell antigen involved in cell adhesion. A high-Man-type *N*-glycosylation in the adhesion domain was characterized, allowing the authors to conclude that the glycan stabilizes an exposed positively charged cluster; removal of the *N*-glycan led to unfolding of the protein, and prevented binding to its counter-receptor (CD58). It was also deduced that the motion of a large region of the attached glycan was restricted in comparison with the conformational mobility described for the corresponding free high-Man oligosaccharides.

This conclusion was indeed interesting. It was in the minds of many scientists that the conformational behavior and, especially, the presentation of the glycan epitopes to their receptors in molecular recognition events, should also depend on the type of attachment to the polypeptide chain in glycoproteins, and to the lipid moieties in glycolipids. This example provided a clear experimental validation of that hypothesis. [21, 215, 407] Interestingly, and related to these investigations, it has also been demonstrated that the interaction outcomes of glycans presented on surfaces (in glycan arrays, for instance) towards glycan-binding proteins may be different from those obtained in solution by NMR, where the partners diffuse freely. [408]

Another system that has been widely studied is human chorionic gonadotropin (hCG), which carries four N-glycans on its two subunits, α and β. αhCG displays N-glycans at Asn52 and Asn78, essential for bio-activity, and which show dramatically different dynamic behavior, due to their different contacts with the protein chain, as could be deduced from extensive NOE analysis. [409-412]

These investigations also exemplified the importance of generating isotopically labelled glycoprotein entities, through the use of mammalian cell systems. A variety of expression and purification protocols have been proposed and successfully employed over time. Simultaneously, the effects of *N*- and *O*-glycosylation on the three dimensional structure of the polypeptide and the sugar were also investigated using simple glycopeptide models. [413-415] Extensive studies by Imperiali and coworkers demonstrated the influence of GlcNAc-glycosylation on the conformation of the peptide backbone. Analysis of the NOEs strongly suggested that the presence of the typical $(GlcNAc)_2$ diacetyl chitobiose moiety induced a packed type I β-turn geometry at the glycosylation site, thus producing a conformational switch from the original extended Asx-turn existing in the naked peptide. [414] Other work showed that the chemical nature of β–GlcNAc was crucial for the existence of such a switch, which did not occur when β-Glc or α-sugars were present at the glycosylation site. [415]

These studies opened the door to related work on different glycoprotein systems. One clear example where NMR analysis of glycoproteins can be of considerable interest is in the search for biomarkers, where simple ^{1}H NMR spectroscopy can identify the so-called ‘GlycA’ signal, which arises from the NAc group signals of GalNAc, GlcNAc, and NeuNAc glycans in glycoproteins. [416] Importantly, its mere observation has diagnostic value for acute-phase inflammation episodes. Further deconvolution of these component signals has recently been achieved. [416] Another important application, this time in the biopharma field, is in the analysis of monoclonal antibodies, which are highly glycosylated molecules. NMR fingerprints can be identified through the analysis of $^{1}H,^{15}N$ and $^{1}H,^{13}C$ cross peaks in heteronuclear spectra, which can in turn be related to high-order structural features and specific glycosylation patterns. [417] This methodology is robust and fast for mAb quality control, although it generally requires isotopic labelling. That said, for samples containing sufficiently concentrated glycoprotein, NMR analysis of non-labeled samples can also provide important information on the glycan chains of intact glycoproteins, as demonstrated by Schubert et al. using simple 2D ^{1}H-^{1}H and ^{1}H-^{13}C correlation methods, [418] differentiating *O*- from *N*-linked glycans using an HSQC experiment, and assessing the components of the glycan skeleton through analysis of spin systems through 2D homonuclear experiments. Given the intrinsic

internal motion of glycan chains described above, such experiments can be successful in identifying glycans regardless of the protein size.

However, with the use of ^{13}C labels, NMR has been increasingly used for the structural characterization of glycoproteins [419] and their interactions. It has been demonstrated that a uniformly ^{13}C-labeled Gal moiety can be enzymatically transferred to a chain of hen ovalbumin, [420] allowing glycan mobility to be monitored by NMR in intact glycoproteins. For instance, in human immunoglobulin G (IgG), when comparing the structural and dynamic features deduced from X-ray crystallography and NMR, subtle differences were detected in the glycan dynamics shown by the two methods. [421]

Different expression systems for stable isotope labeling of eukaryotic glycoproteins are now available, [422] allowing generation of ^{13}C-labelled glycan chains. HEK 293 cells are probably the most commonly employed, since they also display different variants that can be used to generate complex, hybrid, or high-Man-type N-glycans, also playing with glycosyl transferase inhibitors. In seminal work, a glycosylated immunoglobulin G (IgG) was prepared using [U-$^{13}C_6$,$^{2}H_7$]-Glc as sugar precursor. In this manner, a ^{13}C-labeled glycoprotein was isolated and studied by NMR, allowing assignment of the anomeric resonances for the glycan attached to the intact glycoprotein. [423] Nowadays, access to diverse labeling schemes opens new NMR-based avenues to study the structural roles of glycans in glycoproteins, including the modulation of protein conformation and dynamics, stability, and recognition issues. [424-428]

Although the glycan chains can be efficiently labeled just by adding [U-^{13}C]-Glc to the standard culture medium, a key bottleneck is the assignment of the glycan chains to the individual Asn moieties that provide the glycosylation sites. Depending on the target glycoprotein, different strategies can be employed to facilitate assignment. Clear chemical shift differences can be observed for different Asn-linked $^{1}H_1$-$^{13}C_1$ HSQC or TROSY anomeric correlations, depending on their involvement (contacts) with the polypeptide backbone. Obviously, the mutation of the glycosylated Asn moieties to Gln residues impairs *N*-glycosylation and therefore allows assignment of the individual cross peaks to specific positions, [429] provided that the corresponding glycan is not essential for the proper production and folding of the glycoprotein. [430] For instance, HEK293S cells can be used to produce uniformly labeled glycoproteins displaying only high mannose glycans when employing a culture medium with ^{13}C-Glc. Since the glycosylated GlcNAc residues are linked to the side chain NH of Asn moieties, their anomeric cross peaks peaks can be assigned using ^{1}H-^{13}C-HSQC/TROSY experiments. Combinations of single, double, or triple mutations of Asn residues may be used for specific assignments. [429, 431] Moreover, the comparison of the chemical shifts in HSQC/TROSY spectra for these anomeric cross peaks under folded or denatured conditions may indicate whether or not the glycans at the corresponding Asn residues (GlcNAc and beyond) interact with the polypeptide chain; if no GlcNAc-protein interactions take place, the chemical shifts will be identical in the folded and unfolded states. In general, it is now established that the combination of mutagenesis with NMR allows unravelling of site-specific glycosylation, the role of the glycan in influencing protein conformation, shape, dynamics and stability, and the identification of unique sugar residues. [432-435] From the technical NMR perspective, the NMR spectra obtained may be improved by removing those glycans that do not contribute significantly to stabilizing the protein.

Chemical shifts and NOEs, also at the protein level, can be employed to detect conformational changes in the polypeptide chain upon glycosylation. [436, 437] For instance, the Skp1 protein, from the ameba Dictyostelium (DdSkp1), displays a glycosylated hydroxyproline residue at position 143. [436] Analysis of the chemical shift index (CSI) for the non-glycosylated and glycosylated versions of DdSkp1 showed a random coil to α-helix transition for the C-terminal 139−153 segment of DdSkp1, which was verified using ^{15}N-edited NOESY experiments.

Therapeutic monoclonal IgG antibodies display a single glycosylation site (N297). Interestingly, the presence of Gal and Fuc moieties at the ends of glycan chains is linked to toxicity. In this context, NMR methods have been used to quantify these sugars on these IgGs. [438] Simple integration of the relative intensities of the anomeric ^{1}H-^{13}C-HSQC cross peaks for the terminal Gal and Fuc residues versus those measured for the Manα1-3 moiety allows the relative quantitation of these monosaccharides. NMR has been of paramount importance in showing the almost exclusive presence of high-mannose type *N*-glycans on those glycosylation sites, that are hardly accessible for further glycan processing once the polypeptide has been folded. [400, 435, 439, 440]

Given the internal mobility at the glycosidic linkages of glycans, their NMR signals can nowadays be safely assigned using standard 3D experiments. The ^{13}C labeling also paves the way for semi-quantitative, or almost quantitative, analysis of signal intensities, allowing a glycan's heterogeneity to be characterized. Similarly, [435] simultaneous protein labeling would also be highly beneficial for complete analysis of the intact glycoprotein but, depending on the media employed, incorporation will be at a low level. To overcome this problem, Prestegard has proposed an NMR method for assigning sparsely labeled glycoproteins focused on the analysis of intra-residue NOEs, assisted by molecular dynamics. [441]

The conformation of *O*-glycans (Scheme 1) within *O*-glycopeptides or *O*-glycoproteins has also been extensively studied. Different NMR investigations have focused on MUC-1 type structures, to attempt to decipher, at atomic resolution, [442] the differences and similarities that may exist between Ser and Thr-linked *O*-glycopeptides, in many cases to understand the motifs that could build a structure-based protocol for the development of anti-cancer vaccines. [443] As a landmark here, STD-NMR experiments combined with microarray experiments were instrumental in unravelling the epitope specificity of mAbs directed against MUC1. [444] From a basic perspective, the conformational differences between the Tn-antigen variants (α-*O*-GalNAc Ser vs. Thr) have been discussed extensively for almost two decades. All the experimental data lead to the conclusion that the Thr-linked structures are conformationally more restrained than the Ser analogues.

The first such study employed a 24-mer glycopeptide from the HIV-1 V3 loop [445]. NMR structures were in agreement with a greater rigidity for the Thr-linked GalNAc residue, in contrast with the observations for a MUC-7 glycopeptide, for which the authors reported a similar behavior for Ser and Thr-linked motifs of the same glycopeptide [446]. Moreover, Live and coworkers [447] reported that, in a series of penta-glycopeptides displaying contiguous contiguous Ser- and Thr-motifs decorated with the most typical tumor-associated antigens (Tn: GalNAc, TF: Gal-β1,3-GalNAc, or sialyl TF: Gal-β1,3-(α-2,6-Neu5Ac)GalNAc), the NMR features of all those entities were independent of the glycan. According to their analysis, the conformational preferences were shaped by the contacts of the attached α-GalNAc moiety with the polypeptide backbone. They also speculated that the conformational arrangement surrounding the α-GalNAc moiety was influenced by a hydrogen bond between the carbonyl oxygen of the Thr and the NHAc of the GalNAc unit, which did not occur for the Ser-containing series, as supported by NOEs between the peptide backbone and the GalNAc methyl group. A full understanding of the conformational behavior was achieved by systematic NMR studies by Corzana and coworkers, who exhaustively compared the Ser and Thr *O*-linked glycans. [448-451] They first demonstrated that direct interaction between the sugar and the peptide backbone was not driving the conformational preference, but rather bridging water molecules between the sugar and peptide provided the rationale for the observed key differences in Ψ glycosidic torsion (defined by the amino acid ß-carbon of Ser/Thr and the glycosidic oxygen ($C\alpha$-$C\beta$-O-C_{anom}). Indeed, only in the case of Thr *O*-linked glycan did the GalNAc molecule adopt a perpendicular orientation with respect to the amino acid moiety (Fig. 19), allowing the presence of a water molecule.

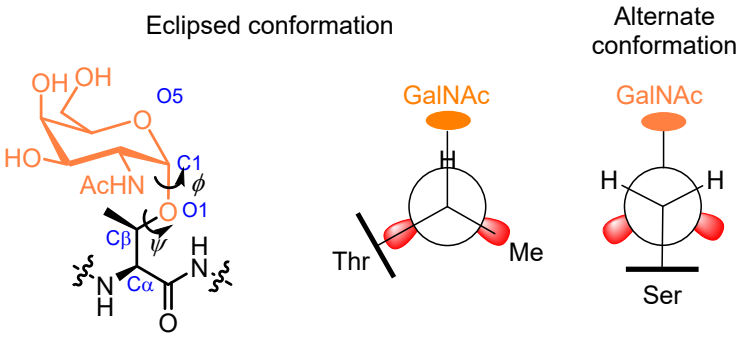

Figure 19. NMR parameters (NOEs and *J* values) allowed the conclusion that the conformations around the torsional degrees of freedom of the Ser-Tn and Thr-Tn antigens are different, especially around Ψ. [448-451]

Further studies have shown that the Tn-Thr antigen displays a well-defined conformation both in solution and when bound state to various mAbs. In contrast, the Tn-Ser antigen is more flexible, and exhibits different conformations around the glycosidic linkage. This feature was also observed when analysing the interactions of α-*O*-GalNAc Ser and Thr MUC1-like glycopeptides with SM3, [452] an anti-MUC1 antibody, now using X-ray crystallography. The glycosidic linkages of the bound Tn-Thr and Ser antigens displayed different geometries, which also impacted on their binding affinities. Interestingly, the analysis of the conformational behavior of these glycopeptides in solution, compared to those obtained in the gas phase by infra-red and microwave methods, showed the existence of specific water molecules bridging the sugar moiety and the peptide backbone, only for the Tn-Thr antigen, as earlier proposed in solution. [451] Also within this research field, NMR studies have been used to assess the glycosylation preferences and mechanism of action of different *N*-acetyl galactosamine transferases, using a MUC1 polypeptide with four tandem repeat domains as substrate, opening new avenues to characterize, at the highest possible resolution, the specificity of the action of other isoforms of *N*-acetyl galactosamine transferase enzymes (GalNAc-Ts) on different mucins. [453]

As can be seen, it has by now been established that NMR is indeed a fantastic tool for studying intact glycoproteins. Nevertheless, the detection of minimally abundant glycans remains elusive, as well as the unequivocal assignment of chemical decorations, such as acetylation, sulfation, or the presence of appendages. It is evident that specifically designed NMR experiments will be required for overcoming these limitations.

6. NMR and molecular recognition: glycan-receptor interactions

NMR spectroscopy is widely regarded as a robust methodology for analysing ligand-receptor recognition events at different levels of complexity. There is a wide variety of different NMR-based techniques to assess molecular interactions, which can be basically divided in two major groups: NMR experiments from the point of view of the ligand (ligand-based NMR experiments), and NMR experiments from the perspective of the receptor (receptor-based NMR experiments).

6.1 The ligand: glycan-based NMR experiments for monitoring interactions

6.1.1. STD-NMR

In the last two decades, Saturation Transfer Difference (STD) NMR has become one of the most robust and widely used NMR tools to analyse glycan-receptor interactions. STD-NMR easily detects the presence of binding in solution, can be employed to screen complex mixtures of putative ligands, and can identify the binding epitope of the saccharide. [454] The STD-NMR experiment is fairly simple, and is based on the transfer of saturation from protein protons, that are saturated by selective irradiation of a protein signal region, to protons of the ligand that are in contact with the protein through binding. (Saturation here means a partial equalisation of spin-state population levels, leading to reduced intensity for the affected signals). Effective intermolecular ^{1}H-^{1}H cross-relaxation mechanisms operate, so that the saturated protein protons transfer their saturation to the nearby ligand protons, whose intensities are affected to an extent that depends on the interproton distance, and can be easily measured using difference spectroscopy.

The STD-NMR experiment has been extensively employed to analyse a large variety of glycan-protein systems of varying degrees of complexity. Indeed, from the seminal publication on STD-NMR, Meyer and Mayer devised the experiment to screen a library of saccharides versus a GlcNAc-specific lectin. [454]

From a technical perspective, STD-NMR relies on the intermolecular nuclear Overhauser effect (NOE) and is especially applicable to systems in chemical exchange under fast kinetics conditions. This is common when studying protein-carbohydrate interactions, which are often characterized by shallow binding sites and transient interactions. [455] Thus, from amongst existing NMR ligand-based techniques, STD-NMR is the most informative one for the structural characterization of glycan binding in solution. In principle, the affinity range over which the technique is applicable is roughly between 10^{-8} and 10^{-3} M. [456] From the practical point of view, the STD-NMR experiment generates saturation selectively on a small group of protons of the receptor. That saturation rapidly spreads throughout the protein protons, and thus when a glycan binds to the saturated protein, it will receive saturation from the protein. Clearly, this will affect the intensities of its NMR signals, a process that can be easily observed. [457] Moreover, the effect on particular ligand signals will be different depending on the distance of the relevant sugar protons from the saturated protein protons. [457]

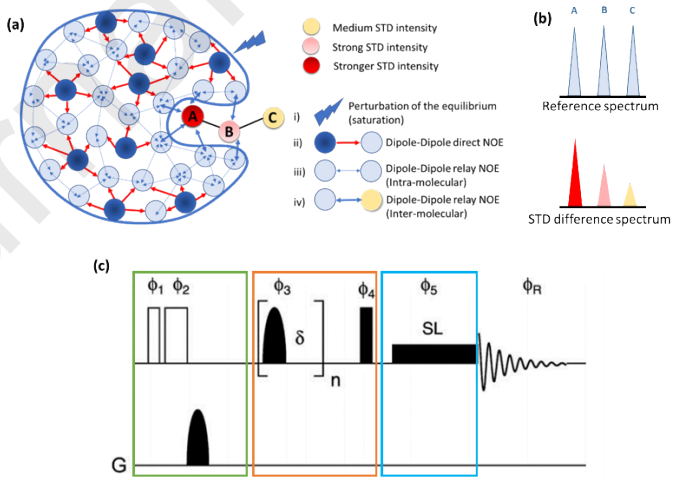

Figure 20. a) Illustration of the sequence of events taking place during an STD-NMR experiment. The outcome is a binding epitope mapping, in this case of the schematic glycan constituted by the three different moieties A–B–C, reporting on its binding mode. (b) Illustration of the reference spectrum (top) and STD difference spectrum (bottom) for the A–B–C ligand in part (a). c) Pulse sequence for STD NMR. The narrow and wide open bars correspond to trim pulses with lengths of 2.5 and 5 ms, respectively, performed at a power level appropriate for spin-locking. The narrow filled bar is a 90° hard pulse. A series of selective pulses (typically 50 ms duration, 1 ms inter-pulse delay, frequency switched between on-resonance and off-resonance spectral locations) is applied for saturation. The first two

radiofrequency pulses and the gradient pulse are applied to dephase any residual magnetization. Figure adapted from [458].

In Figure 20(a), the five processes outlining the STD NMR experiments are schematised: (i) a variable length selective shaped pulse is applied to a given set of protein signals to saturate them; (ii) by dipole–dipole direct NOE, the irradiated protons transfer their perturbed magnetization state (i.e. saturation) to adjacent protons (note that the latter can be on either the protein or the glycan); (iii) by (intramolecular) dipole–dipole relayed NOE, also called spin diffusion, the saturation of protein protons next spreads to the whole protein, through the dense network of proton–proton distances appropriate for NOE propagation, as a result of the rapid cross-relaxation caused by the slow protein rotational tumbling motion; (iv) when a glycan binds to the protein, saturation is transferred to the closest protons of the saccharide via intermolecular NOE interactions; and (v) saturation thus accumulated in the bound state is transferred to the free state, due to the fast exchange between the bound and free states of the ligand and the slow relaxation of the saccharide protons in the free state. Overall, these processes result in an observable reduction in the signal intensities of ligand signals in the ^{1}H NMR spectrum under protein saturation conditions, compared to the reference spectrum, as shown in Figure 20(b). Importantly, those sugar protons that are in closest contact with the macromolecule in the binding pocket receive the most saturation, and hence it is possible to infer the binding epitope of the glycan, i.e. a mapping of which protons are in closest contact with the protein surface. [428, 429]

The STD intensity (I_{STD}) is calculated as:

$$I_{STD\%} = \frac{I_o - I_{sat}}{I_0} \qquad (10)$$

where I_0 is the intensity of a signal in the reference spectrum and I_{sat} is the intensity of the same signal in the saturated spectrum.

There are several experimental aspects of STD NMR approach that should be carefully considered: i) the [Ligand]:[Protein] ratio; ii) the shape and power level of the selective saturating pulses; and iii) the irradiation frequencies used on- and off-resonance. [457] For the ligand to fully populate the binding site of the protein receptor, under the fast exchange conditions discussed above, a large excess of ligand over the protein is needed, so it is usual to aim for a 25:1 to 200:1 ratio. The fact that the absolute amount of protein needed is minimal makes this approach very inexpensive relative to other techniques (mainly protein-based), particularly since there is also no need for isotopic labelling. Turning to the shape of the selective pulse, Figure 20(c) shows the pulse sequence of a general STD NMR experiment. This typically consists of a train of low-power Gaussian-shaped pulses, that are applied to a selected frequency so as to selectively saturate specific protein protons, followed by a 90° hard pulse to convert the spin populations into observable transverse magnetisation (Figure 20(c), orange square). The power and duration of the shaped pulse are set to cover a bandwidth of about 100 Hz, while the number (n) of pulses in the train is adjusted to obtain the desired total saturation time. The experiment is run in an interleaved fashion, in which the reference (off-resonance irradiated) and saturated (on-resonance irradiated) spectra are both averaged over the same time period. Finally, regarding the irradiation frequency, the strongest requirement is for it to be applied to a spectral region devoid of ligand signals. Generally, the aliphatic region is chosen, between δ 0 and 1 ppm. Carbohydrates have the great advantage of also allowing saturation of the protein aromatic residues between δ 6.5 ppm and 8 ppm, which is often not possible when applying STD NMR in drug discovery, since lead compounds are usually very rich in aromatic moieties, whereas carbohydrates have no signals in this spectral region.

STD-NMR has been applied to characterise interactions of glycans and glycomimetics with a variety a lectins, antibodies and enzymes. Different versions and applications of STD-NMR experiments have been developed and presented to the scientific community since the early 2000's, highlighting the concept of group epitope mapping. [457] We will now describe some additional technical aspects that should be considered.

6.1.1.1. Multi-frequency STD NMR

The most relevant outcome of the STD-NMR approach (which can also be used for simple binding screening), is to map the epitope binding, i.e. the binding mode and orientation of the ligand in its binding pocket. Obviously, as a ligand-based NMR technique, STD-NMR does not provide any direct information concerning the protein.

Regarding the technical details of the STD-NMR experiment, saturating the sample at different regions of the protein spectrum will yield different epitope mappings for the same ligand. Detailed analysis of the changes between these different epitopes gives information about the presence of certain amino acid types lining the binding site (for example aliphatic or aromatic, if those regions were irradiated). This is the basis of the DEEP-STD NMR (DiffErential EPitope Mapping) experiment established by Angulo and coworkers. [459] Not only the binding epitope of the ligand is mapped, but key information about the type of amino acid residue near different parts of the ligand is provided. This approach, based on the concept of "multi-frequency STD-NMR", allows extraction of information about the ligand's surroundings. Multiple experiments are carried out, irradiating at different frequencies and measuring the different resulting responses. Carbohydrates, due to their narrow chemical shift distribution around δ 3-4 ppm, are ideal for this kind of study. DEEP-STD NMR is based on the observation of a stronger STD response on those ligand protons receiving saturation from directly irradiated protein residues at a certain on-resonance frequency (dipole-dipole inter-molecular direct NOE), in comparison to the saturation received when the irradiation is applied at another frequency. Comparing these differential STD-NMR responses, a map can be made of the architecture of the residues surrounding the ligand, and of which kinds of residue are contacting which kinds of ligand protons, as sketched in Figure 21a.

For carbohydrate studies, aliphatic and aromatic irradiation enables identification of aromatic-carbohydrate stacking [460] and aliphatic interactions, usually involving N-acetylated sugars. In a seminal study, Monaco *et al*. [459] successfully applied DEEP-STD NMR to two models: 2,7-anhydro-α-N-acetylneuraminic acid bound to GH33 (Figure 21b-d), and 3-nitrophenyl-galactosidase (3NPG) bound to cholera toxin (CTB).

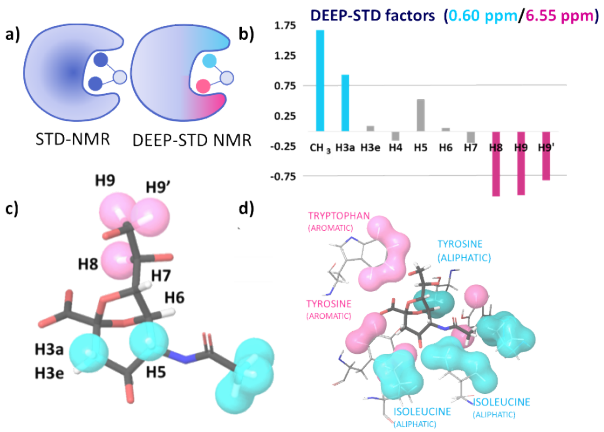

Figure 21. a) Cartoon representing the different kinds of information that are available from traditional STD-NMR and DEEP-STD NMR. b) DEEP-STD factors, highlighting contacts of ligand protons with protein protons in aliphatic residues (teal bars, positive values) and protein protons in aromatic residues (magenta bars, negative values), for 2,7-anhydro-α-N-acetylneuraminic bound to GH33. c) Alternative representation of the DEEP-STD data on the 3D structure of the ligand and d) crystal structure of the 2,7-anhydro-α-N-acetylneuraminic/GH33 complex (PDB ID: 4X4A) , highlighting the different ligand regions contacting aliphatic vs. aromatic residues on the protein, in good agreement with the DEEP-STD factors histogram. Adapted from ref [459].

For the 3PNG/CTB complex, irradiation of the protein aromatic residues would not be helpful as it would also directly irradiate ligand protons. This example shows that, in these situations, the β/γ protons of polar residues can be irradiated instead, at around 2.0-2.5 ppm, as this region is most often free from glycan peaks. In the same work, [459] an alternative approach was also proposed, exploiting differential solvent composition (D_2O:H_2O 10%:90% vs. D_2O:H_2O 90%:10%), showing that ligand protons close to slowly exchanging exchangeable protein protons receive less saturation if the latter are partially exchanged to deuterions instead of protons. This simple method allowed identification of contacts in arginine-rich binding sites, which is also a common scenario in carbohydrate binding. If the binding pocket is known and a crystal structure is available, DEEP-STD NMR can also be used to identify a "fingerprint" for a novel ligand, and compare its DEEP-STD pattern to that of a known ligand. Indeed, the use of the 3NPG/CTB complex as a model to study 6 novel leads [461] allowed confirmation of their binding orientations in the same binding subsite as the 3NPG "probe". In the same system, application of inter-ligand STD-NMR [462] showed that, provided two ligands bind adjacent to each other, multi-frequency STD-NMR can be used to infer their relative orientation, in a similar fashion to the ILOE experiment. [463]

Several applications of multi-frequency STD-NMR have been reported in the carbohydrate field, such as the challenging study of the interaction of the exopolysaccharide produced by *Burkholderia multivorans* C1576 (EpolC1576) with the antibiotics kanamycin and ceftadizime. [464] In this study, the non-canonical carbohydrate receptor was irradiated at 3.2 ppm (on the CH protons) and at 1.2 ppm (on the methyl groups) to study the binding mode of the antibiotics with the biofilm. Interestingly, in this case, the polysaccharide itself acts as the receptor for the antibiotic ligands.

6.1.1.2. Expanding ^{1}H STD-NMR to further dimensions.

The potential of STD-NMR for the study of protein-carbohydrate interactions has been clearly shown to be very wide-reaching for many types of receptors, [465-467] including enzymes [468-476] antibodies, [477-482] and lectins [483-498]. It has also been applied to characterize binding of glycoconjugates to nucleic acids. [499] STD-NMR has been crucial in structural investigations of glycan-receptor complexes of high chemical complexity and biological and therapeutical relevance. Indeed, given the key role of glycans in infection events, there are many studies of the interactions of glycans and glycomimetics with lectins and antibodies related to viral and bacterial infections. STD-NMR data have been of paramount importance in dissecting many of these interactions in systems related to HIV, [500-505] influenza and coronavirus, including SARS-CoV-2. [506-510] Interactions with bacterial receptors have also been the target of numerous investigations, [511-524] also within the fascinating world of gut microbiota. [525-527]

For complex glycans, where the overlap problem may hinder derivation of the binding epitope, analysis of the observed STD signals may be rather difficult or even impossible. Various modifications have been implemented, including the use of homodecoupling. [528] However, the best results have been achieved by the concatenation of the STD element with other NMR experimental pulse sequence modules, such as HSQC/HMQC or COSY/TOCSY, affording 2D

or pseudo-2D STD-NMR versions. [529] These experiments allow discrimination of the signals belonging to a given spin system and therefore identification of the actual STD-NMR signals and thus the real binders and/or epitopes. 1D TOCSY STD-NMR versions were used to study the interaction of three- to six- residue fragments of the *Streptococcus* cell wall with a monoclonal antibody, [530] while the molecular recognition features and the recognised epitope of a complex bi-antennae N-glycan were revealed by using a 2D STD TOCSY experiment, solving the tremendous challenge of analysing the homonuclear STD of a undecasaccharide. [531] The influence of remote branching substituents in N-glycans on the binding mode of the whole glycan entity to a model lectin was also deduced by the use of homonuclear STD-NMR. [532] As further extension of the method, Voghterr and Peters proposed the use of STD-HMQC to efficiently screen entire libraries of randomly methylated ^{13}C labelled monosaccharides (some of which are almost identical and studied as cocktails), as bound to elderberry lectin. [533]

This conceptual advance opened the door to the use of other nuclei. STD INEPT was developed to detect STD-NMR on ^{13}C nuclei. [534] More recently, [535] Casablanca and co-workers showed that this experiment can also be used to acquire build-up curves (consecutive experiments at increasing saturation time). These record the mono-exponential growth of STD as a function of saturation time, before it reaches a maximum value. Analysis of the initial slopes of these curves enables elimination of the impact on the determined binding epitope of processes closely related to fast protein–ligand rebinding and longitudinal relaxation of the ligand protons, which affect the accumulation of saturation in the free ligand. [536] On this basis, the STD-INEPT experiment was especially useful to enable simultaneous characterisation of the epitope maps of a mixture of compounds. [535] The generation of pulse sequences with ^{13}C-filtering or editing modules has permitted the screening of complex mixtures, using a labelled spy molecule (a known binder to the specific target receptor) as a reporter of the possible binding of the molecules in the library to be screened. [537] Moreover, STD-HSQC experiments have been applied to disentangle the molecular recognition features of polyLacNAc moieties with galectins. [398] The chemical shift degeneracy problem was circumvented using the ^{13}C-labelling scheme described above, in which labelled Gal moieties were introduced at selected positions of the glycan chain using chemoenzymatic synthesis (Figure 22). Thus, the specific epitope within the polyLacNAc chain interacting with the different galectins was assessed. Interestingly, despite the strong structural homology that exists among the different galectins, there is a clear discrimination between terminal non-reducing and internal LacNAc moieties, depending on the specific galectin. This selective ^{13}C labelling concept, now applied to sialic acids, has also been used to demonstrate unequivocally the binding of exogeneous sialyl-glycans to the spike glycoprotein trimer of SARS CoV2, which displays 22 glycosylation sites per monomer [538]. The ^{13}C-labelled external sialic acid moieties were identified in a straightforward manner by adding the HSQC module (Figure 22), which facilitated the analysis, also carried out by homonuclear methods. [510, 539]

The use of relaxation-based ^{19}F-NMR to analyse glycan binding to receptors was described in Section 3.2.3. As expected, ^{19}F-NMR methods have also been widely employed in the context of STD-NMR, given the sensitivity (100% natural abundance and high gyromagnetic ratio) of this NMR active spin-½ nucleus. In particular, ^{1}H-^{19}F versions of the STD-NMR experiment have been proposed, using either direct fluorine observation after the protein saturation, or relaying the saturation of the ligand protons to the ^{19}F nuclei through the corresponding two-bond or three-bond ^{1}H-^{19}F couplings. As a proof of concept, STDreF was first proposed [540] using the complex of 2-fluoro-2-deoxy-D-glucose with Concavalin A as a model system, opening the route to applications of ^{19}F-based STD-NMR studies on the interactions of ^{19}F-containing glycomimetics. [154, 156, 541, 542] Since these variations on STD-NMR were mainly designed for efficient ligand screening, optimizing spectral simplicity and resolution, the information on the binding epitope was restricted to the geminal- and trans-vicinal neighboring positions relative to the fluorine atom. To move beyond those limitations, a 2D

STD-TOCSYreF experiment was later proposed. [543] In this case, the use of a TOCSY module allows transfer of the generated STD effects throughout the complete spin system of every fluorinated monosaccharide unit within a given oligosaccharide, thus offering a straightforward method of epitope mapping.

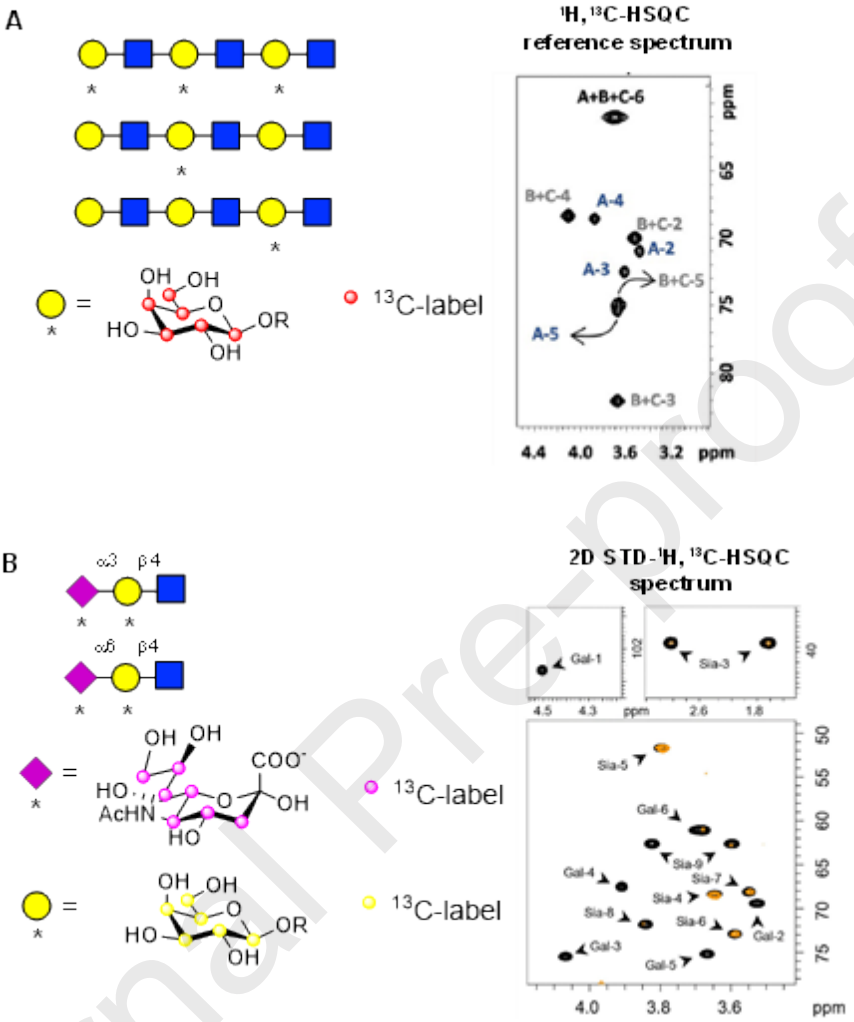

Figure 22. The selective ^{13}C-labelling concept has been applied to distinguish the specific Gal moieties that are recognized by a panel of human galectins [398], and to assess the recognition of exogeneous sialic acids by the highly sialylated spike glycoprotein of SARS-CoV2. Adapted from references [398] and [538].

This concept has been applied to complex branched high-Man-type N-glycans. [544]. In this case, the analysis of the STD buildup curves were acquired and allowed to obtain accurate binding epitopes for the fluorinated Man-9 N-glycan to DC-SIGN, a C-type lectin [545] in dendritic cells that plays a key role in pathogen infection.

It is also worth briefly mentioning that STD-NMR is not only a tool for screening binding and mapping binding epitopes. It can also be used to measure K_D for the interactions under investigation. As initially discussed, due to the K_D window covered by STD-NMR (usually between 10^{-8} and 10^{-3} M), it is an ideal tool to study and characterise weak complexes such as protein-carbohydrate interactions. A thorough explanation of how to use STD-NMR titration to measure K_D has been provided by Angulo and Nieto. [536, 546] Building on this, Monaco

et al. have described Imaging STD-NMR, [547] a novel methodology that is able to measure K_D values directly in a single NMR tube. As model systems for demonstrating a proof of concept, the complexes formed between GcNAc/WGA lectin and 3NPG/cholera toxin were studied.

6.1.1.3. Towards native-like conditions: On-cell STD-NMR

STD-NMR experiments are highly versatile and have been also been employed to monitor interactions between ligands and receptors presented *on-cell*, that is to say on a cell surface, thus providing a first hint of the molecular recognition features in conditions close to those existing in the biological milieu. Given the many crucial cell-pathogen, cell-cell, and cell-matrix processes involving glycans and their receptors that take place *on-cell*, this approach represents a distinct conceptual approach. Following the pioneering work of Jimenez-Barbero and coworkers on DC-SIGN interactions, [548] several applications have employed this experiment, also taking advantage of HR-MAS methods. [549] Other elegant applications from Airoldi's group [550, 551] involved the screening of a series of new adhesin ligands versus bacterial FimH to develop future FimH inhibitors to combat UTIs (urinary tract infections), while the interaction of sialoglycans with the hemagglutinin of influenza-virus expressed in transfected human cells has also been shown by STD-NMR. [552] Usually, STDD (STD difference) variants are employed in which the final STD NMR spectrum recorded for the ligand in the presence of the cells displaying the receptor is subtracted from that recorded for the ligand alone and/or from the cells with the receptor alone and/or from the ligand in the presence of cells without the receptor (if available). With all these control experiments, the epitope can described in a reliable and robust manner. The *on-cell* STD-NMR experiment has also been successfully applied to characterize high-affinity ligands, derived from sialic acid with aromatic fragments at C5 and C9, for CD22 (Siglec-2), using intact Burkitt's lymphoma Daudi cells. [553] The on-cell experiment will also benefit from new approaches to deal with some intrinsic problems with the experiment, such as cell sedimentation and survival. The use of methylcellulose hydrogels, as proposed by Konrad and coworkers, [554] provides new avenues to improve these experiments that take the system into almost native conditions.

A breakthrough field of investigation that has attracted worldwide attention in the last decade or so is the use of NMR spectroscopy directly in-cell. In-cell NMR's aim is to provide a complete description of biological interactions in their natural environment, without losing the atomic resolution offered by NMR. Protein conformation in its natural environment can sometimes differ drastically from the conformation detected *in vitro*, and such a change may affect its recognition properties. The natural cell environment is much more complex than the buffered solution in which purified receptors are normally observed by NMR, since many additional protein-protein interactions, as well as the presence of small binders and protein post-translational modifications, can strongly affect the recognition. Moreover, aspects such as viscosity and pH of the different compartments must be considered. In-cell NMR offers a unique tool to take into account of all these considerations. Although sugar binding studies have not still been carried out, there is no doubt that they will be accomplished in the coming years. Given the promiscuity of lectins, monitoring their conformational, dynamics, and recognition events is rather challenging. Nevertheless, it is expected that new developments of *in-cell* / *on-cell* NMR experiments [555, 556] will also be exploited in the glycan field. Very probably, new advances in hyperpolarization, including the use of Dynamic Nuclear Polarization (DNP) NMR methods [557-559] and new radical molecules, [560, 561] will permit exploration of these events within the cell in the near future. This goes beyond the structural characterization of cell wall polysaccharides, [562-564] a field that is rapidly advancing thanks to the use of dynamic nuclear polarization solid-state NMR, although it is beyond the scope of this review. Nevertheless, the transfer of such new technologies to the liquid state may provide the impetus for breaking the limits in this area.

The STD-NMR experiment has also been applied to direct NMR-based screening of active molecules present in extracts of medicinal species. The crude mixture and the target protein receptor were mixed in the NMR tube and STD-NMR, complemented by tr-NOESY and DOSY experiments, was carried out. When the target receptor is a lectin, the glycans present in the mixture can be detected and further identified by standard NMR methods. [565, 566] It has been shown, with the use of a mushroom extract as model case, that this protocol may provide a fast and simple method to detect the presence of ligands for a target receptor, which would be particularly useful in natural product chemistry.

Given the intrinsic low to medium affinity of glycan-protein interactions, which are rarely at the nanomolar level, multivalency is used in natural systems to enhance binding and to provide the biological signal that affords the biological response. Dealing with multivalent systems is not straightforward, especially from the ligand NMR perspective. [567] Nevertheless, STD-NMR, [568] assisted by DOSY, has been instrumental in accurately establishing the binding epitope of a multivalent ligand bearing a hyaluronic acid glycomimetic when interacting with langerin, [545] a key C-type lectin for viral infection. The STD-NMR data obtained, which included the description of the aggregation behaviour of the multivalent glycomimetic as described by other biophysical techniques such as DLS and TEM, suggested that binding takes place at a non-canonical site, [568] Other alternative NMR methods to deal with multivalent processes are described in section 6.2.

6.1.2. Exchange transferred NOE: the Tr-NOESY experiment

A paradigmatic experiment in ligand-based NMR molecular recognition is based on the so-called exchange transferred Nuclear Overhauser Effect spectroscopy (Tr-NOESY), first proposed in an intermolecular version by Bothner-By in the 1970s, [569] for detecting ligand binding and specific contacts with protein side chains, and later as an intramolecular version by Feeney and co-workers, to report on the conformations of ligands in the bound state. [570]

Although STD NMR provides invaluable information on the contacts of ligand protons with the protein in the bound state, it does not deliver conformational information, being unable to distinguish whether the ligand conformation is changed upon binding or, in contrast, its major conformation in free solution is selected unchanged by the protein. As an excellent complementary technique, the very powerful Tr-NOESY is the technique of choice to probe the ligand bound conformation, [529, 571-576] and has been widely applied in the glycan field. [577] The transfer of structural information (NOEs) from the bound to the free state allows the conformational analysis of ligands in high molecular weight complexes, which otherwise would not be accessible by direct NMR analysis due to extreme line broadening, or in complexes with low solubility that would be intractable by receptor-NMR approaches. [529]

As with STD NMR, the success of the Tr-NOESY experiment depends very strongly on the residence time of the ligand in the binding site (equal to $(k_{off})^{-1}$, the reciprocal of the dissociation rate constant), the molar excess of ligand over receptor, the size of the receptor (its correlation time), the binding affinity, the relaxation delay between scans, and the NOE mixing time. Thus, these are parameters that should be known, guessed, or (better) optimized for each particular system.

In terms of NOE observation, small/medium sized glycans typically show weak/medium positive intramolecular NOE intensities (in practical terms, this means that NOE cross peaks appear inverted with respect to the diagonal peaks in 2D NOESY experiments, Fig. 23). For such molecules, the NOE builds up with mixing time reaching a maximum value on a second- or high millisecond-timescale. In contrast, large molecules such as proteins show strong negative intramolecular NOE intensities (NOE cross peaks appear with the same sign as the diagonal peaks in 2D NOESY experiments) that build up with mixing time reaching a maximum value after a much shorter time (often less than 200 ms). We emphasize here the fact that in

trNOE experiments to determine bound ligand conformation we are dealing with "intramolecular" NOEs, in contrast to "intermolecular" NOEs as would be the case for STD NMR experiments.

When a small molecule, such as a mono- or an oligo-saccharide, binds to a large receptor (e.g. a lectin, an antibody, etc.), its tumbling properties in solution change dramatically, from a fast rotational diffusion (ps timescale) typical of small molecules, to a slow rotational diffusion (ns timescale) typical of macromolecules with large hydrodynamic radius.

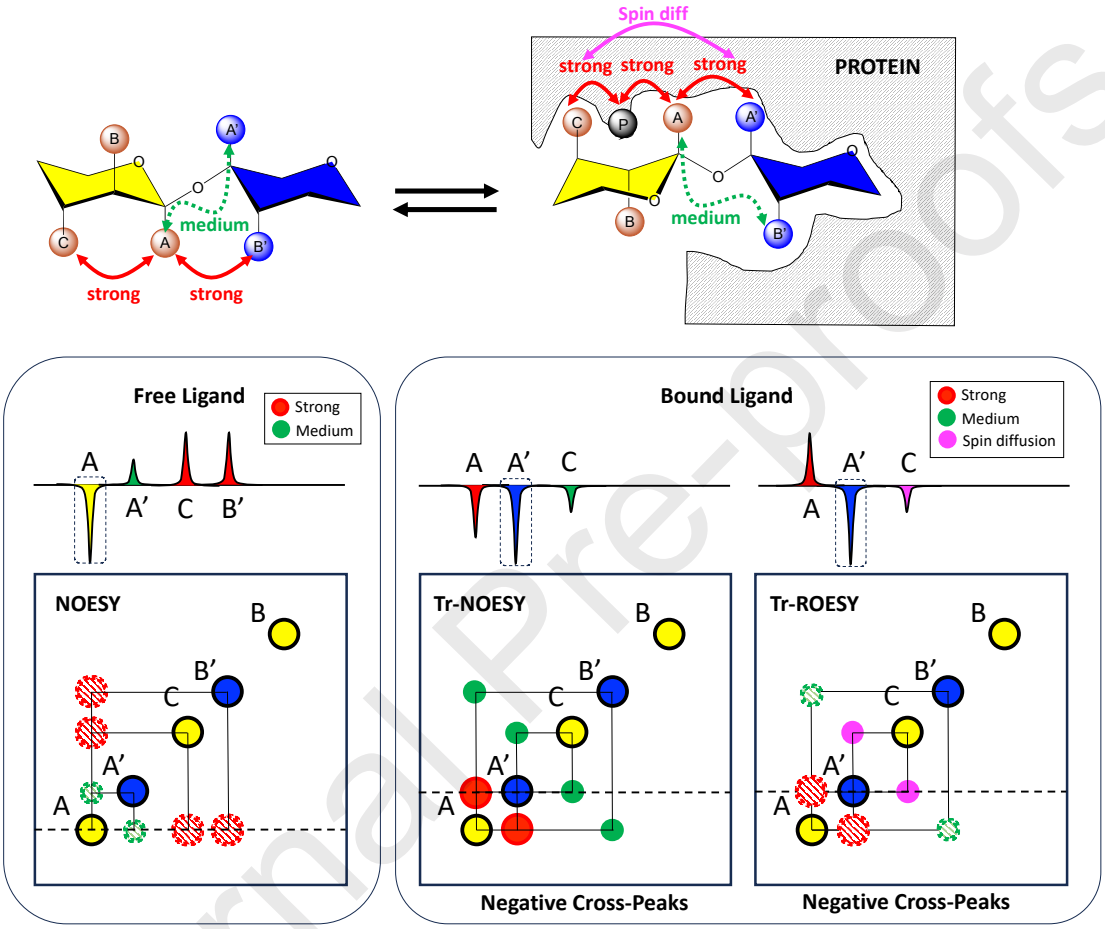

Fig. 23. Tr-NOESY experiments to determine the bioactive conformations of glycan ligands bound to proteins. Cartoon representation of the binding of a disaccharide to a protein receptor involving a ligand conformational change upon binding. In the 2D representations, cross peaks shown as solid colours have the same signs as diagonal peaks, cross peaks shown as cross-hatched colours have opposite signs to the diagonal peaks. Comparison of NOESY and Tr-NOESY experiments demonstrate the change in cross peak signs between the two experiments, indicating binding, and the change in cross peak pattern between the free and bound spectra indicates that there is a conformational transition upon binding. Tr-ROESY experiments [578, 579] may reveal the existence of "false" NOEs due to protein-mediated spin diffusion linking ligand proton pairs that in reality are far apart.

For cases of very strong binding (e.g. for a low nM to pM dissociation constant), a sample containing protein and ligand in a 1:1 ratio would exist almost completely as the complex, exchange between the free and bound states would be negligible, and NOEs between ligand protons would behave in an essentially identical fashion to NOEs between protein protons, i.e.

they would be negative and depend very largely on the internuclear separation in the bound state. In contrast, for cases of medium or weak binding, both the free and bound states would be appreciably populated (depending also on the protein:ligand ratio), and ligand molecules would exchange between the two states at appreciable rates. NOEs between ligand protons then become an average between the free and bound state contributions, making them dependent not just on internuclear separation in the bound state but also on the kinetics and thermodynamics of complex formation, i.e. the rate constants of the association and dissociation processes, k_{on} and k_{off}, as well as the free and bound fractions, f_L^B and f_L^F (in principle, the internuclear separation in the free state could also be relevant, though in practice its influence is very often negligible, see below). [529, 571-577]

$$P + L \underset{k_{off}}{\overset{k_{on}}{\rightleftharpoons}} PL$$

$$k_{ex} = k_{off} + k_{on}[P] \quad (11)$$

Tr-NOESY works for protein-ligand interactions falling within the so-called "fast exchange approximation", i.e. k_{ex} much higher than chemical shift differences of the ligand between free and bound states ($k_{ex} \gg |\Omega_F - \Omega_B|$), and much higher than the relaxation rate differences of the ligand between free and bound states ($k_{ex} \gg |R_F - R_B|$). Under these conditions, for a large excess of ligand over the protein, only one set of ligand NMR signals is detected (basically the free ligand signals) and the measured intramolecular cross-relaxation rates (σ_{obs}) are weighted averages between the intramolecular cross-relaxation rates of the ligand in the free state (σ_F) and the intramolecular cross-relaxation rates of the ligand in the bound state (σ_B) [529, 571-573]:

$$\sigma_{obs} = f_L^F \sigma_F + f_L^B \sigma_B \quad (12)$$

For the sake of simplicity, in this review we use the term NOE as equivalent to cross-relaxation rate, σ_{obs}, though strictly speaking they are only equivalent in the initial rate regime. In this way, the observed intramolecular ligand cross-relaxation rate (σ_{obs}) is termed a transferred NOE (Tr-NOE) because, given fast exchange conditions (in practical terms: $k_{off} \gg \sigma_B$), the much larger absolute magnitude of the NOE in the bound state dominates the average ($|\sigma_B| \gg |\sigma_F|$), so that the observed NOEs report on the conformational properties of the ligand in the bound state, after the bound NOEs are "transferred" to the free state ligand signals where they are observed.

For optimum observation of Tr-NOEs, the NOESY mixing time should be short enough to minimise free state NOE contributions (which grow only slowly), but long enough to allow significant NOE intensity to build up in the bound state (where there is faster growth, but also faster decay). In some cases, for small mono- or oligosaccharides, conditions (viscosity, temperature, magnetic field, etc.) can be found to make free state NOEs intrinsically negligible (by approximating the zero-crossing condition, $\omega\tau_c \approx 1.12$, where ω is the Larmor frequency expressed in rad s^{-1}) so that no contribution from the free ligand will be present. Confirmation of this situation requires recording NOESY spectra on the free ligand alone under the same conditions as for the sample containing the protein.

In order to produce a sufficient concentration of the complex, a large excess of the ligand over the protein is typically used, which makes f_L^B usually much ***smaller*** than f_L^F. On the other hand, to observe Tr-NOEs, the required condition $f_L^B \sigma_B \gg f_L^F \sigma_F$ means that f_L^B has to be sufficiently ***large*** that σ_B can still dominate the average (σ_{obs}). These conditions pose much stricter experimental restraints for Tr-NOE observation than those for STD NMR experiments, where very large ligand-to-protein ratios can be used, providing only that specificity is retained. Ratios from 10:1 to 50:1 are typically found in reported Tr-NOE experiments with carbohydrates,

although if no thermodynamic or kinetic data are available for the studied protein-carbohydrate complex, it is advisable to monitor the Tr-NOE as a function of protein:ligand ratio in a titration experiment, in order to find optimum conditions.

To accurately analyse the NOE information from Tr-NOE experiments, so as to investigate the bound conformation of a ligand, it is very important to take into account the possibility of detecting “false” NOE contacts in the bound state that arise due to indirect pathways of dipolar relaxation, for instance intermolecular spin diffusion processes (Fig. 24). [573-579] In this way, a strong apparent Tr-NOE can develop between two ligand protons that are far apart in the bound state, but which nonetheless interact indirectly due to a relayed exchange of magnetization through an intermediate proton in the protein that is sited in the vicinity of both ligand protons (Fig. 24). Unfortunately, this effect can be very efficient in cases of high molecular weight complexes with long rotational correlation times, so caution is essential to consider this possibility during interpretation. In particular, for carbohydrates, the number of structurally determinant NOE contacts is typically low, in comparison to the situation for other biomolecules, so that very careful interpretation is essential to gain an accurate structural view of the ligand in the bound state.

Despite these caveats, the experiment has been widely employed to deduce the conformations of a variety of saccharides and glycomimetics bound to lectins, enzymes, nucleic acids, and antibodies. [574, 577, 581, 582] For relatively small sugars, the simple observation of a change in sign of the NOE cross peaks of the ligand in the presence of a putative receptor (from positive to negative, given the large difference in the effective correlation time of the ligand between the free and bound forms) affords an unequivocal indication of binding. For more complex molecules, larger than tetrasaccharides (which already show negative NOE cross peaks in the free state at high magnetic fields), the analysis of cross-peak intensities needs to be carefully carried out, and compared with the data observed for the free form. As with regular NOESY-based conformational analysis, the use of build-up curves is highly advisable, given the strong possibility of the existence of spin diffusion, especially for large receptors that contain many protons close to the binding site. The use of semi-quantitative methods, based on analysis of a full relaxation matrix in the presence of exchange, is also highly advisable for obtaining the most accurate estimates of inter-proton ligand distances and, therefore, of the bound conformation. If protein-mediated intermolecular spin diffusion Tr-NOEs are suspected, an easy alternative is to run the equivalent Tr-ROESY experiment, measuring Tr-NOEs in the rotating frame (Tr-ROEs). [578-582] In this experiment, all molecules, independent of their molecular weight and the effective correlation times of the proton pairs that give rise to the NOE, effectively behave as if they were within the fast-tumbling limit, so that direct ROEs are positive (i.e. appear as cross peaks having opposite sign to diagonal peaks), whereas cross peaks dominated by intermolecular spin diffusion appear as negative (Fig. 23).

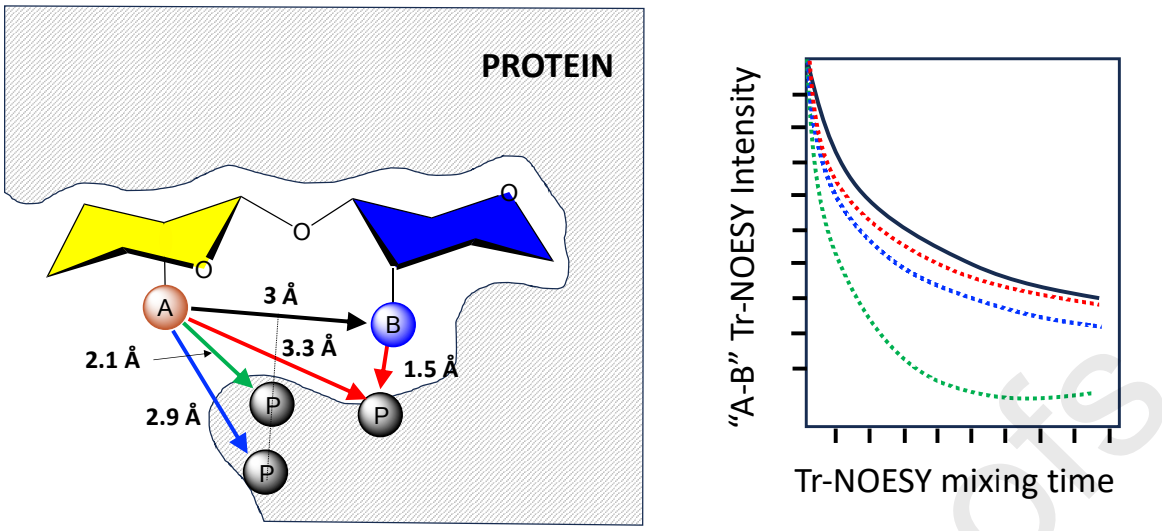

Fig. 24. Protein-mediated spin diffusion in Tr-NOESY experiments. Cartoon representation of the impact of the presence of a protein proton (P) situated in the vicinity of the ligand proton pair (A-B). Even when the ligand interproton distance A-B is fixed, the closer the protein proton P gets to both ligand protons, the larger the observed Tr-NOE intensity becomes, leading to an overestimation of the NOE that can be mistaken for an extremely close proton-proton spatial contact in the ligand. Contributions from protein-mediated spin diffusion can be easily spotted by Tr-ROESY experiments (Fig. 23)

Other methods also allow spin diffusion effects to be detected. For instance, Tr-NOESY and/or Tr-ROESY cross peaks can be quantitatively analysed with a full matrix relaxation approach that includes the exchange process. Other methodology to distinguish direct from spin-diffusion cross peaks is based on using the QUIET-suite of experiments. [583] In this case, a particular region of the spectrum, in which the frequencies of the spin-diffusion-mediating spins is located, is inverted, thus impeding their participation in the cross-relaxation process.

The medium/weak affinities typically found in protein-carbohydrate interactions are particularly suitable for the observation of Tr-NOEs, and many cases have been reported in the literature. [574, 577, 581, 582] In most of the cases, the analysis of NOESY and Tr-NOESY experiments of carbohydrate ligands has reported similar NOE patterns, indicating that there is no conformational selection during the process of protein-carbohydrate complex formation, and typically the global minimum energy conformer of the carbohydrate is what is recognised by the receptor. Cases of interactions of proteins with intrinsically dynamic ligands are of particular interest, as, for example, iduronate-containing heparin-like glycosaminoglycans (GAGs). In contrast to most monosaccharides, iduronate rings are not rigid, and those found internally in GAG chains show a typical conformational equilibrium in the free state between a chair ($^1C_4$) and a skew boat (^2S_O) hexopyranose conformation. Nature has evolved GAG-binding proteins endowed with different architectures and dynamics of their GAG binding sites, so that some of them can preferentially bind to GAG ligands with their iduronate rings only in one of the two limiting conformations, [584, 585] whereas others can recognise GAG ligands preserving the intrinsic iduronate conformational equilibrium. [294, 586]

Tr-NOE studies on the recognition of small heparin-like trisaccharides by langerin (Lg), a C-type lectin important for pathogen recognition and with an ability to recognise sulphated carbohydrates, demonstrated that the Ca^{2+}-dependent binding of the trisaccharides occurs without alteration of the conformational equilibrium of the central iduronate ring. [294] In a study of another biologically relevant GAG-binding receptor, the acidic fibroblast growth factor

(FGF1), NOE data (from ^{13}C filtered NOESY experiments) showed that the protein is able to recognise a heparin-like hexasaccharide without perturbing the equilibrium between the two iduronate conformations. [546] Other examples of protein binding with preservation of the intrinsic conformational equilibrium of the ligand in the free state have also been reported for synthetic non-natural mimetics of carbohydrates (glycomimetics). For example, in the case of *S*-glycosides, [587-589] the interglycosidic linkage shows enhanced flexibility relative to O-glycosides, leading to the existence of a mixture of conformations in the free state. NOE data showed that a model glycosyl hydrolase, *E. coli* β-galactosidase, is able to accommodate different geometries of thiodisaccharide glycomimetics, emulating the distorted geometries present in the transition state for glycosidase-mediated hydrolysis. [212] In all these cases, the ability of the receptor to preserve the intrinsic conformational flexibility of the ligand provides a favourable thermodynamic impetus for binding, as it reduces significantly the entropic penalty that would be incurred by the conformational selection of one of the ligand conformers.

In some cases, Tr-NOE studies have demonstrated that the protein receptor is able to recognise only one of the different conformers of the ligand. For example, in contrast to the above-mentioned case of the thiodisaccharide glycomimetics, the same *E. coli* β-galactosidase was demonstrated to recognise a high-energy conformer of C-lactose, a non-hydrolysable substrate analogue, which has a population in the free state of less than 5% [98, 590]. Other C-glycosyl compounds have also been demonstrated by Tr-NOE studies to undergo conformational selection upon binding to human galectin-1 (hGal-1), again with selection of conformers other than the global minimum energy conformer. [207]

An interesting demonstration of the interplay between kinetics, thermodynamics, and ligand-to-protein ratio for optimum Tr-NOE observation [591] came from the study of molecular recognition of sugar nucleotides UDP-Glc and UDP-Gal by the human blood group B galactosyltransferase (GTB). First STD NMR observations demonstrated that ligand exchange between free and bound forms was fast enough on the relaxation timescale to produce sizeable STD signals. Surprisingly, however, no Tr-NOEs could be detected for either of the two ligands under different ligand-to-protein ratios typical for Tr-NOE experiments (from 10:1 to 30:1). The answer to this puzzle came from a quantitative analysis of the STD NMR build-up curves, yielding dissociation rate constants k_{off} in the range of 10 Hz. The larger kinetics window for STD NMR observation allowed binding to be detected, but such a low k_{off} for weak/medium binders lies at the limit for observation of transferred NOEs. Relaxation rate matrix calculations predict that in such cases the observation of transferred NOEs becomes possible if the ligand-to-protein ratio is significantly reduced. In this way, repetition of the experiments at a much lower ligand-to-protein ratio of 2:1 led to transferred NOEs becoming clearly observable, as predicted by theory for a slow dissociation process. Such a low ligand-to-protein ratio required the use of a perdeuterated enzyme, in order to be able to clearly distinguish the intramolecular ligand Tr-NOEs, while eliminating spin diffusion via protein protons. Finally, the Tr-NOE study in this system showed the existence of ligand conformational selection by GTB, as both sugar nucleotides bind in a folded-back conformation along the pyrophosphate linkage, which is sparsely populated in solution. [591]

Overall, the combination of these methodologies provides a solid perspective on the behavior of glycans at their receptor binding sites. [592] For instance, we can mention the combination of STD and Tr-NOESY experiments, assisted by molecular docking methods, as a robust protocol for analysing the binding of a large number of natural and non-natural ligands to cellodextrin phosphorylase, a natural catalyst for the synthesis of cellulose oligomers. The capacity of this enzyme to interact with a variety of donor and acceptor ligands makes it ideal for accessing a variety of cellulose-based structures with different properties. [593]

As an alternative, Tr-ROESY experiments have shown themselves to be useful for analysing glycan/receptor systems that display slow exchange on the chemical shift time scale. One intrinsic feature of ROESY experiments is that they allow a distinction between direct NOE (positive) and exchange (negative) cross peaks. The exchange cross peaks allow assignment of the chemical shift for a given proton in the bound state, and thus potentially characterisation of its chemical environment. Given the ubiquitous participation of aromatic moieties (Trp and Tyr especially) at the glycan-binding sites in the proteins, the protons of the glycan in the bound state can show dramatic upfield shifts (ca. 2 ppm) and can thus be easily detected. Moreover, from the quantitative analysis of EXSY data, the kinetic parameters of binding can be deduced, allowing energy barriers to be derived. In particular, the conformational entropy of the antigenic determinants of the A and B blood group oligosaccharides when interacting with galectin-3 has been shown to play a major role in the molecular recognition event, opening the door to the design of new binders based on the proper presentation of the glycan binding epitope, without providing additional stabilizing glycan-protein contacts. [120]

6.1.3. Further applications of ligand-based NMR methods: unravelling glycan-virus interactions

One of the major advantages of ligand-based NMR experiments is that the glycan interaction under investigation can involve extremely high molecular weight receptors, as long as the binding falls within the fast exchange range. In particular, STD NMR spectroscopy has been successfully applied to directly investigate the molecular recognition of glycans by various viruses. Key examples include studies on human norovirus, [594] rabbit haemorrhagic disease virus, [595] bovine norovirus, [594] influenza virus, [596-599] rotavirus, [600, 601], polyomavirus, [8] and virus-like particles (VLPs). [594, 596, 602]

From an NMR point of view, there are two favourable conditions for studying glycan-virus interactions: firstly, the extremely high molecular weight of the virus particles allows very efficient spin diffusion to occur, making the experiment very sensitive, and, secondly, the extreme broadening of the protein signals on the virus surface allows the saturation of the viral proteins to be induced very far from typical glycan signals, at chemical shifts for which no efficient saturation would be produced on medium/small sized proteins (e.g. allowing irradiation down to δ -2 or -3 ppm), making the experiment suitable for almost any type of glycan, independent of the ligand chemical shifts.

However, for STD NMR on whole viruses or VLPs, [603, 604] some important parameters of the experimental setup have to be taken into account. The first is the relaxation delay of the STD NMR experiments. [603] Due to the high molecular weight of the virus, long T_1 relaxation time constants are expected, which increase with the correlation time of the particles. As typical STD NMR experiments are recorded in an interleaved manner, i.e. alternating between on- and off-resonance experiments (to avoid the effects of drifts due to instrumental instabilities), the interscan relaxation delay should be long enough to ensure that no saturation remains after the on-resonance experiment. Rademacher and Peters have shown that in some cases relaxation delays in the order of tens of seconds are required, [603] and the optimum can indeed be found experimentally (Fig. 25a,b). Secondly, care must be taken with the off-resonance frequency of the experiment. The extreme broadening of the protein signals from the surface of the virus makes it possible to produce undesirable residual saturation of the proteins even in the off-resonance experiment, if typical chemical shifts for such non-saturating experiments are used (e.g. δ 40-50 ppm). The presence of saturation in the off-resonance experiment can dramatically reduce the sensitivity of the STD NMR experiment, especially considering the very efficient spin diffusion in such large particles, as it reduces the “contrast” of saturated signals (I_{sat}) by reducing the off-resonance intensity (I_0). As an example, Rademacher showed that to study the interactions of glycans with rabbit haemorrhagic disease virus (RHDV), an off-resonance frequency of δ +300 ppm had to be used to ensure maximum sensitivity. [595]

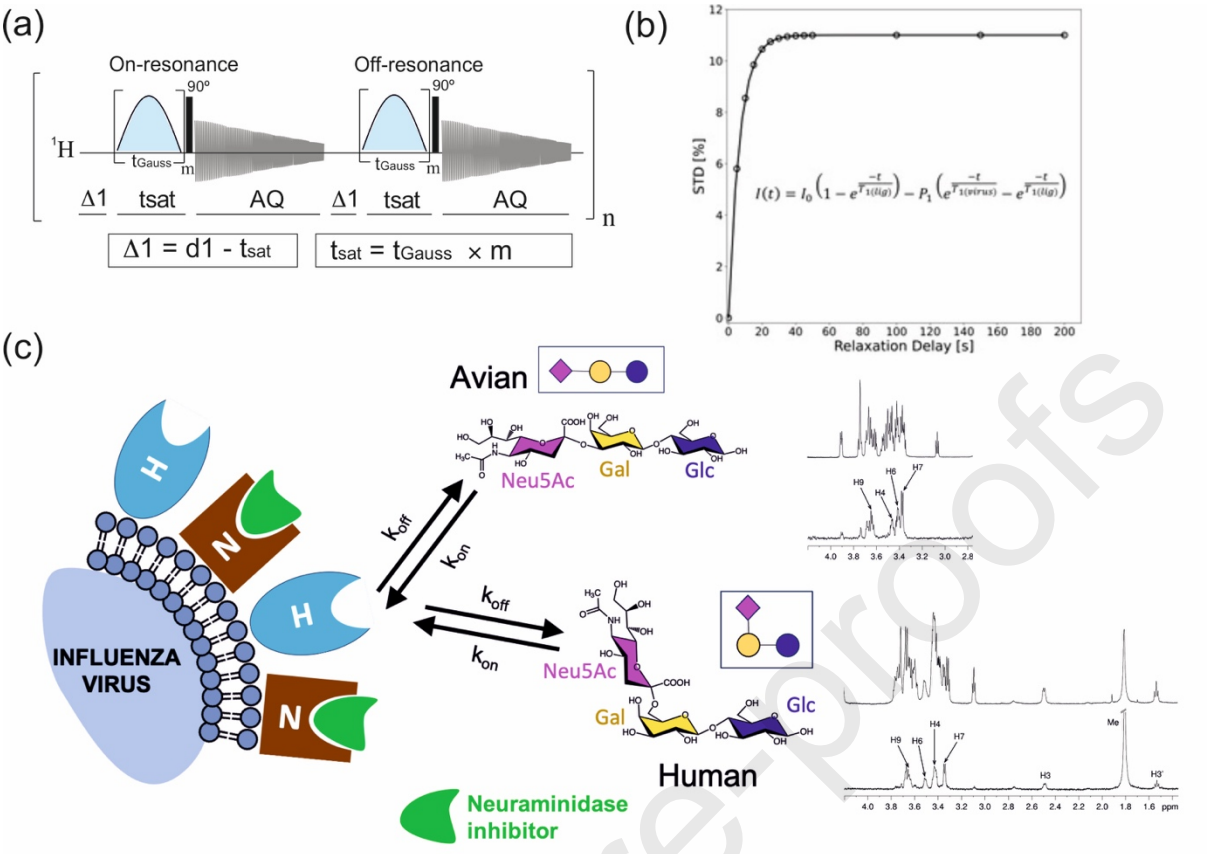

Fig. 25. STD NMR experiments to study glycan-virus interactions. (a) Pulse sequence showing interleaved measurements, where n is the number of scans; m is the number of shaped pulses of t_{Gauss} duration giving rise to the total saturation time t_{sat}; Δ1 is the interscan delay. (b) Effect of the relaxation delay on the observed STD NMR intensities, when the interscan delay Δd1 is varied while keeping on- and off-resonances constant (e.g. at -4 and +300 ppm). (c) Cartoon showing the investigation of sialyllactose binding to the influenza virus. The influenza virus contains the lectin haemagglutinin (H) and the enzyme neuraminidase (N). To prevent hydrolysis of the ligand by the N enzyme, an inhibitor is added at low concentration. Haemagglutinin H is specific for the type of glycan found on the avian respiratory tract (α2,3-sialyllactose) or on the human respiratory tract (α2,6-sialyllactose). STD NMR is able to determine the specificity of the influenza virus on a mixture of both ligands.

Relevant cases of biologically important glycan-virus interactions can be found in the literature. In the case of RHDV, an STD NMR study demonstrated that the minimal structural requirement for histo-blood group antigen (HBGA) recognition by the virus is the presence of fucose and galactose residues. [605] The molecular recognition of HBGAs and other glycans by human and bovine norovirus has also been thoroughly studied by STD NMR, concluding that α2,3-sialyllactose binds noroviruses without much participation of the terminal sialic acid residue. [594] A step-wise behaviour of the STD NMR signals upon titration of HBGAs to norovirus particles warned about an increased complexity in the molecular recognition process of the glycan by the virus, at first interpreted as a cooperative multistep process [565]. Later it was demonstrated that a process of deamidation of a specific asparagine in the proximity of the ligand binding site was responsible for the strange titration behaviour seen by STD NMR. [606] Haselhorst and co-workers have studied thoroughly the molecular recognition of glycans by influenza virus, employing low concentrations of a neuraminidase-specific inhibitor to avoid hydrolysis of the ligand, allowing them to study binding to the hemagglutinin (Fig. 25c). [596-

600] STD NMR has also played a significant role in unveiling the molecular details of the recognition of glycans by rotavirus, helping in determining host cell tropism of intact rotavirus particles. [599-601]

6.2. Receptor-based NMR experiments

Initial receptor-based NMR experiments to investigate glycan binding to lectin receptors employed chemical shift perturbation experiments. [607] The specific methodology focuses on the analysis of the chemical shift perturbations (CSP) of the NMR signals of the receptor upon systematic addition of different equivalents of the glycan, employing a titration protocol with a number of additions.

As in any receptor-based NMR experiment, the binding process is monitored by measuring the CSPs of the receptor's signals that take place due to the alterations in the local environment caused by the presence of the ligand, relative to the control experiment recorded for the protein in the absence of ligand. Increasing amounts of the glycan are added in a systematic manner, with calculated amounts of the titrating species adjusted according to the hypothesised binding affinity, always trying to achieve complete saturation of the system. The observed perturbations are used to calculate the CSP for each protein peak, using which the binding site can be identified. Even without previous assignment of the NMR cross peaks, this methodology allows detection of binding and estimation of binding affinity. Moreover, the exchange regime of the interaction (slow, intermediate or fast on the chemical shift time scale) can be deduced from the behaviour of the peaks during the titration. The K_D value can also be estimated, including quantitatively, if saturation is reached.

The detailed resolution achievable by NMR provides a precise analysis of the molecular recognition processes. In recent decades, with the spectacular advances made in molecular biology, many strategies have been devised for achieving uniform or specific isotope labelling (^{15}N, ^{13}C) of glycan-binding receptors, and dozens of saccharide-recognition events have been scrutinized. Careful analysis of the heteronuclear experiments recorded for labelled receptors in the presence of ligands may provide key information on the accurate location of the interaction site, as well as any accessory areas also perturbed by the glycan and, in some cases, characterization of dynamics.

Initial applications of receptor-based NMR experiments to monitor glycan-protein interactions employed standard homonuclear ^{1}H NMR experiments with unlabelled lectins. [608] In particular, hevein [609] and other proteins containing hevein domains [610] were employed as excellent models for assessing the key features of lectin-glycan interactions. Thus, changes in ^{1}H NMR chemical shifts allowed estimation of the equilibrium dissociation constants, K_D, for a variety of chitooligosaccharides. Moreover, the binding affinity data were complemented by the derivation of three-dimensional structures of the hevein-chitooligosaccharide complexes, using the standard ^{1}H-^{1}H TOCSY/NOESY-based approach to assign the protein NMR signals and the maximum possible number of intra- and inter-molecular sugar-lectin NOEs, sometimes employing ^{13}C-labelled oligosaccharides. The 3D structures provided an unequivocal demonstration of the key role of CH-π stacking sugar-aromatic interactions, [460, 611-615],especially between the less polar faces of the monosaccharides and the acetamide methyl groups with the aromatic side chains of Trp and Tyr moieties of the protein. These investigations in natural receptors have been complemented by other NMR approaches using simple models, usually incorporating ^{13}C labels, that have allowed precise quantification of the CH-π stacking interactions [616] under different conditions, [617] depending on the polarization of the C-H bond, [618, 619] the chemical environment, [620] and the nature of the solvent. [621]. The role of the intermolecular hydrogen bonds generated between, on the sugar, hydroxyl groups and/or the carbonyl and NH moieties of acetamide moieties, and on the protein, the carbonyl or NH groups of polar sidechains (especially those of Asp, Glu, His, Lys, and Arg) [10] has also been demonstrated and quantified by NMR. [622, 623]

Once labelled lectins became available on a routine basis, the standard ^{1}H-^{15}N HSQC-based CSP analysis was extensively employed for moderately sized receptors. [529] As is well known, when the receptor is too large for HSQC, transverse relaxation optimized spectroscopy (TROSY) variants can be used as an alternative, along with deuteration of the H-C protons of the receptor. For extremely large receptors, methyl-TROSY experiments are the method of choice for specifically-designed proteins that display a given methyl labelling pattern. This experiment, supported by mutation analysis, also allows the location of the glycan binding site to be determined.

In this way, the NMR analysis of the interaction of galectins with natural glycans, [624] with special emphasis on lactose and lactosamine derivatives, as well as in the histo blood group antigens and glycomimetics [625] has been extensively studied and described. For instance, the molecular features of interactions of galectin-3, [626] galectin-7, [627] and galectin-1 [628] have been disentangled, while the molecular dynamics associated with ligand binding have been scrutinized using NMR relaxation [629], again emphasising the essential participation of CH-π stacking sugar-Trp interactions and also highlighting the role of ligand conformational entropy, and of the ability of galectins to modulate the recognition. [630-634].NMR relaxation has been instrumental in distinguishing the differences between monomeric galectin-3 [120, 632] and the homodimer galectin-1. [119, 629] The interaction of galectin-4 with CD14, an intact glycoprotein decorated with ^{13}C-labelled glycans, has also been addressed by NMR, [430] as well as the differences in recognition features between different lectins for the same glycan epitope. [635] These investigations have been carried out using either standard CSP methods, hydrogen-deuterium exchange, [636, 637] comparison of data from different solvent mixtures, [638] or paramagnetic NMR. [209, 639, 640] Moreover, as will be described below, galectin-3 has been chosen as a model lectin for scrutinizing the role of crowding in molecular recognition events. [641]

From a global perspective, and to provide a full picture of the interaction between glycan ligands and protein receptors, it is highly beneficial to combine ligand- and receptor-based NMR methods. For instance, STD-NMR and Tr-ROESY, together with ^{1}H-^{15}N-HSQC experiments to monitor CSPs of the backbone amides of the protein upon ligand addition, as well as ITC methods and MD simulations, have been used to probe in depth the fine structural, thermodynamic, kinetic, and dynamic details of the interactions of the different monomer, dimer, and tandem-repeat galectins with blood type antigens and analogues. Depending on the particular galectin and its architecture (monomer: galectin-3; homodimer: Galectin-1, heterodimers: Galectin-4 and Galectin-8), different phenomena were detected, from the existence of subtle selectivity for the type of blood type antigen (Galectin-4), [122] or of exclusive specificity for a given sugar residue depending on the lectin domain at the heterodimer (Galectin-8), [121] or a key role of ligand conformational entropy for the monomer (Galectin-3), [120] through to the transmission of allosteric effects throughout the homodimer interface (Galectin-1). [119]

As mentioned above, the investigation of multivalent processes by NMR is challenging. In this context, the interaction of a variety of multivalent presentations of LacNAc moieties with two galectins (monomer Gal3 CRD and homodimer Gal1) has been addressed through a combination of ligand-based and receptor-based NMR experiments. [407] STD NMR was used purely to describe the interaction of the monovalent LacNAc presentations, while HSQC experiments carried out with the ^{15}N-labelled galectins were employed to monitor binding. Interestingly, no CSPs were observed, but the intensities of ^{1}H-^{15}N cross peaks of the lectin dramatically decreased when the multivalent ligands were added, strongly suggesting the existence of large complexes in solution. Then, competitive ^{1}H-^{15}N HSQC experiments were employed to disentangle the molecular recognition event. In particular, titration with a known competitor (LacNAc) allowed the recovery of the HSQC signal intensities, while analysis of the total intensity at each point permitted an estimation of the relative affinity of the glycopolymers for the galectins. In general, all the molecules tested preferred dimeric galectin-

1 to the monomeric CRD of galectin-3. Interestingly, it was demonstrated that a larger number of LacNAc units in the multivalent presentation of a ligand does not necessarily correlate with higher affinity, while the existence of high-order complexes and cross-linking effects was unequivocally demonstrated by complementary biophysical techniques, including DLS and cryo-EM. [407]

Given their importance in infection and inflammation, C-type lectins, [545] and especially the human innate immune receptor DC-SIGN, have been extensively studied by NMR, using both ligand-based and receptor-based methods, or combinations thereof. Focusing on the receptor-based approach, the key features of the interactions between DC-SIGN and mono- and di-fucosylated glycans of the parasitic worm *Schistosoma mansoni* have been dissected. [642] It was observed that although both ligands provided similar CSP profiles, the mono-fucosylated ligand (LDNF) displayed larger CSPs than the di-fucosylated (LDN-DF) when the same number of equivalents of ligand were employed, suggesting that binding of LDN-DF was weaker. For DC-SIGN and its homologue L-SIGN (or DC-SIGNR), special attention to their interactions with N-glycans, [369, 643] as well as with the Lewis [97] and the histo blood group antigens has also been paid. [644]

Langerin, another member of the C-type family of lectins, has also been the target of numerous NMR investigations, paying special attention to the role of allostery when designing ligands that specifically target this essential lectin, especially in discriminating langerin from DC-SIGN. A number of glycomimetics have been designed that are able to accomplish this task. In most cases, the receptor-based NMR approach has been complemented by ligand-based methods such as STD NMR and ^{19}F relaxation. [645-649]

Another biologically important lectin is cyanovirin-N (CVN), first isolated from the cyanobacterium *Nostoc ellipsosporum*. CVN inactivates different HIV strains through specific binding (in the nanomolar range) to the high-Man *N*-glycans displayed on the viral gp120 glycoprotein. As described in section 3.2.3.1 above, [46, 160] different NMR investigations using ^{19}F- and ^{13}C-labelled glycans have allowed key details of the molecular recognition event to be characterised from the ligand perspective. [650, 504] The receptor-based approach using a number of Man-containing ligands, representing any of the arms of the Man-9 N-glycan, [650-652] as well as their multivalent presentations, [653, 654] complemented the ligand-based information, and allowed determination of the structural details, dynamics, and energetic features of the CVN-glycan interaction. This also resolved the initial discrepancies that were reported when comparing the X-ray and NMR structures, especially regarding the possibility of domain swapping. [655-658]

The binding of the macrophage galactose-type lectin (MGL) to GalNAc has also been studied. [659] Once more, a combination of ligand-based and receptor-based NMR methodology allowed detection of large motions at different timescales in particular protein regions that are coupled to glycan binding, [660] and these results were compared to the X-ray crystal structures of the lectin bound to GalNAc and to the tumor associated Tn antigen. [661] By using receptor-based NMR experiments it was demonstrated that the binding event drastically altered the dynamics of the receptor. In particular, ^{1}H-^{15}N HSQC titration data for ^{15}N labelled MGL-CRD were collected in the presence of different GalNAc containing moieties (α-MeGalNAc, blood group antigen type A, Forssman antigen, GM2 and asialo GM2 glycolipid fragment). Depending on the particular ligand, while several peaks were always perturbed, some others only became visible in the presence of the ligand, strongly suggesting that there is intermediate rate broadening in the apo state resulting from conformational exchange that is quenched in the complex. It is tempting to speculate that some lectin regions adopt different conformations in the apo state, which then become structured in the bound form. The combination of protein NMR based experiments with STD NMR data and MD simulations demonstrated that MGL-CRD is extremely flexible, and that its dynamics in the complex critically depend on the precise GalNAc-containing ligand. [660] Alternatively, it has also been

demonstrated that MGL is able to bind to E. coli lipopolysaccharides through distinct interfaces. [662, 663]

Less common isotopic labels for proteins, such as ^{19}F, can also be exploited. Protein-observed ^{19}F (PrOF) NMR can also be used as a tool for the study of interactions having a wide range of affinities. For instance, standard 1D experiments can be used to obtain binding affinities (K_d). This procedure has been used with ^{19}F labelled LecA lectin from *Pseudomonas aeruginosa*, responsible of biofilm formation in chronic infections. The label was incorporated using 5-fluoroindole as precursor, resulting in protein where all of the tryptophans are modified to become 5-fluorotryptophan (5FT) residues. ^{19}F NMR signals were assigned by site-specific mutagenesis, and the analysis of the NMR titration data with various ligands demonstrated that the presence of a fluorine atom does not modify the binding preferences of the lectin. From the technical perspective, a specific tryptophan residue located in the binding site (W42) was used as the probe to monitor the recognition event (by K_d estimation) with low affinity ligands and with glycomimetics, demonstrating how PrOF NMR has the potential to drive the design of novel molecules with improved affinity. [664] Alternatively, the same methodology has been developed to monitor the binding of the histo blood group antigens and their disaccharide fragments to galectins, [665] given the key role of sugar-galectin CH-π stacking involving a conserved Trp moiety that is essential at the lactose binding site. Investigations were carried out for human galectin-3 (Gal3), with one carbohydrate recognition domain (CRD) and only one Trp residue in its sequence, and also for Galectin-8 (Gal8), which contains two CRDs and three Trp in the polypeptide chain (one not involved in lactose binding). Strikingly, the presence of the fluorine atom in the Trp ring did not decrease the affinity for sugar binding. Moreover, even for the weaker disaccharide ligands, the recognition event was in slow exchange on the ^{19} F NMR chemical-shift timescale, which permitted individual monitoring of the binding events occurring at the two distinct binding sites within Gal-8 heterodimer. [665] This methodology, coupled with paramagnetic relaxation experiments, has been applied to monitor the interactions of cyanovirin with a variety of ^{19}F substitutions in the Trp moiety. [666]

6.3. The determination of 3D structures of low affinity protein-glycan complexes

Specific intermolecular glycan-protein interactions are responsible for triggering, shutting down or controlling processes of signal transduction leading to activation of biological functions, whose significance is well-established in the realms of biochemistry, cell biology, and biomedical research. [2] Ongoing research in this field is critical for further understanding these complex interactions and their potential applications in medical and therapeutic settings. [667]. In this context, an in-depth understanding of the molecular basis of these molecular recognition processes relies on the elucidation of the 3D structures of the interacting glycans and their complexes. Traditionally, most structural biology studies on protein-ligand interactions focus on strong or high-affinity interactions (K_D below 1 μM), which can be studied by various biophysical experimental techniques. X-ray crystallography and cryo-electron-microscopy are the most powerful techniques to characterise high affinity complexes at high resolution. [668]. However, low affinity protein-glycan interactions, frequently with K_D above 10^{-4} M, have also gathered attention. [669]

Within the cellular domain, glycoproteins and glycolipids decorate all living cells, forming a matrix referred to as the ‘glycocalyx’, whose composition differs between different tissue and cell types in multicellular organisms. [670, 671] The glycocalyx plays a pivotal role in cellular interactions and adhesion, i.e. processes involving low affinity interactions. [672] Altered glycosylation is frequently associated with diseases like cancer, where abnormal glycan expression can serve as a prognostic marker and contribute to disease progression. [673, 674] Lectins, carbohydrate-binding proteins, are vital for various biological processes, including immune cell migration, pathogen recognition, and antigen presentation. Indeed, pathogens such as viruses and bacteria often use lectins to mediate infection of host cells and evade immunity, which highlights the importance of such interactions in disease and therapy.

Although considered a challenging or even “undruggable” type of protein receptor, [675] lectins are nonetheless promising drug targets for diverse pathological conditions and can also be exploited for targeted delivery of drugs, [676] imaging agents, and vaccines. However, the challenges for lectin-targeted drug design include to how deal with low ligand affinity and/or shallow binding sites. [675-679]

The structural characterization of these low-affinity protein-glycan complexes is challenging because many conventional experimental approaches fail, or become unreliable, due to the transient nature of the interactions (i.e. the interacting partners are mostly dissociated at equilibrium). Despite providing valuable insights, traditional techniques that employ cryogenic conditions might not accurately represent the physiological states, given that conformational changes could be induced by the extreme cooling conditions required. Non-cryogenic structures are becoming more important for ligand binding studies, as seen with the SARS-CoV-2 main protease. [680] Additionally, low-affinity interactions often result in poor resolution and/or low ligand occupancy in crystal structures, hindering the accurate elucidation of the ligand binding mode. This constitutes a particularly important challenge for Fragment Based Drug Discovery (FBDD) approaches, as these rely on the atomic level characterisation of protein-fragment complexes during the early stages of developing potent drugs; however, a significant proportion of such complexes either do not crystallise or show poor ligand resolution in the X-ray crystallography analysis, given the short residence time of the ligand in the bound state.

NMR has become a key approach for analysing these transient interactions in solution. Techniques like STD NMR, [454] exhaustively described above in section 6.1.1, in the context of glycan interactions are highly effective for studying low-affinity glycan-lectin interactions. In contrast, WaterLOGSY, [681, 682] another methodology that does not require isotopic enrichment and that is widely used to monitor other ligand-receptor interactions, is barely employed in the glycan field, probably due to the fact that lectin binding sites are rather shallow and exposed to solvent so that the required transfer of magnetization from the bound water molecules to the bound glycan is not effective enough. STD NMR, in particular, has demonstrated itself to be a robust and widely-applicable technique for (i) screening of glycan binding to target receptors, [683, 684], (ii) discrimination between specific and unspecific binders, [685] (iii) determination of dissociation constants, [546, 686] (iv) characterization of the glycan epitope mapping, [459] and (v) depiction of glycan orientation in the bound state. [459] This feature, characterised through the (DEEP) STD NMR described in section 6.1.1.1 above, allows identification of the chemical nature of the protein side chains (i.e. aliphatic vs aromatic, polar vs apolar) surrounding the glycan, even in the absence of structural information from the protein side. [459]

6.4. Combining NMR and MM/MD

The combination of NMR and molecular modelling protocols (including docking calculations and molecular dynamics simulations, among others) is essential for deriving the structural features and interactions of carbohydrates. [246, 459, 687, 688] This integrative approach offers a detailed understanding of glycan conformation and dynamics, essential for the advancement of glycosciences in drug discovery. Some examples of the successful combination of NMR and molecular modelling are described below.

6.4.1. Computationally-assisted Structural Determination of Protein-Glycan Complexes. Implications for Fragment Screening and Drug Discovery

NMR provides experimental data on atomic-level details of molecular structures, and this can be used to validate and refine structures obtained from molecular modelling. It has been reported that chemical shifts can be used as structural restraints along with conventional molecular mechanics force fields to determine protein conformations with a backbone rmsd of around 2 Å. [689]. As an example of this paradigm, Hafsa et al. have proposed the use of chemical shift threading (using bioinformatics and a combination of sequence information and low-resolution structural data, either predicted or experimental) for fast and robust determination of protein structures. [690] This method leverages sequence and chemical shift similarity, together with chemical shift-derived secondary structures, shift-derived super-secondary structures, and shift-derived accessible surface areas to generate a high-quality protein 3D structure.

One of the greatest strengths of biomolecular NMR spectroscopy is its ability to identify ligand binding sites and to characterise ligand-protein interactions. In particular, the complementarity of STD NMR with molecular modelling can provide satisfactory 3D pictures of these interactions, aiding in the design of drugs with improved binding properties, especially through fragment-based drug discovery (FBDD).

Importantly, the structural characterisation of these low affinity protein-glycan interactions and the validation of 3D models of protein-glycan complexes have recently benefited from notable developments. Thus, a reduced relaxation matrix theoretical approach has been developed for the very fast validation of static and dynamic 3D models of low-affinity protein-ligand complexes against experimentally determined STD NMR binding epitopes. [691] At the time of writing, this new algorithm, called RedMat, is available on a web server (http://redmat.iiq.us-csic.es/login) and performs with exceptional computational efficiency, greatly accelerating the determination of theoretical binding epitopes from STD initial slopes using the Cartesian coordinates of the 3D structure of the proposed receptor-ligand complex. Furthermore, by combining RedMat with funnel metadynamics MD simulations, [692] the 3D structures of low-affinity protein-ligand complexes can be generated and monitored on the fly (Fig. 26). The development of such an efficient tool is of great interest for the development of new binders through FBDD, since it can easily be used in drug discovery pipelines to rapidly screen and validate a large set of 3D models of protein-fragment complexes, obtained either from docking or MD simulations, against the experimental STD NMR data.

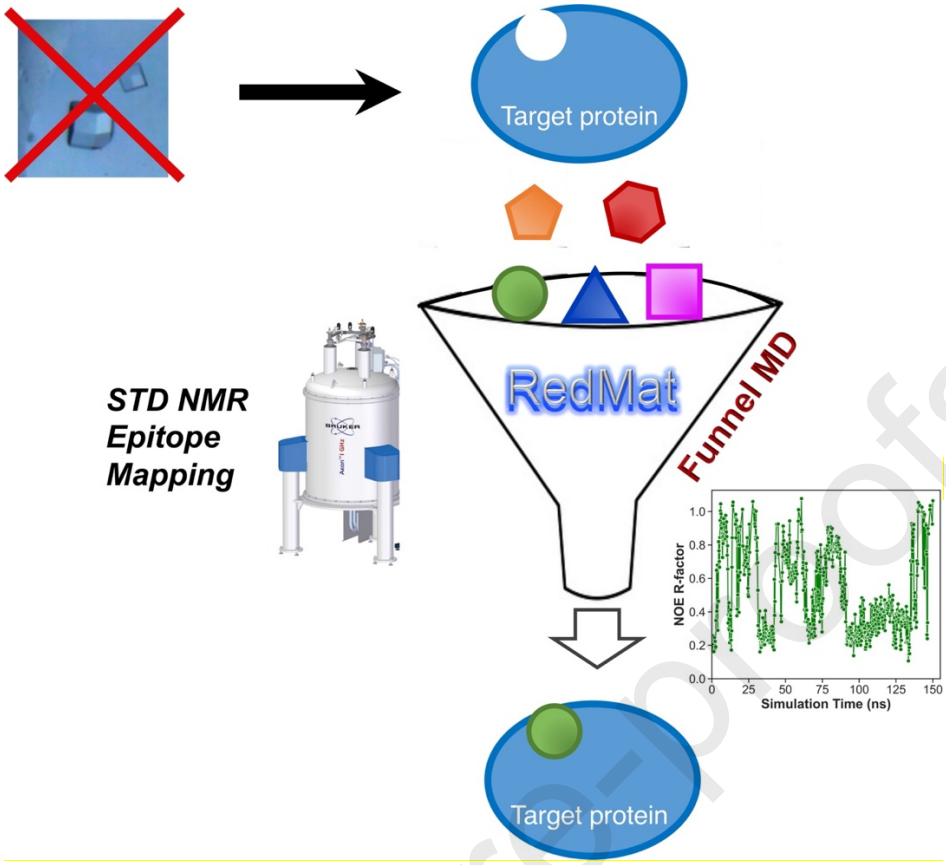

Fig. 26. Cartoon representation of the RedMat protocol for the STD NMR-based validation of 3D models of protein–fragment complexes, in combination with Funnel-MD simulations. From the 3D molecular models, RedMat calculates the theoretical STD initial slopes and compares them with the experimental values. Funnel-MD simulations allow for fast sampling of the conformational space of the bound ligand. The ligand orientations in agreement with the experimental epitope are then validated by RedMat, within minutes. The fragments are here represented as geometrical shapes. The NOE R-factor indicates the quality of the theoretical prediction.

7. Towards the future: the synergy of NMR with computation

Computational software such as Rosetta can be very effectively complemented using sparse NMR data. [693] For instance, the addition of paramagnetic NMR and hydrogen-deuterium exchange data enhances the structural predictions accomplished by programs like AlphaFold2 with NMR-guided Rosetta modelling [694]. Alternatively, coarse-grained MD simulations can handle rather complex molecular systems and predict structures that can be refined with NMR data, in a synergic manner. For glycoscience research, it is expected that continued advancements in both fields will provide access to realistic cell membrane models that represent the large natural diversity of lipids and proteins that provide the plasticity required for cell functioning. [695] These models will constitute an extraordinary tool for predicting large

scale *on-cell* events, [696] that can be complemented with *on-cell* NMR methodologies, further expanding our knowledge.

7.1. AI tools and low affinity protein-ligand interactions

Recent advances in protein structure prediction tools, particularly AlphaFold 3.0 [697] and its variants OpenFold, [698] ESMFold, [699] and RoseTTAFold [700], are poised to significantly impact the field of protein-glycan interactions. These tools already display remarkable accuracy for predicting protein structures, including those containing disordered regions and flexible binding sites, which are crucial for understanding low affinity protein-glycan interactions. Thus, with the recent advent of AlphaFold 3.0 it is now possible to predict protein oligomer structures and the interaction of a protein with some specific sugar (e.g. pectate lyase B bound to mannose, PDB code 7BBV), as well as with RNA and DNA molecules. Recently, a new protocol that leverages AlphaFold2 [701] has been proposed for predicting interactions of non-standard ligands with disordered protein regions that are usually invisible in X-ray and EM structures, [702] and are often associated with low-affinity binding events. Unravelling these "ghost interactions" will be critical for boosting detailed analysis and understanding of the mechanisms behind protein-glycan complexes, thus providing new avenues for developing targeted therapies for those diseases associated with them.

7.2. Towards drug design.

We have seen so far how protein-glycan interactions are ubiquitous in physiological events related to health and disease. We have described the multiple and various ways in which NMR experiments provide precise knowledge for understanding the specific molecular recognition processes behind biological function. A number of glycodrugs for inhibiting pathological processes already exist in the market, ranging from Zanamivir [703] to prevent and treat influenza to Voglibose [704] against diabetes, among many others. [705] However, there are two major challenges associated with glycans as potential therapeutic agents: i) they lack drug-like properties, such as high affinity, adequate bioavailability, and therapeutically relevant plasma half-lives; and ii) their large-scale production may be cumbersome and rather expensive. Therefore, focus has been paid to develop glycomimetic molecules, which can inhibit the pathological response, yet retain appropriate pharmacodynamic and pharmacokinetic properties [705].

As examples, we just highlight two of the many NMR-based studies on the development of glycomimetics, namely cholera toxin targetting and glycosyl transferase inhibition. The cholera toxin (CTB) binding site to GM1 was dissected and characterised at high resolution many years ago. [706] Since then, several libraries of glycomimetic inhibitors have been proposed [706-710] and characterized using NMR. Recent DEEP-STD NMR studies, assisted by computational tools, have uncovered a third, cryptic, binding subsite in the CTB binding pocket, in addition to the canonical sites previously characterized for the physiological binding of GM1. This novel binding pocket can accommodate polyhydroxyalkyl furoate moieties, thus opening new venues for three-finger glycan-based inhibitors. [461]

Glycosyl transferases have been the target of drug discovery campaigns for years. Since aberrant glycosylation, produced by their overexpression, is responsible for or involved in a wide range of diseases, from cancer to microbial infections, the design of glycosyl transferase inhibitors is a very hot topic for academic and pharma research. In particular, iminosugars display higher chemical and enzymatic stability than natural sugars [711] and they have been targeted as potential inhibitors. NMR has been used to study their bioactive conformations using NOESY and heteronuclear HOESY [712]. The buildup and cleavage of glycans involve the generation of glycosyl cations, and NMR investigations have allowed their conformations to be deduced. Moreover, precious information on the inhibitory process produced by mimetics of these intermediates has also been obtained. [713-716] Finally, ligand-based NMR methods

have been applied to disentangle many features of their interactions with the enzymes. [717-719]

These examples represent just the tip of the iceberg concerning the crucial role that NMR plays in the glycometic drug discovery arena. Many more examples exist, and many more still are expected to be disseminated in the coming era, also highlighting new avenues that will be developed through the application of in-cell and on-cell methods.

Glycans and sugars are not only key actors in molecular recognition events, but also can take part in other processes of remarkable interest. For instance, the interaction of the flexible ^{15}N-labeled Aβ (1-42) peptide with amyloid formation inhibitors has been investigated using a combination of CSP-NMR and principal component analysis (PCA). Several sugars, such as sucrose, glucose and trehalose, were used as osmolytes, and their ability to stabilize some of the possible compact conformations of the peptide was examined. It was expected that the presence of the sugar osmolytes could inhibit amyloid fibril formation inhibition. The CSP analyses with the osmolytes and with other described inhibitory compounds were carried out at different temperatures. Interestingly, the process was shown to be rather complex, since a wide variety of chemical shift changes were detected in all cases, hampering the understanding of the dynamic changes caused by each molecule. Nevertheless, the PCA diagram allowed to describe two physico-chemical events. [720]

7.3. Expanding applications

Obviously, glycan-lectin interactions in nature may take place under highly crowded conditions, both in-cell and on-cell, as described in section 6.1.1.3 above, [548-556] and a variety of methodologies have been employed to mimic the natural environment. As landmark, the molecular recognition events involving ^{15}N-labeled human galectin 3 (Gal-3) in a number of crowding environments have been monitored using ^{1}H-^{15}N HSQC experiments. [721] As crowders, different proteins, such as bovine and human serum albumin, as well as synthetic molecules, including Ficoll 70 and PEG3350, were employed. Although the HSQC cross peaks for Galectin-3 experienced shift perturbations and line broadening in the presence of crowders, due both to the increase in viscosity and to the presence of large entities, the signal intensities were recovered upon addition of lactose, suggesting that, even in crowded environments, the interaction still takes place and the glycan finds its recognition site. [721]

Besides the use of Dynamic Nuclear Polarization (DNP) methods to study the structure of cell-wall polysaccharides *in situ,* [557-564] this methodology also offers possibilities to monitor lectin-binding recognition. Under favourable conditions, Selective DNP (Sel-DNP), exploiting DNP-enhanced NMR under magic angle spinning, may allow identification of the lectin residues involved in a specific binding event without previous knowledge and without limits on receptor size. The interaction of galactose (Gal) with a ^{13}C/^{15}N double labelled LecA lectin was used as a proof of concept. The Gal ligand was connected to the bis-nitroxide TOTAPOL paramagnetic tag through a linker, in order to facilitate the transfer of polarization. Sel-DNP combines localized Paramagnetic Relaxation Enhancement (PRE) with difference spectroscopy to obtain information from a hyperpolarized binding site through highly resolved multi-dimensional NMR experiments. In particular, two datasets of experiments (^{13}C–^{13}C DQ/SQ one-bond correlation spectra) were acquired using a labelled protein with general polarizing agents AMUPol (S_0, where signals are uniformly enhanced) and with the functionalized ligand (S_1, where signal broadening is only detected for the signals of the nearby nuclei). The difference between the two spectra revealed the residues involved in binding. [722]

8. Brief summary

In this review, we have addressed the standard NMR protocols used to assign the NMR spectra of glycans, and to identify their chemical nature. The NMR parameters and experiments employed to study their conformation and dynamic features have also been described, paying attention to the influence of internal motions, and to the intrinsic chemical characteristics of the glycosidic linkages. A perspective on the NMR properties of the natural glycans and the relationship with their conformational and dynamic features has also been presented, expanding the discussion to include the analysis of glycomimetics. The use of ^{19}F NMR to investigate fluorosugars has also been highlighted, as well as the use of paramagnetic NMR. The NMR study of intact glycoproteins is reaching maturity, especially when accompanied by the labeling of glycans with NMR-active stable isotopes. The review has also addressed the use of NMR and molecular recognition methodologies and approaches, both from the perspective of the glycan, with special emphasis on STD NMR and Tr-NOESY methodologies, and from that of the receptor. New avenues such as on-cell NMR have also been described, providing a basis for current and future advances and developments that hold the promise of many future applications in the flourishing field of glycans in heath and disease.

Glossary of Abbreviations

BLI: Biolayer interferometry

CAMELSPIN: Cross-relaxation appropriate for minimolecules emulated by locked spins

COSY: Correlated spectroscopy

Cov: Coronavirus

Covid: Coronavirus disease

CPMG: Carr Purcell Meiboom Gill

CRD: Carbohydrate recognition domain

CS: chondroitin sulfate

CSP: Chemical shift perturbation

CT: Constant time

CVN: Cyanoviridin-N

DC-SIGN: Dendritic cell-specific intercellular adhesion molecule-3-grabbing non-integrin

DEEP-STD: Differential epitope mapping STD

DFT: Density functional theory

D-GlcA: D-glucopyranosyluronic acid

DMSO: Dimethylsulfoxide

DNA: deoxyribonucleic acid

DNP: Dynamic nuclear polarization

DOSY: Diffusion ordered spectroscopy

DQ: Double quantum

DS: dermatan sulfate

DSL: *Datura stramonium* seed Lectin

FAXS: Fluorine chemical shift anisotropy and exchange for screening

FBDD: Fragment based drug discovery

FGF: Fibroblast growth factor

Fuc: fucose

GAG: glycosaminoglycan

Gal: galactose

GalN: galactosamine

gg: gauche-gauche

Glc: glucose

GlcA: glucuronic acid

GlcN: glucosamine

gt: gauche-trans

HA: hyaluronan

HB: hydrogen bonding

HEP: heparin

HMBC: Heteronuclear multiple bond correlation

HMQC: Heteronuclear multiple quantum correlation

HOESY: Heteronuclear Overhauser effect spectroscopy

HS: heparan sulfate

HSEA: Hard Sphere Exo-Anomeric

HSQC: Heteronuclear single quantum correlation

IdoA: iduronic acid

INEPT: Insensitive nucleus enhancement by polarisation transfer

ITC: Isothermal titration calorimetry

Kdo: 3-deoxy-d-*manno*-oct-2-ulosonic acid

Ko: d-*manno*-oct-2-ulosonic acid

KS: keratan sulfate

LBT: lanthanide binding tag

LeX: Lewis-X antigen

L-IdoA: L-idopyranosyluronic acid

L-IdoA2S: 2-*O*-sulfo-L-iduronic acid

L-PROSY: Looped projected spectroscopy

Man: mannose

MD: molecular dynamics simulations

MGL: Macrophage galactose-type lectin

Neu5Ac: Sialic acid, N-acetyl neuraminic acid

NMR: Nuclear magnetic resonance

NOE: Nuclear Overhauser Enhancement

NOESY: NOE spectroscopy

PCA: Principle component analysis

PCS: pseudo-contact shift

PEG: Polyethylene glycol

PRE: paramagnetic relaxation enhancement

PROF: Protein-observed fluorine

QM: quantum mechanical

RCA: *Ricinus communis* agglutinin

RDC: residual dipolar coupling

RNA: Ribonucleic acid

ROE: Rotating frame NOE

ROESY: Rotating frame NOE spectroscopy

SARS: Severe acute respiratory syndrome

SNFG: Signal nomenclature for glycans

SQ: Single quantum

SPR: Surface plasmon resonance

STD: saturation transfer difference

TEMPO: 2,2,6,6-Tetramethylpiperidine

tg: trans-gauche

TOCSY: Total correlation spectroscopy

TOTAPOL: 1-(TEMPO-4-oxy)-3-(TEMPO-4-amino)propan-2-ol

Tr-NOE: transferred NOE

WATERLOGSY: Water-ligand observed via gradient spectroscopy

Xyl: xylose

Acknowledgments

This work was supported by the European Research Council (788143-RECGLYCANMR to J.J.-B) and Marie-Skłodowska-Curie actions (ITN Glytunes grant agreement No 956758 to J.E.-O; and ITN Glyco-N under grant agreement no. 101119499 to J.J.B.). We also acknowledge the European Commission for the GLYCOTWINNING project and CIBERES, an initiative of Instituto de Salud Carlos III (ISCIII, Madrid, Spain). We thank Agencia Estatal de Investigación of Spain for grants PID2019-107770RA-I00 (J.E.-O.), PDI2021-1237810B-C21 (J.J.B. & A-A.), and the Severo Ochoa Center of Excellence Accreditation CEX2021-001136-S, all funded by MCIN/AEI/10.13039/501100011033. J.A. and J.C.M.-G. acknowledges the Ministerio de Ciencia e Innovación for funding through grant PID2022-142879NB-I00. S.M. thanks UKRI for funding via a Future Leaders Fellowship awarded to Prof. Matthew Wallace (MR/T044020/1). We also thank Dr. Unai Atxabal for his support with some figures.

REFERENCES

[1] A. Varki, R.D. Cummings, J. D. Esko, P. Stanley, G. W. Hart, M. Aebi, A. G. Darvill, T. Kinoshita, N. H. Packer, J. H. Prestegard, R. L. Schnaar, P. H. Seeberger, Essentials of Glycobiology, third ed., Cold Spring Harbor (NY): Cold Spring Harbor Laboratory Press (NY), 2015-2017.

[2] A. Varki, Biological Roles of Glycans. Glycobiology 27 (2017) 3–49.

[3] R.A. Flynn, K. Pedram, S.A. Malaker, P.J. Batista, B.A.H. Smith, A.G. Johnson, B.M. George, K. Majzoub, P.W. Villalta, J.E. Carette, C.R. Bertozzi, Small RNAs Are Modified with N-Glycans and Displayed on the Surface of Living Cells. Cell 184 (2021), 3109-3124.e22.

[4] M. Dalziel, M. Crispin, C.N. Scanlan, N. Zitzmann, R.A. Dwek, Emerging principles for the therapeutic exploitation of glycosylation. Science 343 (2014) 1235681.

[5] R.A. Laine, The information-storing potential of the sugar code, in: Glycosciences, Wiley-VCH Verlag GmbH, 2008, pp. 1–14.

[6] H.-J. Gabius, S. Andre, J. Jimenez-Barbero, A. Romero, D. Solis, From Lectin Structure to Functional Glycomics: Principles of the Sugar Code. Trends Biochem. Sci. 36 (2011) 298–313.

[7] D.F. Thieker, J.A. Hadden, K. Schulten, R.J. Woods, 3D implementation of the symbol nomenclature for graphical representation of glycans. Glycobiology, 26 (2016) 786–787.

[8] B.S. Blaum, U. Neu, T. Peters, T. Stehlea, Spin ballet for sweet encounters: saturation-transfer difference NMR and X-ray crystallography complement each other in the elucidation of protein−glycan interactions. Acta Crystallogr., Sect. F: Struct. Biol. Commun. 74 (2018) 451−462.

[9] J. Agirre, Strategies for carbohydrate model building, refinement and validation. Acta Crystallogr., Sect. D: Struct. Biol. 73 (2017) 171−186.

[10] W.I. Weis, K. Drickamer, Structural Basis of Lectin-Carbohydrate Recognition. Annu. Rev. Biochem. 65 (1996) 441–473.

[11] J. Agirre, G. Davies, K. Wilson, K. Cowtan, Carbohydrate anomalies in the PDB. Nat. Chem. Biol. 11 (2015) 303-303.

[12] J. Agirre, G.J. Davies, K.S. Wilson, K.D. Cowtan, Carbohydrate structure: the rocky road to automation, Curr. Opin. Struct. Biol. 44 (2017) 39–47.

[13] T.J. Yang, T-J. Yang, Y-C. Chang, T-P. Ko, P. Draczkowski, Y-C. Chien, Y-C. Chang, K-P. Wu, K-H. Khoo, H-W. Chang, S-T. D. Hsu, Cryo-EM analysis of a feline coronavirus spike protein reveals a unique structure and camouflaging glycans. Proc. Natl. Acad. Sci. U. S. A., 117 (2020) 1438–1446.

[14] R. Wild, J. Kowal, J. Eyring, E. M. Ngwa, M. Aebi, K. P. Locher, Structure of the yeast oligosaccharyltransferase complex gives insight into eukaryotic N-glycosylation, Science, 359 (2018) 545–550.

[15] M. Atanasova, H. Bagdonas, J. Agirre, Structural Glycobiology in the Age of Electron Cryo-Microscopy. Curr. Opin. Struct. Biol. 62 (2020) 70–78.

[16] E. Duverger, N. Lamerant-Fayel, N. Frison, M. Monsigny, Carbohydrate-Lectin Interactions Assayed by SPR. Methods Mol. Biol. 627 (2010) 157–178.

[17] J. Wallner, B. Sissolak, W. Sommeregger, N. Lingg, G. Striedner, K. Vorauer-Uhl, Lectin Bio-Layer Interferometry for Assessing Product Quality of Fc- Glycosylated Immunoglobulin G. Biotechnol. Prog. 35 (2019) e2864.

[18] O. Blixt, B.E. Collins, I.M. van den Nieuwenhof, P.R. Crocker, J.C. Paulson, Sialoside Specificity of the Siglec Family Assessed Using Novel Multivalent Probes. J. Biol. Chem. 278 (2003) 31007–31019.

[19] S. Serna, J. Etxebarria, N. Ruiz, M. Martin-Lomas, N.C. Reichardt, Construction of N-glycan microarrays by using modular synthesis and on-chip nanoscale enzymatic glycosylation. Chem. Eur J. 16 (2010) 13163-13175.

[20] M.A. Campanero-Rhodes, D. Solís, Bacterial Microarrays for Examining Bacterial Glycosignatures and Recognition by Host Lectins. Methods Mol. Biol. 2460 (2022) 147-160.

[21] O.C. Grant, H.M.K. Smith, D. Firsova, E. Fadda, R.J. Woods, Presentation, Presentation, Presentation! Molecular-Level Insight into Linker Effects on Glycan Array Screening Data. Glycobiology. 24 (2014), 17–25.

[22] E.J. Toone, Structure and Energetics of Protein-Carbohydrate complexes. Curr. Opin. Struct. Biol. 4 (1994) 719–728.

[23] T.K. Dam, C.F. Brewer, Multivalent Lectin—Carbohydrate Interactions: Energetics and Mechanisms of Binding. Adv. Carbohydr. Chem. Biochem. 63 (2010) 139–164.

[24] Y. Takeda, I. Matsuo, Isothermal Calorimetric Analysis of Lectin-Sugar Interaction. Methods Mol. Biol. 1200 (2014) 207–214.

[25] W.B. Turnbull, A.H. Daranas, On the Value of c: Can Low Affinity Systems Be Studied by Isothermal Titration Calorimetry? J. Am. Chem. Soc. 125 (2003) 14859-14866.

[26] T.J. Wenzel, C.D. Chisholm, Using NMR spectroscopic methods to determine enantiomeric purity and assign absolute stereochemistry, Prog. Nucl. Magn. Reson. Spectrosc. 59 (2011) 1-63.

[27] S. Nerli, A.C. McShan, N.G. Sgourakis, Chemical shift-based methods in NMR structure determination, Prog. Nucl. Magn. Reson. Spectrosc. 106–107 (2018) 1-25.

[28] M.E. Elyashberg, A.J. Williams, G.E. Martin, Computer-assisted structure verification and elucidation tools in NMR-based structure elucidation, Prog. Nucl. Magn. Reson. Spectrosc. 53 (2008) 1-104.

[29] A.D. Gossert, W. Jahnke, NMR in drug discovery: A practical guide to identification and validation of ligands interacting with biological macromolecules, Prog. Nucl. Magn. Reson. Spectrosc. 97 (2016) 82-125.

[30] L. Fielding, NMR methods for the determination of protein–ligand dissociation constants, Prog. Nucl. Magn. Reson. Spectrosc. 51 (2007) 219-242.

[31] C. Dalvit, I. Gmür, P. Rößler, A.D. Gossert, Affinity measurement of strong ligands with NMR spectroscopy: Limitations and ways to overcome them, Prog. Nucl. Magn. Reson. Spectrosc. 138–139 (2023) 52-69.

[32] C.F. Tormena, Conformational analysis of small molecules: NMR and quantum mechanics calculations, Prog. Nucl. Magn. Reson. Spectrosc. 96 (2016) 73-88.

[33] D. A. Torchia, NMR studies of dynamic biomolecular conformational ensembles, Prog. Nucl. Magn. Reson. Spectrosc. 84-85 (2015) 14-32.

[34] A.D. Bain, Chemical exchange in NMR, Prog. Nucl. Magn. Reson. Spectrosc. 43 (2003) 63-103.

[35] V. Tugarinov, A. Ceccon, G.M. Clore, NMR methods for exploring ‘dark’ states in ligand binding and protein-protein interactions, Prog. Nucl. Magn. Reson. Spectrosc. 128 (2022) Pages 1-24.

[36] D. K. Yadav, P. J. Lukavsky, NMR solution structure determination of large RNA-protein complexes, Prog. Nucl. Magn. Reson. Spectrosc. 97 (2016) 57-81.

[37] J. Duus, C.H. Gotfredsen, K. Bock, Carbohydrate structural determination by NMR spectroscopy: modern methods and limitations, Chem. Rev. 100 (2000) 4589–4614.

[38] M.D. Battistel, H.F. Azurmendi, B. Yu, D.I. Freedberg, NMR of glycans: shedding new light on old problems, Prog. Nucl. Magn. Reson. Spectrosc. 79 (2014) 48-68.

[39] M.R. Wormald, A. J. Petrescu, Y-L. Pao, A. Glithero, T. Elliott, R.A., Conformational studies of oligosaccharides and glycopeptides: complementarity of NMR, X-ray crystallography, and molecular modelling, Chem. Rev. 102 (2002) 371-386.

[40] S. Bekiroglu, C. Sandström, T. Norberg, L. Kenne, Hydroxy protons in conformational study of a Lewis b tetrasaccharide derivative in aqueous solution by NMR spectroscopy, Carbohydr. Res. 328 (2000) 409-418.

[41] L. Poppe, H. van Halbeek, NMR spectroscopy of hydroxyl protons in supercooled carbohydrates, Nat. Struct. Biol. 1 (1994) 215-216.

[42] G. Batta, K.E. Kövér, Heteronuclear coupling constants of hydroxyl protons in a water solution of oligosaccharides: trehalose and sucrose, Carbohydr. Res. 320 (1999) 267-272.

[43] M.D. Battistel, R. Pendrill, G. Widmalm, D.I. Freedberg, Direct evidence for hydrogen bonding in glycans: a combined NMR and molecular dynamics study, J. Phys. Chem. B, 117 (2013) 4860-4869.

[44] T.E. Vasquez, J.M. Bergset, M.B. Fierman, A. Nelson, J. Roth, S.I. Khan, D.J. O'Leary, Using equilibrium isotope effects to detect intramolecular OH/OH hydrogen bonds: structural and solvent effects, J. Am. Chem. Soc. 124 (2002) 2931-2938.

[45] M. Novakovic, M. D. Battistel, H.F. Azurmendi, M.G. Concilio, D.I. Freedberg, L. Frydman, The Incorporation of Labile Protons into Multidimensional NMR Analyses: Glycan Structures Revisited. J. Am. Chem. Soc. 143 (2021) 8935−8948.

[46] G. Nestor, T. Andreson, S. Oscarson, A.M. Gronenborn, Direct observation of carbohydrate hydroxyl protons in hydrogen bonds with a protein, J. Am. Chem. Soc. 140 (2018) 339-345.

[47] E. F. Hounsell, 1H NMR in the structural and conformational analysis of oligosaccharides and glycoconjugates, Prog. Nucl. Magn. Reson. Spectrosc. 27 (1995) 445-474.

[48] C. Fontana, G. Widmalm, Primary structure of glycans by NMR spectroscopy, Chem. Rev. 123 (2023) 1040-1102.

[49] B. Coxon, Developments in the Karplus equation as they relate to the NMR coupling constants of carbohydrates. Adv. Carbohydr. Chem. Biochem. 62 (2009) 17-82.

[50] K. Gheysen, C. Mihai, K. Conrath, J.C. Martins, Rapid identification of common hexapyranose monosaccharide units by a simple TOCSY matching approach. Chem. Eur. J. 14 (2008) 8869-8878.

[51] A. Furevi, A. Ruda, T. Angles d'Ortoli, H. Mobarak, J. Ståhle, C. Hamark, C. Fontana, O. Engström, P. Apostolica, G. Widmalm, Complete (1)H and (13)C NMR chemical shift assignments of mono-to tetrasaccharides as basis for NMR chemical shift predictions of oligo- and polysaccharides using the computer program CASPER. Carbohydr. Res. 513 (2022) 513, 108528.

[52] a) b) I. Speciale, A. Notaro, P. Garcia-Vello, F. Di Lorenzo, S. Armiento, A. Molinaro, R. Marchetti, A. Silipo, C. De Castro, Liquid-state NMR spectroscopy for complex carbohydrate structural analysis: A hitchhiker's guide, Carbohydr. Polym. 277 (2022) 118885.

[53] Widmalm, G., A Perspective on the Primary and Three-dimensional Structures of Carbohydrates, Carbohydr. Res. (2013) 378, 123-132.

[54] L.B. Krivdin, Computational NMR of carbohydrates: theoretical background, applications, and perspectives, Molecules. 2021, 26, 2450.

[55] R. Marchetti, F. Nieto Fabregat, M. Pallach, D. Gully, E. Giraud, A. Molinaro, K.A. Duda, A. Silipo, The peculiar structure of acetobacter pasteurianus CIP103108 LPS core oligosaccharide, ChembioChem. 22 (2021) 147-150.

[56] G. Widmalm, Glycan shape, motions, and interactions explored by NMR spectroscopy, JACS Au. 4 (2024) 20-39.

[57] A. Imberty, S. Perez, Structure, conformation, and dynamics of bioactive oligosaccharides: theoretical approaches and experimental validations, Chem. Rev. 100 (2000) 4567–4588.

[58] C. A. Bush, M. Martin-Pastor, A. Imberty, Structure and conformation of complex carbohydrates of glycoproteins, glycolipids, and bacterial polysaccharides, Annu. Rev. Biophys. Biomol. Struct. 28 (1999) 269-293.

[59] K. Bock, J.Ø. Duus, A conformational ctudy of hydroxymethyl groups in carbohydrates investigated by ^{1}H NMR spectroscopy. J. Carbohydr. Chem. 13 (1994) 513-543.

[60] R.U. Lemieux, S. Koto, The conformational properties of glycosidic linkages. Tetrahedron 30 (1974) 1933-1944.

[61] J.L. Asensio, F.J. Cañada, A. García-Herrero, M. T. Murillo, A. Fernández-Mayoralas, B. A. Johns, J. Kozak, Z. Zhu, C. R. Johnson, J. Jiménez-Barbero, Conformational behavior of aza-C-glycosides: experimental demonstration of the relative role of the exo-anomeric effect and 1,3-type interactions in controlling the conformation of regular glycosides, J. Am. Chem. Soc. 121 (1999) 11318-11320.

[62] J.L. Asensio, F.J. Cañada, X. Cheng, N. Khan, D.R. Mootoo, J. Jiménez-Barbero, Conformational differences between O- and C-glycosides: the alpha-O-man-(1-->1)-beta-Gal/alpha-C-Man-(1-->1)-beta-Gal case--a decisive demonstration of the importance of the exo-anomeric effect on the conformation of glycosides. Chem. Eur. J. 6 (2000) 1035-1041.

[63] R. Marchetti, S. Perez, A. Arda, A. Imberty, J. Jimenez-Barbero, A. Silipo, A. Molinaro, "Rules of engagement" of protein-glycoconjugate interactions: a molecular view achievable by using NMR spectroscopy and molecular modeling, ChemistryOpen. 5 (2016) 274-296.

[64] M. Karplus, Vicinal proton coupling in nuclear magnetic resonance. J. Am. Chem. Soc. 85 (1963) 2870–2871.

[65] I. Tvaroska, and F.R. Taravel, Carbon-proton coupling constants in the conformational analysis of sugar molecules. Adv. Carbohydr. Chem. Biochem. 51 (1995) 15-61.

[66] P. E. Hansen, Carbon—hydrogen spin—spin coupling constants. Prog. NMR Spectr. 14 (1981) 175-295.

[67] R.J. Meredith, I. Carmichael, R.J. Woods, A.S. Serianni, MA'AT analysis: probability distributions of molecular torsion angles in solution from NMR spectroscopy, Acc. Chem. Res. 56 (2023) 2313-2328.

[68] R.U. Lemieux, R.K. Kullnig, H.J. Bernstein, W.G. Schneider, Configurational effects on the proton magnetic resonance spectra of six-membered ring compounds, J. Am. Chem. Soc. 80 (1958) 6098-6105.

[69] F.H. Cano, C. Foces-Foces, J. Jiménez-Barbero, A. Alemany, M. Bernabe, M. Martín-Lomas, Experimental evidence of deviations from a Karplus-like relationship of vicinal carbon-proton coupling constants in some conformationally rigid carbohydrate derivatives. J. Org. Chem. 52 (1987) 3367–3372.

[70] R.J. Meredith, R.J. Woods, I. Carmichael, AS. Serianni, Reconciling MA′AT and molecular dynamics models of linkage conformation in oligosaccharides, Phys. Chem. Chem. Phys. 22 (2020) 14454-14457.

[71] B. Bose; S. Zhao, R. Stenutz, F. Cloran, P.B. Bondo, G. Bondo, B. Hertz, I. Carmichael, A.S. Serianni, Three-bond C-O-C-C spin-coupling constants in carbohydrates: development of a Karplus relationship. J. Am. Chem. Soc. 120 (1998) 11158-11173.

[72] Y. Nishida, H. Hori, H. Ohrui, H. Meguro, 1H NMR analyses of rotameric distribution of C5-C6 bonds of D-glucopyranoses in solution. J. Carbohydr. Chem. 7 (1988) 239-250.

[73] J. Gonzalez-Outeiriño, K.N. Kirschner, S. Thobhani, R.J. Woods, Reconciling solvent effects on rotamer populations in carbohydrates: a joint MD and NMR analysis. Can. J. Chem. 84 (2006), 569-579.

[74] G. D. Rockwell, T. B. Grindley, Effect of solvation on the rotation of hydroxymethyl groups in carbohydrates. J. Am. Chem. Soc. 120 (1998) 10953-10963.

[75] R. H. Marchessault, S. Perez, Conformations of the hydroxymethyl group in crystalline aldohexopyranoses. Biopolymers. 18 (1979) 2369-2374.

[76] S. Wolfe, The gauche effect. Some stereochemical consequences of adjacent electron pairs and polar bonds. Acc. Chem. Res. 5 (1972) 102-111.

[77] K.N. Kirschner, R.J. Woods, Solvent interactions determine carbohydrate conformation. Proc. Natl. Acad. Sci. USA 98 (2001) 10541-10545.

[78] D. Neuhaus, M.P. Williamson, The nuclear Overhauser effect in structural and conformational analysis, VCH, New York, NY, U.S.A.,1989.

[79] S.W. Homans, Oligosaccharide conformations: application of NMR and energy calculations, Prog. NMR Spectrosc. 22 (1990) 55-81.

[80] D.A. Cumming, J.P. Carver, Virtual and solution conformations of oligosaccharides. Biochemistry. 26 (1987) 6664-6676.

[81] T. Peters, T. Weimar, Assessing glycosidic linkage flexibility: conformational analysis of the repeating trisaccharide unit of *Aeromonas salmonicida*. J. Biomol. NMR, 4 (1994) 97-116.

[82] J.P.M. Lommerse, L.M.J. Kroon-Batenburg, J. Kroon, J.P. Kamerling, J.F.G. Vliegenthart, Conformations and internal mobility of a glycopeptide derived from bromelain using molecular dynamics simulations and NOESY analysis. J. Biomol. NMR, 6 (1995) 79–94.

[83] A. Poveda, J.L. Asensio, M. Martín-Pastor, J. Jiménez-Barbero, Solution conformation and dynamics of a tetrasaccharide related to the Lewis(x) antigen deduced by NMR relaxation measurements. J. Biomol. NMR, 10 (1997) 29-43.

[84] P. Berthault, N. Birlirakis, G. Rubinstenn, P. Sinaÿ, H.J. Desvaux , Solution structure of a Lewis(x) analogue by off-resonance 1H NMR spectroscopy without use of an internal distance reference. J. Biomol. NMR. 8 (1996) 23-35.

[85] A. Poveda, M. Santamaría, M. Bernabé, A. Rivera, J. Corzo, J. Jiménez-Barbero, Solution conformation and dynamics of an extracellular polysaccharide isolated from Bradyrhyzobium as deduced from 1H-NMR off resonance ROESY and 13C-NMR relaxation measurements. Carbohydr. Res. 304 (1997) 219-228.

[86] R.U. Lemieux, K. Bock, L.T.J. Delbaere, S. Koto, V.S. Rao, The conformations of oligosaccharides related to the ABH and Lewis human blood group determinants, Can. J. Chem. 58 (1980) 631-653.

[87] RJ. Woods, Predicting the structures of glycans, glycoproteins, and their complexes. Chem. Rev. 118 (2018) 8005-8024.

[88] P. Cagas, C. A. Bush, Determination of the conformation of Lewis blood group oligosaccharides by simulation of two-dimensional nuclear Overhauser data. Biopolymers. 30 (1990) 1123-1138.

[89] H.F. Azurmendi, M. Martin-Pastor, C.A. Bush, Conformational studies of Lewis X and Lewis A trisaccharides using NMR residual dipolar couplings. Biopolymers. 63 (2002) 89-98.

[90] S. Bekiroglu, L. Kenne, C. Sandström, NMR study on the hydroxy protons of the Lewis X and Lewis Y oligosaccharides. Carbohydr. Res. 339 (2004) 2465-2468.

[91] S.W. Homans, M. Forster, Application of restrained minimization, simulated annealing and molecular dynamics simulations for the conformational analysis of oligosaccharides. Glycobiology. 2 (1992) 143-151.

[92] K. Scheffler, J.R. Brisson, R. Weisemann, J.L. Magnani, W.T. Wong, B. Ernst, T.J. Peters, Application of homonuclear 3D NMR experiments and 1D analogs to study the conformation of sialyl Lewis^x bound to E-selectin. J. Biomol. NMR. 9 (1997) 423-436.

[93] C. Hoog, C. Landersjo, G. Widmalm, Oligosaccharides display both rigidity and high flexibility in water as determined by 13C NMR relaxation and 1H,1H NOE spectroscopy: evidence of anti-ϕ and anti-ψ torsions in the same glycosidic linkage. Chem. Eur. J. 7 (2001) 3069-3077.

[94] T. Haselhorst, T. Weimar, T. Peters, Molecular recognition of sialyl Lewis(x) and related saccharides by two lectins. J. Am. Chem. Soc. 123 (2001) 10705-10714.

[95] M.J. Milton, D.R. Bundle, Observation of the anti conformation of a glycosidic linkage in an antibody-bound oligosaccharide, J. Am. Chem. Soc. 120 (1998) 10547-10548.

[96] J. Topin, M. Lelimousin, J. Arnaud, A. Audfray, S. Pérez, A. Varrot, A. Imberty, The hidden conformation of Lewis x, a human histo-blood group antigen, is a determinant for recognition by pathogen lectins. ACS Chem. Biol. 11 (2016) 2011-2020.

[97] K. Pederson, D. A. Mitchell, J. H. Prestegard, Structural characterization of the DC-SIGN-Lewis(X) complex. Biochemistry. 53 (2014) 5700-5709.

[98] J.F. Espinosa, E. Montero, A. Vian, J.L. García, H. Dietrich, R.R. Schmidt, M. Martín-Lomas, A. Imberty, F.J. Cañada, J. Jiménez-Barbero, *Escherichia coli* β-Galactosidase recognizes a high-energy conformation of C-lactose, a nonhydrolizable substrate analogue. NMR and modeling studies of the molecular complex. J. Am. Chem. Soc. 120 (1998) 1309-1318.

[99] A. García-Herrero, E. Montero, J.L. Muñoz, J.F. Espinosa, A. Vián, J.L. García, J.L. Asensio, F.J. Cañada, J. Jiménez-Barbero, Conformational selection of glycomimetics at enzyme catalytic sites: experimental demonstration of the binding of distinct high-energy distorted conformations of C-, S-, and O-glycosides by E. Coli beta-galactosidases. J. Am. Chem. Soc. 124 (2002) 4804-4810.

[100] M.R. Wormald, C.J. Edge, R.A. Dwek, The solution conformation of the LeX group. Biochem. Biophys. Res Commun. 180 (1991) 1214-1221.

[101] K.E. Miller, C. Mukhopadhyay, P. Cagas, C.A. Bush, Solution structure of the Lewis x oligosaccharide determined by NMR spectroscopy and molecular dynamics simulations. Biochemistry. 31 (1992) 6703-6709.

[102] H. Kogelberg, TJ. Rutherford, Studies on the three-dimensional behaviour of the selectin ligands Lewis^a and sulphated Lewis^a using NMR spectroscopy and molecular dynamics simulations. Glycobiology. 4 (1994) 49-57.

[103] T.J. Rutherford, D.G. Spackman, P.J. Simpson, S.W. Homans, 5 nanosecond molecular dynamics and NMR study of conformational transitions in the sialyl-Lewis X antigen. Glycobiology 4 (1994) 59-68.

[104] A. Poveda, J.L. Asensio, M. Martín-Pastor, J. Jiménez-Barbero, Solution conformation dynamics of a tetrasaccharide related to the Lewis^x antigen deduced by 1H NMR NOESY, ROESY, and T-ROESY measurements. Carbohydr. Res. 300 (1997) 3-10.

[105] A. Poveda, J.L. Asensio, M. Martín-Pastor, J. Jiménez-Barbero, Exploration of the conformational flexibility of the Le^X related oligosaccharide GalNAcα(1→3)Galβ(1→4)[Fucα1→3)]Glc by 1H NMR relaxation measurements and molecular dynamics simulations. Chem. Commun. (1996) 421-422.

[106] S. V. Ley, D. Neuhaus, D. J. Williams, A conformational study of elaiophylin by x-ray crystallography and difference 1h nmr methods; observation of a selective sign reversal of the nuclear overhauser effect. Tetrahedron Lett. 23 (1982) 1207-1210.

[107] R.U. Lemieux, K.Bock, The conformational analysis of oligosaccharides by H-NMR and HSEA calculation. Arch. Biochem. Biophys. 221 (1983) 125-134.

[108] T. Aeschbacher, M. Zierke, M. Smieško, M. Collot, J. M. Mallet, B. Ernst, F. Allain, M. A Schubert, Secondary structural element in a wide range of fucosylated glycoepitopes. Chem. Eur. J. 23 (2017) 11598-11610.

[109] B. Wagner, F.P.C. Binder, X. Jiang, T. Mühlethaler, R.C. Preston, S. Rabbani, M. Smieško, O. Schwardt, B. Ernst, A Structural-Reporter Group to Determine the Core Conformation of Sialyl Lewisx Mimetics. Molecules. 28 (2023) 2595.

[110] M. Zierke, M. Smieško, S. Rabbani, T. Aeschbacher, B. Cutting, F.H. Allain, M. Schubert, B. Ernst. J Am Chem Soc. 135 (2013) 13464-13472.

[111] M.D. Battistel, H.F. Azurmendi, M. Frank, D. I. Freedberg, Uncovering Nonconventional and Conventional Hydrogen Bonds in Oligosaccharides through NMR Experiments and

Molecular Modeling: Application to Sialyl Lewis-X. J. Am. Chem. Soc. 137 (2015) 13444−13447.

[112] J. Kwon, A. Ruda, H.F. Azurmendi, J. Zarb, M.D. Battistel, L. Liao, A. Asnani, F.I. Auzanneau, G. Widmalm, D.I. Freedberg, Glycan Stability and Flexibility: Thermodynamic and Kinetic Characterization of Nonconventional Hydrogen Bonding in Lewis Antigens. J. Am. Chem. Soc. 145 (2023) 10022-10034.

[113] Y. Zhang, M. Gómez-Redondo, G. Jiménez-Osés, A. Arda, H.S. Overkleeft, G.A .van der Marel, J. Jiménez-Barbero, J.D.C. Codée. Synthesis and structural analysis of *Aspergillus fumigatus* galactosaminogalactans featuring α-galactose, α-galactosamine and α-N-acetyl galactosamine linkages. Angew. Chem. Int. Ed. 59 (2020) 12746-12750.

[114] G. Fittolani, T. Tyrikos-Ergas, A. Poveda, Y. Yu, N. Yadav, P.H. Seeberger, J. Jiménez-Barbero, M. Delbianco, Synthesis of a glycan hairpin. Nat. Chem. 15 (2023) 1461-1469.

[115] N. Yadav, S. Djalali, A. Poveda, M.G. Ricardo, P.H. Seeberger, J. Jiménez-Barbero, M. Delbianco, Dissecting the Conformational Stability of a Glycan Hairpin. J. Am. Chem Soc. 146 (2024) 6369-6376.

[116] F. Casset, T. Peters, M. Etzler, E. Korchagina, N. Nifant'ev, S. Pérez, A. Imberty, Conformational Analysis of Blood Group A Trisaccharide in Solution and in the Binding Site of *Dolichos biflorus* Lectin Using Transient and Transferred Nuclear Overhauser Enhancement (NOE) and Rotating-Frame NOE Experiments. Eur. J. Biochem. 239 (1996) 710-709.

[117] Y. Zhang, B. Dausse, P. Sinaÿ, M. Afsahi, P. Berthault, H. Desvaux, Synthesis and NMR study of a heptasaccharide, epitope of the stage-specific embryonic antigen-1 (SSEA-1). Carbohydr. Res. 324 (2000) 231-241.

[118] P.J. Meloncelli, L.J. West, T.L. Lowary, Synthesis and NMR studies on the ABO histo-blood group antigens: synthesis of type III and IV structures and NMR characterization of type I-VI antigens. Carbohydr. Res. 346 (2011) 1406-1426.

[119] S. Bertuzzi, A. Gimeno, R. Núñez-Franco, G. Bernardo-Seisdedos, S. Delgado, G. Jiménez-Osés, O. Millet, J. Jiménez-Barbero, A. Ardá, Unravelling the time scale of conformational plasticity and allostery in glycan recognition by human galectin-1. Chem. Eur. J. 26 (2020) 15643-15653.

[120] A. Gimeno, S. Delgado, P. Valverde, S. Bertuzzi, M. A. Berbís, J. Echavarren, A. Lacetera, S. Martín-Santamaría, A. Surolia, F.J. Cañada, J. Jiménez-Barbero, A. Ardá, Minimizing the entropy penalty for ligand binding: lessons from the molecular recognition of the histo blood-group antigens by human galectin-3. Angew. Chem. Int. Ed. 131 (2019) 7346-7350.

[121] M. Gómez-Redondo, S. Delgado, R. Núñez-Franco, G. Jiménez-Osés, A. Ardá, J. Jiménez-Barbero, A. Gimeno, The two domains of human galectin-8 bind sialyl- and fucose-containing oligosaccharides in an independent manner. A 3D view by using NMR. RSC Chem. Biol. 2 (2021) 932-941.

[122] J.I. Quintana, S. Delgado, R. Núñez-Franco, F.J. Cañada, G. Jiménez-Osés, J. Jiménez-Barbero, A. Ardá. Galectin-4 N-terminal domain: binding preferences toward A and B antigens with different peripheral core presentations. Front. Chem. 9 (2021) 664097.

[123] T. Rundlöf, L. Eriksson, G. Widmalm, A conformational study of the trisaccharide β-D-Glcp-(1→2)[β-D-Glcp-(1→3)]α-D-Glcp-OMe by NMR NOESY and TROESY experiments, computer simulations, and X-ray cystal structure analysis. Chem. Eur. J. 7 (2001) 1750-1758.

[124] A.M. Dixon, R. Venable, G. Widmalm, T.E. Bull, R.W. Pastor, Application of NMR, molecular simulation, and hydrodynamics to conformational analysis of trisaccharides. Biopolymers. 69 (2003) 448-460.

[125] M. Yang, T. Angles d'Ortoli, E. Säwén, M. Jana, G. Widmalm, A.D. MacKerell, Delineating the conformational flexibility of trisaccharides from NMR spectroscopy experiments and computer simulations. Phys. Chem. Chem. Phys. 18 (2016) 18776-18794.

[126] E. Hatcher, E. Säwén, G. Widmalm, A.D. MacKerell Jr., Conformational properties of methyl β-maltoside and methyl α- and β-cellobioside disaccharides. J. Phys. Chem. B. 115 (2011) 597-608.

[127] H.C. Siebert, S. André, J.L. Asensio, F.J. Cañada, X. Dong, J.F. Espinosa, M. Frank, M. Gilleron, H. Kaltner, T. Kozár, N.V. Bovin, C.W. von Der Lieth, J.F.G. Vliegenthart, J. Jiménez-Barbero, H.J. Gabius. A new combined computational and NMR-spectroscopical strategy for the identification of additional conformational constraints of the bound ligand in an aprotic solvent. Chembiochem. 1 (2000) 181-195.

[128] S. Perez, O. Makshakova, J. Angulo, E. Bedini, A. Bisio, J.L. de Paz, E. Fadda, M. Guerrini, M. Hricovini, M. Hricovini, F. Lisacek, P.M. Nieto, K. Pagel, G. Paiardi, R. Richter, S.A. Samsonov, R.R. Vivès, D. Nikitovic, S. Ricard Blum, Glycosaminoglycans: What Remains To Be Deciphered? JACS Au 3 (2023) 628–656.

[129] J.C. Muñoz-García, E. Chabrol, R.R. Vivès, A. Thomas, J.L. de Paz, J. Rojo, A. Imberty, F. Fieschi, P.M. Nieto, J. Angulo, Langerin–Heparin Interaction: Two Binding Sites for Small and Large Ligands As Revealed by a Combination of NMR Spectroscopy and Cross-Linking Mapping Experiments. J. Am. Chem. Soc. 137 (2015) 4100–4110.

[130] D. Shi, A. Sheng, L. Chi, Glycosaminoglycan-Protein Interactions and Their Roles in Human Disease. Front. Mol. Biosci. 8 (2021) 639666.

[131] S.D. Vallet, O. Clerc, S. Ricard-Blum, Glycosaminoglycan-Protein Interactions: The First Draft of the Glycosaminoglycan Interactome. J. Histochem. Cytochem. 69 (2021) 93–104.

[132] J.M. Whitelock, R.V. Iozzo, Heparan Sulfate: A Complex Polymer Charged with Biological Activity. Chem. Rev. 105 (2005) 2745–2764.

[133] M. Hricovíni, A. Bisio, G. Torri, A. Naggi, B. Casu, M. Guerrini, Active Conformations of Glycosaminoglycans. NMR Determination of the Conformation of Heparin Sequences Complexed with Antithrombin and Fibroblast Growth Factors in Solution. Semin. Thromb. Hemost. 28 (2002) 325–334.

[134] M. Guerrini, M. Hricovíni, G. Torri, Interaction of Heparins with Fibroblast Growth Factors: Conformational Aspects. Curr. Pharm. Des. 13 (2007) 2045–2056.

[135] I. McEwen, B. Mulloy, E. Hellwig, L. Kozerski, T. Beyer, U. Holzgrabe, R. Wanko, J.-M. Spieser, A. Rodomonte, Determination of Oversulphated Chondroitin Sulphate and Dermatan Sulphate in unfractionated heparin by (1)H-NMR - Collaborative study for quantification and analytical determination of LoD. Pharmeuropa Bio 2008 (2008) 31–39.

[136] Y. Song, F. Zhang, R.J. Linhardt, Analysis of the Glycosaminoglycan Chains of Proteoglycans. J. Histochem. Cytochem. 69 (2020) 121–135.

[137] S. Furlan, G. La Penna, A. Perico, A. Cesàro, Hyaluronan chain conformation and dynamics. Carbohydr. Res. 340 (2005) 959–970.

[138] A. Almond, P.L. DeAngelis, C.D. Blundell, Dynamics of Hyaluronan Oligosaccharides Revealed by 15N Relaxation. J. Am. Chem. Soc. 127 (2005) 1086–1087.

[139] O. Guvench, Atomic-Resolution Experimental Structural Biology and Molecular Dynamics Simulations of Hyaluronan and Its Complexes. Molecules 27 (2022) 7276.

[140] T.N. Huckerby, R.M. Lauder, Keratan sulfates from bovine tracheal cartilage, Eur. J. Biochem. 267 (2000) 3360–3369.

[141] R.M. Lauder, T.N. Huckerby, I.A. Nieduszynski, I.H. Sadler, Characterisation of oligosaccharides from the chondroitin/dermatan sulphates: 1H and 13C NMR studies of oligosaccharides generated by nitrous acid depolymerization. Carbohydr. Res. 346 (2011) 2222–2227.

[142] O.F. Restaino, C. Schiraldi, Chondroitin sulfate: are the purity and the structural features well assessed? A review on the analytical challenges. Carbohydr. Polym. 292 (2022) 119690.

[143] G.C.B. Gardini, M. Guerrini, E. Kellenbach, M. Lunenburg, J.Y. van der Meer; A. Naggi, E. Urso, Quantitative 2D 1H, 13C HSQC NMR Spectroscopy for the Determination of Chondroitin Sulfate and Dermatan Sulfate Content in Danaparoid Sodium. Thromb. Haemost. 123 (2023) 856–866.

[144] A. Silipo, Z. Zhang, F.J. Cañada, A. Molinaro, R.J. Linhardt, J. Jiménez-Barbero. Conformational analysis of a dermatan sulfate-derived tetrasaccharide by NMR, molecular modeling, and residual dipolar couplings. Chembiochem. 9 (2008) 240-252.

[145] B. Mulloy, M.J. Forster, Conformation and dynamics of heparin and heparan sulfate. Glycobiology 10 (2000) 1147–1156.

[146] M. Hochuli, K. Wüthrich, B. Steinmann, Two-dimensional NMR spectroscopy of urinary glycosaminoglycans from patients with different mucopolysaccharidoses. NMR Biomed. 16 (2003) 224–236.

[147] U. Lindahl, G. Bäckström, L. Thunberg, I.G. Leder, Evidence for a 3-O-sulfated D-glucosamine residue in the antithrombin-binding sequence of heparin. Proc. Nat. Acad. Sci. 77 (1980) 6551–6555.

[148] G. Gatti, B. Casu, A.S. Perlin, Conformations of the major residues in heparin. 1H-NMR spectroscopic studies. Biochem. Biophys. Res. Commun. 85 (1978) 14–20.

[149] B. Casu, Structure and Biological Activity of Heparin. Adv. Carbohydr. Chem. Biochem. (1985) 51–134.

[150] B. Casu, P. Oreste, G. Torri, G. Zoppetti, J. Choay, J.C. Lormeau, M. Petitou, P. Sinay, The structure of heparin oligosaccharide fragments with high anti-(factor Xa) activity containing the minimal antithrombin III-binding sequence Chemical and13C nuclear-magnetic-resonance studies. Biochem. J. 197 (1981) 599–609.

[151] B. Casu, J. Choay, D. R. Ferro, G. Gatti, J.-C. Jacquinet, M. Petitou, A. Provasoli, M. Ragazzi, P. Sinay, G. Torri, Controversial Glycosaminoglycan Conformations. Nature 322 (1986) 215–216.

[152] Z.M. Merchant, Y.S. Kim, K.G. Rice, R.J. Linhardt, Structure of heparin-derived tetrasaccharides. Biochem. J. 229 (1985) 369–377.

[153] A. Larnkjaer, S.H. Hansen, P.B. Østergaard, Isolation and charaterization of hexasaccharides derived from heparin. Analysis by HPLC and elucidation of structure by 1H NMR, Carbohydr. Res. 266 (1995) 37–52.

[154] S. Beni, J.F.K. Limtiaco, C.K. Larive, Analysis and characterization of heparin impurities. Anal. Bioanal. Chem. 399 (2011) 527–539.

[155] C.D. Blundell, P.L. DeAngelis, A.J. Day, A. Almond, Use of 15N-NMR to resolve molecular details in isotopically-enriched carbohydrates: sequence-specific observations in hyaluronan oligomers up to decasaccharides. Glycobiology 14 (2004) 999–1009.

[156] M. Guerrini, A. Bisio, G. Torri, Combined Quantitative 1H and 13C Nuclear Magnetic Resonance Spectroscopy for Characterization of Heparin Preparations. Semin. Thromb. Hemost. 27 (2001) 473–482.

[157] M. Guerrini, S. Guglieri, A. Naggi, R. Sasisekharan, G. Torri, Low Molecular Weight Heparins: Structural Differentiation by Bidimensional Nuclear Magnetic Resonance Spectroscopy. Semin. Thromb. Hemost. 33 (2007) 478–487.

[158] J. Sitkowski, E. Bednarek, W. Bocian, L. Kozerski, Assessment of Oversulfated Chondroitin Sulfate in Low Molecular Weight and Unfractioned Heparins Diffusion Ordered Nuclear Magnetic Resonance Spectroscopy Method. J. Med. Chem. 51 (2008) 7663–7665.

[159] V.H. Pomin, NMR Chemical Shifts in Structural Biology of Glycosaminoglycans. Anal. Chem. 86 (2014) 65–94.

[160] V.H. Pomin, B. Mulloy, Nuclear Magnetic Resonance Methods in Structural Characterization of Glycosaminoglycans, in: K. Balagurunathan, H. Nakato, U. Desai, Y. Saijoh (Eds.), Glycosaminoglycans: Methods and Protocols, Springer US, New York, (2022) 183–207.

[161] C. Bu, L. Jin, NMR Characterization of the Interactions Between Glycosaminoglycans and Proteins. Front. Mol. Biosci. 8 (2021) 646808.

[162] V.H. Pomin, X. Wang, Glycosaminoglycan-Protein Interactions by Nuclear Magnetic Resonance (NMR) Spectroscopy. Molecules. 23 (2018) 2314.

[163] V.H. Pomin, K. Rajarathnam, NMR Methods for Characterization of Glycosaminoglycan–Chemokine Interactions, in: A.R. Lucas (Ed.), Chemokine-Glycosaminoglycan Interactions: Methods and Protocols, Springer US, New York, (2023) 143–157.

[164] V.H. Pomin, Solution NMR conformation of glycosaminoglycans. Prog. Biophys. Mol. Biol. 114 (2014) 61–68.

[165] V.H. Pomin, Advances in glycosaminoglycanomics by 15N-NMR spectroscopy. Anal. Bioanal. Chem. 405 (2013) 3035–3048.

[166] L. Rodén, S. Ananth, P. Campbell, T. Curenton, G. Ekborg, S. Manzella, D. Pillion, E. Meezan, Heparin — An Introduction, in Heparin and Related Polysaccharides, D.A. Lane, I. Bjork, U. Lindahl (eds). (1992) 1–20.

[167] E.I. Oduah, R.J. Linhardt, S.T. Sharfstein, Heparin: Past, Present, and Future, Pharmaceuticals. 9 (2016) 38.

[168] A. Hughes, M. Meneghetti, T.-Y. Huang, S.-C. Hung, S. Elli, M. Guerrini, T. Rudd, M. Lima, E. Yates, Investigating the relationship between temperature, conformation and calcium binding in heparin model oligosaccharides. Carbohydr. Res. 438 (2017) 58–64.

[169] X. Zhang, V. Pagadala, H.M. Jester, A.M. Lim, T.Q. Pham, A.M.P. Goulas, J. Liu, R.J. Linhardt, Chemoenzymatic synthesis of heparan sulfate and heparin oligosaccharides and NMR analysis: paving the way to a diverse library for glycobiologists. Chem. Sci. 8 (2017) 7932–7940.

[170] M. Bernfield, R. Kokenyesi, M. Kato, M.T. Hinkes, J. Spring, R.L. Gallo, E.J. Lose, Biology of the Syndecans: A Family of Transmembrane Heparan Sulfate Proteoglycans. Annu. Rev. Cell. Dev. Biol. 8 (1992) 365–393.

[171] J.T. Gallagher, J.E. Turnbull, M. Lyon, Heparan Sulphate Proteoglycans: Molecular Organisation of Membrane-Associated Species and an Approach to Polysaccharide Sequence Analysis, Heparin and Related Polysaccharides. Springer US, Boston, MA, (1992) 49–57.

[172] M. Bernfield, M. Götte, P.W. Park, O. Reizes, M.L. Fitzgerald, J. Lincecum, M. Zako, Functions of cell surface heparan sulfate proteoglycans. Annu. Rev. Biochem. 68 (1999) 729–777.

[173] J.D. Esko, Special considerations for proteoglycans and glycosaminoglycans and their purification, Curr. Protoc. Mol. Biol. Chapter 17 (2001) Unit17.2.

[174] D.R. Ferro, Augusto. Provasoli, Massimo. Ragazzi, Giangiacomo. Torri, Benito. Casu, Giuseppe. Gatti, J.Claude. Jacquinet, Pierre. Sinay, Maurice. Petitou, Jean. Choay, Evidence for conformational equilibrium of the sulfated L-iduronate residue in heparin and in synthetic heparin mono- and oligo-saccharides: NMR and force-field studies. J. Am. Chem. Soc. 108 (1986) 6773–6778.

[175] S.K. Das, J.-M. Mallet, J. Esnault, P.-A. Driguez, P. Duchaussoy, P. Sizun, J.-P. Hérault, J.-M. Herbert, M. Petitou, P. Sinaÿ, Synthesis of Conformationally Locked

Carbohydrates: A Skew-Boat Conformation of L-Iduronic Acid Governs the Antithrombotic Activity of Heparin. Angew. Chem. Intern. Ed. 40 (2001) 1670–1673.

[176] D.A. Rees, E.R. Morris, J.F. Stoddart, E.S. Stevens, Controversial glycosaminoglycan conformations. Nature 317 (1985) 480.

[177] F. Demeter, T. Gyöngyösi, Z. Bereczky, K.E. Kövér, M. Herczeg, A. Borbás, Replacement of the L-iduronic acid unit of the anticoagulant pentasaccharide idraparinux by a 6-deoxy-L-talopyranose – Synthesis and conformational analysis. Sci. Rep. 8 (2018) 13736.

[178] J.C. Muñoz-García, J. López-Prados, J. Angulo, I. Díaz-Contreras, N. Reichardt, J.L. de Paz, M. Martín-Lomas, P.M. Nieto, Effect of the Substituents of the Neighboring Ring in the Conformational Equilibrium of Iduronate in Heparin-like Trisaccharides. Chem. Eur. J. 18 (2012) 16319–16331.

[179] D.R. Ferro, A. Provasoli, M. Ragazzi, B. Casu, G. Torri, V. Bossennec, B. Perly, P. Sinaÿ, M. Petitou, J. Choay, Conformer populations of l-iduronic acid residues in glycosaminoglycan sequences. Carbohydr. Res. 195 (1990) 157–167.

[180] J.C. Muñoz-García, F. Corzana, J.L. de Paz, J. Angulo, P.M. Nieto, Conformations of the iduronate ring in short heparin fragments described by time-averaged distance restrained molecular dynamics. Glycobiology. 23 (2013) 1220–1229.

[181] L. Unione, B. Xu, D. Díaz, S. Martín-Santamaría, A. Poveda, J. Sardinha, A.P. Rauter, Y. Blériot, Y. Zhang, F.J. Cañada, M. Sollogoub, J. Jiménez-Barbero, Conformational plasticity in glycomimetics: fluorocarbamethyl-L-idopyranosides mimic the intrinsic dynamic behaviour of natural idose rings. Chem. Eur. J. 21 (2015) 10513-10521.

[182] L. Jin, M. Hricovíni, J.A. Deakin, M. Lyon, D. Uhrín, Residual dipolar coupling investigation of a heparin tetrasaccharide confirms the limited effect of flexibility of the iduronic acid on the molecular shape of heparin. Glycobiology. 19 (2009) 1185–1196.

[183] Z. Zhang, S.A. McCallum, J. Xie, L. Nieto, F. Corzana, J. Jiménez-Barbero, M. Chen, J. Liu, R.J. Linhardt, Solution Structures of Chemoenzymatically Synthesized Heparin and Its Precursors. J. Am. Chem. Soc. 130 (2008) 12998–13007.

[184] M. Ragazzi, D.R. Ferro, A. Provasoli, A force-field study of the conformational characteristics of the iduronate ring. J. Comput. Chem. 7 (1986) 105–112.

[185] J. Angulo, P.M. Nieto, M. Martín-Lomas, A molecular dynamics description of the conformational flexibility of the L-iduronate ring in glycosaminoglycans. Chem. Commun. (2003) 1512–1513.

[186] C.F. Becker, J.A. Guimarães, H. Verli, Molecular dynamics and atomic charge calculations in the study of heparin conformation in aqueous solution. Carbohydr. Res. 340 (2005) 1499–1507.

[187] E. Stancanelli, S. Elli, P.-H. Hsieh, J. Liu, M. Guerrini, Recognition and Conformational Properties of an Alternative Antithrombin Binding Sequence Obtained by Chemoenzymatic Synthesis. ChemBioChem. 19 (2018) 1178–1188.

[188] M. Petitou, C. A A van Boeckel, A synthetic antithrombin III binding pentasaccharide is now a drug! What comes next?. Angew. Chem. Int. Ed. Engl. 43 (2004) 3118–3133.

[189] L. Jin, J.P. Abrahams, R. Skinner, M. Petitou, R.N. Pike, R.W. Carrell, The anticoagulant activation of antithrombin by heparin. Proc. Nat. Acad. Sci. 94 (1997) 14683–14688.

[190] J. Angulo, R. Ojeda, J.-L. de Paz, R. Lucas, P.M. Nieto, R.M. Lozano, M. Redondo-Horcajo, G. Giménez-Gallego, M. Martín-Lomas, The activation of fibroblast growth factors (FGFs) by glycosaminoglycans: influence of the sulfation pattern on the biological activity of FGF-1. Chembiochem. 5 (2004) 55–61.

[191] J.C. Muñoz-García, C. Solera, P. Carrero, J.L. de Paz, J. Angulo, P.M. Nieto, 3D structure of a heparin mimetic analogue of a FGF-1 activator. A NMR and molecular modelling study. Org. Biomol. Chem. 11 (2013) 8269–8275.

[192] L. Nieto, Á. Canales, I.S. Fernández, E. Santillana, R. González-Corrochano, M. Redondo-Horcajo, F.J. Cañada, P. Nieto, M. Martín-Lomas, G. Giménez-Gallego, J. Jiménez-Barbero, Heparin Modulates the Mitogenic Activity of Fibroblast Growth Factor by Inducing Dimerization of its Receptor. A 3D View by Using NMR. ChemBioChem. 14 (2013) 1732–1744.

[193] J. Hanske, R. Wawrzinek, A. Geissner, E.-C. Wamhoff, K. Sellrie, H. Schmidt, P.H. Seeberger, C. Rademacher, Calcium-Independent Activation of an Allosteric Network in Langerin by Heparin Oligosaccharides. ChemBioChem. 18 (2017) 1183–1187.

[194] J.L. de Paz, E.A. Moseman, C. Noti, L. Polito, U.H. von Andrian, P.H. Seeberger, Profiling Heparin–Chemokine Interactions Using Synthetic Tools. ACS Chem Biol 2 (2007) 735–744.

[195] I.C. Severin, J.-P. Gaudry, Z. Johnson, A. Kungl, A. Jansma, B. Gesslbauer, B. Mulloy, C. Power, A.E.I. Proudfoot, T. Handel, Characterization of the Chemokine CXCL11-Heparin Interaction Suggests Two Different Affinities for Glycosaminoglycans. J. Biol. Chem. 285 (2010) 17713–17724.

[196] K. Kobayashi, R. Takano, H. Takemae, T. Sugi, A. Ishiwa, H. Gong, F.C. Recuenco, T. Iwanaga, T. Horimoto, H. Akashi, K. Kato, Analyses of Interactions Between Heparin and the Apical Surface Proteins of Plasmodium falciparum. Sci. Rep. 3 (2013) 3178.

[197] A. Canales, R. Lozano, B. López-Méndez, J. Angulo, R. Ojeda, P.M. Nieto, M. Martín-Lomas, G. Giménez-Gallego, J. Jiménez-Barbero, Solution NMR structure of a human FGF-1 monomer, activated by a hexasaccharide heparin-analogue. FEBS J. 273 (2006) 4716-4727.

[198] J. Angulo, M. Hricovíni, M. Gairi, M. Guerrini, J.L. de Paz, R. Ojeda, M. Martín-Lomas, P.M. Nieto, Dynamic properties of biologically active synthetic heparin-like hexasaccharides. Glycobiology. 15 (2005) 1008–1015.

[199] M. Hricovíni, Solution Structure of Heparin Pentasaccharide: NMR and DFT Analysis, J. Phys. Chem. B. 119 (2015) 12397–12409.

[200] H. Verli, J.A. Guimar, Molecular dynamics simulation of a decasaccharide fragment of heparin in aqueous solution, Time 339 (2004) 281–290.

[201] S. Faham, R.E. Hileman, J.R. Fromm, R.J. Linhardt, D.C. Rees, Heparin Structure and Interactions with Basic Fibroblast Growth Factor. Science. 271 (1996) 1116–1120.

[202] A. Canales, J. Angulo, R. Ojeda, M. Bruix, R. Fayos, R. Lozano, G. Giménez-Gallego, M. Martín-Lomas, P.M. Nieto, J. Jiménez-Barbero, Conformational Flexibility of a Synthetic Glycosylaminoglycan Bound to a Fibroblast Growth Factor. FGF-1 Recognizes Both the 1C4 and 2SO Conformations of a Bioactive Heparin-like Hexasaccharide. J. Am. Chem. Soc, 127 (2005) 5778–5779.

[203] J. Jiménez-Barbero, J.F. Espinosa, J.L. Asensio, F.J. Cañada, A. Poveda, The conformation of C-glycosyl compounds, Adv. Carbohydr. Chem. Biochem. 56 (2000) 235-284.

[204] I. Raich, Z. Lövyová, L. Trnka, K. Parkan, J. Kessler, R. Pohl, J. Kaminský, Limitations in the description of conformational preferences of C-disaccharides: The (1 → 3)-C-mannobiose case. Carbohydr. Res. 451 (2017) 42-50.

[205] P. Vidal, J. Jiménez-Barbero, J.F. Espinosa, Conformational flexibility around the Gal-β-(1 → 3)-Glc linkage: Experimental evidence for the existence of the anti-ψ conformation in aqueous solution. Carbohydr. Res. 433 (2016) 36-40.

[206] P. Vidal, B. Vauzeilles, Y. Blériot, M. Sollogoub, P. Sinaÿ, J. Jiménez-Barbero, J.F. Espinosa, Conformational behaviour of glycomimetics: NMR and molecular modelling studies

of the C-glycoside analogue of the disaccharide methyl beta-D-galactopyranosyl-(1-->3)-beta-D-glucopyranoside. Carbohydr. Res. 342 (2007) 12-23.

[207] P. Vidal, V. Roldós, M.C. Fernández-Alonso, B. Vauzeilles, Y. Bleriot, F.J. Cañada, S. André, H.J. Gabius, J. Jiménez-Barbero, J.F. Espinosa, S. Martín-Santamaría, Conformational selection in glycomimetics: human galectin-1 only recognizes syn-Ψ-type conformations of β-1,3-linked lactose and its C-glycosyl derivative. Chem. Eur. J. 19 (2013) 14581-14590.

[208] K. Mazeau, I. Tvaroska, PCILO quantum-mechanical relaxed conformational energy map of methyl 4-thio-α-maltoside in solution. Carbohydr. Res. 225 (1992) 27-41.

[209] K. Bock, J. Defaye, H. Drigues, E. Bar-Guilloux, Conformations in solution of α,α-trehalose, α-d-glucopyranosyl α-d-Mannopyranoside, and their 1-thioglycosyl analogs, and a tentative correlation of their behaviour with respect to the enzyme trehalase. Eur. J. Biochem. 131 (1983) 595-600.

[210] C. Sandström, G. Magnusson, U. Nilsson, L. Kenne, Comparative 1H NMR study of hydroxy protons in galabioside and its S-linked 4-thiodisaccharide analogue in aqueous solution. Carbohydr. Res. 322 (1999) 46-56.

[211] T. Weimar, B. Stoffer, B. Svensson, B. M. Pinto, Complexes of glucoamylase with maltoside heteroanalogues: bound ligand conformations by use of transferred NOE experiments and molecular modelling. Biochemistry. 39 (2000) 300–306.

[212] L. Calle, V. Roldós, F.J. Cañada, M.L. Uhrig, A.J. Cagnoni, V.E. Manzano, O. Varela, J. Jiménez-Barbero, Escherichia coli β-galactosidase inhibitors through modifications at the aglyconic moiety: experimental evidence of conformational distortion in the molecular recognition process. Chem. Eur. J. 19 (2013) 4262-4270.

[213] S. Martín-Santamaría, S. André, E. Buzamet, R. Caraballo, G. Fernández-Cureses, M. Morando, J.P. Ribeiro, K. Ramírez-Gualito, B. de Pascual-Teresa, F.J. Cañada, M. Menéndez, O. Ramström, J. Jiménez-Barbero, D. Solís, H-J. Gabius. Symmetric dithiodigalactoside: strategic combination of binding studies and detection of selectivity between a plant toxin and human lectins. **Org. Biomol. Chem. 9 (**2011) 5445-5455.

[214] J. Uzawa, J. Shimabukuro, T. Suzuki, A. Imamura, H. Ishida, H. Ando, Y. Yamaguchi, J(^{77}Se,^{1}H) and J(^{77}Se,^{13}C) couplings of seleno-carbohydrates obtained by ^{77}Se satellite 1D ^{13}C spectroscopy and ^{77}Se selective HR-HMBC spectroscopy. Magn. Res. Chem. 56 (2018) 836-846.

[215] T. Diercks, F.J. Medrano, F.G. FitzGerald, D. Beckwith, M. J. Pedersen, M. Reihill, A-K. Ludwig, A. Romero, S. Oscarson, M. Cudic, H-J. Gabius, Galectin–glycan interactions: Guidelines for monitoring by ^{77}Se NMR spectroscopy, and solvent (H_2O/D_2O) impact on binding. Chem. Eur. J. 27 (2021) 316-325.

[216] M. Raics, I. Timári, T. Diercks, L. Szilágyi, H-J. Gabius, K. E. Kövér, Selenoglycosides as lectin ligands: 77 Se-edited CPMG-HSQMBC NMR spectroscopy to monitor biomedically relevant interactions. ChemBioChem. 20 (2019) 1688-1692.

[217] E. Montero, A. García, JL. Asensio, FJ. Cañada, F. Santoyo, S. Ogawa, J. Jiménez-Barbero, The conformational behaviour of non-hydrolizable lactose analogues. The thioglycoside, carbaglycoside, and carba-iminoglycoside cases. Eur. J. Org. Chem. (2000) 1945-1952.

[218] E.M: Sánchez-Fernández, R. Rísquez-Cuadro, C. Ortiz Mellet, J.M. García Fernández, P.M. Nieto, J. Angulo, Sp2-Iminosugar O-, S-, and N-glycosides as conformational mimics of α-linked disaccharides; implications for glycosidase inhibition. Chem. Eur. J. 18 (2012) 8527-8539.

[219] A. Tamburrini, C. Colombo, A. Bernardi, Design and synthesis of glycomimetics: Recent advances. Med. Res. Rev. 40 (2020) 495-531.

[220] B. Linclau, A. Ardá, N.C. Reichardt, M. Sollogoub, L. Unione, S.P. Vincent, J. Jiménez-Barbero, Fluorinated carbohydrates as chemical probes for molecular recognition studies. Current status and perspectives. Chem Soc Rev. 49 (2020) 3863-3888.

[221] G. M. Alter, J. A. Magnuson, Characterization of concanavalin A sugar binding site by F-19 nuclear magnetic resonance. Biochemistry. 13 (1974) 4038-4045.

[222] P. Midoux, J.-P. Grivet, M. Monsigny, Lectin-sugar interactions: the binding of -O-methyl-di-N-trifluoroacetyl-β-chitobioside to wheat germ agglutinin. Febs Lett. 120 (1980) 29-32.

[223] F. Jordan, H. Bahr, J. Patrick, P. W. K. Woo, Nuclear magnetic resonance studies on wheat germ agglutinin-monomeric amino sugar interactions. Arch. Biochem. Biophys. 207 (1981) 81–86.

[224] B. Xu, L. Unione, J. Sardinha, S. Wu, M. Ethève-Quelquejeu, A.P. Rauter, Y. Blériot, Y. Zhang, S. Martín-Santamaría, D. Díaz, J. Jiménez-Barbero, M. Sollogoub, gem-difluorocarbadisaccharides: restoring the exo-anomeric effect. Angew. Chem. Int. Ed. 53 (2014) 9597-9602.

[225] L. Unione, M. Alcalá, B. Echeverria, S. Serna, A. Ardá, A. Franconetti, F. J. Cañada, T. Diercks, N. Reichardt, J. Jiménez-Barbero, Fluoroacetamide moieties as NMR spectroscopy probes for the molecular recognition of GlcNAc-containing sugars: modulation of the CH-π stacking interactions by different fluorination patterns. Chem. Eur. J. 23 (2017) 3957-3965.

[226] C. Dalvit, P.E. Fagerness, D.T. Hadden, R.W. Sarver, B.J. Stockman, Fluorine-NMR experiments for high-throughput screening: theoretical aspects, practical considerations, and range of applicability. J. Am. Chem. Soc. 125 (2003) 7696-7703.

[227] C. Dalvit, N. Mongelli, G. Papeo, P. Giordano, M. Veronesi, D. Moskau, R. Kümmerle, Sensitivity improvement in 19F NMR-based screening experiments: theoretical considerations and experimental applications. J. Am. Chem. Soc. 127 (2005) 13380-13385.

[228] A. Vulpetti, U. Hommel, G. Landrum, R. Lewis, C. Dalvit, Design and NMR-based screening of LEF, a library of chemical fragments with different local environment of fluorine. J. Am. Chem. Soc. 131 (2009) 12949-12959.

[229] U. Atxabal, A. Fernández, M.J. Moure, K. Sobczak, C. Nycholat, V. Almeida-Marrero, I. Oyenarte, J.C. Paulson, A. de la Escosura, T. Torres, N.C. Reichardt, J. Jiménez-Barbero, J. Ereño-Orbea, Quantifying Siglec-Sialylated Ligand Interactions: A versatile 19F-T2 CPMG Filtered Competitive NMR Displacement Assay. Chem. Sci. 15 (2024) https://doi.org/10.1039/D4SC01723D.

[230] E. C. Wamhoff, J. Hanske, L. Schnirch, J. Aretz, M. Grube, D. Varón Silva, C. Rademacher, 19F NMR-guided design of glycomimetic langerin ligands. ACS Chem. Biol. 11 (2016) 2407-2413.

[231] J. D. Martínez, P. Valverde, S. Delgado, C. Romanò, B. Linclau, N. C. Reichardt, S. Oscarson, A. Ardá, J. Jiménez-Barbero, F. J. Cañada, Unraveling sugar binding modes to DC-SIGN by employing fluorinated carbohydrates. Molecules 24 (2019) 2337.

[232] J.D. Martínez, A.I. Manzano, E. Calviño, A. Diego, B. Rodriguez de Francisco, C. Romanò, S. Oscarson, O. Millet, H.J. Gabius, J. Jiménez-Barbero, F.J. Cañada. Fluorinated Carbohydrates as Lectin Ligands: Simultaneous Screening of a Monosaccharide Library and Chemical Mapping by ^{19}F NMR Spectroscopy. J Org Chem. 85 (2020) 16072-16081.

[233] G. Fittolani, E. Shanina, M. Guberman, P. H. Seeberger, C. Rademacher, M. Delbianco, Automated Glycan Assembly of ^{19}F-labeled Glycan Probes Enables High-Throughput NMR Studies of Protein–Glycan Interactions. Angew. Chem. Int. Ed. 60 (2021) 13302-13309.

[234] E. Shanina, S Kuhaudomlarp, K. Lal, P. H. Seeberger, A, Imberty, C. Rademacher, Druggable Allosteric Sites in b-Propeller Lectins. Angew. Chem. Int. Ed. 60 (2021) 2-11.

[235] E. Matei, S. André, A. Glinschert, A.S. Infantino, S. Oscarson, H.J. Gabius, A.M. Gronenborn. Fluorinated carbohydrates as lectin ligands: dissecting glycan-cyanovirin interactions by using 19F NMR spectroscopy. Chem. Eur. J. 19 (2013) 5364-5374.

[236] K.F. Morris, C.S. Johnson Jr., J Diffusion-ordered two-dimensional nuclear magnetic resonance spectroscopy. J. Am. Chem. Soc. 114 (1992) 3139-3141.

[237] E.J. Cabrita, S. Berger, HR-DOSY as a new tool for the study of chemical exchange phenomena. Magn. Reson. Chem. 40 (2002) S122-S127.

[238] J. Camponovo, C. Hadad, J. Ruiz, E. Cloutet, S. Gatard, J. Muzart, S. Bouquillon, D. Astruc. "Click" glycodendrimers containing 27, 81, and 243 modified xylopyranoside termini. J. Org. Chem. 74 (2009) 5071-5074.

[239] R. Cao, F. Komura, A. Nonaka, T. Kato, J. Fukumashi, T. Matsui, Quantitative analysis of D-(+)-glucose in fruit juices using diffusion ordered-1H nuclear magnetic resonance spectroscopy. Anal. Sci. 30 (2014) 383-368.

[240] M. Politi, P. Groves, M.I. Chávez, F.J. Cañada, J. Jiménez-Barbero, Useful applications of DOSY experiments for the study of mushroom polysaccharides. Carbohydr. Res. 341 (2006) 84-89.

[241] W.L. De Man, E. Vaneeckhaute, N. De Brier, A.G.B. Wouters, J.A. Martens, E. Breynaert, J.A. Delcour, 1H Diffusion-Ordered Nuclear Magnetic Resonance Spectroscopic Analysis of Water-Extractable Arabinoxylan in Wheat Triticum aestivum Flour. J. Agric. Food Chem. 69 (2021) 3912-3922.

[242] M. C. Miller, A. Klyosov, D. Platt, K. H. Mayo Using pulse field gradient NMR diffusion measurements to define molecular size distributions in glycan preparations. Carbohydr.Res. 344 (2009) 1205-1212.

[243] A. Bellomaria, R. Nepravishta, U. Mazzanti, M. Marchetti, P. Piccioli, M. Paci, Determination of the presence of hyaluronic acid in preparations containing amino acids: the molecular weight characterization. Eur. J. Pharm. Sci. 63 (2014) 199-203.

[244] Y.B. Monakhova, B.W.K. Diehl. Nuclear magnetic resonance spectroscopy as an elegant tool for a complete quality control of crude heparin material. J. Pharm. Biomed. Anal. 219 (2022) 114915.

[245] A. Mola, F.F. Summa, P. Oliva, F. Lelj, S. Remiddi, L. Silvani, A. Massa., Synergistic Properties of Arabinogalactan (AG) and Hyaluronic Acid (HA) Sodium Salt Mixtures. Molecules. 26 (2021) 7246.

[246] E. Bednarek, J. Sitkowski, W. Bocian, B. Mulloy, L. Kozerski. An assessment of polydispersed species in unfractionated and low molecular weight heparins by diffusion ordered nuclear magnetic resonance spectroscopy method. J. Pharm. Biomed. Anal. 53 (2010) 302-308.

[247] Y. B. Monakhova, B. W. K. Diehl, T. X. Do, M. Schulze, S. Witzleben, A. Eletsky. Novel method for the determination of average molecular weight of natural polymers based on 2D DOSY NMR and chemometrics: Example of heparin. J. Pharm. Biomed Anal. 149 (2018) 128-132.

[248] S. Viel, D. Capitani, L. Mannina, A. Segre, Diffusion-ordered NMR spectroscopy: a versatile tool for the molecular weight determination of uncharged polysaccharides. Biomacromolecules. 4 (2003) 1843-1847.

[249] J. Sitkowski, E. Bednarek, W. Bocian, L. Kozerski, Assessment of oversulfated chondroitin sulfate in low molecular weight and unfractioned heparins diffusion ordered nuclear magnetic resonance spectroscopy method. J. Med. Chem. 51 (2008) 7663-7665.

[250] P. Groves, M.O. Rasmussen, M.D. Molero, E. Samain, F.J. Cañada, H. Driguez, J. Jiménez-Barbero, Diffusion ordered spectroscopy as a complement to size exclusion chromatography in oligosaccharide analysis. Glycobiology. 14 (2004) 451-456.

[251] J.L. Asensio, F.J. Cañada, H.C. Siebert, J. Laynez, A. Poveda, P.M. Nieto, U.M. Soedjanaamadja, H.J. Gabius, J. Jiménez-Barbero. Structural basis for chitin recognition by defense proteins: GlcNAc residues are bound in a multivalent fashion by extended binding sites in hevein domains. Chem Biol. 7 (2000) 529-543.

[252] M.D. Díaz, S. Berger, Studies of the complexation of sugars by diffusion-ordered NMR spectroscopy. Carbohydr Res. 329 (2000) 1-5.

[253] L. Jia, R. Liu, J. Lv, L. Liu, Z. Zhang, Y. Wang, X. Hou, Probing the interactions of GlcNH2 with boric acid via NMR spectroscopy. Phys. Chem. Chem. Phys. 23 (2021) 15758-15765.

[254] T. Fujimoto, S. Sakurai, A. Tsutsui, K. Furihata, T. Machinami, M. Tashiro, Observation of 1,6-anhydro-beta-maltose and 1,6-anhydro-beta-D-glucopyranose complexed with rubidium by NMR spectroscopy and electrospray ionization mass spectrometry. Anal. Sci. 21 (2005) 1245-1247.

[255] J.I. Santos, A. Carvalho de Souza, F.J. Cañada, S. Martín-Santamaría, J.P. Kamerling, J. Jiménez-Barbero, Assessing carbohydrate-carbohydrate interactions by NMR spectroscopy: the trisaccharide epitope from the marine sponge Microciona prolifera. Chembiochem. 10 (2009) 511-519.

[256] L. Jütten, K. Ramírez-Gualito, A. Weilhard, B. Albrecht, G. Cuevas, M.C. Fernández-Alonso, J. Jiménez-Barbero, N.E. Schlörer, M.D. Díaz-Hernández, Exploring the Role of Solvent on Carbohydrate–Aryl Interactions by Diffusion NMR-Based Studies. ACS Omega. 3 (2018) 536-543.

[257] T. Yamanoi, Y. Oda, K. Katsuraya, Separation of the α-and β-Anomers of Carbohydrates by Diffusion-Ordered NMR Spectroscopy. Magnetochemistry. 3 (2017) 38.

[258] K. Vermillion, N.P. Price, Stable isotope-enhanced two- and three-dimensional diffusion ordered 13C NMR spectroscopy (SIE-DOSY 13C NMR). J. Magn. Reson. 198 (2009) 209-14.

[259] Y. Belabassi, J. Moreau, V. Gheran, C. Henoumont, A. Robert, N. Callewaert, G. Rigaux, C. Cadiou, L. Vander Elst, S. Laurent, R.N. Muller, A. Dinischiotu, S.N. Voicu, F. Chuburu, Synthesis and Characterization of PEGylated and Fluorinated Chitosans: Application to the Synthesis of Targeted Nanoparticles for Drug Delivery Biomacromolecules. 18 (2017) 2756-2766.

[260] I. Bertini, C. Luchinat, G. Parigi, R. Pierattelli, NMR spectroscopy of paramagnetic metalloproteins. ChemBioChem. 6 (2005) 1536-1549.

[261] A. Leonov, B. Voigt, F. Rodríguez-Castañeda, P. Sakhaii, C. Griesinger, Convenient Synthesis of Multifunctional EDTA-Based Chiral Metal Chelates Substituted with an S-Mesylcysteine Chem. Eur. J. 11 (2005) 3342 – 3348.

[262] K. Barthelmes, A.M. Reynolds, E. Peisach, H.R. Jonker, N.J. DeNunzio, K.N. Allen, B. Imperiali, H. Schwalbe, Engineering encodable lanthanide-binding tags into loop regions of proteins. J. Am. Chem. Soc. 133 (2011) 808-19.

[263] T. Müntener, D. Joss, D. Haussinger, S. Hiller, Pseudocontact shifts in biomolecular NMR spectroscopy. Chem. Rev. 122 (2022) 9422-9467.

[264] C. Luchinat, M. Nagulapalli, G. Parigi, L. Sgheri, Maximum occurrence analysis of protein conformations for different distributions of paramagnetic metal ions within flexible two-domain proteins. J. Mag. Reson. 215 (2012) 85-93.

[265] K. Kato, T. Yamaguchi, Paramagnetic NMR probes for characterization of the dynamic conformations and interactions of oligosaccharides. Glycoconj. J. 2015, 32 (2015) 505-513.

[266] D. Joss, D. Häussinger, Design and applications of lanthanide chelating tags for pseudocontact shift NMR spectroscopy with biomacromolecules. Prog. Nucl. Magn. Reson. Spectrosc. 114-115 (2019) 284-312.

[267] Q. Miao, C. Nitsche, H. Orton, M. Overhand, G. Otting, M. Ubbink, Paramagnetic Chemical Probes for Studying Biological Macromolecules. Chem. Rev. 122 (2022) 9571-9642.

[268] A. Mallagaray, A. Canales, G. Domínguez, J. Jiménez-Barbero, J. Pérez-Castells. A rigid lanthanide binding tag for NMR structural analysis of carbohydrates. Chem. Commun. 47 (2011) 7179-7181.

[269] T. Yamaguchi, Y. Sakae, Y. Zhang, S. Yamamoto, Y. Okamoto, K. Kato K. Exploration of conformational spaces of high-mannose-type oligosaccharides by an NMR-validated simulation. Angew. Chem. Int. Ed. Engl. 53 (2014) 10941-10944.

[270] A. Canales, A. Mallagaray, J. Pérez-Castells, I. Boos, C. Unverzagt, S. André, H.J. Gabius, F.J. Cañada, J. Jiménez-Barbero. Breaking pseudo-symmetry in mutiantennary complex N-glycans using lanthanide binding tagging and NMR pseudo-contact shifts. Angew. Chem. Int. Ed. Engl. 52 (2013) 13789-13793.

[271] A. Canales, J. Jimenez-Barbero, M. Martin-Pastor, Use of RDCs to determine the conformation of carbohydrates, Magn Reson Chem, 50 (2012) Suppl 1: S80-5.

[272] M. Erdélyi, E. d'Auvergne, A. Navarro-Vázquez, A. Leonov, C. Griesinger. Dynamics of the glycosidic bond: conformational space of lactose. Chem. Eur. J. 17 (2011), 9368-9376.

[273] M.L. Demarco, R.J. Woods, J.H. Prestegard, F. Tian, Presentation of membrane anchored glycosphingolipids determined from molecular dynamics simulations and NMR paramagnetic relaxation enhancement. J. Am. Chem. Soc. 132 (2010) 1334-1338.

[274] G. Otting. Prospects for lanthanides in structural biology by NMR. J. Biomol. NMR. 42 (2008) 1-9.

[275] M. Weiss, D. Ott, T. Karagiannis, M. Weishaupt, N. Niemietz, S. Eller, M. Lott, M. Martínez-Orts, A. Canales, N. Razi, J.C. Paulson, C. Unverzagt. Efficient Chemoenzymatic Synthesis of N-Glycans with a β1,4-Galactosylated Bisecting GlcNAc Motif. ChemBiochem. 21 (2020) 3212-3215.

[276] A. Canales, I. Boos, L. Perkams, L. Karst, T. Luber, T. Karagiannis, G. Domínguez, F.J. Cañada., J. Pérez-Castells, D. Häussinger, C. Unverzagt, J. Jiménez-Barbero, Breaking the limits in analyzing carbohydrate recognition by NMR spectroscopy: Resolving branch-selective interaction of a tetra-Antennary N-Glycan with lectins. Angew Chem. Int. Ed. Engl. 56 (2017) 14987-14991.

[277] T. Suzuki, M. Kajino, S. Yanaka, T. Zhu, H. Yagi, T. Satoh, T. Yamaguchi, K. Kato, Conformational Analysis of a High-Mannose-Type Oligosaccharide Displaying Glucosyl Determinant Recognised by Molecular Chaperones Using NMR-Validated Molecular Dynamics Simulation. Chembiochem. 18 (2017) 396-401.

[278] Y. Zhang, T. Yamaguchi, T. Satoh, M. Yagi-Utsumi, Y. Kamiya, Y. Sakae, Y. Okamoto, K. Kato. Conformational dynamics of oligosaccharides characterized by paramagnetism-assisted NMR spectroscopy in conjunction with molecular dynamics simulation. Adv. Exp. Med. Biol. 842 (1015) 217-30.

[279] T. Yamaguchi, Y. Sakae, Y. Zhang, S. Yamamoto, Y. Okamoto, K. Kato. Exploration of conformational spaces of high-mannose-type oligosaccharides by an NMR-validated simulation. Angew Chem Int Ed Engl. 53 (2014) 10941-10944.

[280] Y. Zhang, S. Yamamoto, T. Yamaguchi, K. Kato. Application of paramagnetic NMR-validated molecular dynamics simulation to the analysis of a conformational ensemble of a branched oligosaccharide. Molecules. 17 (2012) 6658-6671.

[281] S. Yamamoto, T. Yamaguchi, M. Erdélyi, C. Griesinger, K. Kato. Paramagnetic lanthanide tagging for NMR conformational analyses of N-linked oligosaccharides. Chem. Eur. J. 17 (2011) 9280-9282.

[282] https://mestrelab.com/software/mnova-software/

[283] A. Canales, A. Mallagaray, M. A. Berbís, A. Navarro-Vázquez, G. Domínguez, F. J. Cañada, S. André, H. J. Gabius, J. Pérez-Castells, J. Jiménez-Barbero. Lanthanide-chelating Carbohydrate conjugates are useful tools to characterize carbohydrate conformation in

solution and sensitive sensors to detect carbohydrate–protein interactions. J. Am. Chem. Soc. 136 (2014) 8011–8017.

[284] T. Zhuang, L.S. Lee, B. Imperiali, J.H. Prestegard, Structure determination of a Galectin-3-carbohydrate complex using paramagnetism-based NMR constraints. Prot. Sci. 17 (2008) 1220-1231.

[285] Q. Gao, C.Y. Chen, C. Zong, S. Wang, A. Ramiah, L.C. Prabhakar, L.C. Morris, G.J. Boons, K.W. Moremen, J.H. Prestegard, Structural Aspects of Heparan Sulfate Binding to Robo1-Ig1-2. ACS Chem. Biol. 11 (2016) 3106-3113.

[286] A.J. Thompson, N.C. Wu, A. Canales, C. Kikuchi, X. Zhu, B.F. de Toro, F.J. Cañada, C. Worth, S. Wang, R. McBride, W. Peng, C.M: Nycholat, J. Jiménez-Barbero, I.A. Wilson, J.C. Paulson. Evolution of human H3N2 influenza virus receptor specificity has substantially expanded the receptor-binding domain site. Cell Host Microbe. 32 (2024) 261-275.

[287] B. Fernández de Toro, W. Peng, A.J. Thompson, G. Domínguez, F.J. Cañada, J. Pérez-Castells, J.C. Paulson, J. Jiménez-Barbero, A. Canales. Avenues to Characterize the Interactions of Extended N-Glycans with Proteins by NMR Spectroscopy: The Influenza Hemagglutinin Case. Angew. Chem. Int. Ed. Engl. 57 (2018) 15051-15055.

[288] A. Canales, J. Sastre, J.M. Orduña, C. M. Spruit, J. Pérez-Castells, G. Domínguez, K.M. Bouwman, R. van der Woude, F.J. Cañada, C.M. Nycholat, J.C. Paulson, G.-J. Boons, J. Jiménez-Barbero, R. P. de Vries Revealing the Specificity of Human H1 Influenza A Viruses to Complex N-Glycans. JACS Au. 3 (2023) 868-878.

[289] T. Yamaguchi, Y. Kamiya, Y.-M. Choo, S. Yamamoto, K.Kato, Terminal Spin Labeling of a High-mannose-type Oligosaccharide for Quantitative NMR Analysis of Its Dynamic Conformation, Chem. Lett. 42 (2013) 544–546.

[290] M.G. Lete, A. Franconetti, S. Delgado, J. Jiménez-Barbero, A. Ardá, Oligosaccharide Presentation Modulates the Molecular Recognition of Glycolipids by Galectins on Membrane Surfaces. Pharmaceuticals. 15 (2022) 145.

[291] A. Mallagaray, G. Domínguez, T. Peters, J. Pérez-Castells, A rigid lanthanide binding tag to aid NMR studies of a 70 kDa homodimeric coat protein of human norovirus Chem. Commun. 52 (2016) 601-604.

[292] C. Deshauer, A.M. Morgan, E.O. Ryan, T.M. Handel, J.H. Prestegard, X. Wang. Interactions of the Chemokine CCL5/RANTES with Medium-Sized Chondroitin Sulfate Ligands. Structure. 23 (2015) 1066-1077.

[293] M.J. Moure, A. Eletsky, Q. Gao, L.C. Morris, J.-Y. Yang, D. Chapla, Y. Zhao, C. Zong, I.J. Amster, K.W. Moremen, G.-J. Boons, J.H. Prestegard. Paramagnetic Tag for Glycosylation Sites in Glycoproteins: Structural Constraints on Heparan Sulfate Binding to Robo1. ACS Chem. Biol. 13 (2018) 2560-2567.

[294] M.A. Macnaughtan, M. Kamar, G. Alvarez-Manilla, A. Venot AJ. Glushka, J.M. Pierce, J.H. Prestegard. NMR structural characterization of substrates bound to N-acetylglucosaminyltransferase V. J Mol Biol. 366 (2007) 1266-1281.

[295] C. S. Chaitanya, A. J. Robertson, Y. Shen, D. A. Torchia, A. Bax Advances in NMR Spectroscopy of Weakly Aligned Biomolecular Systems. Chem Rev. 122 (2022) 9307-9330.

[296] H. F. Azurmendi, C. A. Bush, Tracking Alignment from the Moment of Inertia Tensor (TRAMITE) of Biomolecules in Neutral Dilute Liquid Crystal Solutions. J. Am. Chem. Soc., 124 (2002) 2426–2427.

[297] A. Poveda, G. Fittolani, P. H. Seeberger, M. Delbianco, J. Jiménez-Barbero, The Flexibility of Oligosaccharides Unveiled Through Residual Dipolar Coupling Analysis. Front. Mol. Biosci. 8 (2021) 784318.

[298] P. Berthault, D. Jeannerat, F. Camerel, F. Alvarez Salgado, Y. Boulard, J.C. Gabriel, H. Desvaux. Dilute liquid crystals used to enhance residual dipolar couplings may alter conformational equilibrium in oligosaccharides. Carbohydr. Res. 338 (2003) 1771-1785.

[299] M. Ottiger, F. Delaglio, A. Bax, Measurement of J and Dipolar Couplings from Simplified Two-Dimensional NMR Spectra. J. Magn. Reson. 131 (1998) 373-378.

[300] Yu B, van Ingen H, Freedberg DI. Constant time INEPT CT-HSQC (CTi-CT-HSQC) - A new NMR method to measure accurate one-bond J and RDCs with strong 1H-1H couplings in natural abundance J. Magn. Reson. 228 (2013) 159-165.

[301] M. Martín-Pastor, A. Canales, J. Jiménez-Barbero. NMR experiments for the measurement of proton–proton and carbon–carbon residual dipolar couplings in uniformly labelled oligosaccharides. J. Biomol. NMR, 26 (2003) 345-353.

[302] V. Gargiulo, M.A. Morando, A. Silipo, A. Nurisso, S. Pérez S, A. Imberty, F.J. Cañada, M. Parrilli, J. Jiménez-Barbero, C. De Castro. Insights on the conformational properties of hyaluronic acid by using NMR residual dipolar couplings and MD simulations. Glycobiology. 20 (2010) 1208-1216

[303] J. Xia, C. Margulis. A tool for the prediction of structures of complex sugars, J. Biomol. NMR. 42 (2008) 241-256.

[304] M. Martin-Pastor, C.A. Bush. Conformational studies of human milk oligosaccharides using (1)H-(13)C one-bond NMR residual dipolar couplings, Biochemistry. 39 (2000) 4674-4683.

[305] E. Säwén, F. Hinterholzinger, C. Landersjö, G. Widmalm. Conformational flexibility of the pentasaccharide LNF-2 deduced from NMR spectroscopy and molecular dynamics simulations, Org. Biomol. Chem. 10 (2012) 4577-4585.

[306] M. Martin-Pastor, C.A. Bush. The use of NMR residual dipolar couplings in aqueous dilute liquid crystalline medium for conformational studies of complex oligosaccharides. Carbohydr. Res. 323 (2000) 147-155.

[307] H. F. Azurmendi, C. Allen Bush. Conformational studies of blood group A and blood group B oligosaccharides using NMR residual dipolar couplings. Carbohydr. Res. 2002, 227 (2002) 905-915.

[308] A. Almond, J. Bunkenborg, T. Franch, C.H. Gotfredsen, J.O. Duus. Comparison of aqueous molecular dynamics with NMR relaxation and residual dipolar couplings favors internal motion in a mannose oligosaccharide, J. Am. Chem. Soc. 123 (2001) 4792-4802.

[309] F. Tian, H.M. Al-Hashimi, J.L. Craighead, J.H. Prestegard. Conformational analysis of a flexible oligosaccharide using residual dipolar couplings, J. Am. Chem. Soc. 123 (2001) 485-492.

[310] M. Martin-Pastor MC.A. Bush. Refined structure of a flexible heptasaccharide using 1H-13C and 1H-1H NMR residual dipolar couplings in concert with NOE and long range scalar coupling constants, J. Biomol. NMR. 19 (2001) 125-139.

[311] J. Xia, C.J. Margulis, D.A. Case. Searching and optimizing structure ensembles for complex flexible sugars, J. Am. Chem. Soc. 133 (2011) 15252-15255.

[312] G.R. Kiddle, S.W. Homans, Residual dipolar couplings as new conformational restraints in isotropically 13C-enriched oligosaccharides FEBS Lett. 436 (1998) 128-130.

[313] M. Martín-Pastor, A. Canales, F. Corzana, J. L. Asensio, J. Jiménez-Barbero. Limited Flexibility of Lactose Detected from Residual Dipolar Couplings Using Molecular Dynamics Simulations and Steric Alignment Methods. J. Am. Chem. Soc. 127 (2005) 3589–3595.

[314] J. H. Prestegard, A. Eletsky, Paramagnetic, RDC and RCSA Constraints in the Structural Analysis of Glycans. Chapter in NMR in Glycoscience and Glycotechnology 2017, pp.123-149.

[315] H. Shimizu, A. Donohue-Rolfe, S.W. Homans Derivation of the Bound-State Conformation of a Ligand in a Weakly Aligned Ligand−Protein Complex. J. Am. Chem. Soc. 2005 (127) 3589–3595.

[316] N.U. Jain, S. Noble, J.H. Prestegard. Structural characterization of a mannose-binding protein-trimannoside complex using residual dipolar couplings. J. Mol. Biol., 328 (2003) 451-462.

[317] T. Zhuang, H. Leffler, J. H. Prestegard, Enhancement of bound-state residual dipolar couplings: Conformational analysis of lactose bound to Galectin-3. Prot. Sci. 15 (2006) 1780-1790.

[318] L. Unione, G. Ortega, A. Mallagaray, F. Corzana, J. Pérez-Castells, A. Canales, J. Jiménez-Barbero, O. Millet. Unraveling the Conformational Landscape of Ligand Binding to Glucose/Galactose-Binding Protein by Paramagnetic NMR and MD Simulations. ACS Chem. Biol. 11 (2016) 2149-2157.

[319] H.R.A. Jonker, K. Saxena, A. Shcherbakova, B. Tiemann, H. Bakker, H. Schwalbe, NMR Spectroscopic Characterization of the C-Mannose Conformation in a Thrombospondin Repeat Using a Selective Labeling Approach. Angew. Chem. Int. Ed. Engl. 59 (2020) 20659-20665.

[320] J.F.G. Vliegenthart, L. Dorland, H. Van Halbeek, High resolution 1H-NMR spectroscopy as a tool in the structural analysis of carbohydrates related to glycoproteins. Adv. Carbohydr. Chem. Biochem. 41 (1983) 209–374.

[321] J.F.G. Vliengenthart, The complexity of glycoprotein-derived glycans. Proc. Jpn. Acad., Ser. B 93 (2017) 64-93.

[322] G. W. Vuister, P. De Waard, R. Boelens, J. F. G. Vliegenthart, R. Kaptein, The use of three-dimensional NMR in structural studies of oligosaccharides. J. Am. Chem. Soc. 112 (1990) 3232-3234.

[323] T.J. Rutherford, S.W. Homans, Restrained vs free dynamics simulations of oligosaccharides: application to solution dynamics of biantennary and bisected biantennary N-linked glycans. Biochemistry. 33 (1994) 9606-9614.

[324] S.W. Homans, A. Pastore, R.A. Dwek, T.W. Rademacher, Structure and dynamics in oligomannose-type oligosaccharides Biochemistry. 26 (1987) 6649-6655.

[325] J.P. Lommerse, L.M. Kroon-Batenburg, J.P. Kamerling, J.F.G. Vliegenthart, Conformational analysis of the xylose-containing N-glycan of pineapple stem bromelain as part of the intact glycoprotein, Biochemistry. 34 (1995) 8196-8206.

[326] J.R. Brisson, J.P. Carver, Solution conformation of asparagine-linked oligosaccharides: alpha(1-2)-, alpha(1-3)-, beta(1-2)-, and beta(1-4)-linked units. Biochemistry. 22 (1983) 3671-3680.

[327] J.R. Brisson, J.P. Carver, Solution conformation of asparagine-linked oligosaccharides: alpha(1-6)-linked moiety, Biochemistry. 22 (1983) 3680-3686.

[328] S.W. Homans, R.A. Dwek, J. Boyd, M. Mahmoudian, W.G. Richards, T.W. Rademacher, Conformational transitions in N-linked oligosaccharides, Biochemistry. 25 (1986) 6342-6350.

[329] H. Paulsen, T. Peters, V. Sinnwell, M. Heume, B. Meyer, Conformational analysis of the double pentasaccharide sequence of the "bisected" structure of N-glycoproteins. Carbohydr. Res.156 (1986) 87-106.

[330] J.B. Bouwstra, E.C. Spoelstra, P. De Waard, B.R. Leeflang, J.P. Kamerling, J.F.G. Vliegenthart, Conformational studies on the N-linked carbohydrate chain of bromelain. Eur. J. Biochem. 190 (1990) 113-122.

[331] D.A. Cumming, R.N. Shah, J.J. Krepinsky, A.A. Grey, J.P. Carver, Solution conformation of the branch points of N-linked glycans: synthetic model compounds for tri-antennary and tetraantennary glycans. Biochemistry. 26 (1987) 6655-6663.

[332] S. Perez, A. Imberty, S. Engelsen, J. Gruza, K. Mazeau, J. Jimenez-Barbero, A. Poveda, J.F. Espinosa, B.P. van Eyck, G. Johnson, A.D. French, M.L:C.E. Kouwijzer, P.D.J. Grootenuis, A. Bernardi, L. Raimondi, H. Senderowitz, V. Durier, G. Vergoten, K. Rasmussen, A Comparison and Chemometric Analysis of Several Molecular Mechanics Force Fields and Parameter Sets applied to Carbohydrates. Carbohydr. Res. 314 (1998) 141-155.

[333] C.A Stortz, G.P Johnson, A.D French, G.I Csonka, Comparison of different force fields for the study of disaccharides. Carbohydr Res. 344 (2009) 2217-2228.

[334] O. Engström, H. Mobarak, J. Ståhle, G. Widmalm, Conformational Dynamics and Exchange Kinetics of N-Formyl and N-Acetyl Groups Substituting 3-Amino-3,6-dideoxy-α-d-galactopyranose, a Sugar Found in Bacterial O-Antigen Polysaccharides. J Phys Chem B, 121 (2017) 9487-9497.

[335] J. Jimenez-Barbero, O, Noble, C. Pfeffer, S. Perez, Solvent-Specific Surfaces of Carbohydrates: The Mannobiose Case. New. J. Chem. 12 (1988) 941-946.

[336] A. Bastida, A. Hidalgo, J.L: Chiara, M. Torrado, F. Corzana, J.M: Pérez-Cañadillas, P. Groves, E. Garcia-Junceda, C. Gonzalez, J. Jimenez-Barbero, J.L. Asensio, Exploring the Use of Conformationally Locked Aminoglycosides as a New Strategy to Overcome Bacterial Resistance. J. Am. Chem. Soc. 128 (2006) 100-116.

[337] S.W. Homans, Conformation and dynamics of oligosaccharides in solution, Glycobiology. 3 (1993) 551-555.

[338] C.J. Edge, U.C. Singh, R. Bazzo, G.L. Taylor, R.A. Dwek, T.W. Rademacher. 500-picosecond molecular dynamics in water of the Man alpha 1-2Man alpha glycosidic linkage present in Asn-linked oligomannose-type structures on glycoproteins. Biochemistry. 29 (1990) 1971-1974.

[339] R.J. Woods, Computational carbohydrate chemistry: what theoretical methods can tell us. Glycoconj J. 15 (1998) 209-216.

[340] M. Hricovíni, R.N. Shah, J.P. Carver, Detection of internal motions in oligosaccharides by 1H relaxation measurements at different magnetic fields. Biochemistry. 31 (1992) 10018-10023.

[341] M. Zerbetto, A. Polimeno, D. Kotsyubynskyy, L. Ghalebani, J. Kowalewski, E. Meirovitch, U. Olsson, G. Widmalm, An integrated approach to NMR spin relaxation in flexible biomolecules: application to beta-D-glucopyranosyl-(1-->6)-alpha-D-mannopyranosyl-Ome. J. Chem. Phys. 131 (2009) 234501.

[342] O. Jardetzky, On the nature of molecular conformations inferred from high-resolution NMR. Biochim. Biophys. Acta 621 (1980) 227-232.

[343] A. Imberty, S. Pérez, M. Hricovíni, R.N. Shah, J.P. Carver, Flexibility in a tetrasaccharide fragment from the high mannose type of N-linked oligosaccharides. Int J Biol Macromol. 15 (1993) 17-23.

[344] I. Braccini, V. Michon, C. Hervé du Penhoat, A. Imberty, S. Pérez, Internal motion in carbohydrates as probed by n.m.r. spectroscopy. Int J Biol Macromol. 15 (1993) 52-55.

[345] M. Hricovíni, G. Torri, Dynamics in aqueous solutions of the pentasaccharide corresponding to the binding site of heparin for antithrombin III studied by NMR relaxation measurements. Carbohydr. Res. 268 (1995) 159-175.

[346] G. LIpari, A. Szabo, Model-free approach to the interpretation of nuclear magnetic resonance relaxation in macromolecules. 1. Theory and range of validity, J. Am. Chem. Soc. 104 (1982) 4546-4559.

[347] S. Cros, C.H. du Penhoat, N. Bouchemal, H. Ohassan, A. Imberty, S. Pérez. Solution conformation of a pectin fragment disaccharide using molecular modelling and nuclear magnetic resonance. Int. J. Biol. Macromol. 14 (1992) 313-320.

[348] L. Catoire, I. Braccini, N. Bouchemal-Chibani, L. Jullien, C. Herve du Penhoat, S. Perez, NMR analysis of carbohydrates with model-free spectral densities: the dispersion range revisited Glycoconj. J. 14 (1997) 935-943.

[349] A. Poveda, Martin-Pastor M, Bernabe M, Leal JA, J. Jimenez-Barbero, Solution conformation and dynamics of a fungal cell wall polysaccharide isolated from Microsporum gypseum. Glycoconj. J. 15 (1998) 309-321.

[350] A. Andersson, A. Ahl, R. Eklund, G. Widmalm, L. Mäler, Dynamics in the cyclic Enterobacterial common antigen as studied by 13C NMR relaxation. J. Biomol. NMR. 31 (2005) 311-320.

[351] B.J. Hardy, W.G. Egan, G. Widmalm, Conformational analysis of the disaccharide alpha-L-Rhap-(1-->2)-alpha-L-Rhap-OMe: comparison of dynamics simulations with NMR experiments. Int. J. Biol. Macromol. 17 (1995) 149-160.

[352] R. Pendrill, O. Engström, A. Volpato, M. Zerbetto, A. Polimeno, G. Widmalm, Flexibility at a glycosidic linkage revealed by molecular dynamics, stochastic modeling, and 13C NMR spin relaxation: conformational preferences of α-L-Rhap-α-(1 → 2)-α-L-Rhap-OMe in water and dimethyl sulfoxide solutions. Phys. Chem. Chem. Phys. 18 (2016) 3086-3096.

[353] A.A. Bothner-By, R.L. Stephens, J.M. Lee, C.D. Warren, R.W. Jeanloz, Structure determination of a tetrasaccharide: transient nuclear Overhauser effects in the rotating frame. J. Am. Chem. Soc. 106 (1984) 811-813.

[354] M. Hricovini, S. Bystrický, A. Malovíková, Conformations of (1-4)-linked alpha-D-galacturono-di- and -tri-saccharides in solution analysed by n.m.r. measurements and theoretical calculations. Carbohydr. Res. 220 (1991) 23-31.

[355] K. Lycknert, G. Widmalm Dynamics of the Escherichia coli O91 O-antigen polysaccharide in solution as studied by carbon-13 NMR relaxation. Biomacromolecules. 5 (2004) 1015-1020.

[356] P. Dais, S. Vlachou, F.R. Taravel. 13C nuclear magnetic relaxation study of segmental dynamics of the heteropolysaccharide pullulan in dilute solutions. Biomacromolecules. 2 (2001) 1137-1147.

[357] M. Soltesova, J. Kowalewski, G. Widmalm Dynamics of exocyclic groups in the Escherichia coli O91 O-antigen polysaccharide in solution studied by carbon-13 NMR relaxation. J. Biomol. NMR. 57 (2013) 37-45.

[358] D. Live, L.A.P. Silks, J. Schmidt, 13C Isotopic Enrichment for Nuclear Magnetic Resonance Studies of Carbohydrates and Glycoconjugates. Methods Enzymol. 338 (2001) 305-319.

[359] R. Gitti, G. X. Long, C. A. Bush, Measurement of long-range2 13C-1H coupling constants of 95% uniformly 13C-labeled polysaccharide from Streptococcus mitis J22. Biopolymers 34, (1994) 1327.

[360] E. Samain, S. Drouillard, A. Heyraud, H. Driguez, R.A. Geremia, Gram-scale synthesis of recombinant chitooligosaccharides in Escherichia coli. Carbohydr. Res. 302 (1997) 35-42.

[361] D. Fujinami, J. Nyirenda, S. Matsumoto, D. Kohda, Carbohydr. Res. 413 (2015), 55–62.

[362] C. Fontana, H. Kovacs, G. Widmalm, NMR structure analysis of uniformly 13C-labeled carbohydrates. J. Biomol. NMR. 59 (2014) 95–110.

[363] E. Vinogradov , B.O. Petersen, J.O. Duus, Isolation and characterization of non-labeled and 13C-labeled mannans from Pichia pastoris yeast. Carbohydr. Res. 325 (2000) 216-221.

[364] H. Shimizu, R. A. Field, S. W. Homans, A. Donohue-Rolfe,Solution Structure of the Complex between the B-Subunit Homopentamer of Verotoxin VT-1 from Escherichia coli and the Trisaccharide Moiety of Globotriaosylceramide. Biochemistry. 37 (1988) 11078–11082.

[365] M.J. Milton, R. Harris, M.A. Probert, R.A. Field, S.W. Homans, New conformational constraints in isotopically (13C) enriched oligosaccharides. Glycobiology. 8 (1998) 147-153.

[366] R. Harris, T.J. Rutherford, M.J. Milton, S.W. Homans.,Three-dimensional heteronuclear NMR techniques for assignment and conformational analysis using exchangeable protons in uniformly 13C-enriched oligosaccharides. J. Biomol. NMR. 9 (1997) 47-54.

[367] C.D. Blundell, P.L. DeAngelis, A. Day, A. Almond, Use of 15N-NMR to Resolve Molecular Details in Isotopically-Enriched Carbohydrates: Sequence-Specific Observations in Hyaluronan Oligomers up to Decasaccharides. Glycobiology. 14 (2004) 999−1009.

[368] Y. Kamiya, K. Yanagi, T. Kitajima, T. Yamaguchi, Y. Chiba, K. Kato, Application of Metabolic 13C Labeling in Conjunction with High-Field Nuclear Magnetic Resonance Spectroscopy for Comparative Conformational Analysis of High Mannose-Type Oligosaccharides. Biomolecules. 3 (2013) 108−123.

[369] S. Shahzad-ul-Hussan, M. Sastry, T. Lemmin, C. Soto, S. Loesgen, D.A. Scott, J.R. Davison, K. Lohith, R. O'Connor, P.D. Kwong, C.A. Bewley, Insights from NMR Spectroscopy into the Conformational Properties of Man-9 and Its Recognition by Two HIV Binding Proteins. ChemBioChem. 18 (2017) 764–771.

[370] H. Shimizu, J.M. Brown, S.W. Homans, R.A. Field, Tetrahedron. 54 (1998) 9489-9506.

[371] F. Yu, J.H. Prestegard, Structural monitoring of oligosaccharides through 13C enrichment and NMR observation of acetyl groups. Biophys J. 91 (2006) 1952-9.

[372] C. Thibaudeau, R. Stenutz, B. Hertz, T. Klepach, S. Zhao, Q. Wu, I. Carmichael, A.S. Serianni, Correlated C-C and C-O bond conformations in saccharide hydroxymethyl groups: parametrization and application of redundant 1H-1H, 13C-1H, and 13C-13C NMR J-couplings. J. Am. Chem. Soc. 126 (2004) 15668-15685.

[373] Y. Zhu, Q. Pan, C. Thibaudeau, S. Zhao, I. Carmichael, A.S. Serianni, [13C,15N]2-Acetamido-2-deoxy-D-aldohexoses and their methyl glycosides: synthesis and NMR investigations of J-couplings involving 1H, 13C, and 15N. J. Org. Chem. 71 (2006) 466-479.

[374] C. Murruzzu, M. Alonso, A. Canales, J. Jiménez-Barbero, A. Riera, Synthesis and NMR experiments of (4,5,6-13C)-deoxymannojirimycin. A new entry to 13C-labeled glycosidase inhibitors. Carbohydr. Res. 342 (2007) 1805-1812.

[375] T. Klepach, W. Zhang, I. Carmichael, A.S. Serianni, (13)C-(1)H and (13)C-(13)C NMR J-couplings in (13)C-labeled N-acetyl-neuraminic acid: correlations with molecular structure. J. Org. Chem. 73 (2008) 4376-4387.

[376] Zhang W, Hu X, I. Carmichael, A.S. Serianni, Methyl [13C]glucopyranosiduronic acids: effect of COOH ionization and exocyclic structure on NMR spin-couplings. J. Org. Chem. 77 (2012) 9521-9534.

[377] U. Olsson, E. Säwén, R. Stenutz, G. Widmalm, Conformational flexibility and dynamics of two (1-->6)-linked disaccharides related to an oligosaccharide epitope expressed on malignant tumour cells. Chem. Eur. J. 15 (2009) 8886-8894.

[378] A. Ruda, A.H. Aytenfisu, T. Angles d'Ortoli, A.D. MacKerell Jr, G. Widmalm, Glycosidic α-linked mannopyranose disaccharides: an NMR spectroscopy and molecular dynamics simulation study employing additive and Drude polarizable force fields. Phys. Chem. Chem. Phys. 25 (2023) 3042-3060.

[379] K.H. Jonsson, E. Säwén, G. Widmalm, Studies on the conformational flexibility of α-L-rhamnose-containing oligosaccharides using 13C-site-specific labeling, NMR spectroscopy and molecular simulations: implications for the three-dimensional structure of bacterial rhamnan polysaccharides. Org. Biomol. Chem. 10 (2012) 2453-2463.

[380] W. Zhang, Q. Pan, A.S. Serianni, A chemical synthesis of a multiply 13C-labeled hexasaccharide: a high-mannose N-glycan fragment. J. Labelled Comp. Radiopharm. 59 (2016) 673-679.

[381] A. Hughes, M. Meneghetti, T.Y. Huang, S.C. Hung, S. Elli, M. Guerrini, T. Rudd, M. Lima, E. Yates, Investigating the relationship between temperature, conformation and calcium binding in heparin model oligosaccharides. Carbohydr. Res. 438 (2017) 58-64.

[382] S.A. Colebrooke, C.D. Blundell, P.L. DeAngelis, I.D. Campbell, A. Almond, Exploiting the carboxylate chemical shift to resolve degenerate resonances in spectra of 13C-labelled glycosaminoglycans. Magn. Reson. Chem. 43 (2005) 805-815.

[383] F. Yu, J.J. Wolff, I.J. Amster, J.H. Prestegard, Conformational preferences of chondroitin sulfate oligomers using partially oriented NMR spectroscopy of 13C-labeled acetyl groups. J. Am. Chem. Soc. 129 (2007) 13288-13297.

[384] M. Ichikawa, Y. Otsuka, T. Minamisawa, N. Manabe, Y. Yamaguchi, NMR characterization of uniformly 13C- and/or 15N-labeled, unsulfated chondroitins with high molecular weights. Magn. Reson. Chem. 62 (2024) 439-451.

[385] H.F. Azurmendi, J. Vionnet, L. Wrightson, L.B. Trinh, J. Shiloach, D.I. Freedberg, Extracellular Structure of Polysialic Acid Explored by on Cell Solution NMR. Proc. Natl. Acad. Sci. U. S. A. 104 (2007) 11557−11561.

[386] W. Zou, J.R. Brisson, Q.L. Yang, M. van der Zwan, H.J. Jennings, Synthesis and NMR assignment of two repeating units (decasaccharide) of the type III group B Streptococcus capsular polysaccharide and its 13C-labeled and N-propionyl substituted sialic acid analogues. Carbohydr. Res. 295 (1996) 209-228.

[387] S. Sheng, R. Cherniak, Structure of the 13C-enriched O-deacetylated glucuronoxylomannan of Cryptococcus neoformans serotype A determined by NMR spectroscopy. Carbohydr. Res. 301 (1997) 33-40.

[388] F.J. Cañada, A Canales, P Valverde, B.F. de Toro, M. Martínez-Orts, P. O. Phillips, A. Pereda, Conformational and Structural Characterization of Carbohydrates and their Interactions Studied by NMR. Curr Med Chem. 29 (2022) 1147-1172.

[389] R. Harris, G.R. Kiddle, R.A. Field, M.J. Milton, B. Ernst, J.L. Magnani, S.W. Homans: Stable isotope assisted NMR studies on 13C-enriched sialyl LewisX in solution and bound to E-selectin. J. Am. Chem. Soc. 121 (1999) 2546-2551.

[390] D. Uhrin, A.V.K. Prasad, J.R. Brisson, D.R. Bundle, Carbohydrate antibody interactions by NMR for a 13C-labelled disaccharide ligand. Can. J. Chem. 80 (2002) 904-907.

[391] G. Nestor, T. Anderson, S. Oscarson, A. M. Gronenborn, Exploiting Uniformly 13C-Labeled Carbohydrates for Probing Carbohydrate-Protein Interactions by NMR Spectroscopy. J. Am.Chem. Soc. 139 (2017) 6210–6216.

[392] G. Nestor, A. Ruda, T. Anderson, S. Oscarson, Widmalm, A.M. Gronenborn, A detailed picture of a protein-carbohydrate hydrogen-bonding network revealed by NMR and MD simulations. Glycobiology. 31(2021) 508-518.

[393] O. J. Plante, P. H. Seeberger, Automated Solid-Phase Synthesis of Oligosaccharides. Science. 291 (2001) 1523-1527.

[394] M. Guberman, P. H. Seeberger, Automated Glycan Assembly: A Perespective. J. Am. Chem. Soc. 141 (2019) 5581-5592.

[395] H. S. Hahm, M. K. Schlegel, M. Hurevich, S. Eller, F. Schuhmacher, J. Hofmann, K. Pagel, P H. Seeberger, Automated Glycan Assembly Using the Glyconeer 2.1 Synthesizer. Proc. Natl. Acad. Sci. U.S.A, 114 (2021) E3385-E3389.

[396] M. Delbianco, A. Kononov, A. Poveda, Y. Yu, T. Diercks, J. Jiménez-Barbero, P. H Seeberger, Well-Defined Oligo- and Polysaccharides as Ideal Probes for Structural Studies. J. Am. Chem. Soc. 140 (2018) 5421-5426.

[397] G. Fittolani, E. Shanina, M. Guberman, P. H. Seeberger, C. Rademacher, M. Delbianco, Automated Glycan Assembly of 19 F-labeled Glycan Probes Enables High-Throughput NMR Studies of Protein-Glycan Interactions. Angew. Chem. Int. Ed. 60 (2021) 13302-13309.

[398] M.J. Moure, A. Gimeno, S. Delgado, T. Diercks, G. J Boons, J. Jiménez-Barbero, A. Ardá, Selective 13 C-Labels on Repeating Glycan Oligomers to Reveal Protein Binding Epitopes through NMR: Polylactosamine Binding to Galectins. Angew. Chem. Int. Ed. 60 (2021) 18777-18782.

[399] L. Unione, A. Ammerlaan, G.P. Bosman, E. Uslu, R. Liang, F. Broszeit, R. van der Woude, Y. Liu, S. Ma, L. Liu, M. Gómez-Redondo, I.A. Bermejo, P. Valverde, T. Diercks, A. Ardá, R.P. de Vries, G.J. Boons. Probing altered receptor specificities of antigenically drifting human H3N2 viruses by chemoenzymatic synthesis, NMR, and modelling. Nat Commun. 15 (2024) 2979.

[400] M. A. Macnaughtan, F. Tian, S. Liu, L. Meng, S. Park, P. Azadi, K. W. Moremen and J. H. Prestegard, ^{13}C-Sialic Acid Labeling of Glycans on Glycoproteins Using ST6Gal-I. J. Am. Chem. Soc. 13 (2008) 11864–11865.

[401] A. W. Barb, L. Meng, Z. Gao, R. W. Johnson, K. W. Moremen and J. H. Prestegard, NMR characterization of immunoglobulin G Fc glycan motion on enzymatic sialylation. Biochemistry. 51 (2012) 4618–4626.

[402] Y. Yamaguchi, K. Kato, M. Shindo, S. Aoki, K. Furusho, K. Koga, N. Takahashi, Y. Arata, I. Shimada, Dynamics of the carbohydrate chains attached to the Fc portion of immunoglobulin G as studied by NMR spectroscopy assisted by selective 13C labeling of the glycans. J. Biomol. NMR. 12 (1998) 385–394.

[403] A.W. Barb, Intramolecular N-Glycan/Polypeptide Interactions Observed at Multiple N-Glycan Remodeling Steps through [13C,15N]-N-Acetylglucosamine Labeling of Immunoglobulin G1. Biochemistry, 54 (2015) 313–322.

[404] A. W. Barb and J. H. Prestegard, NMR analysis demonstrates immunoglobulin G N-glycans are accessible and dynamic. Nat. Chem. Biol. 7 (2011) 147–153.

[405] Van den Steen P, Rudd PM, Dwek RA, Opdenakker G. Concepts and principles of O-linked glycosylation. Crit. Rev. Biochem. Mol. Biol. 33 (1998) 151-208.

[406] D.F. Wyss, J.S. Choi, J. Li, M.H. Knoppers, K.J. Willis, A.R.N. Arulanandam, A. Smolyar, E.L. Reinherz, G. Wagner, Conformation and Function of the N-Linked Glycan in the Adhesion Domain of Human CD2. Science. 269 (1995) 1273-1278.

[407] M.G. Lete, M. Hoffmann, N. Schomann, A. Martínez-Castillo, F. Peccati, P.B. Konietzny, S. Delgado, N.L. Snyder, G. Jiménez-Oses, N.G.A. Abrescia, A. Ardá, L. Hartmann, J. Jiménez-Barbero, Molecular Recognition of Glycan-Bearing Glycomacromolecules Presented at Membrane Surfaces by Lectins: An NMR View. ACS Omega. 8 (2023) 16883-16895.

[408] S. Bertuzzi, F. Peccati, S. Serna, R. Artschwager, S. Notova, M. Thépaut, G. Jiménez-Osés, F. Fieschi, N.C. Reichardt, J. Jiménez-Barbero, A. Ardá, Immobilization of Biantennary N-Glycans Leads to Branch Specific Epitope Recognition by LSECtiN. ACS Cent Sci. 8 (2022) 1415-1423.

[409] J.W. Lustbader, S. Pollak, L. Lobel, I. Trakht, S.W. Homans, J.M. Brown, R.E. Canfield, Three-dimensional structures of gonadotropins. Mol. Cell. Endocrinol. 125 (1996) 21.

[410] C.T. Weller, J. Lustbader, K. Seshadri, J.M. Brown, C.A. Chadwick, C.E. Kolthoff, S. Ramnarain, S. Pollak, R. Canfield, S.W. Homans, Structural and conformational analysis of glycan moieties in situ on isotopically 13C, 15N-enriched recombinant human chorionic gonadotropin. Biochemistry. 35 (1996) 8815.

[411] T. De Beer, C.W. Van Zuylen, B.R. Leeflang, K. Hard, R. Boelens, R. Kaptein, J.P. Kamerling, J.F.G. Vliegenthart, NMR Studies of the Free α Subunit of Human Chorionic Gonadotropin. Structural Influences of N-Glycosylation and the β Subunit on the Conformation of the α Subunit. Eur J Biochem. 241 (1996) 229.

[412] C.W. Van Zuylen, BJ.P. Kamerling, J.F.G. Vliegenthart, Glycosylation beyond the Asn78-linked GlcNAc residue has a significant enhancing effect on the stability of the alpha subunit of human chorionic gonadotropin. Biochem. Biophys. Res. Commun. 232 (1997) 117.

[413] S.E. O'Connor, B. Imperiali, Conformational Switching by Asparagine-Linked Glycosylation. J. Am. Chem. Soc. 119 (1997) 2295-2296.

[414] S.E. O'Connor, B. Imperiali, A molecular basis for glycosylation-induced conformational switching. Chem. Biol. 5 (1998) 427-437.

[415] C.J. Bosques, S.M. Tschampel, R.J. Woods, B. Imperiali, Effects of Glycosylation on Peptide Conformation: A Synergistic Experimental and Computational Study. J. Am. Chem. Soc. 126 (2004) 8421.

[416] A. Mallagaray, L. Rudolph, M. Lindloge, J. Mölbitz, H. Thomsen, F. Schmelter, M.W. Alhabash, M.R. Abdullah, R. Saraei, M. Ehlers, T. Graf, C. Sina, A. Petersmann, M. Nauck, U.L. Günther, Towards a Precise NMR Quantification of Acute Phase Inflammation Proteins from Human Serum. Angew Chem Int Ed. 62 (2023) e202306154.

[417] R.G. Brinson, J.P. Marino, F. Delaglio, L.W. Arbogast, R.M. Evans, A. Kearsley, G. Gingras, H. Ghasriani, Y. Aubin, G.K. Pierens, et al., Enabling adoption of 2D-NMR for the higher order structure assessment of monoclonal antibody therapeutics. mAbs. 11 (2019) 94-105.

[418] M. Schubert, M.J. Walczak, M. Aebi, G. Wider, Posttranslational modifications of intact proteins detected by NMR spectroscopy: application to glycosylation. Angew. Chem. Int. Ed. 54 (2015) 7096.

[419] S. Yanaka, S. Yagi, H. Yogo, R. Yagi-Utsumi, K. Kato, Stable isotope labeling approaches for NMR characterization of glycoproteins using eukaryotic expression systems. J. Biomol. NMR. 71 (2018) 193.

[420] W.J. Goux, C. Perry, T. L. James, An NMR study of 13C-enriched galactose attached to the single carbohydrate chain of hen ovalbumin. Motions of the carbohydrates of glycoproteins. J. Biol. Chem. 25 (1982) 1829.

[421] A.M. Gilhespy-Muskett, J. Partridge, R. Jefferis, S.W. Homans, A novel 13C isotopic labelling strategy for probing the structure and dynamics of glycan chains in situ on glycoproteins. Glycobiology. 4 (1994) 485-489.

[422] M. Sastry, C.A. Bewley, P. D. Kwong, Effective isotope labeling of proteins in a mammalian expression system. Methods Enzymol. 565 (2015) 289–307.

[423] Y. Yamaguchi, T. Takizawa, Y. Arata and I. Shimada, 1H and 13C NMR assignments for the glycans in glycoproteins by using 2H/13C-labeled glucose as a metabolic precursor. J. Biomol. NMR. 18 (2000) 357-360.

[424] L. Skrisovska, M. Schubert, F. H.-T. Allain, Recent advances in segmental isotope labeling of proteins: NMR applications to large proteins and glycoproteins. J. Biomol. NMR. 46 (2010) 51–65.

[425] K. Kato, Y. Yamaguchi, Y. Arata, Stable-isotope-assisted NMR approaches to glycoproteins using immunoglobulin G as a model system. Prog. Nucl. Magn. Reson. Spectrosc. 56 (2010) 346–359.

[426] H. Yagi, Y. Zhang, M. Yagi-Utsumi, T. Yamaguchi, S. Iida, Y. Yamaguchi, K. Kato, Backbone ^{1}H, ^{13}C, and ^{15}N resonance assignments of the Fc fragment of human immunoglobulin G glycoprotein. Biomol. NMR Assign. 9, (2015) 257–260.

[427] Y. Yamaguchi, M. Nishimura, M. Nagano, H. Yagi, H. Sasakawa, K. Uchida, K. Shitara, K. Kato, Glycoform-dependent conformational alteration of the Fc region of human immunoglobulin G1 as revealed by NMR spectroscopy. Biochim. Biophys. Acta. 1760 (2006) 693–700.

[428] S. Matsumiya, Y. Yamaguchi, J. Saito, M. Nagano, H. Sasakawa, S. Otaki, M. Satoh, K. Shitara, K. Kato, Structural comparison of fucosylated and nonfucosylated Fc fragments of human immunoglobulin G1. J. Mol. Biol. 368 (2007) 767–779.

[429] G.P. Subedi, A.W. Barb, The Structural Role of Antibody N-Glycosylation in Receptor Interactions. Structure. 23 (2015) 1573–1583.

[430] J.I. Quintana, S. Delgado, M. Rábano, M. Azkargorta, M. Florencio-Zabaleta, L. Unione, M.D. Vivanco, F. Elortza, J. Jiménez-Barbero, A. Ardá, The impact of glycosylation on the structure, function, and interactions of CD14. Glycobiology. 34 (2024) cwae002.

[431] A.W. Barb, D.J. Falconer, G.P. Subedi,. The Preparation and Solution NMR Spectroscopy of Human Glycoproteins Is Accessible and Rewarding. Methods Enzymol. 614 (2019) 239-261.

[432] G.P. Subedi, D.J. Falconer, A.W. Barb, Carbohydrate–polypeptide contacts in the antibody receptor CD16A identified through solution NMR spectroscopy. Biochemistry. 56 (2017) 3174-3177.

[433] G.P. Subedi, A.V. Sinitskiy, J.T. Roberts, K.R. Patel, V.S. Pande, A.W. Barb, Intradomain interactions in an NMDA receptor fragment mediate N-glycan processing and conformational sampling. Structure. 27 (2019) 55-65.e3.

[434] Patel KR, J.T. Roberts, G.P. Subedi, A.W. Barb, Restricted processing of CD16a/Fc g receptor IIIa N -glycans from primary human NK cells impacts structure and function. J. Biol. Chem. 293 (2018) 3477-3489.

[435] L. Unione, M.P. Lenza, A. Arda, P. Urquiza, A. Laın, J.M. Falcon-Perez, J. Jimenez-Barbero, O. Millet, Glycoprofile analysis of an intact glycoprotein as inferred by NMR spectroscopy. ACS Cent. Sci. 5 (2019) 1554-1561.

[436] K. Rahman, P. Zhao, M. Mandalasi, H. van der Wel, L. Wells, I.J. Blader, C.M. West, The E3 Ubiquitin Ligase Adaptor Protein Skp1 Is Glycosylated by an Evolutionarily Conserved Pathway That Regulates Protist Growth and Development. J. Biol. Chem. 291 (2016) 4268-4280.

[437] G.P. Subedi, A.W. Barb: The structural role of antibody N-glycosylation in receptor interactions. Structure. 23 (2015) 1573-1583.

[438] J.N. Peng, S.M. Patil, D.A. Keire, K. Chen, Chemical Structure and Composition of Major Glycans Covalently Linked to Therapeutic Monoclonal Antibodies by Middle-Down Nuclear Magnetic Resonance. Anal. Chem. 90 (2018) 11016.

[439] I. Hang, C. Lin, O.C. Grant, S. Fleurkens, T.K. Villiger, M. Soos, M. Morbidelli, R.J. Woods, R. Gauss, M. Aebi: Analysis of site-specific N-glycan remodeling in the endoplasmic reticulum and the Golgi. Glycobiology. 25 (2015) 1335-1349.

[440] K. Khatri K, J.A. Klein JA, M.R. White MR, O.C. Grant OC, N. Leymarie N, R.J. Woods, K.L. Hartshorn KL, J. Zaia J: Integrated omics and computational glycobiology reveal structural basis for influenza A virus glycan microheterogeneity and host interactions. Mol Cell Proteomics. 15 (2016) 1895-1912.

[441] G.R. Chalmers, A. Eletsky, L.C. Morris, J.Y. Yang, F. Tian, R.J. Woods, K.W. Moremen, J.H. Prestegard, NMR resonance assignment methodology: characterizing large sparsely labeled glycoproteins. J. Mol. Biol. 431 (2019) 2369-2382.

[442] J.J. Barchi, Mucin-type glycopeptide structure in solution: Past, present, and future. Biopolymers. 99 (2013), 713–723.

[443] N. Martínez-Sáez, J. M. Peregrina, F. Corzana, Principles of mucin structure: implications for the rational design of cancer vaccines derived from MUC1-glycopeptides. Chem. Soc. Rev. 46 (2017) 7154-7175.

[444] H. Coelho, T. Matsushita, G. Artigas, H. Hinou, F. J. Cañada, R. Lo-Man, C. Leclerc, E.J. Cabrita, J. Jiménez-Barbero, S-I. Nishimura, F. Garcia-Martín and F. Marcelo, The Quest

for Anticancer Vaccines: Deciphering the Fine-Epitope Specificity of Cancer-Related Monoclonal Antibodies by Combining Microarray Screening and Saturation Transfer Difference NMR. J. Am. Chem. Soc. 137 (2015) 12438-12441.

[445] X.L. Huang, J.J. Barchi, F.D. Lung, P.P. Roller, P.L. Nara, J. Muschik, R.R. Garrity, (Glycosylation affects both the three-dimensional structure and antibody binding properties of the HIV-1 (IIIB) GP120 peptide RP135. Biochemistry. 36 (1997) 10846–10856.

[446] G.A. Naganagowda, T.L. Gururaja, J. Satyanarayana, M.J. Levine, NMR analysis of human salivary mucin (MUC7) derived O-linked model glycopeptides: Comparison of structural features and carbohydrate-peptide interactions. J. Peptide Res. 54 (1999) 290–310.

[447] D.M. Coltart, A.K. Royyuru, A. K., L.J. Williams, L. P.W. Glunz, D. Sames, S.D. Kuduk, J.B. Schwarz, X.T. Chen, S.J. Danishefsky, D.H. Live, Principles of mucin architecture: Structural studies on synthetic glycopeptides bearing clustered mono-di-tri-and hexasaccharide glycodomains. J. Am. Chem. Soc. 124 (2002) 9833–9844.

[448] F. Corzana, J.H. Busto, G. Jimenez-Oses, J.L. Asensio, J. Jimenez-Barbero, J.M. Peregrina, A. Avenoza, New insights into alpha-GalNAc-Ser motif: Influence of hydrogen bonding versus solvent interactions on the preferred conformation. J. Am. Chem. Soc. 128 (2006) 14640–14648.

[449] F. Corzana, J.H. Busto, G. Jimenez-Oses, M. Garcia de Luis, J.L. Asensio, J. Jimenez-Barbero, J.M: Peregrina, A. Avenoza, Serine versus threonine glycosylation: The methyl group causes a drastic alteration on the carbohydrate orientation and on the surrounding water shell. J. Am. Chem. Soc. 129 (2007) 9458–9467.

[450] F. Corzana, J.H. Busto, M. Garcia de Luis, J. Jimenez-Barbero, A. Avenoza, J.M. Peregrina, The nature and sequence of the amino acid aglycone strongly modulates the conformation and dynamics effects of Tn antigen's clusters. Chem. Eur. J. 15 (2009) 3863–3874.

[451] I. A. Bermejo, I. Usabiaga, I. Compañón, J. Castro-López, A. Insausti, J. A. Fernandez, A. Avenoza, J. H Busto, J. Jiménez-Barbero, J. Luis Asensio, J. M. Peregrina, G. Jiménez-Osés, R. Hurtado-Guerrero, E. J. Cocinero, F. Corzana, J. Am. Chem. Soc. 2018, 140 (2018) 9952-9960.

[452] N. Martínez-Sáez, J. Castro-López, J. Valero-González, D. Madariaga, I. Compañón, V. J. Somovilla, M. Salvadó, J. L. Asensio, J. Jiménez-Barbero, A. Avenoza, J. H. Busto, G. J. L. Bernardes, J. M. Peregrina, R. Hurtado-Guerrero, F. Corzana, Angew. Chem. Int. Ed. 127 (2015) 9968–9972.

[453] M. de las Rivas, E. Lira-Navarrete, E.J.P. Daniel, I. Companon, H. Coelho, A. Diniz, J. Jiménez-Barbero, J.M. Peregrina, H. Clausen, F. Corzana, F. Marcelo, G. Jiménez-Osés, T.A. Gerken, R. Hurtado-Guerrero. The interdomain flexible linker of the polypeptide GalNAc transferases dictates their long-range glycosylation preferences. Nat. Commun. 8 (2017) 1959.

[454] M. Mayer, B. Meyer, Characterization of ligand binding by saturation transfer difference NMR spectroscopy. Angew. Chem. Int. Ed. 38 (1999) 1784-1788.

[455] F.A. Quiocho, Carbohydrate-binding proteins: tertiary structures and protein-sugar interactions. Ann. Rev. Biochem. 55 (1986) 287-315.

[456] S. Walpole, S. Monaco, R. Nepravishta, J. Angulo, STD NMR as a technique for ligand screening and structural studies. Methods Enzymol. (2019) 423-451.

[457] M. Mayer, B. Meyer, Group epitope mapping by saturation transfer difference NMR to identify segments of a ligand in direct contact with a protein receptor. J. Am. Chem. Soc. 123 (2001) 6108-6117.

[458] S. Monaco, J. Angulo, Multi-frequency Saturation Transfer Difference NMR to Characterize Weak Protein–Ligand Complexes, in NMR Spectroscopy for Probing Functional Dynamics at Biological Interfaces. Royal Society of Chemistry (2022) 179-202.

[459] S. Monaco, L. Tailford, N. Juge, J. Angulo, Differential Epitope Mapping by STD NMR Spectroscopy To Reveal the Nature of Protein-Ligand Contacts. Angew. Chem. Int. Ed. 56 (2017) 15289-15293.

[460] J.L. Asensio, A. Ardá, J. Cañada, J. Jimenez-Barbero, Carbohydrate–aromatic interactions. Acc. Chem. Res. 46 (2013) 946-954.

[461] S. Monaco, S. Walpole, H. Doukani, R. Nepravishta, M. Martinez-Bailen, A. T. Carmona, J. Ramos-Soriano, M. Bergstrom, I. Robina, J. Angulo, Exploring Multi-Subsite Binding Pockets in Proteins: DEEP-STD NMR Fingerprinting and Molecular Dynamics Unveil a Cryptic Subsite at the GM1 Binding Pocket of Cholera Toxin B. Chem. Eur. J. 26 (2020) 10024-10034.

[462] S. Monaco, J. Ramirez-Cardenas, A. T. Carmona, I. Robina, J. Angulo, Inter-ligand STD NMR: An efficient 1D NMR approach to probe relative orientation of ligands in a multi-subsite protein binding pocket. Pharmaceuticals. 15 (2022) 1030.

[463] B. Becattini, M. Pellecchia, SAR by ILOEs: An NMR-based approach to reverse chemical genetics. Chem. Eur. J. 12 (2006) 2658-2662.

[464] R. Nepravishta, S. Monaco, M. Distefano, R. Rizzo, P. Cescutti, J. Angulo, Multifrequency STD NMR unveils the interactions of antibiotics with Burkholderia multivorans biofilm exopolysaccharide. Front. Mol. Biosci. 8 (2021) 727980.

[465] P. M. Nieto, The Use of NMR to Study Transient Carbohydrate-Protein Interactions. Front. Mol. Biosci. 5 (2018) 33.

[466] C. Di Carluccio, M. C. Forgione, S. Martini, F. Berti, A. Molinaro, R. Marchetti, A. Silipo, Investigation of protein-ligand complexes by ligand-based NMR methods. Carbohydr Res. 503 (2021) 108313.

[467] T. Haselhorst, A. C. Lamerz, M. Itzstein, Saturation transfer difference NMR spectroscopy as a technique to investigate protein-carbohydrate interactions in solution. Methods Mol. Biol. 534 (2009) 375-86.

[468] L. Brecker, A. Schwarz, C. Goedl, R. Kratzer, C. E. Tyl, B. Nidetzky, Studying non-covalent enzyme carbohydrate interactions by STD NMR. Carbohydr. Res. 12 (2008) 2153-2161.

[469] Y. Yuan, D. W. Bleile, X. Wen, D.A. Sanders, K. Itoh, H. W. Liu, B. M. Pinto, Investigation of binding of UDP-Galf and UDP-[3-F]Galf to UDP-galactopyranose mutase by STD-NMR spectroscopy, molecular dynamics, and CORCEMA-ST calculations. J. Am. Chem. Soc. 130 (2008) 3157-3168.

[470] S. M. L. Gagnon, M. S. G. Legg, N. Sindhuwinata, J. A. Letts, A. R. Johal, B. Schuman, S. N. Borisova, M. M. Palcic, T. Peters, S. V. Evans, High-resolution crystal structures and STD NMR mapping of human ABO(H) blood group glycosyltransferases in complex with trisaccharide reaction products suggest a molecular basis for product release. Glycobiology. 27 (2017) 966-977.

[471] C. Puchner, T. Eixelsberger, B. Nidetzky, L. Brecker, Binding pattern of intermediate UDP-4-keto-xylose to human UDP-xylose synthase: Synthesis and STD NMR of model keto-saccharides. Carbohydr Res. 437 (2017) 50-58.

[472] I. N'Go, S. Golten, A. Ardá, J. Cañada, J. Jiménez-Barbero, B. Linclau, S. P. Vincent, Tetrafluorination of sugars as strategy for enhancing protein-carbohydrate affinity: application to UDP-Galp mutase inhibition. Chem. Eur. J. 20 (2014) 106-112.

[473] J. Landström J, M. Bergström, C. Hamark, S. Ohlson, G. Widmalm, Combining weak affinity chromatography, NMR spectroscopy and molecular simulations in carbohydrate-lysozyme interaction studies. Org. Biomol. Chem. 10 (2012) 3019-3032.

[474] O. Berteau, C. Sandström, J. Bielicki, D.S. Anson, L. Kenne, Glycosidase-substrate interactions analysis by STD-NMR spectroscopy: study of alpha-L-fucosidase, J. Am. Chem. Soc. 120 (2003) 15296-15297.

[475] S. Liu, L. Meng, K. W. Moremen, J. H. Prestegard, Nuclear magnetic resonance structural characterization of substrates bound to the alpha-2,6-sialyltransferase, ST6Gal-I. Biochemistry. 47 (2009) 11211-1129.

[476] J. Angulo, B. Langpap, A. Blume, T. Biet, B. Meyer, N. R. Krishna, H. Peters, M. M. Palcic, T. Peters, Blood group B galactosyltransferase: insights into substrate binding from NMR experiments. J. Am. Chem. Soc. 128 (2006) 13529-13538.

[477] H. Möller, N. Serttas, H. Paulsen, J. M. Burchell, J. Taylor-Papadimitriou, B. Meyer. NMR-based determination of the binding epitope and conformational analysis of MUC-1 glycopeptides and peptides bound to the breast cancer-selective monoclonal antibody SM3. Eur J Biochem. 296 (2002) 1444-1455.

[478] S. Robakiewicz, C. Bridot, S. Serna, A. Gimeno, B. Echeverria, S. Delgado, J. de Ruyck, S. Semwal, D. Charro, A. Dansercoer, K. Verstraete, M. Azkargorta, K. van Noort, R. H. P Wilbers RHP, S. N. Savvides, N. Abrescia, A. Arda, N. C. Reichardt, J. Jiménez-Barbero, J. Bouckaert, Minimal epitope for Mannitou IgM on paucimannose-carrying glycoproteins. Glycobiology. 31 (2021) 1005-1017.

[479] R. Amon, O. C. Grant, S. Leviatan Ben-Arye, S. Makeneni, A. K. Nivedha, T. Marshanski, C. Norn, H. Yu, J. N. Glushka, S. J. Fleishman, X. Chen, R. J. Woods, V. Padler-Karavani, A combined computational-experimental approach to define the structural origin of antibody recognition of sialyl-Tn, a tumor-associated carbohydrate antigen. Sci. Rep. 8 (2018) 10786.

[480] R. van de Weerd, M. A. Berbís, M. Sparrius, J. J. Maaskant, M. Boot, N. J. Paauw, N. de Vries, L. Boon, O. Baba, F. J. Cañada, J. Geurtsen, J. Jiménez-Barbero, B. J. Appelmelk, A murine monoclonal antibody to glycogen: characterization of epitope-fine specificity by saturation transfer difference (STD) NMR spectroscopy and its use in mycobacterial capsular α-glucan research. Chembiochem. 16 (2015) 977-989.

[481] Y. E. Tsvetkov, M. Burg-Roderfeld, G. Loers, A. Ardá, E. V. Sukhova, E. A. Khatuntseva, A. A. Grachev, A. O. Chizhov, H. C. Siebert, M. Schachner, J. Jiménez-Barbero, N. E. Nifantiev. Synthesis and molecular recognition studies of the HNK-1 trisaccharide and related oligosaccharides. The specificity of monoclonal anti-HNK-1 antibodies as assessed by surface plasmon resonance and STD NMR. J. Am. Chem. Soc. 134 (2012) 426-435.

[482] M. Plum, Y. Michel, K. Wallach, T. Raiber, S. Blank, F. I. Bantleon, A. Diethers, K. Greunke, I. Braren, T. Hackl, B. Meyer, E. Spillner, Close-up of the immunogenic α1,3-galactose epitope as defined by a monoclonal chimeric immunoglobulin E and human serum using saturation transfer difference (STD) NMR. J. Biol. Chem. 286 (2011) 43103-43111.

[483] F. Hőgye, L. B. Farkas, A. K. Balogh, L. Szilágyi, S. Alnukari, I. Bajza, A. Borbás, K. Fehér, T. Z. Illyés, I. Timári, Saturation Transfer Difference NMR and Molecular Docking Interaction Study of Aralkyl-Thiodigalactosides as Potential Inhibitors of the Human-Galectin-3 Protein. Int. J. Mol. Sci. 25 (2024) 1742.

[484] S. Hanashima, A. Ikeda, H. Tanaka, Y. Adachi, N. Ohno, T. Takahashi, Y. Yamaguchi, NMR study of short β(1-3)-glucans provides insights into the structure and interaction with Dectin-1. Glycoconj J. 31 (2014) 199-207.

[485] M. Thépaut, C. Guzzi, I. Sutkeviciute, S. Sattin, R. Ribeiro-Viana, N. Varga, E. Chabrol, J. Rojo, A. Bernardi, J. Angulo, P. M. Nieto, F. Fieschi, Structure of a glycomimetic ligand in the carbohydrate recognition domain of C-type lectin DC-SIGN. Structural requirements for selectivity and ligand design. J. Am. Chem. Soc. 135 (2013) 2518-2529.

[486] A. B. Yongye, L. Calle, A. Ardá, J. Jiménez-Barbero, S. André, H. J. Gabius, K. Martínez-Mayorga, M. Cudic, Molecular recognition of the Thomsen-Friedenreich antigen-threonine conjugate by adhesion/growth regulatory galectin-3: nuclear magnetic resonance studies and molecular dynamics simulations. Biochemistry. 51 (2012) 7278-7289.

[487] D. Schwizer, J. T. Patton, B. Cutting, M. Smieško, B. Wagner, A. Kato, C. Weckerle, F. P. Binder, S. Rabbani, O. Schwardt, J. L. Magnani, B. Ernst, Pre-organization of the core structure of E-selectin antagonists. Chem. Eur. J. 18 (2012) 1342-1351.

[488] M. C. Miller, J. P. Ribeiro, V. Roldós, S. Martín-Santamaría, F. J. Cañada, I. A. Nesmelova, S. André, M. Pang, A. A. Klyosov, L. G. Baum, J. Jiménez-Barbero, H. J. Gabius, K. H. Mayo, Structural aspects of binding of α-linked digalactosides to human galectin-1. Glycobiology. 21 (2011) 1627-1641.

[489] C. Guzzi, J. Angulo, F. Doro, J. J. Reina, M. Thépaut, F. Fieschi, A. Bernardi, J. Rojo, P. M. Nieto, Insights into molecular recognition of Lewis(X) mimics by DC-SIGN using NMR and molecular modelling. Org. Biomol. Chem. 9 (2011) 7705-7712.

[490] J. M. Teixeira, D. M. Dias, F. J. Cañada, J. A. Martins, J. P. André, J. Jiménez-Barbero, C. F. Geraldes, The interaction of La(3+) complexes of DOTA/DTPA glycoconjugates with the RCA(120) lectin: a saturation transfer difference NMR spectroscopic study. J. Biol. Inorg. Chem. 16 (2011) 725-734.

[491] M. Kaszowska, A. S. Norgren, P. I. Arvidson, C. Sandström, Studies on the interactions between glycosylated beta3-peptides and the lectin Vicia villosa by saturation transfer difference NMR spectroscopy. Carbohydr, Res. 344 (2009) 2577-2580.

[492] B. N. Murthy, S. Sinha, A. Surolia, N. Jayaraman, L. Szilágyi, I. Szabó, K. E. Kövér, Interactions of aromatic mannosyl disulfide derivatives with concanavalin A: synthesis, thermodynamic and NMR spectroscopy studies. Carbohydr. Res. 344 (2009) 1758-1763.

[493] C. Clavel, A. Canales, G. Gupta, J. I. Santos, F. J. Cañada, S. Penadés, A. Surolia, J. Jiménez-Barbero, NMR studies on the conformation of oligomannosides and their interaction with banana lectin. Glycoconj. J. 24 (2007) 449-464.

[494] S. Castro, M. Duff, N. L. Snyder, M. Morton, C. V. Kumar, M. W. Peczuh, Recognition of septanose carbohydrates by concanavalin A. Org. Biomol. Chem. 3 (2005) 3869-3872.

[495] K. Lycknert, M. Edblad, A. Imberty, G. Widmalm, NMR and molecular modeling studies of the interaction between wheat germ agglutinin and the beta-D-GlcpNAc-(1-->6)-alpha-D-Manp epitope present in glycoproteins of tumor cells. Biochemistry. 43 (2004) 9647-9654.

[496]: A. Bhunia, V. Jayalakshmi, A. J. Benie, O. Schuster, S. Kelm, N. Rama Krishna, T. Peters, Saturation transfer difference NMR and computational modeling of a sialoadhesin-sialyl lactose complex. Carbohydr. Res. 339 (2004) 259-267.

[497]: M. Rinnbauer, B. Ernst, B. Wagner, J. Magnani, A. J. Benie, T. Peters. Epitope mapping of sialyl Lewis(x) bound to E-selectin using saturation transfer difference NMR experiments. Glycobiology. 13 (2003) 435-443.

[498] J. P. Ribeiro, S. André, F. J. Cañada, H. J. Gabius, A. P. Butera, R. J. Alves, J. Jiménez-Barbero, Lectin-based drug design: combined strategy to identify lead compounds using STD NMR spectroscopy, solid-phase assays and cell binding for a plant toxin model. Chem. Med. Chem. 5 (2010) 41541-9.

[499] F. Souard, E. Muñoz, P. Peñalver, C. Badía, R. del Villar-Guerra, J. L. Asensio, J. Jiménez-Barbero, C. Vicent, Sugar-oligoamides: bound-state conformation and DNA minor-groove-binding description by TR-NOESY and differential-frequency saturation-transfer-difference experiments. Chem. Eur. J. 14 (2008) 2435-2442.

[500] J. C. Muñoz-García, E. Chabrol, R. R. Vives, A. Thomas, J. L. de Paz, J. Rojo, A. Imberty, F. Fieschi, P. M. Nieto, J. Angulo. Langerin–heparin interaction: Two binding sites for small and large ligands as revealed by a combination of nmr spectroscopy and cross-linking mapping experiments. J. Am. Chem. Soc., 137 (2015) 4100-4110.

[501] I. Huettner, S. A. Krumm, S. Serna, K. Brzesicka, S. Monaco, S. Walpole, A. van Diepen, F. Allan, T. Hicks, S. Kimuda, A. M. Emery, E. Landais, C. H. Hokke, J. Angulo, N. Reichardt,

K. Doores, Cross-reactivity of glycan-reactive HIV-1 broadly neutralizing antibodies with parasite glycans. Cell Rep. 38 (2022) 110611.

[502] P. M. Enríquez-Navas, F. Chiodo, M. Marradi, J. Angulo, S. Penadés, STD NMR studyof the interactions between antibody 2G12 and synthetic oligomannosides that mimic selected branches of gp120 glycans. Chembiochem. 13 (2012) 1357-1365.

[503] P. M. Enríquez-Navas, M. Marradi, D. Padro, J. Angulo, S. Penadés. A solution NMR study of the interactions of oligomannosides and the anti-HIV-1 2G12 antibody reveals distinct binding modes for branched ligands. Chem. Eur. J. 17 (2011) 1547-1560.

[504] C. Sandström, B. Hakkarainen, E. Matei, A. Glinchert, M. Lahmann, S. Oscarson, L. Kenne, A. M. Gronenborn, Atomic mapping of the sugar interactions in one-site and two-site mutants of cyanovirin-N by NMR spectroscopy. Biochemistry. 47 (2008) 3625-3635.

[505] C. Sandström, O. Berteau, E. Gemma, S. Oscarson, L. Kenne, A. M. Gronenborn AM. Atomic mapping of the interactions between the antiviral agent cyanovirin-N and oligomannosides by saturation-transfer difference NMR. Biochemistry. 43 (2004) 13926-13931.

[506] M. Pascolutti, L. Dirr, P. Guillon, A. Van Den Bergh, T. Ve, R. J. Thomson, M. von Itzstein, Structural Insights into Human Parainfluenza Virus 3 Hemagglutinin-Neuraminidase Using Unsaturated 3- N-Substituted Sialic Acids as Probes. ACS Chem. Biol. 13 (2018) 1544-1550.

[507] Z. Li, L. Unione, L. Liu, Y. Lang, R. P. de Vries, R. J. de Groot, G. J. Boons, Synthetic Acetylated Sialosides and their Acetamido-deoxy Analogues as Probes for Coronaviral Hemagglutinin-esterase Recognition. J. Am. Chem. Soc. 144 (2022) 424-435.

[508] T. Maass, G. Ssebyatika, M. Brückner, L. Breckwoldt, T. Krey, A. Mallagaray, T. Peters, M. Frank, R. Creutznacher, Binding of Glycans to the SARS CoV-2 Spike Protein, an Open Question: NMR Data on Binding Site Localization, Affinity, and Selectivity. Chem. Eur. J. 28 (2022) e202202614.

[509] I. Tomris, L. Unione, L. Nguyen, P. Zaree, K. M. Bouwman, L. Liu, Z. Li, J. A. Fok, M. Ríos Carrasco, R. van der Woude, A. L. M. Kimpel, M. W. Linthorst, S. E. Kilavuzoglu, E. Verpalen, T. G. Caniels, R. W. Sanders, B. A. Heesters, R. J. Pieters, J. Jiménez-Barbero, J. S. Klassen, G. J. Boons, R. P. de Vries, SARS-CoV-2 Spike N-Terminal Domain Engages 9-O-Acetylated α2-8-Linked Sialic Acids. ACS Chem. Biol. 18 (2023) 1180-1191.

[510] C. J. Buchanan, B. Gaunt, P. J. Harrison, Y. Yang, J. L., A. Khan, A. M. Giltrap, A. Le Bas, P. N. Ward, K. Gupta, M. Dumoux, T. K. Tan, L. Schimaski, S. Daga, N. Picchiotti, M. Baldassarri, E. Benetti, C. Fallerini, F. Fava, A. Giliberti, P. I. Koukos, M. J. Davy, A. L. Rayanan, X. Xue, G. Papadakis, L. P. Deimel, Vi. Casablancas-Antràs, T. D. W. Claridge, A. M. J. J. Bonvin, Q. J. Sattentau, S. Furin, I. Gori, J. Huo, R. J. Owens, C. Schaffitzel, I. Berger, A. Renieri, Gen-Covid Multicenter Study, J. H. Naismith, A. J. Baldwin, B. G. Davis, Pathogen-sugar interactions revealed by universal saturation transfer analysis. Science. 377 (2022) 6604.

[511] Haselhorst T, Wilson JC, Thomson RJ, McAtamney S, Menting JG, Coppel RL, von Itzstein M. Saturation transfer difference (STD) 1H-NMR experiments and in silico docking experiments to probe the binding of N-acetylneuraminic acid and derivatives to Vibrio cholerae sialidase. Proteins. 56 (2004) 346-353.

[512] A. Maggioni, J. Meier, F. Routier, T. Haselhorst, J. Tiralongo, Direct investigation of the Aspergillus GDP-mannose transporter by STD NMR spectroscopy. Chembiochem. 12 (2011) 2421-2425.

[513] A. Blume, B. Neubacher, J. Thiem, T. Peters, Donor substrate binding to trans-sialidase of Trypanosoma cruzi as studied by STD NMR. Carbohydr. Res. 342 (2007) 1904-1909.

[514] A. C. Lamerz, T. Haselhorst, A. K. Bergfeld, M. von Itzstein, R. Gerardy-Schahn, Molecular cloning of the Leishmania major UDP-glucose pyrophosphorylase, functional

characterization, and ligand binding analyses using NMR spectroscopy. J. Biol. Chem. 281 (2006) 16314-16322.

[515] F. Vasile, J. J. Reina, D. Potenza, J. E. Heggelund, A. Mackenzie, U. Krengel, A. Bernardi, Comprehensive analysis of blood group antigen binding to classical and El Tor cholera toxin B-pentamers by NMR. Glycobiology. 24 (2014) 766-778.

[516] H. Maaheimo, P. Kosma, L. Brade, H. Brade, T. Peters, Mapping the binding of synthetic disaccharides representing epitopes of chlamydial lipopolysaccharide to antibodies with NMR. Biochemistry. 39 (2000) 12778-12788.

[517] F. Corzana, I. Cuesta, A. Bastida, A. Hidalgo, M. Latorre, C. González, E. García-Junceda, J. Jiménez-Barbero, J. L. Asensio, Molecular recognition of aminoglycoside antibiotics by bacterial defence proteins: NMR study of the structural and conformational features of streptomycin inactivation by Bacillus subtilis aminoglycoside-6-adenyl transferase. Chem. Eur. J. 11 (2005) 5102-5113.

[518] J. Boutet, P. Blasco, C. Guerreiro, F. Thouron, S. Dartevelle, F. Nato, F. J. Cañada, A. Ardá, A. Phalipon, J. Jiménez-Barbero, L. A. Mulard, Detailed Investigation of the Immunodominant Role of O-Antigen Stoichiometric O-Acetylation as Revealed by Chemical Synthesis, Immunochemistry, Solution Conformation and STD-NMR Spectroscopy for Shigella flexneri 3a. Chem. Eur. J. 22 (2016) 10892-108911.

[519] R. Marchetti, A. Canales, R. Lanzetta, I. Nilsson, C. Vogel, D. E. Reed, D. P. Aucoin, J. Jiménez-Barbero, A. Molinaro, A. Silipo, Unraveling the interaction between the LPS O-antigen of Burkholderia anthina and the 5D8 monoclonal antibody by using a multidisciplinary chemical approach, with synthesis, NMR, and molecular modeling methods. Chembiochem. 14 (2013) 1485-1493.

[520] M. G. Szczepina, R. B. Zheng, G. C. Completo, T. L. Lowary, B. M. Pinto, STD-NMR studies of two acceptor substrates of GlfT2, a galactofuranosyltransferase from Mycobacterium tuberculosis: epitope mapping studies. Bioorg. Med. Chem. 18 (2010) 5123-5128.

[521] M.G. Szczepina, R.B. Zheng, G.C. Completo, T.L. Lowary, B.M. Pinto, STD-NMR studies suggest that two acceptor substrates for GlfT2, a bifunctional galactofuranosyltransferase required for the biosynthesis of Mycobacterium tuberculosis arabinogalactan, compete for the same binding site. Chembiochem. 10 (2009) 2052-2059.

[522] S. Mazzotta, G. Antonini, F. Vasile, E. Gillon, J. Lundstrøm, A. Varrot, L. Belvisi, A. Bernardi, Identification of New L-Fucosyl and L-Galactosyl Amides as Glycomimetic Ligands of TNF Lectin Domain of BC2L-C from Burkholderia cenocepacia. Molecules. 28 (2023) 1494.

[523] F. Berni, E. Kalfopoulou, A. M. Gimeno Cardells, F. Carboni, D. van der Es, F. Romero-Saavedra, D. Laverde, K. Miklic, S. Malic S, T. L. Rovis, S. Jonjic, S. Ali, H. S. Overkleeft, C. H. Hokke, A. van Diepen, R. Adamo, J. Jiménez-Barbero, G. A. van der Marel, J. Huebner, J. D. C. Codée, Epitope Recognition of a Monoclonal Antibody Raised against a Synthetic Glycerol Phosphate Based Teichoic Acid. ACS Chem. Biol. 16 (2021) 1344-1349.

[524] Q. Zhang, A. Gimeno, D. Santana, Z. Wang, Y. Valdés-Balbin, L. M. Rodríguez-Noda, T. Hansen, L. Kong, M. Shen, H. S. Overkleeft, V. Vérez-Bencomo, G. A. van der Marel, J. Jiménez-Barbero, F. Chiodo, J. D. C. Codée, Synthetic, Zwitterionic Sp1 Oligosaccharides Adopt a Helical Structure Crucial for Antibody Interaction. ACS Cent. Sci. 5 (2019) 1407-1416.

[525] C. D. Owen, L. Tailford, S. Monaco, T. Suligoj, L. Vaux, R. Lallament, Z. Khedri, H. Yu, K. Lecointe, J. Walshaw, S. Tribolo, M. Horrex, A. Bell, X. Chen, G. Taylor, A. Varki, J. Angulo, N. Juge, Unravelling the specificity and mechanism of sialic acid recognition by the gut symbiont Ruminococcus gnavus. Nat. Comm. 8 (2017) 2196-2213.

[526] A. Bell, J. Brunt, E. Crost, L. Vaux, R. Nepravishta, C. D. Owen, D. Latousakis, A. Xiao, W. Li, X. Chen, M. A. Walsh, J. Claesen, J. Angulo, G. H. Thomas, M. Juge. Elucidation of a

sialic acid metabolism pathway in mucus-foraging Ruminococcus gnavus unravels mechanisms of bacterial adaptation to the gut. Nat. Microbiol. 4 (2019) 2393-2404.

[527] H. Wu, E. Crost, C. D. Owen, W. van Bakel, A. Martinez-Guascuena, D. Dimitrios Latousakis, T. Hicks, S. Walpole, P. Urbanowicz, D. Ndeh, S. Monaco, L. Sanchez Salom, R. Griffiths, R. S. Reynolds, A. Colvile, D. I. R. Spencer, M. Walsh, J. Angulo, N. Juge. The human gut symbiont Ruminococcus gnavus shows specificity to blood group A antigen during mucin glycan foraging: Implication for niche colonisation in the gastrointestinal tract. PLoS Biol. 19 (2021) 1-32.

[528] M. Martín-Pastor, M. Vega-Vázquez, A. De Capua, A. Canales, S. André, H. J. Gabius, J. Jiménez-Barbero, Enhanced signal dispersion in saturation transfer difference experiments by conversion to a 1D-STD-homodecoupled spectrum. J. Biomol. NMR. 36 (2006) 103-109.

[529] B. Meyer, T. Peters, NMR Spectroscopy Techniques for Screening and Identifying Ligand Binding to Protein Receptors, Angew Chem Int Ed 42 (2003) 864-890.

[530] M. A. Johnson, B.M. Pinto, Saturation transfer difference 1D-TOCSY experiments to map the topography of oligosaccharides recognized by a monoclonal antibody directed against the cell-wall polysaccharide of Group A Streptococcus. J. Am. Chem. Soc. 124 (2002) 15368-15374.

[531] A. Ardá, P. Blasco, D. Varón Silva, V. Schubert, S. André, M. Bruix, F. J. Cañada, H. J. Gabius, C. Unverzagt, J. Jiménez-Barbero, Molecular recognition of complex-type biantennary N-glycans by protein receptors: a three-dimensional view on epitope selection by NMR. J. Am. Chem. Soc. 135 (2013) 2667-2675.

[532] A. Gimeno, N. C. Reichardt, F. J. Cañada, L. Perkams, C. Unverzagt, J. Jiménez-Barbero, A. Ardá, NMR and Molecular Recognition of N-Glycans: Remote Modifications of the Saccharide Chain Modulate Binding Features. ACS Chem. Biol. 12 (2017) 1104-1112.

[533] M. Vogtherr, T. Peters, Application of NMR based binding assays to identify key hydroxy groups for intermolecular recognition. J. Am. Chem. Soc.122 (2000) 6093-6099.

[534] C. Räuber, S. Berger, 13C-NMR detection of STD spectra. Magn. Reson. Chem. 48 (2010) 91-93.

[535] H. Xu, D. Lustig, L.B. Casabianca, 13C Saturation-Transfer Difference (STD)-NMR Experiments Using INEPT Polarization Transfer. Appl. Magn. Reson. 51 (2020) 277-286.

[536] J. Angulo, P.M. Nieto, STD-NMR: application to transient interactions between biomolecules—a quantitative approach. Eur. Biophys. J. 40 (2011) 1357-1369.

[537] K. Fehér, P. Groves, G. Batta, J. Jiménez-Barbero, C. Muhle-Goll, K. E. Kövér, Competition saturation transfer difference experiments improved with isotope editing and filtering schemes in NMR-based screening. J. Am. Chem. Soc. 130 (2008) 17148-17153.

[538] L. Unione, M. J. Moure, M. P. Lenza, I. Oyenarte, J. Ereño-Orbea, A. Ardá, J. Jiménez-Barbero, The SARS-CoV-2 Spike Glycoprotein Directly Binds Exogeneous Sialic Acids: A NMR View. Angew Chem Int Ed Engl. 134 (2022) e202201432.

[539] R. Creutznacher, T. Maass, B. Veselkova, G. Ssebyatika, T. Krey, M. Empting, N. Tautz, M. Frank, K. Kölbel, C. Uetrecht, T. Peters, NMR Experiments Provide Insights into Ligand-Binding to the SARS-CoV-2 Spike Protein Receptor-Binding Domain. J. Am. Chem. Soc. 144 (2022) 13060-13065.

[540] T. Diercks, J. Ribeiro, F. J. Cañada, S. A. Priv-Doz, J. Jimenez-Barbero, H. J. Gabius. Fluorinated Carbohydrates as Lectin Ligands: Versatile Sensors in 19F-Detected Saturation Transfer Difference NMR Spectroscopy, Chem. Eur. J. 15 (2009) 5666-5668.

[541] J. P. Ribeiro, T. Diercks, J. Jiménez-Barbero, S. André, H. J. Gabius, F. Cañada, Fluorinated Carbohydrates as Lectin Ligands: (19)F-Based Direct STD Monitoring for Detection of Anomeric Selectivity. Biomolecules. 5 (2015) 3177-3192.

[542] J. D. Martínez, A. S. Infantino, P. Valverde, T. Diercks, S. Delgado, N. C. Reichard, A. Ardá, F. J. Cañada, S. Oscarson, J. Jiménez-Barbero, The Interaction of Fluorinated Glycomimetics with DC-SIGN: Multiple Binding Modes Disentangled by the Combination of NMR Methods and MD Simulations. Pharmaceuticals. 13 (2020) 179-188.

[543] T. Diercks, A. S. Infantino, L. Unione, J. Jimenez-Barbero, S. Oscarson, H. J. Gabius, Fluorinated Carbohydrates as Lectin Ligands: Synthesis of OH/F-Substituted N-Glycan Core Trimannoside and Epitope Mapping by 2D STD-TOCSYreF NMR spectroscopy. Chem. Eur. J. 24 (2018) 15761-15765.

[544] A. Silva-Díaz, J. Ramirez-Cardeans, J. C. Munoz-Garcia, M. Carmen de la Fuente, M. Thepaut, F. Fieschi, J. Ramos-Soriano, J. Angulo, J. Rojo, Fluorinated Man9 as a High Mannose Mimetic to Unravel Its Recognition by DC-SIGN Using NMR. J. Am. Chem. Soc. 145 (2023) 26009-26015.

[545] P. Valverde, J. D. Martínez, F. J. Cañada, A. Ardá, J. Jiménez-Barbero, Molecular Recognition in C-Type Lectins: The Cases of DC-SIGN, Langerin, MGL, and L-Sectin, Chembiochem. 21 (2020) 2999-3025.

[546] J. Angulo, P.M. Enríquez-Navas, and P.M. Nieto, Ligand–receptor binding affinities from saturation transfer difference (STD) NMR spectroscopy: the binding isotherm of STD initial growth rates. Chem. Eur. J. 16 (2010) 7803-7812.

[547] S. Monaco, J. Angulo, M. Wallace, Imaging Saturation Transfer Difference (STD) NMR: Affinity and Specificity of Protein–Ligand Interactions from a Single NMR Sample. J. Am. Chem. Soc. 145 (2023) 16391-16397.

[548] S. Mari, D. Serrano-Gómez, F. J. Cañada, A. L. Corbí, J. Jiménez-Barbero, 1D saturation transfer difference NMR experiments on living cells: the DC-SIGN/oligomannose interaction, Angew Chem Int Ed 44 (2005) 298-298.

[549] C. Airoldi, S. Giovannardi, B. La Ferla, J. Jiménez-Barbero, F. Nicotra, Saturation transfer difference NMR experiments of membrane proteins in living cells under HR-MAS conditions: the interaction of the SGLT1 co-transporter with its ligands. Chem. Eur. J. 17 (2011) 13395-13399.

[550] A. Palmioli, P. Sperandeo, S. Bertuzzi, A. Polissi, C. Airoldi, On-cell saturation transfer difference NMR for the identification of FimH ligands and inhibitors. Bioorg. Chem. 112 (2021) 104876-104889.

[551] A. Palmioli, L. Moretti, C. A. Vezzoni, L. Legnani, P. Sperandeo, L. Baldini, F. Sansone, C. Airoldi, A. Casnati, Multivalent calix[4]arene-based mannosylated dendrons as new FimH ligands and inhibitors. Bioorg Chem. 138 (2023) 106613.

[552] F. Vasile, F. Gubinelli, M. Panigada, E. Soprana, A. Siccardi, D. Potenza, NMR interaction studies of Neu5Ac-α-(2,6)-Gal-β-(1-4)-GlcNAc with influenza-virus hemagglutinin expressed in transfected human cells. Glycobiology. 28 (2018) 42-49.

[553] P.D. Madge, A. Maggioni, M. Pascolutti, M. Amin, M. Waespy, B. Bellett, R.J. Thomson, S. Kelm, M. von Itzstein, T. Haselhorst, Structural characterisation of high affinity Siglec-2 (CD22) ligands in complex with whole Burkitt's lymphoma (BL) Daudi cells by NMR spectroscopy. Sci. Rep. 6 (2016) 36012.

[554] B. Mateos, M. Sealey-Cardona, K. Balazs, J. Konrat, G. Staffler, R. Konrat, NMR Characterization of Surface Receptor Protein Interactions in Live Cells Using Methylcellulose Hydrogels. Angew. Chem. Int. Ed. Engl. 59 (2020) 3886-3890.

[555] E. Luchinat, L. Banci, In-cell NMR: From target structure and dynamics to drug screening. Curr. Opin. Struct. Biol. 74 (2022) 102374.

[556] F.X. Theillet, E. Luchinat, In-cell NMR: Why and how? Prog. Nucl. Magn. Reson. Spectrosc. 132-133 (2022) 1-112.

[557] M.H. Lerche, S. Meier, P.R. Jensen, H. Baumann, B.O. Petersen, M. Karlsson, J.Ø. Duus, J.H. Ardenkjaer-Larsen, Study of molecular interactions with 13C DNP-NMR. J. Magn. Reson. 203 (2010) 52-56.

[558] H. Takahashi, I. Ayala, M. Bardet, G. De Paëpe, J.P. Simorre, S. Hediger. Solid-state NMR on bacterial cells: selective cell wall signal enhancement and resolution improvement using dynamic nuclear polarization, J. Am. Chem. Soc. 135 (2013) 5105-10.

[559] D. Dai, X. Wang, Y. Liu, X.L. YanL, C. Glaubitz, V. Denysenkov, X. He, T. Prisner, J. Mao, Room-temperature dynamic nuclear polarization enhanced NMR spectroscopy of small biological molecules in water. Nat. Commun. 12 (2021) 6880.

[560] B.C. Dollmann, A.L. Kleschyov, V. Sen, V. Golubev, L.M. Schreiber, H.W. Spiess, K. Münnemann, D. Hinderberger, Spin-labeled heparins as polarizing agents for dynamic nuclear polarization. Chemphyschem. 11 (2010) 3656-3663.

[561] K.R. Keshari, D.M. Wilson, A.P. Chen, R. Bok, P.E. Larson, S. Hu, M. Van Criekinge, J.M. Macdonald, D.B. Vigneron, J. Kurhanewicz, Hyperpolarized [2-13C]-fructose: a hemiketal DNP substrate for in vivo metabolic imaging. J. Am. Chem. Soc. 131 (2009) 17591-17596.

[562] A. Chakraborty, F. Deligey, J. Quach, F. Mentink-Vigier, P. Wang, T. Wang, Biomolecular complex viewed by dynamic nuclear polarization solid-state NMR spectroscopy. Biochem. Soc. Trans. 48 (2020) 1089-1099.

[563] R. Bastos, I. Marín-Montesinos, S.S. Ferreira, F. Mentink-Vigier, M. Sardo, L. Mafra, M.A. Coimbra, E. Coelho, Covalent connectivity of glycogen in brewer's spent yeast cell walls revealed by enzymatic approaches and dynamic nuclear polarization NMR. Carbohydr. Polym. 324 (2024) 121475.

[564] W. Zhao, F. Deligey, S.S. Chandra, F. Mentink-Vigier, T. Wang, Current limitations of solid-state NMR in carbohydrate and cell wall research. J. Magn. Reson. 341 (2022) 107263.

[565] M. Politi, M. I. Chávez, F. J. Cañada, J. Jiménez-Barbero, Screening by NMR: A New Approach for the Study of Bioactive Natural Products? The Example of Pleurotus ostreatus Hot Water Extract. Eur. J. Org. Chem. (2005) 1392-1396.

[566] M. Politi, J. Alvaro-Blanco, P. Groves, A. Prieto, J. A. Leal, F. J. Cañada, J. Jiménez-Barbero, Screening of Garlic Water Extract for Binding Activity with Cholera Toxin B Pentamer by NMR Spectroscopy – An Old Remedy Giving a New Surprise. Eur. J. Org. Chem. (2006) 2067-2073.

[567] J. I. Quintana, U. Atxabal, L. Unione, A. Ardá, J. Jiménez-Barbero, Exploring multivalent carbohydrate-protein interactions by NMR. Chem. Soc. Rev. 52 (2023) 1591-1613.

[568] A. E. Cristófalo, P. M. Nieto, M. Thépaut, F. Fieschi, P. H. Di Chenna, M. L. Uhrig, Synthesis, self-assembly and Langerin recognition studies of a resorcinarene-based glycocluster exposing a hyaluronic acid thiodisaccharide mimetic. Org. Biomol. Chem. 19 (2021) 6455-6467.

[569] A.A. Bothner-By, R Gassend, Binding of small molecules to proteins. Ann N Y Acad Sci. 222 (1973) 668-676.

[570] J.P. Albrand, B. Birdsall, J. Feeney, G.C.K. Roberts, A.S.V. Burgen, The use of transferred nuclear Overhauser effects in the study of the conformations of small molecules bound to proteins. Int. J. Biol. Macromol. 1 (1979) 37–41.

[571] G.M. Clore, A.M. Gronenborn, Theory and applications of the transferred nuclear overhauser effect to the study of the conformations of small ligands bound to proteins. J. Magn. Reson. 48 (1982) 402–417.

[572] G.M. Clore, A.M. Gronenborn, Theory of the time dependent transferred nuclear Overhauser effect: Applications to structural analysis of ligand-protein complexes in solution. J J. Magn. Reson. 53 (1983) 423–42.

[573] F. Ni, Recent developments in transferred NOE methods. Prog. Nucl. Magn. Reson. Spectrosc. 26 (1994) 517–606.

[574] T. Peters, Transfer NOE Experiments for the Study of Carbohydrate-Protein Interactions, in: Carbohydr. Chem. Biol., 2000: pp. 1003–1023.

[575] C.B. Post, Exchange-transferred NOE spectroscopy and bound ligand structure determination. Curr. Opin. Struct. Biol. 13 (2003) 581–588.

[576] G.C. Roberts, NMR spectroscopy in structure-based drug design. Curr. Opin. Biotechnol. 10 (1999) 42–47.

[577] A. Poveda, J. Jiménez-Barbero, NMR studies of carbohydrate–protein interactions in solution. Chem. Soc. Rev. 27 (1998) 133–144.

[578] S.R. Arepalli, C.P.J. Glaudemans, G.D. Daves, P. Kovac, A. Bax, Identification of Protein-Mediated Indirect Noe Effects in a Disaccharide-Fab′ Complex by Transferred ROESY. J. Magn. Reson. B 106 (1995) 195–198.

[579] J.L. Asensio, F.J. Cañada, J. Jiménez-Barbero, Studies of the Bound Conformations of Methyl α-Lactoside and Methyl β-Allolactoside to Ricin B Chain Using Transferred NOE Experiments in the Laboratory and Rotating Frames, Assisted by Molecular Mechanics and Dynamics Calculations, Eur. J. Biochem. 233 (1995) 618–630.

[580] T. Haselhorst, J.-F. Espinosa, J. Jiménez-Barbero, T. Sokolowski, P. Kosma, H. Brade, L. Brade, T. Peters, NMR Experiments Reveal Distinct Antibody-Bound Conformations of a Synthetic Disaccharide Representing a General Structural Element of Bacterial Lipopolysaccharide Epitopes. Biochemistry. 38 (1999) 6449–6459.

[581] L. Unione, S. Galante, D. Díaz, F.J. Cañada, J. Jiménez-Barbero, NMR and molecular recognition. The application of ligand-based NMR methods to monitor molecular interactions. Med. Chem. Commun. 5 (2014) 1280–1289.

[582] R. Marchetti, S. Perez, A. Arda, A. Imberty, J. Jimenez-Barbero, A. Silipo, A. Molinaro, “Rules of Engagement” of Protein–Glycoconjugate Interactions: A Molecular View Achievable by using NMR Spectroscopy and Molecular Modeling, ChemistryOpen. 5 (2016) 274–296.

[583] S.J.F. Vincent, C. Zwahlen, C.B. Post, J.W. Burgner, G. Bodenhausen, The conformation of NAD+ bound to lactate dehydrogenase determined by nuclear magnetic resonance with suppression of spin diffusion, Proc. Nat. Acad. Sci. USA. 94 (1997) 4383–4388.

[584] M.F. García-Mayoral, Á. Canales, D. Díaz, J. López-Prados, M. Moussaoui, J.L. de Paz, J. Angulo, P.M. Nieto, J. Jiménez-Barbero, E. Boix, M. Bruix, Insights into the Glycosaminoglycan-Mediated Cytotoxic Mechanism of Eosinophil Cationic Protein Revealed by NMR, ACS Chem. Biol. 8 (2013) 144–151.

[585] L. Nieto, Á. Canales, G. Giménez-Gallego, P.M. Nieto, J. Jiménez-Barbero, Conformational Selection of the AGA*IAM Heparin Pentasaccharide when Bound to the Fibroblast Growth Factor Receptor. Chem. Eur. J. 17 (2011) 11204–11209.

[586] A. Canales, J. Angulo, R. Ojeda, M. Bruix, R. Fayos, R. Lozano, G. Giménez-Gallego, M. Martín-Lomas, P.M. Nieto, J. Jiménez-Barbero, Conformational Flexibility of a Synthetic Glycosylaminoglycan Bound to a Fibroblast Growth Factor. FGF-1 Recognizes Both the 1C4 and 2SO Conformations of a Bioactive Heparin-like Hexasaccharide, J. Am. Chem. Soc. 127 (2005) 5778–5779.

[587] E. Montero, Querol, Perez Pons, J. Jimenez-Barbero, J. Cañada Studies on the bound conformation of thiocellobiose bound to Streptomyces Sp. Glucosidase. Febs Lett. 421 (1998) 243-248

[588] B. Aguilera, J. Jimenez-Barbero, A. Fernández-Mayoralas, Conformational differences between L-Fuc-(1->3)-GlcNAc and its thioglycoside analogue. Carbohydr. Res. 308 (1998) 19-27

[589] J. L Muñoz, A. García-Herrero, J. L. Asensio, F. J. Cañada, J. Jiménez-Barbero, Conformational selection of non-hydrolizable glycomimetics: the conformation of N, N'- di-acetyl thiochitobiose bound to wheat germ agglutinnin. J. Chem. Soc. Perkin I (2001) 867-872.

[590] J.L. Asensio, J.F. Espinosa, H. Dietrich, F.J. Cañada, R.R. Schmidt, M. Martín-Lomas, S. André, H.-J. Gabius, J. Jiménez-Barbero, Bovine Heart Galectin-1 Selects a Unique (Syn) Conformation of C-Lactose, a Flexible Lactose Analogue. J. Am. Chem. Soc. 121 (1999) 8995–9000.

[591] J. Angulo, B. Langpap, A. Blume, T. Biet, B. Meyer, N.R. Krishna, H. Peters, M.M. Palcic, T. Peters, Blood Group B Galactosyltransferase: Insights into Substrate Binding from NMR Experiments, J. Am. Chem. Soc. 128 (2006) 13529–13538.

[592] A. Ardá, J. Jiménez-Barbero, The recognition of glycans by protein receptors. Insights from NMR spectroscopy, Chem. Commun. 54 (2018) 4761–4769.

[593] V. Gabrielli, J.C. Muñoz-García, G. Pergolizzi, P. de Andrade, Y.Z. Khimyak, R.A. Field, J. Angulo, Molecular Recognition of Natural and Non-Natural Substrates by Cellodextrin Phosphorylase from Ruminiclostridium Thermocellum Investigated by NMR Spectroscopy, Chem. Eur. J. 27 (2021) 15688-15698.

[594] B. Fiege, C. Rademacher, J. Cartmell, P.I. Kitov, F. Parra, T. Peters, Molecular Details of the Recognition of Blood Group Antigens by a Human Norovirus as Determined by STD NMR Spectroscopy. Angew. Chem. Int. Ed. 51 (2012) 928–32.

[595] C. Rademacher, N.R. Krishna, M. Palcic, F. Parra, T. Peters, NMR Experiments Reveal the Molecular Basis of Receptor Recognition by a Calicivirus. J. Am. Chem. Soc. 130 (2008) 3669–75.

[596] T. Haselhorst, J.M. Garcia, T. Islam, J.C.C. Lai, F.J. Rose, J.M. Nicholls, J.S.M. Peiris, M. von Itzstein, Avian Influenza H5-Containing Virus-Like Particles (VLPs) Host-Cell Receptor Specificity by STD NMR Spectroscopy. Angew. Chem. Int. Ed. 47 (2008) 1910–1912.

[597] P.S.K. Ng, R. Böhm, L.E. Hartley-Tassell, J.A. Steen, H. Wang, S.W. Lukowski, P.L. Hawthorne, A.E. Trezise, P.J. Coloe, S.M. Grimmond, T. Haselhorst, M. von Itzstein, A.W. Paton, J.C. Paton, M.P. Jennings, Ferrets exclusively synthesize Neu5Ac and express naturally humanized influenza A virus receptors. Nat. Commun. 5 (2014) 5750.

[598] J.C.C. Lai, J.M. Garcia, J.C. Dyason, R. Böhm, P.D. Madge, F.J. Rose, J.M. Nicholls, J.S. Peiris, T. Haselhorst, M.A. von Itzstein, Secondary Sialic Acid Binding Site on Influenza Virus Neuraminidase: Fact or Fiction? Angew. Chem. Int. Ed. 51 (2012) 2221–2224.

[599] J.M. Garcia, J.C.C. Lai, T. Haselhorst, K.T. Choy, H.L. Yen, J.S.M. Peiris, M.A. von Itzstein, J.M. Nicholls, Investigation of the binding and cleavage characteristics of N1 neuraminidases from avian, seasonal, and pandemic influenza viruses using saturation transfer difference nuclear magnetic resonance. Influenza and Other Respiratory Viruses. 8 (2014) 235–242.

[600] T. Haselhorst, F.E. Fleming, J.C. Dyason, R.D. Hartnell, X. Yu, G. Holloway, K. Santegoets, M.J. Kiefel, H. Blanchard, B.S. Coulson, M. von Itzstein, Sialic acid dependence in rotavirus host cell invasion. Nat. Chem. Biol. 5 (2009) 91–93.

[601] T. Haselhorst, T. Fiebig, J.C. Dyason, F.E. Fleming, H. Blanchard, B.S. Coulson, M. von Itzstein, Recognition of the GM3 Ganglioside Glycan by Rhesus Rotavirus Particles. Angew. Chem. Internat. Ed. 50 (2011) 1055–1058.

[602] J. Mayr, K. Lau, J.C.C. Lai, I.A. Gagarinov, Y. Shi, S. McAtamney, R.W.Y. Chan, J. Nicholls, M. von Itzstein, T. Haselhorst, Unravelling the Role of O-glycans in Influenza A Virus Infection. Sci. Rep. 8 (2018) 16382.

[603] C. Rademacher, T. Peters, Molecular Recognition of Ligands by Native Viruses and Virus-Like Particles as Studied by NMR Experiments. In: T. Peters, editor. Bioactive Conformation II [Internet]. Berlin, Heidelberg: Springer Berlin Heidelberg; 2008. p. 183–202.

[604] T. Haselhorst, Studying the interaction of glycans with intact virions and virus-like particles by ligand-observed NMR spectroscopy. Magn. Reson. Chem. 62 (2024) 337-344.

[605] A. Mallagaray, J. Lockhauserbäumer, G. Hansman, C. Uetrecht, T. Peters,. Attachment of Norovirus to Histo Blood Group Antigens: A Cooperative Multistep Process. Angew. Chem. Internat. Ed. 54 (2015) 12014–12019.

[606] A. Mallagaray, R. Creutznacher, J. Dülfer, P.H.O. Mayer, L.L. Grimm, J.M: Orduña, et al., A post-translational modification of human Norovirus capsid protein attenuates glycan binding. Nat. Commun. 10 (2019) 1320.

[607] M.P: Williamson, Using chemical shift perturbation to characterise ligand binding. Prog. Nucl. Magn. Reson. Spectrosc. 73 (2013) 1–16.

[608] J.L. Asensio. F.J. Cañada, M. Bruix, A. Rodriguez-Romero, J. Jimenez-Barbero, The Interaction of Hevein with N-acetylglucosamine-containing Oligosaccharides. Eur. J. Biochem. 230 (1995) 621–633.

[609] J.L. Asensio. F.J. Cañada, M. Bruix, C. González, N. Khiar, A. Rodriguez-Romero, J. Jimenez-Barbero, NMR investigations of protein-carbohydrate interactions: refined three-dimensional structure of the complex between hevein and methyl β-chitobioside. Glycobiology. 1998, 8 (1998) 569–577.

[610] J. Jiménez-Barbero, J. Cañada, J. L. Asensio, N. Aboitiz, P. Groves, A. Canales, H.-J. Gabius, H. C. Siebert, Hevein domains: a simple model to study carbohydrate-protein interactIons at atomic resolution Adv. Carbohydr. Chem. Biochem. 60 (2006) 303-354.

[611] M.C. Fernández-Alonso F.J. Cañada,J. Jiménez-Barbero, G. Cuevas, Molecular recognition of saccharides by proteins. Insights on the origin of the carbohydrate-aromatic interactions, J. Am. Chem .Soc. 127 (2005) 7379-86.

[612] K.L. Hudson, G.J. Bartlett, R.C. Diehl, J. Agirre, T. Gallagher, L.L. Kiessling, D.N. Woolfson, Carbohydrate-Aromatic Interactions in Proteins. J. Am. Chem. Soc. 137 (2015) 15152−15160.

[613] S. Vandenbussche, D. Díaz, M.C. Fernández-Alonso, W. Pan, S.P. Vincent, G. Cuevas, F.J. Cañada, J. Jiménez-Barbero, K. Bartik, Aromatic-Carbohydrate Interactions: An NMR and Computational Study of Model Systems. Chem. Eur. J. 14 (2008) 7570−7578.

[614] K. Ramírez-Gualito, R. Alonso-Ríos, B. Quiroz-García, A. Rojas-Aguilar, D. Díaz, J. Jiménez-Barbero, G. Cuevas, Enthalpic Nature of the CH/π Interaction Involved in the Recognition of Carbohydrates by Aromatic Compounds, Confirmed by a Novel Interplay of NMR, Calorimetry, and Theoretical Calculations. J. Am. Chem. Soc. 131 (2009) 18129−18138.

[615] V. Spiwok, CH/π Interactions in Carbohydrate Recognition. Molecules. 22 (2017) 1038.

[616] C.H. Hsu, S. Park, D.E. Mortenson, B.L. Foley, X. Wang, R.J. Woods, D.A. Case, E.T. Powers, C.H. Wong, H.J. Dyson, J.W. Kelly, The Dependence of Carbohydrate-Aromatic Interaction Strengths on the Structure of the Carbohydrate. J. Am. Chem. Soc. 138 (2016) 7636-7648.

[617] E. Jiménez-Moreno, G. Jiménez-Osés, A.M. Gómez, A.G. Santana, F. Corzana, A. Bastida, J. Jiménez-Barbero, J.L. Asensio, A thorough experimental study of CH/π interactions in water: quantitative structure-stability relationships for carbohydrate/aromatic complexes. Chem. Sci. 6 (2015) 6076-6085.

[618] A.G. Santana, E. Jiménez-Moreno, A.M. Gómez, F. Corzana, C. González, G. Jiménez-Oses, J. Jiménez-Barbero, J.L. Asensio, A dynamic combinatorial approach for the analysis

of weak carbohydrate/aromatic complexes: dissecting facial selectivity in CH/π stacking interactions. J. Am. Chem. Soc. 135 (2013) 3347-3350.

[619] E. Jiménez-Moreno, A.M. Gómez, A. Bastida A, F. Corzana, G. Jiménez-Oses, J. Jiménez-Barbero, J.L. Asensio, Modulating weak interactions for molecular recognition: a dynamic combinatorial analysis for assessing the contribution of electrostatics to the stability of CH-π bonds in water. Angew. Chem. Int. Ed. Engl. 54 (2015) 4344-4348.

[620] L. Montalvillo-Jiménez, A.G. Santana, F. Corzana, G. Jiménez-Osés, J. Jiménez-Barbero, A.M. Gómez, J.L. Asensio, Impact of Aromatic Stacking on Glycoside Reactivity: Balancing CH/π and Cation/π Interactions for the Stabilization of Glycosyl-Oxocarbenium Ions. J. Am. Chem. Soc. 141(2019) 13372-13384.

[621] L. Díaz-Casado, A. Villacampa, F. Corzana, J. Jiménez-Barbero, A.M. Gómez, A.G. Santana, J.L. Asensio, Illuminating a Solvent-Dependent Hierarchy for Aromatic CH/π Complexes with Dynamic Covalent Glyco-Balances. JACS Au. 4 (2024) 476-490.

[622] N. Aboitiz, M. Vila-Perelló, P. Groves, J.L. Asensio, D. Andreu, F.J. Cañada, J. Jiménez-Barbero, NMR and modeling studies of protein-carbohydrate interactions: synthesis, three-dimensional structure, and recognition properties of a minimum hevein domain with binding affinity for chitooligosaccharides. Chembiochem. 5 (2004) 1245-1255.

[623] M.I. Chávez, C. Andreu, P. Vidal, N. Aboitiz, F. Freire, P. Groves, J.L. Asensio, G. Asensio, M. Muraki, F.J. Cañada, J. Jiménez-Barbero, On the importance of carbohydrate-aromatic interactions for the molecular recognition of oligosaccharides by proteins: NMR studies of the structure and binding affinity of AcAMP2-like peptides with non-natural naphthyl and fluoroaromatic residues. Chem. Eur. J. 11 (2005) 7060-7074.

[624] Y.C. Chan, H.Y. Lin, Z. Tu, Y.H. Kuo, S.D. Hsu, C.H. Lin, Dissecting the Structure-Activity Relationship of Galectin-Ligand Interactions. Int J Mol Sci. 9 (2018) 392.

[625] S. Bertuzzi, J.I. Quintana, A. Ardá, A. Gimeno, J. Jiménez-Barbero, Targeting Galectins With Glycomimetics. Front Chem. 8 (2020) 593.

[626] H. Ippel, M.C. Miller, S. Vértesy, Y. Zheng, F.J. Cañada, D. Suylen, K. Umemoto, C. Romanò, T. Hackeng, G. Tai, H. Leffler, J. Kopitz, S. André, D. Kübler, J. Jiménez-Barbero, S. Oscarson, H.J. Gabius, K.H. Mayo, Intra- and intermolecular interactions of human galectin-3: assessment by full-assignment-based NMR. Glycobiology. 26 (2016) 888-903.

[627] E. Ermakova, M.C. Miller, I.V. Nesmelova, L. López-Merino, M.A. Berbís, Y. Nesmelov, Y.V. Tkachev, L. Lagartera, V.A. Daragan, S. André, F.J. Cañada, J. Jiménez-Barbero, D. Solís, H.J. Gabius, K.H. Mayo, Lactose binding to human galectin-7 (p53-induced gene 1) induces long-range effects through the protein resulting in increased dimer stability and evidence for positive cooperativity. Glycobiology. 23 (2013) 508-523.

[628] M.C. Miller, J.P. Ribeiro, V. Roldós, S. Martín-Santamaría, F.J. Cañada, I.A. Nesmelova, S. André, M. Pang, A.A. Klyosov, L.G. Baum, J. Jiménez-Barbero, H.J. Gabius, K.H. Mayo, Structural aspects of binding of α-linked digalactosides to human galectin-1. Glycobiology. 21 (2011) 1627-1641.

[629] I.V. Nesmelova, E. Ermakova, V.A. Daragan, M. Pang, M. Menéndez, L. Lagartera, D. Solís, L.G. Baum, K.H. Mayo, Lactose binding to galectin-1 modulates structural dynamics, increases conformational entropy, and occurs with apparent negative cooperativity. J. Mol. Biol. 97 (2010) 1209-1230.

[630] J. Wallerstein, V. Ekberg, M.M. Ignjatović, R. Kumar, O. Caldararu, K. Peterson, S. Wernersson, U. Brath, H. Leffler, E. Oksanen, D.T. Logan, U.J. UJ, U. Ryde, M. Akke, Entropy-Entropy Compensation between the Protein, Ligand, and Solvent Degrees of Freedom Fine-Tunes Affinity in Ligand Binding to Galectin-3C. JACS Au. 1 (2021) 484-500.

[631] O. Stenström, C. Diehl, K. Modig, U.J. Nilsson, M. Akke, Mapping the energy landscape of protein-ligand binding via linear free energy relationships determined by protein NMR relaxation dispersion. RSC Chem. Biol. 2 (2020) 259-265.

[632] M.L. Verteramo, O. Stenström, M.M. Ignjatović, O. Caldararu, M.A. Olsson, F. Manzoni, H. Leffler, E. Oksanen, D.T. Logan, U.J. Nilsson, U. Ryde, M. Akke, Interplay between Conformational Entropy and Solvation Entropy in Protein-Ligand Binding. J. Am. Chem. Soc. 141 (2019) 2012-2026.

[633] C. Diehl, O. Engström, T. Delaine, M. Håkansson, S. Genheden, K. Modig, H. Leffler, U. Ryde, U.J. Nilsson, M. Akke, Protein flexibility and conformational entropy in ligand design targeting the carbohydrate recognition domain of galectin-3. J. Am. Chem. Soc. 132 (2010) 14577-14589.

[634] O. Stenström, C. Diehl, K. Modig, M. Akke, Ligand-induced protein transition state stabilization switches the binding pathway from conformational selection to induced fit. Proc. Natl. Acad. Sci. USA. 121 (2024) e2317747121.

[635] C.D.L. Lima, H. Coelho, A. Gimeno, F. Trovão, A. Diniz, J.S. Dias, J. Jiménez-Barbero, F. Corzana, A.L. Carvalho, E.J. Cabrita, F. Marcelo, Structural Insights into the Molecular Recognition Mechanism of the Cancer and Pathogenic Epitope LacdiNAc by Immune-Related Lectins. Chem. Eur. J. 27 (2021) 7951-7958.

[636] A. Schedlbauer, U. Gilles, A.K. Ludwig, A. Adler, H. Kaltner, I. Lindner, K.H. Mayo, T. Diercks, D. Reusch, H.J. Gabius, Characterizing ligand-induced conformational changes in clinically relevant galectin-1 by HN/H2O (D2O) exchange. Biochimie. 187 (2021) 48-56.

[637] C.H. Chien, M.R. Ho, C.H. Lin, S.D. Hsu, Lactose Binding Induces Opposing Dynamics Changes in Human Galectins Revealed by NMR-Based Hydrogen-Deuterium Exchange Molecules. 22 (2017) 1357.

[638] S. Wernersson, S. Birgersson, M. Akke, Cosolvent Dimethyl Sulfoxide Influences Protein-Ligand Binding Kinetics via Solvent Viscosity Effects: Revealing the Success Rate of Complex Formation Following Diffusive Protein-Ligand Encounter. Biochemistry. 62 (2023) 44-52.

[639] K. Umemoto, H. Leffler, A. Venot, H. Valafar, J.H. Prestegard, Conformational differences in liganded and unliganded states of Galectin-3. Biochemistry. 42 (2003) 3688-3695.

[640] R.D. Seidel 3rd, T. Zhuang, J.H. Prestegard, Bound-state residual dipolar couplings for rapidly exchanging ligands of His-tagged proteins. J. Am. Chem. Soc. 129 (2007) 4834-4839.

[641] A. Diniz, J.S. Dias, J. Jiménez-Barbero, F. Marcelo, E.J. Cabrita, Protein-Glycan Quinary Interactions in Crowding Environment Unveiled by NMR Spectroscopy. Chem. Eur. J. 23 (2017) 13213-13220.

[642] Srivastava, A.D.; Unione, L.; Wolfert, M.A.; Valverde, P.; Ardá, A.; Jiménez-Barbero, J.; Boons, G.J. Mono- and Di-Fucosylated Glycans of the Parasitic Worm S. mansoni are Recognized Differently by the Innate Immune Receptor DC-SIGN. Chem. Eur. J. 2020, 26, 15605–15612.

[643] F. Probert, S.B. Whittaker, M. Crispin, D.A. Mitchell, A.M. Dixon, Solution NMR analyses of the C-type carbohydrate recognition domain of DC-SIGNR protein reveal different binding modes for HIV-derived oligosaccharides and smaller glycan fragments J. Biol. Chem. 288 (2013) 22745-22757.

[644] P Valverde, S. Delgado, J.D. Martínez, J.B. Vendeville, J. Malassis, B. Linclau, N.C. Reichardt, F.J. Cañada, J. Jiménez-Barbero, A. Ardá A, Molecular Insights into DC-SIGN Binding to Self-Antigens: The Interaction with the Blood Group A/B Antigens. ACS Chem Biol. 14 (2019) 1660-1671.

[645] R. Wawrzinek, E.C. Wamhoff, J. Lefebre, M. Rentzsch, G. Bachem, G. Domeniconi, J. Schulze, F.F. Fuchsberger, H. Zhang, C. Modenutti, L. Schnirch, M.A. Marti, O. Schwardt, M. Bräutigam, M. Guberman, D. Hauck, P.H. Seeberger, O. Seitz, A. Titz, B. Ernst, C. Rademacher, A Remote Secondary Binding Pocket Promotes Heteromultivalent Targeting of DC-SIGN. J. Am. Chem. Soc. 143 (2021) 18977-18988.

[646] E.C. Wamhoff, J. Schulze, L. Bellmann, M. Rentzsch, G. Bachem, F.F. Fuchsberger, J. Rademacher, M. Hermann, B. Del Frari, R. van Dalen, D. Hartmann, N.M. van Sorge, O. Seitz, P. Stoitzner, C. Rademacher, A Specific, Glycomimetic Langerin Ligand for Human Langerhans Cell Targeting. ACS Cent. Sci. 5 (2019) 808-820.

[647] J. Aretz, U.R. Anumala, F.F. Fuchsberger, N. Molavi, N. Ziebart, H. Zhang, M. Nazaré, C. Rademacher, Allosteric Inhibition of a Mammalian Lectin. J. Am. Chem. Soc. 140 (2018) 14915-14925.

[648] H. Zhang, C. Modenutti, Y.P.K. Nekkanti, M. Denis, I.A. Bermejo, J. Lefèbre, K. Che, D. Kim, M. Kagelmacher, D. Kurzbach, M. Nazaré, C. Rademacher, Identification of the Allosteric Binding Site for Thiazolopyrimidine on the C-Type Lectin Langerin. ACS Chem. Biol. 17 (2022) 2728-2733.

[649] L. P. Calle, B. Echeverria, A. Franconetti, S. Serna, M. C. Fernández-Alonso, T. Diercks, F.J. Cañada, A. Ardá, N. C. Reichardt, J. Jiménez-Barbero, Monitoring glycan-protein interactions by NMR spectroscopic analysis: A simple chemical tag that mimics natural CH-π interactions. Chem. Eur. J. 21 (2015) 11408-11416.

[650] C.A. Bewley, Solution structure of a cyanovirin-N:Man alpha 1-2Man alpha complex: structural basis for high-affinity carbohydrate-mediated binding to gp120. Structure. 9 (2001) 931-940.

[651] L.C. Chang LC, C.A. Bewley, Potent inhibition of HIV-1 fusion by cyanovirin-N requires only a single high affinity carbohydrate binding site: characterization of low affinity carbohydrate binding site knockout mutants. J. Mol. Biol. 318 (2002) 1-8.

[652] S.R. Shenoy, L.G. Barrientos, D.M. Ratner, B.R. O'Keefe, P.H. Seeberger, A.M. Gronenborn, M.R. Boyd, Multisite and multivalent binding between cyanovirin-N and branched oligomannosides: calorimetric and NMR characterization. Chem. Biol. 9 (2002) 1109-18.

[653] S.L. Mangold, J.R. Morgan, G.C. Strohmeyer, A.M. Gronenborn, M.J. Cloninger, Cyanovirin-N binding to Manalpha1-2Man functionalized dendrimers. Org. Biomol. Chem. 3 (2005) 2354-2358.

[654] J. Mares, J.U. Müller, A. Skirgailiene, A. Neumoin, C.A. Bewley, R.R. Schmidt, O. Zerbe, A model for cell-surface-exposed carbohydrate moieties suitable for structural studies by NMR spectroscopy. Chembiochem. 7 (2006) 1764-1773.

[655] F. Yang, C.A. Bewley, J.M. Louis, K.R. Gustafson, M.R. Boyd, A.M. Gronenborn, G.M. Clore, A. Wlodawer, Crystal structure of cyanovirin-N, a potent HIV-inactivating protein, shows unexpected domain swapping. J. Mol. Biol. 288 (1999) 403-412.

[656] L.G. Barrientos, J.M. Louis, I. Botos, T. Mori, Z. Han, B.R. O'Keefe, M.R. Boyd, A. Wlodawer, A.M. Gronenborn, The domain-swapped dimer of cyanovirin-N is in a metastable folded state: reconciliation of X-ray and NMR structures. Structure.10 (2002) 673-686.

[657] E. Matei, W. Furey, A.M. Gronenborn, Solution and crystal structures of a sugar binding site mutant of cyanovirin-N: no evidence of domain swapping. Structure. 16 (2008) 1183-1194.

[658] L. Liu, I.J. Byeon, I. Bahar, A.M. Gronenborn, Domain swapping proceeds via complete unfolding: a 19F- and 1H-NMR study of the Cyanovirin-N protein. J. Am. Chem. Soc. 134 (2012) 4229-4235.

[659] F. Marcelo, F. Garcia-Martin, T. Matsushita, J. Sardinha, H. Coelho, A. Oude-Vrielink, C. Koller, S. André, E.J. Cabrita, H.J. Gabius, S. Nishimura, J. Jiménez-Barbero, F.J. Cañada, Delineating binding modes of Gal/GalNAc and structural elements of the molecular recognition of tumor-associated mucin glycopeptides by the human macrophage galactose-type lectin. Chem. Eur. J. 20 (2014) 16147-16155.

[660] A. Diniz, H. Coelho, J.S. Dias, S.J. van Vliet, J. Jiménez-Barbero, F. Corzana, E.J. Cabrita, F. Marcelo, The Plasticity of the Carbohydrate Recognition Domain Dictates the

Exquisite Mechanism of Binding of Human Macrophage Galactose-Type Lectin. Chem. Eur. J. *25*, (2019) 13945–13955.

[661] A. Gabba, A. Bogucka, J.G. Luz, A. Diniz, H. Coelho, F. Corzana, F.J. Cañada, F. Marcelo, P.V. Murphy, G. Birrane, Crystal Structure of the Carbohydrate Recognition Domain of the Human Macrophage Galactose C-Type Lectin Bound to GalNAc and the Tumor-Associated Tn Antigen. Biochemistry. 60 (2021) 1327-1336.

[662] M. Maalej, R.E. Forgione, R. Marchetti, F. Bulteau, M. Thépaut, R. Lanzetta, C. Laguri, J.P. Simorre, F. Fieschi, A. Molinaro, A. Silipo, Human Macrophage Galactose-Type Lectin (MGL) Recognizes the Outer Core of Escherichia coli Lipooligosaccharide. Chembiochem. 20 (2019) 1778-1782.

[663] M. Abbas, M. Maalej, F. Nieto-Fabregat, M. Thépaut, J.P. Kleman, I. Ayala, A. Molinaro, J.P. Simorre, R. Marchetti, F. Fieschi, C. Laguri, The unique 3D arrangement of macrophage galactose lectin enables Escherichia coli lipopolysaccharide recognition through two distinct interfaces. PNAS Nexus. 2 (2023) pgad310.

[664] E. Shanina, E. Siebs, H. Zhang, D. Varón Silva, I. Joachim, A. Titz, C. Rademacher, Protein-observed 19F NMR of LecA from Pseudomonas aeruginosa. Glycobiology. 31 (2021) 159–165.

[665] M.G. Lete, A. Franconetti, S. Bertuzzi, S. Delgado, G. Jiménez-Oses, A. Ardá, J. Jiménez-Barbero, NMR Investigations of Protein-Carbohydrate Interactions: The Recognition of Glycans by Galectins Engineered with Fluorotryptophan Residues,.Chem. Eur. J. 29 (2023) e202202208.

[666] E. Matei, A.M. Gronenborn, (19)F Paramagnetic Relaxation Enhancement: A Valuable Tool for Distance Measurements in Proteins. Angew. Chem. Int. Ed. Engl. 55 (2016) 150-154.

[667] T.R. McKitrick, M.E. Ackerman, R.M. Anthony, C.S. Bennett, M. Demetriou, G.A. Hudalla, K. Ribbeck, S. Ruhl, C.M. Woo, L. Yang, S.J. Zost, R.L. Schnaar, T.L. Doering, The Crossroads of Glycoscience, Infection, and Immunology. Front. Microbiol. 12 (2021) 731008.

[668] X. Du, Y. Li, Y.-L. Xia, S.-M. Ai, J. Liang, P. Sang, X.-L. Ji, S.-Q. Liu, Insights into Protein–Ligand Interactions: Mechanisms, Models, and Methods. Int. J. Mol. Sci. 17 (2016) 144.

[669] J. Qin, A.M. Gronenborn, Weak protein complexes: challenging to study but essential for life. FEBS J. 281 (2014) 1948–1949.

[670] A. Martínez-Palomo, The Surface Coats of Animal Cells. Int Rev Cytol (1970) 29–75.

[671] J.W. Costerton, R.T. Irvin, K.J. Cheng, The Bacterial Glycocalyx in Nature and Disease. Annu. Rev. Microbiol. 35 (1981) 299–324.

[672] L. Möckl, The Emerging Role of the Mammalian Glycocalyx in Functional Membrane Organization and Immune System Regulation. Front. Cell. Dev. Biol. 8 (2020) 253.

[673] C. Reily, T.J. Stewart, M.B. Renfrow, J. Novak, Glycosylation in health and disease. Nat. Rev. Nephrol. 15 (2019) 346–366.

[674] J.C. Lumibao, J.R. Tremblay, J. Hsu, D.D. Engle, Altered glycosylation in pancreatic cancer and beyond. J. Exp. Med. 219 (2022) e20211505.

[675] J. Aretz, E.-C. Wamhoff, J. Hanske, D. Heymann, C. Rademacher, Computational and Experimental Prediction of Human C-Type Lectin Receptor Druggability. Front. Immunol. 5 (2014) 323.

[676] S. Leusmann, P. Ménová, E. Shanin, A. Titz, C. Rademacher, Glycomimetics for the inhibition and modulation of lectins. Chem. Soc. Rev. 52 (2023) 3663–3740.

[677] M. Rentzsch, R. Wawrzinek, C. Zelle-Rieser, H. Strandt, L. Bellmann, F.F. Fuchsberger, J. Schulze, J. Busmann, J. Rademacher, S. Sigl, B. Del Frari, P. Stoitzner, C. Rademacher,

Specific Protein Antigen Delivery to Human Langerhans Cells in Intact Skin. Front. Immunol. 12 (2021) 732298.

[678] G. Timpano, G. Tabarani, M. Anderluh, D. Invernizzi, F. Vasile, D. Potenza, P.M. Nieto, J. Rojo, F. Fieschi, A. Bernardi, Synthesis of Novel DC-SIGN Ligands with an α-Fucosylamide Anchor. ChemBioChem. 9 (2008) 1921–1930.

[679] D. van Dinther, D.A. Stolk, R. van de Ven, Y. van Kooyk, T.D. de Gruijl, J.M.M. den Haan, Targeting C-type lectin receptors: a high-carbohydrate diet for dendritic cells to improve cancer vaccines. J. Leukoc. Biol. 102 (2017) 1017–1034.

[680] A. Ebrahim, B.T. Riley, D. Kumaran, B. Andi, M.R. Fuchs, S. McSweeney, D.A. Keedy, The temperature-dependent conformational ensemble of SARS-CoV-2 main protease (M pro). IUCrJ. 9 (2022) 682–694.

[681] C. Dalvit, P. Pevarello, M. Tatò, M. Veronesi, A. Vulpetti, M. Sundström, Identification of compounds with binding affinity to proteins via magnetization transfer from bulk water. J. Biomol. NMR 18 (2000) 65–68.

[682] C. Dalvit, G. Fogliatto, A. Stewart, M. Veronesi, B. Stockman, WaterLOGSY as a method for primary NMR screening: practical aspects and range of applicability. J. Biomol. NMR 21 (2001) 349–359.

[683] A. Viegas, J. Manso, F.L. Nobrega, E.J. Cabrita, Saturation-Transfer Difference (STD) NMR: A Simple and Fast Method for Ligand Screening and Characterization of Protein Binding. J. Chem. Educ. 88 (2011) 990–994.

[684] S. Walpole, S. Monaco, R. Nepravishta, J. Angulo, Chapter Twelve - STD NMR as a Technique for Ligand Screening and Structural Studies, in: A.J.B.T.-M. in E. Wand (Ed.), Biological NMR Part B, Academic Press, 2019: pp. 423–451.

[685] O. Cala, I. Krimm, Ligand-Orientation Based Fragment Selection in STD NMR Screening. J. Med. Chem. 58 (2015) 8739–8742.

[686] G. Rocha, J. Ramírez-Cárdenas, M.C. Padilla-Pérez, S. Walpole, R. Nepravishta, M.I. García-Moreno, E.M. Sánchez-Fernández, C. Ortiz Mellet, J. Angulo, J.C. Muñoz-García, Speeding-up the Determination of Protein–Ligand Affinities by STD NMR: The Reduced Data Set STD NMR Approach (rd-STD NMR). Anal. Chem. 96 (2024) 615-619.

[687] V. Gabrielli, J.C. Muñoz-García, G. Pergolizzi, P. de Andrade, Y.Z. Khimyak, R.A. Field, J. Angulo, Molecular Recognition of Natural and Non-Natural Substrates by Cellodextrin Phosphorylase from Ruminiclostridium Thermocellum Investigated by NMR Spectroscopy. Chem. Eur. J. 27 (2021) 15688–15698.

[688] U. Atxabal, C. Nycholat, J.M. Pröpster, A. Fernández, I. Oyenarte, M.P. Lenza, A. Franconetti, C.O. Soares, H. Coelho, F. Marcelo, M. Schubert, J.C. Paulson, J. Jiménez-Barbero, J. Ereño-Orbea, Unraveling Molecular Recognition of Glycan Ligands by Siglec-9 via NMR Spectroscopy and Molecular Dynamics Modeling. ACS Chem. Biol. 19 (2024) 483–496.

[689] A. Cavalli, X. Salvatella, C.M. Dobson, M. Vendruscolo, Protein structure determination from NMR chemical shifts. Proc. Nat. Acad. Sci. USA 104 (2007) 9615–9620.

[690] N.E. Hafsa, M. V Berjanskii, D. Arndt, D.S. Wishart, Rapid and reliable protein structure determination via chemical shift threading. J. Biomol. NMR 70 (2018) 33–51.

[691] R. Nepravishta, J. Ramírez-Cárdenas, G. Rocha, S. Walpole, T. Hicks, S. Monaco, J.C. Muñoz-García, J. Angulo, Fast Quantitative Validation of 3D Models of Low-Affinity Protein–Ligand Complexes by STD NMR Spectroscopy. J Med Chem (2024) doi: 10.1021/acs.jmedchem.4c00204.

[692] V. Limongelli, M. Bonomi, M. Parrinello, Proc. Nat. Acad. Sci. USA. 110 (2013) 6358-6363. Funnel metadynamics as accurate binding free-energy method.

[693] A. Mittermaier, L.E. Kay, New tools provide new insights in NMR studies of protein dynamics. Science 312 (2006) 224–228.

[694] J.K. Leman, G. Künze, Recent Advances in NMR Protein Structure Prediction with ROSETTA.,Int J Mol Sci 24 (2023) 7835.

[695] S.J. Marrink, V. Corradi, P.C.T. Souza, H.I. Ingólfsson, D.P. Tieleman, M.S.P. Sansom, Computational Modeling of Realistic Cell Membranes. Chem. Rev. 119 (2019) 6184–6226.

[696] A. Yu, A.J. Pak, P. He, V. Monje-Galvan, L. Casalino, Z. Gaieb, A.C. Dommer, R.E. Amaro, G.A. Voth, A multiscale coarse-grained model of the SARS-CoV-2 virion. Biophys. J. 120 (2021) 1097–1104.

[697] J. Abramson, J. Adler, J. Dunger, R. Evans, T. Green, A. Pritzel, O. Ronneberger, L. Willmore, A.J. Ballard, J. Bambrick, S.W. Bodenstein, D.A. Evans, C.-C. Hung, M. O'Neill, D. Reiman, K. Tunyasuvunakool, Z. Wu, A. Žemgulytė, E. Arvaniti, C. Beattie, O. Bertolli, A. Bridgland, A. Cherepanov, M. Congreve, A.I. Cowen-Rivers, A. Cowie, M. Figurnov, F.B. Fuchs, H. Gladman, R. Jain, Y.A. Khan, C.M.R. Low, K. Perlin, A. Potapenko, P. Savy, S. Singh, A. Stecula, A. Thillaisundaram, C. Tong, S. Yakneen, E.D. Zhong, M. Zielinski, A. Žídek, V. Bapst, P. Kohli, M. Jaderberg, D. Hassabis, J.M. Jumper, Accurate structure prediction of biomolecular interactions with AlphaFold 3. Nature. 630 (2024) 493–500.

[698] J. Jumper, R. Evans, A. Pritzel, T. Green, M. Figurnov, O. Ronneberger, K. Tunyasuvunakool, R. Bates, A. Žídek, A. Potapenko, A. Bridgland, C. Meyer, S.A.A. Kohl, A.J. Ballard, A. Cowie, B. Romera-Paredes, S. Nikolov, R. Jain, J. Adler, T. Back, S. Petersen, D. Reiman, E. Clancy, M. Zielinski, M. Steinegger, M. Pacholska, T. Berghammer, S. Bodenstein, D. Silver, O. Vinyals, A.W. Senior, K. Kavukcuoglu, P. Kohli, D. Hassabis, Highly accurate protein structure prediction with AlphaFold. Nature. 596 (2021) 583–589.

[699] G. Ahdritz, N. Bouatta, C. Floristean, S. Kadyan, Q. Xia, W. Gerecke, T.J. O'Donnell, D. Berenberg, I. Fisk, N. Zanichelli, B. Zhang, A. Nowaczynski, B. Wang, M.M. Stepniewska-Dziubinska, S. Zhang, A. Ojewole, M.E. Guney, S. Biderman, A.M. Watkins, S. Ra, P.R. Lorenzo, L. Nivon, B. Weitzner, Y.-E.A. Ban, S. Chen, M. Zhang, C. Li, S.L. Song, Y. He, P.K. Sorger, E. Mostaque, Z. Zhang, R. Bonneau, M. AlQuraishi, OpenFold: retraining AlphaFold2 yields new insights into its learning mechanisms and capacity for generalization, Nat. Meth. (2024) doi: 10.1038/s41592-024-02272-z.

[700] Z. Lin, H. Akin, R. Rao, B. Hie, Z. Zhu, W. Lu, N. Smetanin, R. Verkuil, O. Kabeli, Y. Shmueli, A. dos Santos Costa, M. Fazel-Zarandi, T. Sercu, S. Candido, A. Rives, Evolutionary-scale prediction of atomic-level protein structure with a language model. Science. 379 (2023) 1123–1130.

[701] M. Baek, F. DiMaio, I. Anishchenko, J. Dauparas, S. Ovchinnikov, G.R. Lee, J. Wang, Q. Cong, L.N. Kinch, R.D. Schaeffer, C. Millán, H. Park, C. Adams, C.R. Glassman, A. DeGiovanni, J.H. Pereira, A. V Rodrigues, A.A. van Dijk, A.C. Ebrecht, D.J. Opperman, T. Sagmeister, C. Buhlheller, T. Pavkov-Keller, M.K. Rathinaswamy, U. Dalwadi, C.K. Yip, J.E. Burke, K.C. Garcia, N. V Grishin, P.D. Adams, R.J. Read, D. Baker, Accurate prediction of protein structures and interactions using a three-track neural network. Science. 373 (2021) 871–876.

[702] N. Escobedo, T. Saldaño, J. Mac Donagh, L.R. Sawicki, N. Palopoli, S.F. Alberti, M.S. Fornasari, G. Parisi, Ghost interactions: revealing missing protein-ligand interactions using AlphaFold predictions. BioRxiv. (2023) 10.18.561916.

[703] M. Von Itzstein, W.Y. Wu, G.B. Kok, M.S. Pegg, J.C. Dyason, B. Jin, T. Van Phan, M.L. Smythe, H.F. White, S.W. Oliver, Rational design of potent sialidase-based inhibitors of influenza virus replication. Nature. 363 (1993) 418-423.

[704] X. Chen, Y. Zheng, Y. Shen, Voglibose (Basen®, AO-128), one of the most important α-glucosidase inhibitors. Curr. Med. Chem. 13 (2006) 109-116.

[705] B. Ernst, J.L. Magnani, From carbohydrate leads to glycomimetic drugs. Nat. Rev. Drug Discov. 8 (2009) 661-677.

[706] W.B. Turnbull, B.L. Precious, S.W. Homans, Dissecting the cholera toxin−ganglioside GM1 interaction by isothermal titration calorimetry. J. Am. Chem. Soc. 126 (2004) 1047-1054.

[707] A. Bernardi, J. Jiménez-Barbero, D. Potenza, A. García-Herrero, F. J. Cañada, A. Capelli, Synthesis and Structural Studies on Second Generation Mimics of Ganglioside GM1. A Three-Dimensional View of their Interactions with Bacterial Enterotoxins by NMR and Computational methods. Chem. Eur. J. 8 (2002) 4597-4612.

[708] A. Bernardi, D. Arosio, L. Manzoni, D. Monti, H. Posteri, D. Potenza, S. Mari, J. Jimenez-Barbero, Mimics of ganglioside GM1 as cholera toxin ligands: replacement of the GalNAc residue. Org. Biomol. Chem. 1 (2003) 785-792.

[709] I. Vrasidas, J. Kemmink, R.M. Liskamp, R. Pieters, R. Synthesis and cholera toxin binding properties of a lactose-2-aminothiazoline conjugate. Org. Lett. 4 (2002) 1807-1808.

[710] A. Bernardi, D. Arosio, D. Potenza, I. Sanchez-Medina, S. Mari, F.J. Cañada, J. Jimenez-Barbero, Mimics of ganglioside GM1 as Cholera Toxin ligands: The importance of carbohydrate-aromatic interactions in molecular recognition processes. Chem. Eur. J. 10 (2004) 4395-4405.

[711] I. Conforti, A. Marra, Iminosugars as glycosyltransferase inhibitors. Org. Biomol. Chem. 19 (2021) 5439-5475.

[712] F. Massicot, R. Plantier-Royon, J.L. Vasse, J.B. Behr, Synthesis and glycosidase inhibition potency of all-trans substituted 1-C-perfluoroalkyl iminosugars. Carbohydr. Res. 464 (2018) 2-7.

]713] Y. Blériot, Contributing to the Study of Enzymatic and Chemical Glycosyl Transfer Through the Observation and Mimicry of Glycosyl Cations. Synthesis. 53 (2021) 904-924.

[714] T. G. Frihed, M. Bols, C.M. Pedersen, Mechanisms of glycosylation reactions studied by low-temperature nuclear magnetic resonance. Chem. Rev. 115 (2015) 4963-5013.

[715] A. Martin, N. Probst, A. Arda, J. Desire, A. Mingot, P. Sinay, J. Jimenez-Barbero, S. Thibaudeau, Y. Bleriot, Catching elusive glycosyl cations in a condensed phase with HF/SbF_5 superacid. Nat. Chem. 8 (2016) 186-91.

[716] L. Lebedel, A. Ardá, A. Martin, J. Désiré, A. Mingot, M. Aufiero, N. Aiguabella Font, R. Gilmour, J. Jiménez-Barbero, Y. Blériot, S. Thibaudeau, Structural and Computational Analysis of 2-Halogeno-Glycosyl Cations in Superacid. Angew. Chem. Int. Ed. 58 (2019) 13758-13762.

[717]. A. Blume, J. Angulo, T. Biet, H. Peters, A.J. Benie, M. Palcic, T. Peters, Fragment-based screening of the donor substrate specificity of human blood group B galactosyltransferase using saturation transfer difference NMR. J. Biol. Chem. 281 (2006) 32728-32740.

[718] H. Zafar, M. Atif, M.I. Choudhary, Fucosyltransferase 2 inhibitors: Identification via docking and STD-NMR studies. PLoS One. 16 (2021) e0257623.

[719] K.C. Martin, J. Tricomi, F. Corzana, A. García-García, L. Ceballos-Laita, T. Hicks, S. Monaco, J. Angulo, R. Hurtado-Guerrero, B. Richichi, R. Sackstein, Fucosyl transferase-specific inhibition via next generation of fucose mimetics. Chem. Commun. 57 (2021) 1145-1148.

[720] N. Iwaya, N. Goda, M. Matsuzaki, A. Narita, Y. Shigemitsu, T. Tenno, Y. Abe, M. Hoshi, H. Hiroaki, Principal component analysis of data from NMR titration experiment of uniformly 15N labeled amyloid beta (1–42) peptide with osmolytes and phenolic compounds. Arch. Biochem. Biophys. 2020, 690 (2020) 108446.

[721] A. Diniz, J.S. Dias, J. Jiménez-Barbero, F. Marcelo, E.J. Cabrita. Protein-Glycan Quinary Interactions in Crowding Environment Unveiled by NMR Spectroscopy. Chem. Eur. J. 23 (2017) 13213-13220.

[722] I. Marin-Montesinos, D. Goyard, E. Gillon, O. Renaudet, A. Imberty, S. Hediger, G. De Paëpe, Selective high-resolution DNP-enhanced NMR of biomolecular binding sites. Chem. Sci. 10 (2019) 3366–3374.

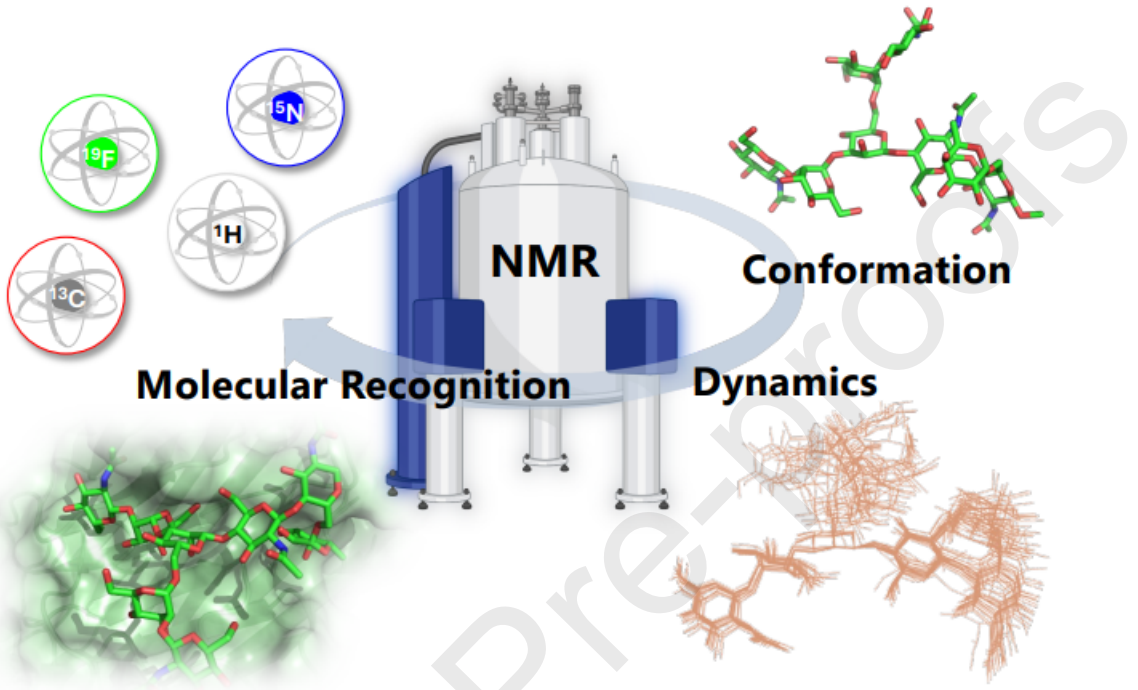

NMR investigations of glycans are essential to deduce their conformation and dynamic features • Diverse NMR methodologies can be applied to decipher their molecular recognition properties • STD NMR and Tr-NOE methods have been widely used to understand how glycans bind to lectins • Paramagnetic NMR and the use of isotope labelling have allowedd accessing to challenging systems, including intact glycoproteins